Transcriptomic and proteomic changes in the different zones of the articular cartilage during osteoarthritis and ageing

Thesis submitted in accordance with the requirements of the University of Liverpool for the degree of Doctor in Philosophy

by

Aibek Smagul

March 2023

Table of contents

CHAPTER 1

General introduction

1.1 Human articular cartilage

Cartilage is a connective tissue found in the synovial joints, spine, ribs, external ears and nose. Dependant on their biomechanical properties and the extracellular matrix (ECM) content there are three distinct types of cartilage found in human body: hyaline, fibrous and elastic cartilage (Wachsmuth et al., 2006). The type of hyaline cartilage found in the articulating surfaces of bones is articular cartilage (Krishnan & Grodzinsky, 2018). Articular cartilage can withstand high compressive strength and provides low-friction surface to ensure smooth joint movement, and also functions as a shock absorber (Bhosale & Richardson, 2008; Buckwalter & Mankin, 1998). The tissue structure of the articular cartilage is devoid of blood vessels, nerves and lymphatic vessels, it mainly consists of ECM and sparsely populated cells (Buckwalter & Mankin, 1998). Water is a major constituent of articular cartilage accounting for up to 80 per cent of total wet weight (Bhosale & Richardson, 2008). Water content differs from the surface (80%) to the deeper zones (65%) of the cartilage, this provides natural biomechanical properties to the tissue in a load-dependant manner (Bhosale & Richardson, 2008). Articular cartilage is composed of cells called chondrocytes and ECM, the majority of which are collagens and proteoglycans. The other molecules include glycoproteins and small leucine rich proteoglycans in a lesser amount (Brody, 2015).

1.2 Structural components of articular cartilage

1.2.1 Chondrocyte

Chondrocytes are the only cells residing in the tissue that maintain the tissue homeostasis by producing collagen and other ECM proteins (Urban, 1994). Chondrocytes react to mechanical loading of the cartilage during the movement which results in biosynthesis of molecules, the processes called mechanotransduction (Bader et al., 2011; Urban, 1994). Biosynthesis or inhibition of the matrix upon loading is dependent on strain rate and loading amplitude. Amplitude exceeding the dynamic range results in the inhibition of matrix synthesis, the same as static loading. Loading amplitude in the dynamic range induces matrix production within the cartilage tissue (Gilbert & Blain, 2018).

Mature chondrocytes are postmitotic cells have low proliferative capacity thus limiting the healing processes of cartilage tissue (Gilbert & Blain, 2018; Lin et al., 2006). In normal articular cartilage chondrocytes sustain a balance between anabolic and catabolic processes, ensuring the synthesis and degradation of ECM proteins respectively (Gilbert & Blain, 2018).

1.2.2 Extracellular matrix (ECM)

The ECM accounts for the majority of cartilage dry weight, of which collagen makes up to 60% and the rest includes proteoglycans, non-collagenous proteins and glycoproteins (Sophia Fox et al., 2009). The ECM is comprised of a pericellular, territorial and interterritorial regions (Heinegård & Saxne, 2011). Each chondrocyte is encircled with a pericellular matrix; together they are termed the chondron (C Anthony Poole, 1997). Pericellular matrix plays an important role in the mechanotransduction and helps to maintain chondrocyte homeostasis (Wilusz et al., 2014). Matrix proteins found exclusively or at higher proportion in the pericellular matrix include collagen type VI (Zelenski et al., 2015), perlecan, aggrecan monomers, hyaluronan, biglycan, collagen type XI and XIII, fibronectin (Heinegård & Saxne, 2011; Wilusz et al., 2014) (Fig. 1.1). In turn pericellular matrix is enclosed by territorial matrix and maintains biomechanical properties of cartilage by transducing signals to cells together with pericellular matrix (Gilbert & Blain, 2018). Territorial matrix is rich in procollagen II, matrilins 1 and 3, fibulin and the matrix is encompassed in fibrillar collagen (Heinegård & Saxne, 2011; Xia et al., 2018). Interterritorial matrix surrounds the space around the territorial matrix and takes up the highest proportion of the total area. It consists of fibrillar and non-fibrillar collagens, proteoglycans, asporin, fibromodulin, cartilage oligometric matrix protein (COMP) and other interconnected complex of matrix proteins (Heinegård & Saxne, 2011).
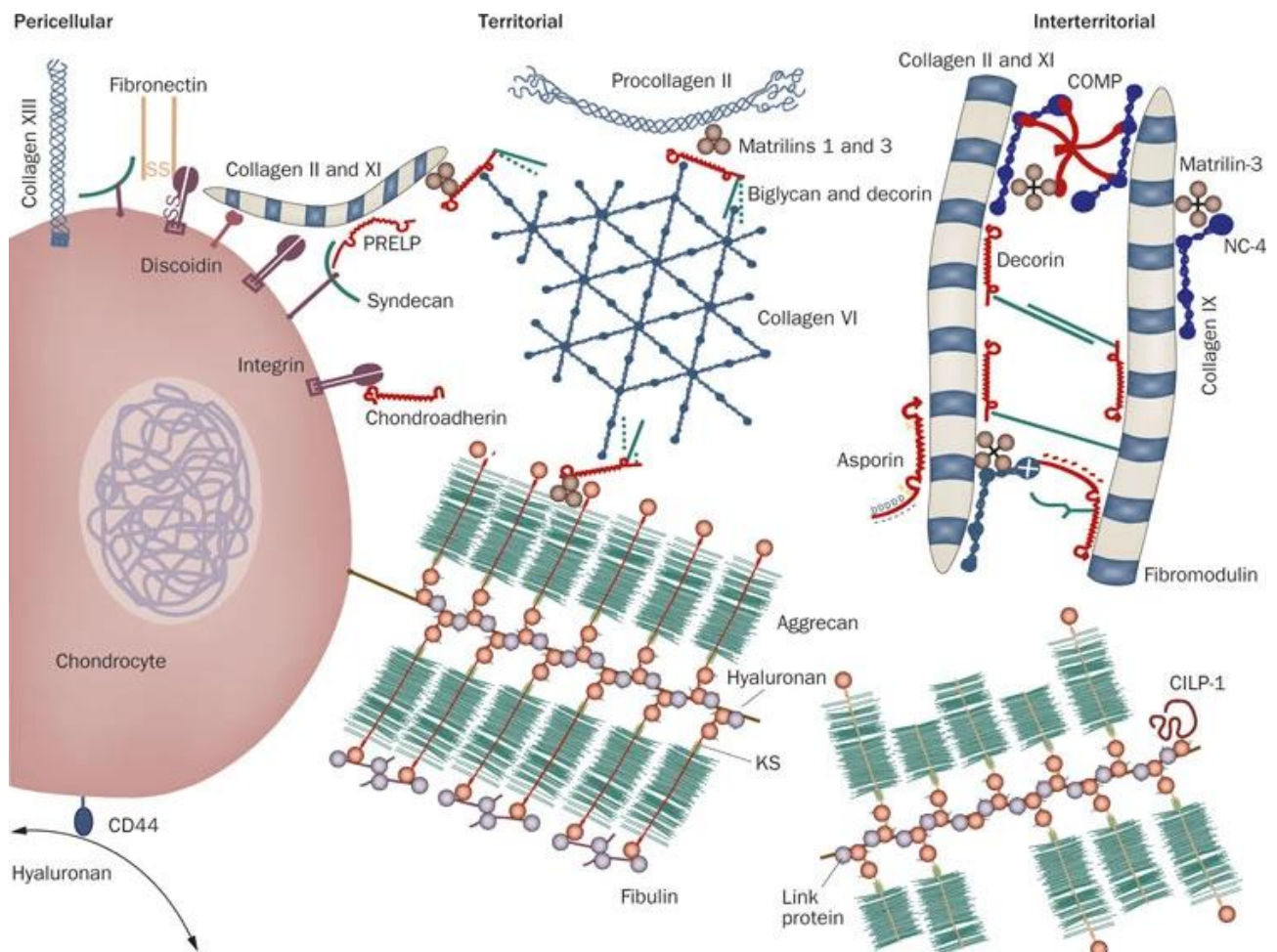
Figure 1.1: Molecular organisation of cartilage regions.

Cartilage regions are divided into three: pericellular, territorial and interterritorial regions with the pericellular region the thinnest of all three. It envelopes chondrocyte and forms a "chondron". The pericellular region is rich in collagen type VI, XI, XIII, hyaluronan, chondroadherin and fibronectin. The territorial region is next to the pericellular region, both of these regions play important roles in mechantransduction. The territorial region has higher abundance in procollagen II, precursor to collagen type II. Interterritorial matrix covers largest areas of cartilage tissue, especially in the middle zone. Collagen fibrils in this region have wider diameter and are rich in aggrecan, asporin and cartilage intermediate layer protein (CILP-1). Figure copied from (Heinegård & Saxne, 2011). Copyright license number 5151770858932 .

1.2.2.1 Collagen

Collagens are the most abundant molecules found in the articular cartilage responsible for the load-bearing function of the tissue. Collagen type II accounts for the 95% of total collagen in the tissue, it has close resemblance to fibril forming collagen type I and III (D. R. Eyre, 1991). Collagen types IX

and XI form heteropolymer templates with collagen type II (D. Eyre, 2002). The function of collagen type IX may be in restraining collagen type II with which it links covalently and forms a bridge between the fibrils (D. Eyre, 2002). In turn the majority of collagen type XI is mostly cross-linked with itself. However, there is evidence that collagen type XI might restrict lateral growth of collagen type II by linking laterally between the collagen type II fibrils (Blaschke et al., 2000; J. J. Wu & Eyre, 1995). The abundance of collagen types IX and XI is higher in the pericellular matrix of the cartilage region (C A Poole et al., 1987).

One of the collagens found in lesser amount in the articular cartilage is type III. This covalently cross-links with other collagen type III molecules. Furthermore the telopeptides of collagen type III link to helical cross-linking sites on the surface of collagen type II fibrils (J.-J. Wu et al., 2010). Collagen type VI can be attached to the chondrocytes via cell surface receptors and is abundantly present in the pericelluar matrix of cartilage (Marcelino & McDevitt, 1995; Zelenski et al., 2015). Collagen type VI plays an important role in mechanotransduction of signals to chondrocytes and maintains mechanical properties of the pericellular matrix (Zelenski et al., 2015).

Collagen types IX, XII, XIV, XVI, and XXII are members of the fibril-associated collagen with interrupted triple helix (FACIT). These types of collagen do not form fibrils by themselves but are associated with the surface of various fibrils (Y. Luo et al., 2017). Collagen type XII was found to co-localise with organised fibril direction. This may indicate its function in maintaining such organisation of fibrils and withstanding the load-bearing properties of cartilage (Gregory et al., 2001). Moreover, collagen type XII is involved in hyaline cartilage formation, as it was found to be abundantly secreted by chondrocytes during redifferentiation (Taylor et al., 2015). Type XIV collagen is structurally comparable to collagen type XII and has a similar function based on the localisation of the protein in the tissue (Y. Luo et al., 2017).

Collagen type XVI may have tissue specific functions. In papillary dermis it was found in fibrillin-1 containing microfibers (Kassner et al., 2003). However, in the articular cartilage it is localised with thin collagen fibrils of collagen type II and XI in the territorial matrix (Kassner et al., 2003). Another member of FACIT type XXII collagen is expressed specifically at tissue junctions. In the joint it is restricted to the articular cartilage and synovial fluid junction (Koch et al., 2004). Homotrimeric collagen type X is synthesised mainly by hypertrophic chondrocytes and is crucial for endochondral ossification (Shen, 2005).

1.2.2.2 Proteoglycans

Second to collagen in terms of abundance in the articular cartilage matrix are proteoglycans. Proteoglycans provide cartilage with biomechanical properties to withstand suppressive loads, with the hydrophilic nature of proteoglycans attracting water to aid load dispersal . The structure of proteoglycans includes one or more glycosaminoglycans (GAGs) covalently attached to a core protein. The principle GAGs found in the articular cartilage which are also negatively charged include keratin sulphate, chondroitin sulphate and dermatan sulphate (Brody, 2015). Proteoglycans form aggregates by linking to hyaluronan via a link protein. As many as 50 monomers can attach to the hyaluronan chain; the formed aggregate is called aggrecan (Knudson & Knudson, 2001). The main proteoglycans present in the articular cartilage are aggrecan, biglycan and decorin (Gilbert & Blain, 2018).

Aggrecan is the major glycoprotein in the articular cartilage. The core protein of aggrecan contains three disulphide-bonded globular domains, G1, G2 and G3, separated by three interglobular domains. Aggrecan also includes monomers of chondroitin sulphate and keratin sulphate. The G1 domain of aggrecan is responsible for attaching to hyaluronan. Although the G2 domain shares some structural similarities with G1 it lacks the ability of attaching to hyaluronan (Dudhia, 2005). The G2 domain may act as an inhibitor of aggrecan secretion, whilst the G3 domain along with the glycosylated core protein facilitate the secretion of aggrecan to ensure that only fully glycosylated molecules are secreted from the cell (Kiani et al., 2001; W. Luo et al., 1996).

Biglycan and decorin are smaller molecules in comparison to aggrecan and they have a different composition of GAGs. Thus, biglycan has one and decorin has two dermatan sulphate chains. Moreover, biglycan interacts with collagen type II fibrils, whereas, decorin links with collagen type VI (Sophia Fox et al., 2009).

1.3 Zonal composition of the articular cartilage

Articular cartilage is divided into four distinct zones: superficial, middle, deep and calcified zones; each of them differ in ECM structure and molecular composition at the cellular level (Heinegård & Saxne, 2011) (Fig. 1.2).
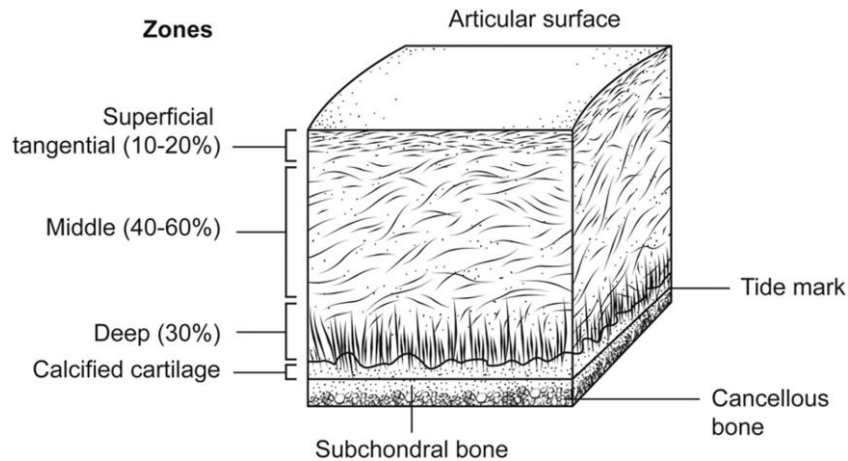
Figure 1.2 Articular cartilage zones.

Articular cartilage consists of three main zones: superficial (10-20%), middle (40-60%) and deep (30%) zones. Beneath the deep zone lies calcified cartilage followed by subchondral bone. Chondrocytes are flattened and collagen fibrils directed parallel to the surface of the cartilage in the superficial zone. The middle zone accounts for the majority of the cartilage thickness with sparsely distributed cells. Chondrocytes in the deep zone form a columnar structure, and collagen fibrils have a perpendicular direction relatively to the underlying bone. Figure copied from (Brody, 2015). License number 5151411065626.

1.3.1 Superficial zone

Situated on the surface of the gliding articular cartilage the superficial zone is the thinnest of all zones, providing the shear force resistance of the tissue (Heinegård & Saxne, 2011). Chondrocytes residing in the superficial zone appear flattened with ellipsoid shape, furthermore the superficial zone has increased number of cells in comparison to other zones (Killen & Charalambous, 2020) (Fig. 1.2). Collagen content in the superficial zone differs in comparison to the underlying zones. Collagen type I is found in the superficial zone has higher proportion to collagen type II in comparison to the deeper zones (Duance, 1983; Hidaka et al., 2006). Moreover, collagen types II, IX and XI are the main constituents of the superficial zone, with collagen fibrils oriented parallel to the surface of the articular cartilage (Gilbert & Blain, 2018). The proportion of the synthesised collagen is much higher in the superficial zone in comparison to proteoglycans, as the water content is increased in the superficial zone in comparison to the deep zone (Killen & Charalambous, 2020). One of the zone specific protein synthesised by chondrocytes in the superficial zone is proteoglycan 4 (PRG4), also known as lubricin, which functions as joint lubricant (Flannery et al., 1999; Ikegawa et al., 2000). Chondrocytes in the superficial zone exclusively express clusterin, commonly found in tissue-fluid junctions. It is involved in cell death and complement activation (Khan et al., 2001). The superficial zone accounts

for a higher amount of progenitor cells in comparison to the middle and deep zones (Dowthwaite et al., 2004). These cells have chondrogenic and osteogenic capabilities, similar to mesenchymal stem cells (MSC) found in bone marrow (Grogan et al., 2009). Progenitor cells express Notch1, Stro-1, VCAM (Grogan et al., 2009), CD105 and CD166 cell surface markers (Alsalameh et al., 2004), and demonstrate high affinity for fibronectin (Dowthwaite et al., 2004). However, these progenitor cells are found in higher proportions than expected and also in osteoarthritic cartilage, indicating that the progenitor cells may be activated chondrocytes (Alsalameh et al., 2004; Grogan et al., 2009).

1.3.2 Middle zone

The middle zone makes up to 60% of the cartilage total thickness, in comparison to the superficial zone collagen fibrils appear thicker and proteoglycan content is increased (Sophia Fox et al., 2009) (Fig. 1.2). Chondrocytes in the middle zone have spheroid shape and are sparsely situated within the matrix (Killen & Charalambous, 2020). It provides transition from the shearing forces of the superficial zone to the compressive forces in the deep zone (Killen & Charalambous, 2020). Cartilage intermediate layer protein (CILP1) is exclusively abundant in the middle zone of articular cartilage, and localised in the interterritorial matrix (Lorenzo et al., 1998). A highly homologous gene to CILP1 is cartilage intermediate layer protein, isoform 2 (CILP2). It is localised in the lower part of the middle zone and has different responses to experimental osteoarthritis in comparison to CILP1 (Bernardo et al., 2011).

1.3.3 Deep zone and calcified zone

Collagen fibrils are oriented perpendicularly to the underlying bone in the deep zone of articular cartilage, and chondrocytes appear to have ellipsoid shape with a principal axis directed vertically, similarly to fibrils (Killen & Charalambous, 2020; Youn et al., 2006) (Fig. 1.2). The deep zone provides the greatest compressive force in the articular cartilage (Killen & Charalambous, 2020). Chondrocytes in the deep zone form columnar structures where several chondrocytes can be placed in the same chondron (Youn et al., 2006). Collagen type X is specific for the deep zone chondrocytes, and facilitates endochondral ossification via mineralisation of cartilage matrix (Shen, 2005). Proteoglycan content is higher in the deep zone and it contains fibrils with larger diameter in comparison to the superficial and middle zones (Killen & Charalambous, 2020). The transcription factor RUNX2 plays important role in chondrocyte maturation and regulates the expression of collagen type X (Komori, 2017). RUNX2 is the main hypertrophy marker, and chondrocytes found in the deep zone of articular cartilage have a hypertrophic phenotype.

The tidemark delineates the deep zone from the underlying calcified cartilage (Killen & Charalambous, 2020). The calcified cartilage is connected to the subchondral bone and has low numbers of cells with limited metabolic activity (Killen & Charalambous, 2020). Mature articular cartilage take up nutrition from the synovial fluid, whilst the calcified cartilage prevents the supply of nutrition from the subchondral bone to the cartilage (Brody, 2015).

1.4 Ageing processes in the articular cartilage

Ageing is considered as the accumulation of damages at organism, cellular and molecular levels to the extent where whole organism or a tissue fails to restore itself. Ageing is an inevitable process affecting almost all living organisms (Xi et al., 2013). Ageing of the articular cartilage introduces broad changes in tissue composition predisposing it to a disease progression such as osteoarthritis (Martin & Buckwalter, 2002). Both chondrocytes and the ECM undergo age-related changes caused by oxidative stress, telomere erosion, cell senescence and matrix degeneration (Martin & Buckwalter, 2002). Processes driven by ageing in the articular cartilage are discussed below.

1.4.1 Age-related changes in ECM

Biomechanical properties of articular cartilage ECM are essential for the tissue to withstand repetitive loading and shearing forces needed to provide normal movement of the joints. However, changes during ageing affect these properties, including decrease in water content and proteoglycan degradation (Killen & Charalambous, 2020). Water in the articular cartilage is attracted by negatively charged proteoglycans abundantly present in the cartilage tissue. In turn normal water content helps to attenuate loading and makes articular cartilage resistant to the compression (Sophia Fox et al., 2009). A decline in water content can lead to the calcification of the cartilage tissue. Common crystals found in the cartilage are calcium pyrophosphate dihydrate and basic calcium phosphate crystals (Mitsuyama et al., 2007). Cartilage calcification can cause inflammatory arthritis and increase the severity of osteoarthritis (OA). Ageing is positively correlated with cartilage calcification and was shown to be the main cause of it, not (OA) (Moyer et al. 2021).

Aggrecan undergoes age-related changes, specifically proteolytic degradation of proteoglycan-rich regions (Dudhia, 2005). Furthermore, chondroitin sulphate content diminishes enabling elongation of keratan sulphate in aggrecan structure, leaving heterogeneously sized aggrecan. A decline in the synthesis of aggrecan by chondrocytes and low protein turnover results in a high proportion of proteolytically cleaved aggrecan in the tissue. It was also shown that newly synthesised aggrecan in

the cartilage during ageing has low rate of linking to hyaluronan, which could be partially due to a decrease in link protein (Vincent, 2000). Proteoglycan loss in the articular cartilage also predispose chondrocytes to cell death. It was shown that depletion of proteoglycans does not affect cell viability directly, however, cartilage tissue with depleted proteoglycan content demonstrated significant cell death after mechanical loading, especially in the superficial zone (Otsuki et al., 2008).

During articular cartilage ageing advanced glycation end products (AGEs) start to accumulate in the tissue affecting biomechanical properties and cellular homeostasis (Verzijl et al., 2003). AGEs formation can be initiated by nonenzymatic glycation of proteins via sugar reduction, metal-catalysed glucose autooxidation or lipid peroxidation. Firstly, cross-linking of AGEs with collagen results in an increased diameter of collagen fibrils, which impairs elasticity and leads to brittleness of collagen network. Secondly, the slow turnover of collagen in the articular cartilage adds to the accumulation of higher levels of AGEs in the tissue (Bank et al., 1998). Intact collagen type IX is lost from the interterritorial region of cartilage during ageing. This compounds the fact that collagen type II fibrils are less restrained and available for other molecules to link (Vaughan-Thomas et al., 2008).

1.4.2 Chondrocyte senescence

1.4.2.1 Telomere erosion

The cellular senescence process initiates permanent cell-cycle arrest with cells unable to proliferate and developing a senescent phenotype (Campisi & d'Adda di Fagagna, 2007). However, even before reaching proliferation arrest, cells begin dividing at slower rate and cell function starts to deteriorate, impairing tissue homeostasis (Martin & Buckwalter, 2002). Senescence can be prompted by many factors including telomere erosion, DNA damage, expression of oncogenes and changes in chromatin organisation (Campisi & d'Adda di Fagagna, 2007). Telomeres are repetitive DNA sequences and associated proteins that cap the end of chromosomes. They can reach up to 15kbp in sequence length (Campisi & d'Adda di Fagagna, 2007). Telomeres shorten by 100-200bp after each mitosis, and after 40-50 cycles of mitosis cells can enter cell-cycle arrest. Chondrocytes extracted from cartilage during ageing demonstrate the shortening of telomeres and low mitotic activity, suggesting cellular senescence. However, chondrocytes in mature cartilage in general have low mitotic activity which may imply that telomeres shortening alone is not a cause of chondrocyte senescence (Martin & Buckwalter, 2002). However, trauma to the cartilage tissue can initiate mitotic activity in chondrocytes, hence repetitive injuries could accelerate telomeres shortening.

1.4.2.2 Oxidative stress

One of the other major factors leading to chondrocyte senescence is oxidative stress. Free radicals are any molecules with an unpaired electron in the outer shell. Reactive free radicals (ROS) associated with oxygen are the most central to ageing (Valko et al., 2007). The mitochondrial respiration process forms ROS superoxide or hydrogen peroxide. ROS plays an essential role in cell homeostasis; in defence against infectious agents and different cellular signalling pathways (Valko et al., 2007). However, excessive levels of ROS have negative effects on cells and DNA, subsequently triggering cell senescence. Chondrocytes reside in an aneural, avascular, low oxygen environment obtaining the nutrients through diffusion. Due to this chondrocytes may withstand higher levels of oxidative stress in comparison to fibroblasts (Brandl et al., 2011). Mitochondrial function has been shown to decline during ageing, and is linked with oxidative stress and cellular senescence (Hui et al., 2016). Chondrocytes from OA cartilage have reduced mitochondrial mass and mitochondrial DNA content, together with reduced levels of electron transport chain proteins and proteins involved in mito-chondrial biogenesis (Wang et al., 2015). However, mouse cartilage sections demonstrated that some of the changes were initiated during ageing and were independent of the disease state. In addition to the increase of oxidative stress in cells the antioxidants involved in eliminating ROS decrease with age and disease (Martin Lotz & Loeser, 2012). Furthermore, overloading of articular cartilage *in vivo* promotes mitochondrial ROS production and downregulates mitochondrial superoxide dismutase (SOD2) (Koike et al., 2015). ROS can induce MAP kinases activation in chondrocytes. This has been shown to initiate downstream catabolic signalling events including the release of cartilage matrix degrading enzymes (Forsyth et al., 2005). ROS activation of MAP kinases also contributes to inhibition of pro-anabolic signalling, downregulation of cartilage matrix synthesis, and chondrocyte cell death (Bolduc et al., 2019). All of the above demonstrate that a continuous rise in ROS causes oxidative damage to proteins and DNA, resulting in increased cell death, and moreover can disrupt cell signalling pathways.

1.4.2.3 Inflammation and apoptosis during ageing

Reduction in the capability to cope with a variety of stress factors and a progressive increase in the proinflammatory status is a major characteristic of the ageing process termed inflammageing (Franceschi et al., 2000). In ageing chondrocytes develop senescence-associated secretory phenotype, defined by the production of high levels of proinflammatory cytokines and matrix-degrading enzymes (Freund et al., 2010). One of the main cytokines found to be elevated during ageing is IL-6. Increased expression of IL-6 is linked with age-related joint diseases. Levels of IL-6 in the systemic circulation

increase with age and are strongly associated with the risk of OA progression (Loeser et al., 2016). Production of pro-inflammatory cytokines such as IL-1 results in upregulation of matrix metallopeptidase 13 (MMP13) which degrades collagen type II (Mengshol et al., 2001).

Apoptosis is programmed cell death occurring under physiological and pathological stimuli (Kerr et al., 1972). Ageing has been associated with progressively reduced cellularity in the articular cartilage as a result of cell death (Temple et al., 2007). Changes in the structure of the chondrocyte environment during ageing can alter the biomechanical forces experienced by the cell, as well as the mechanotransduction that regulates the cell response (Grogan & D'Lima, 2010). As degeneration continues, the loss of matrix leads to cell death and tissue degeneration. Some chondrocytes especially in the superficial zone express Fas antigen. In the event of cross-linking with antibody apoptosis is induced (M Lotz et al., 1999). Chondrocyte apoptosis can be triggered by trauma and oxidative stress, subsequently resulting in cartilage calcification in addition to matrix degeneration (M Lotz et al., 1999). Nitric oxide is a further factor inducing cell death, and it has been shown that IL-1 and tumour necrosis factor (TNF) can stimulate high levels of expression of nitric oxide (M Lotz et al., 1999). It is evident that changes in ageing are interconnected were oxidative stress and inflammation induces apoptosis, and further matrix degeneration including proteoglycan loss leads to cell death under mechanical loading. Overarching processes triggered by ageing in the cartilage impede the search for a single solution to overturn the destructive transformation in the tissue. Thus, to address the ageing changes a complex approach needs to be implemented considering the structural and zonal composition of articular cartilage.

1.5 Osteoarthritis epidemiology and pathogenesis

OA is a degenerative joint disease, the most common form of arthritis, affecting the whole joint. It is associated with ageing and affects the joints that have been continually stressed throughout life including the knees, hips, fingers, and lower spine region (Martel-Pelletier et al., 2016b). OA is a multifactorial condition of joint characterised by articular cartilage loss, subchondral bone sclerosis, and inflammation leading to progressive joint degradation, structural alterations, loss of mobility and pain. (Tuhina Neogi & Zhang, 2013). In the UK approximately one in 10 adults have symptomatic clinically diagnosed OA, the knee being the most frequent (Swain et al., 2020). Females are subject to a twice-fold higher risk of developing knee OA in comparison to males (Phinyomark et al., 2016). In Kazakhstan in 2012 the incidence of musculoskeletal disorders was 22,864 people, including 2,160 cases of OA (hip and knee OA only), the increase rate per 100,000 population was 2% (Nogaeva, 2015). Increasing lifespan of people worldwide would make age-related diseases such as OA even more prevalent in the future.

Signs of OA onset may include pain, transient morning stiffness and crepitus on joint motion that lead to instability and physical disability, thus impairing quality of life. OA can be divided as primary and secondary depending on the cause of the disease emergence (Martel-Pelletier et al., 2016a). Primary OA, also called idiopathic, is diagnosed due to a combination of risk factors including ageing, obesity, knee malalignment, increased biomechanical loading of joints, genetics, and low-grade systemic inflammation. Whereas secondary OA results from trauma, surgery or abnormal joints at birth (Martel-Pelletier et al., 2016b). OA can be also divided in two subclasses based on the presence or absence of symptoms. Symptomatic OA indicates the presence of both radiographic OA and symptoms including pain or stiffness in the joint (T Neogi, 2013). Whereas patients with asymptomatic OA have classic radiographic features of OA, however, do not experience clinically relevant symptoms of the disease (Roos & Arden, 2016). Patients with asymptomatic OA are defined by the presence of bony enlargements (osteophytes) and the loss of cartilage in the radiographic findings (Fig. 1.3).
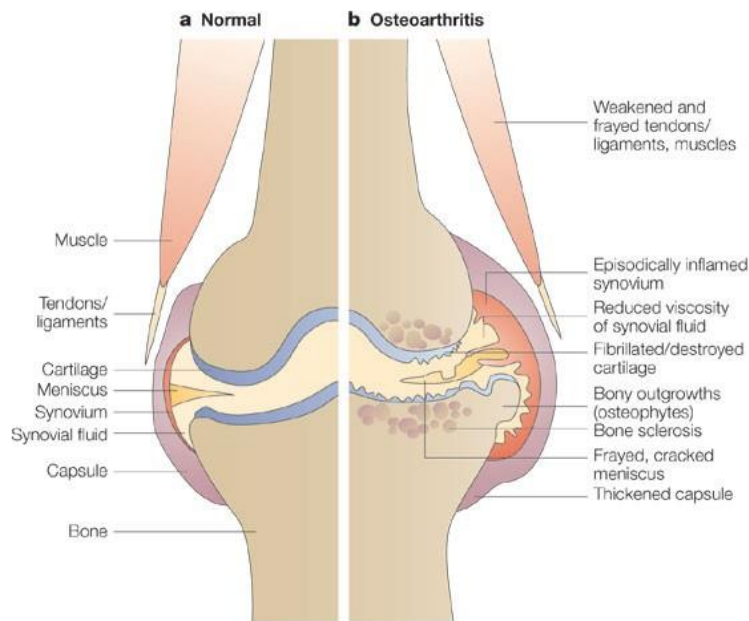
Nature Reviews | Drug Discovery

Figure 1.3 Normal and osteoarthritic synovial joint. In normal joint (a) no synovial inflammation and no cartilage degradation are present. During osteoarthritis (b) degenerative changes occur in the joint, including synovium inflammation, degradation of cartilage tissue, osteophyte outgrowth and thickened capsule. Figure copied from (Wieland et al., 2005). License number 5604681148967.

OA is commonly diagnosed based on the radiographic findings, with the Kellgren-Lawrence (KL) grading system usually applied (H & Lawrence, 1957). There are five grades of OA severity in the KL scoring system based on x-ray findings: grade 0 (normal), grade 1 (doubtful), grade 2 (minimal), grade 3 (moderate) and grade 4 (severe). This grading system is based on the presence or absence of various morphological features, such as formation of osteophytes, narrowing of the joint space, sclerosis of subchondral bone and altered shape of the bone ends (H & Lawrence, 1957).

1.5.1 OA risk factors and therapy

Ageing is the main factor of OA development, other factors include obesity, genetic predisposition and trauma (Bijlsma et al., 2011). Articular cartilage changes introduced by ageing were mentioned in the section 1.5, however it is evident that matrix degradation and chondrocyte senescence predispose cartilage to OA. Among the other risk factors obesity and being overweight are recognised as modifiable risk factor leading to OA (King et al., 2013). Obesity may increase the chances of OA development in the knee by up to seven times. The risk of knee OA is higher in patients with obesity

in comparison to patients with previous joint trauma (Coggon et al., 2001). Moreover, the additive effect of both trauma, definite Heberden's nodes and obesity brings the relative risk of knee OA from 24% to 78%. While it was shown that obesity results in higher chances of OA occurrence in the hip and knee, the latter group is by far the more susceptible to OA and subsequent surgical intervention in the knee are more frequent due to obesity (Liu et al., 2007).

The prevalence and incidence of knee OA is much higher in females in comparison to males, furthermore females older than 55 years tend to have more severe knee OA (Srikanth et al., 2005). Low serum levels of endogenous oestradiol, progesterone and testosterone in females are associated with increased knee effusion-synovitis and possibly other OA-related structural changes (Jin et al., 2017).

Genetics is considered as one of the factors contributing to OA. Genome-wide findings in the knee OA revealed single nucleotide polymorphisms in genes including collagen type VI alpha 4 pseudogene 1 (DVWA), Glycosyltransferase 8 domain-containing protein 1 (GLT8D1), HMG-Box Transcription Factor 1 (HBP1), Major Histocompatibility Complex Class II DQ Beta 1 (HLA-DQB1), alpha-ketoglutarate-dependent dioxygenase (FTO) (Warner & Valdes, 2017). However, candidate genes with variants linked to OA may demonstrate population-based predisposition, in which genetic predisposition of the variant is found in one population alone. Recently, a genome-wide association study on a UK biobank cohort identified two genetic loci in growth differentiation factor 5 (GDF5) and collagen type XXVII alpha 1 chain (COL27A1) had a strong association with OA (Meng et al., 2019). GDF5 and COL27A1 may play important roles during cartilage formation, suggesting that polymorphisms in these gene could have functional changes to the cartilage.

For weight-bearing joints such as knees, hips and ankles altered loading mechanisms, increased mechanical forces and changing biomechanics are significant contributing factors for initiation and progression of OA (Egloff et al., 2012). Other musculoskeletal tissues are involved in the OA. Knee ligament injuries decrease joint stability and, therefore, could be responsible for joint degeneration (Madry et al., 2016). Even after a successful anterior cruciate ligament (ACL) reconstruction the risk of OA development remains. Patients with ACL injury and meniscal tear are 2.5 times more likely to develop OA and 4 times more likely to undergo total knee arthoplasty (TKA) surgery than those without injury (Suter et al., 2017). Moreover, muscle weakness could be a risk factor for OA development. In early OA weakness of the quadriceps was previously established (Baert et al., 2013). Thus, OA is a disease of the whole joint, including muscles, tendons, ligaments, synovium and bone.

Currently there are no officially registered disease-modifying OA drugs available, and treatment of OA mostly focused on relief of symptoms such as pain, and at the end-stage OA total knee replacement (TKA) surgery is performed if possible. As previously mentioned obesity increases the

risk of OA onset, thus weight management has been demonstrated as a positive effect in lowering the risk of disease development (Bliddal et al., 2014). Moreover, weight loss can alleviate the symptoms of OA and prevent TKA in patients with obesity (body mass index > 25). Supervised exercise therapy has a positive effect on pain management and function of the joints, along with weight loss (Skou & Roos, 2019).

Medication used for symptomatic improvement in pain and joint function include paracetamol, nonsteroidal anti-inflammatory drugs (NSAIDs), opioid analgesics, and intra-articular medications such as steroids and hyaluronic acids (Oo et al., 2021). Since these drugs are mainly focused on pain relief they have no effect on disease progression. Thus, pain relief medications can be regarded as a temporarily solution with the risk of side-effects for long term use. Potential therapies for OA based on trials include colchicine, hydroxychlorquine, TNF inhibitors and injectable corticosteroids, although the trials for these drugs had no long term reduction in pain and no improvement in radiographic findings (Ghouri & Conaghan, 2019). Currently there are promising disease-modifying OA drugs undergoing trials in man including ADAMTS-5 inhibitors, fibroblast growth factor 18 (FGF-18), Wnt/b-catenin signalling pathway inhibitors and senolytic agents (Oo et al., 2021).

Patients with severe symptomatic knee OA may be presented with options for surgeries such as osteoctomy and TKA. TKA remains one of the most successful medical procedures to date for improving knee function and alleviate pain when nonoperative methods have been exhausted (Papas et al., 2019). TKA has high rate of patient satisfaction and implant durability is between 10-15 years. To ensure the patients get the most satisfactory outcomes after the surgery four predictive factors were set including Western Ontario and McMaster University OA Index score, comorbidities, number of joints affected and type of arthritis (rheumatoid arthritis or OA) (Gress et al., 2020). It was shown that patients with high levels of pain and a smaller number of joints affected had higher rates of positive outcomes following TKA. Following a five year assessment postoperative a quality of life satisfaction rate of 75% was reported (Canovas & Dagneaux, 2018). Despite the success of TKA complications such as polyethylene wear, aseptic loosening, infection, instability, and patellofemoral complications can result in the revision TKA surgery (Lum et al., 2018).

1.5.2 Macroscopic and microscopic changes in the articular cartilage during OA

Articular cartilage undergoes substantial changes that can be assessed on macroscopic and microscopic levels. One of the common scoring system applied for chondral lesions in the tissue is the Outerbridge classification (Killen & Charalambous, 2020). The Outerbridge classification was initially introduced as a simple grading system for chondromalacia patellae but has since been extrapolated and is now in use for joints throughout the body It grades lesions from 1 to 4 in order

of increasing severity according to their macroscopic appearance: grade 1 is characterised by softening and swelling; grade 2 lesion describes a partial-thickness defect with fissures that do not exceed 0.5 inches in diameter or reach subchondral bone; grade 3 is fissuring of the cartilage with a diameter > 0.5 inches with an area reaching subchondral bone; grade 4 includes erosion of the articular cartilage that exposes subchondral bone (Outerbridge, 1961; Slattery & Kweon, 2018).

Histological assessment of the articular cartilage is the main method used to identify structural and cellular differences in the tissue. The most widely used scoring systems for articular cartilage OA are Histological-Histochemical Grading System (HHGS) introduced by Mankin (Mankin et al., 1971) and the Osteoarthritis Research Society International (OARSI) scoring systems (Pritzker et al., 2006). The HHGS scores cartilage structure, cell distribution, Safranin-O staining and tidemark integrity as separate features, the sum of the separate scores ranges from 0 (normal) to 14 (severe OA) (Rutgers et al., 2010). However, limitations in this grading system were reported including difficulties of separating early and mild OA phases; no staging presented to account for variation of cartilage quality within the same section. Additionally the inter- and intra-observer variability of this system has repeatedly been described to be high (Custers et al., 2007).

The OARSI system assesses the severity and the extent of cartilage surface involvement in the local OA process. In contrast to the HHGS and most other OA scores, the OARSI system emphasises the extent of cartilage damage over the articular surface through a 'stage' component, in addition to damage analysed at several levels of the cartilage layers (Rutgers et al., 2010). However, histological scoring is not limited to the above-mentioned systems, there are at least eight other scoring systems for OA cartilage. In addition other scoring systems are available for *in vivo* cartilage repair scores and *in vitro* tissue engineering scoring (Rutgers et al., 2010).

1.5.3 Molecular changes in the articular cartilage during OA

OA development in the articular cartilage results in tissue degeneration initiated by the dysregulation of the molecular mechanisms. In normal cartilage the balance between anabolic and catabolic processes are closely regulated to maintain the turnover of ECM. During the OA progression of catabolic processes outweigh the anabolic properties leading to further degradation of cartilage tissue (Goldring & Marcu, 2009). Moreover, anabolic reaction of chondrocytes to restore the matrix produces mostly fibrous cartilage, in which mechanical capacities are different compared to healthy hyaline cartilage (Lorenz & Richter, 2006). Catabolic processes including matrix metalloproteases

21

(MMP) synthesis is increased and their inhibitors are decreased by inflammatory cytokines such as interleukin (IL)-1, IL-17 and IL-18 and TNF-α (Lorenz & Richter, 2006) (Fig. 1.4). IL-1β expression is found in normal articular cartilage and may play a role in matrix turnover, however, increase in IL-1β within the cartilage tissue in addition to its diffusion from the synovial fluid could result in tissue degradation (Fan et al., 2007). Increase of IL-1β is linked to the upregulation of cyclooxygenase-2 (COX2), MMP13 and nitric oxide synthase (NOS2) gene expression, along with the suppression of cartilage specific proteins including COL2A1 synthesis (Goldring & Marcu, 2009). Subsequently, upregulation of catabolic COX2, NOS2 and MMP13 genes lead to proteoglycan loss and deterioration of matrix structure. IL-6 has both pro-inflammatory and anti-inflammatory properties, which is regulated via soluble IL-6 receptor (IL-6R) and membrane bound IL-6R respectively (Scheller et al., 2011). In chondrocytes lower amounts of membrane-bound IL-6R are found in comparison to other cell types, suggesting they are more susceptible undergoing the pro-inflammatory pathway via soluble IL-6R (Porée et al., 2008). Pro-inflammatory IL-6 and IL-6R can repress COL2A1 transcription by affecting the promoter region of that gene. Therefore, increased levels of IL-6 can deteriorate cartilage matrix structure during OA. TNF-α is another pro-inflammatory cytokine involved in OA pathogenesis, TNF-α promotes the secretion of MMPs by synovial fibroblasts resulting in degradation of the cartilage matrix (Chisari et al., 2020). Furthermore, chondrogenesis can be inhibited by TNF-α through the nuclear factor-κb (NF-κb) pathway and downregulation of SRY-Box Transcription Factor 9 (SOX9). Inhibition of TNF-α demonstrated chondroprotective effect, stimulated chondrogenesis and restored osteochondral lesions (Chisari et al., 2020).
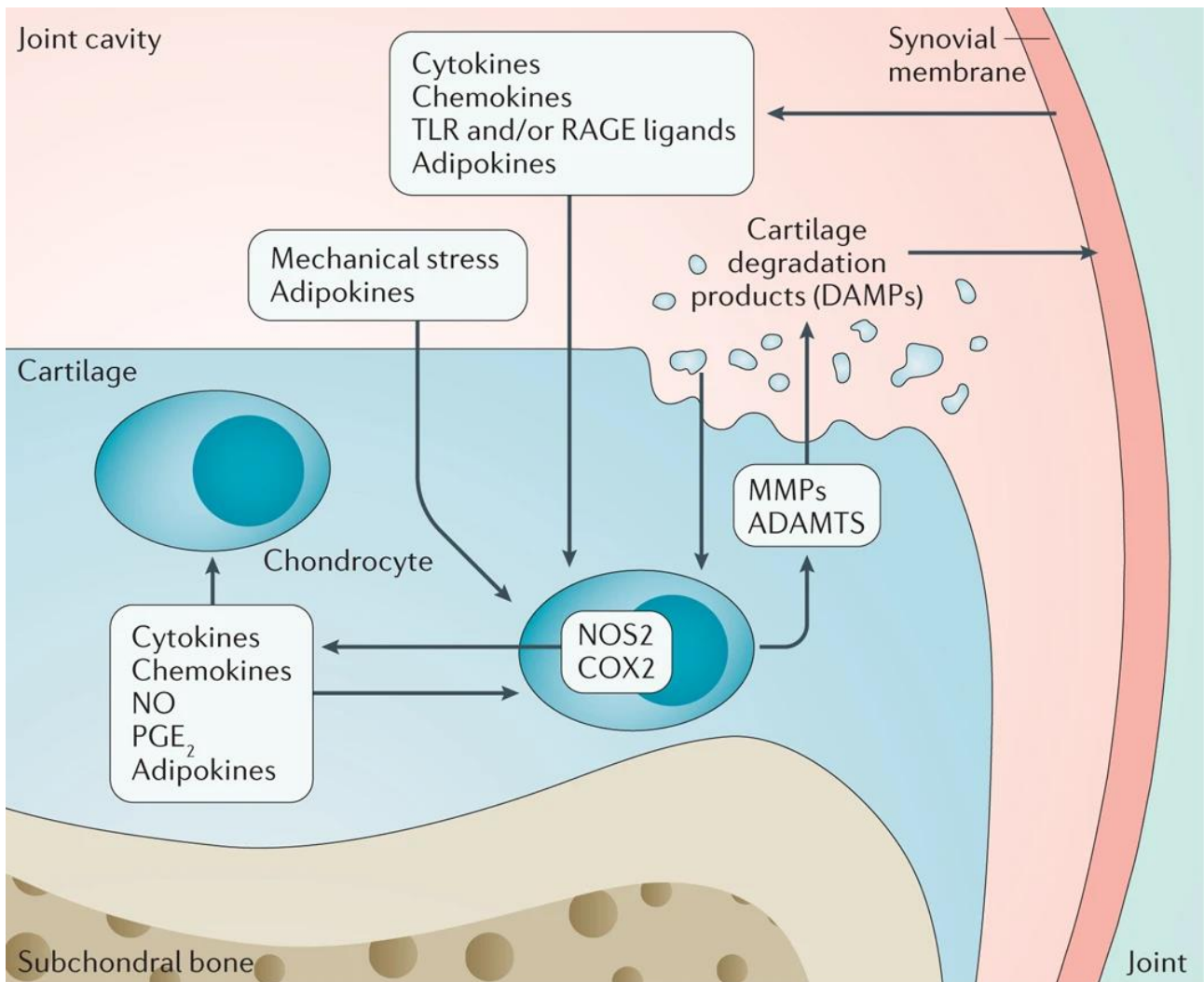
Figure 1.4: Molecular changes in the articular cartilage during OA. Copied from (Martel-Pelletier et al., 2016b). License 5155911413674 .

Several signalling pathways are involved directly in cartilage homeostasis and the development of OA including NF-κB, Wnt signalling, PI3K/AKT/mTOR, and Rhoa/Rock pathways. NF-κb pathway includes a family of transcription factors that play critical role in the immunity, inflammation, cell growth and apoptosis. NF-κB pathway can regulate transcription of various genes including cytokines, cell adhesion molecules, stress response genes and growth factors. There are two types of the pathway: canonical and non-canonical NF-κB pathways, which differ in signalling mechanisms and biological functions (Gilmore, 2006). The canonical NF-κB signalling mechanism is initiated by ligand binding to the TNF-receptor (TNF-R) or a Toll-like receptor (Hayden & Ghosh, 2008). This can in sequence recruit TRAF/RIP adapter proteins, which together with MAP3-kinase TGF-β-activated kinase 1 (TAK1) recruit IKK complex. IKK complex in canonical NF-κB pathways consists of two kinase subunits IKKa and IKKb, and a regulatory subunit NEMO. IKK kinases phosphorylate IkBa and IκB-like molecule p105 prompting their degradation and releasing NF-κB dimers into the nucleus. It results in binding of these canonical NF-kB dimers (p50/RELA, p50/c-REL and p50/50)

to the enhancers of target genes and inducing their expression (Hayden & Ghosh, 2008). In comparison to the canonical NF-κB pathway ligand binding to TNF-Rs (e.g. LTBR) can initiate the non-canonical NF-κB signalling (Sun, 2011). This in turn recruits TRAF adapter protein followed by the activation of NIK. NIK subsequently phosphorylates the IKKa dimer that is needed for the induction of p100 processing to p52. Finally, nuclear translocation of NF-κB dimer p52/RELB leads to the expression non-canonical NF-κB target genes. The activation of NF-κb is positively correlated with cartilage destruction, while member of non-canonical NF-κB pathway TAK1 have been implicated in OA pathogenesis (Choi et al., 2019). Moreover, excessive mechanical loading and inflammatory cytokines such as IL-1b and TNF-a can activate NF-κb leading to the upregulation of catabolic markers including MMP13 in the cartilage.

The Wnt signalling pathway is involved in the regulation of cell fate determination, motility, polarity, primary axis formation and organogenesis (Komiya & Habas, 2008). The Wnt signaling pathway plays an important role in the development and maintenance of articular cartilage. This pathway is a complex network of proteins and signaling molecules that are involved in various cellular processes such as proliferation, differentiation, and cell survival. The Wnt pathway has been shown to regulate the production and maintenance of the ECM in articular cartilage, which is essential for the proper function of this tissue. In particular, the Wnt pathway has been implicated in the regulation of chondrocyte differentiation and maturation, which are important processes for the development and maintenance of articular cartilage. Several studies have demonstrated that activation of the Wnt pathway can promote chondrocyte differentiation and enhance the production of ECM proteins such as type II collagen and aggrecan (Blaney Davidson et al., 2006; Dell'accio et al., 2008). However, aberrant activation of the Wnt pathway has also been associated with the development of osteoarthritis (OA), a common degenerative joint disease characterised by the breakdown of articular cartilage. In OA, the Wnt pathway is often activated, leading to the excessive production of catabolic enzymes and pro-inflammatory cytokines that contribute to cartilage degradation (Dell'accio et al., 2008).

1.6 Mass-spectrometry based proteomics as a tool to study OA in the articular cartilages

Proteomics based on mass spectrometry is a powerful tool for investigating the molecular mechanisms underlying OA in articular cartilage. This technique allows for a thorough examination of cartilage protein composition, providing insights into the changes in protein expression, post-translational modifications, and protein-protein interactions that occur as OA progresses.

Several studies have investigated OA in articular cartilage using mass spectrometry-based proteomics. One study, for example, examined the mitochondrial proteome of OA human articular chondrocytes and discovered changes in oxidative phosphorylation and antioxidant defence pathways (Ruiz-Romero et al., 2009). Another study used proteomics to identify proteins that were differentially expressed in OA cartilage versus healthy cartilage and discovered that proteins involved in ECM remodeling and cell signaling were upregulated in OA cartilage (Collins et al., 2018). Furthermore, mass spectrometry-based proteomics has been used to investigate the role of post-translational modifications in OA cartilage. One study discovered that protein carbamylation, a modification linked to inflammation and oxidative stress, was higher in OA cartilage than in healthy cartilage (Wu et al., 2019). All of the above show that proteomics has provided important insights into the molecular mechanisms underlying OA in articular cartilage.

1.7 The use of RNA-seq based transcriptomics in articular cartilage molecular mechanisms

Transcriptomics based on RNA sequencing (RNA-seq) is a powerful tool for studying the molecular mechanisms underlying articular cartilage homeostasis and disease. This technique identifies and quantifies transcripts expressed in articular cartilage, providing insights into gene expression regulation and the signaling pathways involved in cartilage development, maintenance, and disease progression. RNA-seq-based transcriptomics has been used in several studies to investigate the molecular mechanisms of articular cartilage. For instance, to compare the gene expression profiles of healthy human articular cartilage and cartilage from OA patients. The study using this approach discovered differences in the expression of genes involved in ECM organization, inflammation, and oxidative stress (Wu et al., 2017). Another study looked at the transcriptomic changes that occurred during chondrogenesis, or the formation of cartilage during embryonic development, and identified key signaling pathways involved in chondrocyte differentiation (Takahashi et al., 2018).

Transcriptomics based on RNA-seq has also been used to investigate the role of non-coding RNAs in articular cartilage. Swärd et al. (2013) discovered that differentially expressed microRNAs (miRNAs) in OA cartilage compared to healthy cartilage regulate key signaling pathways involved in cartilage homeostasis. In conclusion, RNA-seq based approach can be employed to study the molecular mechanisms in the articular cartilage during the development and disease. It could be also used to identify novel biomarkers for early diagnosis and targeted therapeutics.

This thesis hypothesises that articular cartilage undergoes distinctive molecular changes at protein and gene expression level during osteoarthritis and ageing in the different zones of the tissue. The following aims were set to test the hypothesis:

1.   Establish differentially abundant proteins in the superficial, middle and deep zones of articular cartilage during osteoarthritis and ageing using liquid chromatography-tandem mass spectrometry.

2.   Identify differentially expressed genes in the superficial, middle and deep zones of articular cartilage during osteoarthritis and ageing using RNA sequencing.

3.   Establish differentially abundant proteins in the chondrocytes extracted from superficial and deep zones of articular cartilage from young and old OA donors using liquid chromatography-tandem mass spectrometry.

CHAPTER 2

Articular cartilage proteome during osteoarthritis and ageing

2.1 INTRODUCTION

Articular cartilage is deprived of blood vessel and nerves, and the only cells residing in this tissue are chondrocytes. The molecular properties of the articular cartilage and the architecture of the extracellular matrix (ECM) demonstrate a complex structure that differentiate on the depth of tissue. Articular cartilage biology is well studied with the focus on the musculoskeletal diseases and cartilage development. However, there are relatively few studies on cartilage ageing. Published mass spectrometry studies on cartilage proteomics are reviewed here.

Early cartilage proteomic studies mostly used 1D and 2D SDS-PAGE (2DE) gels separate samples prior to mass-spectrometry MS analysis. Garcia *et al.* used articular cartilage samples from patients undergoing total knee replacement surgeries. Cartilage samples were digested using liberase enzyme and cells removed using centrifugation. ECM extracts were run on 1D-SDS-PAGE and cut into eight equal pieces, each sample was run for 1h on liquid chromatography-tandem mass spectrometry (LC-MS/MS). In this study over 100 proteins were identified, the majority were ECM proteins (35%). Among the biological processes the proteins were involved in were signal transduction and cell communication (14%), immune response (11%). Metabolism and energy pathways (11%) were also identified (Garcia et al., 2006) .

Hermansson *et al.* used [35S] methionine/cysteine to radiolabel newly synthesized proteins in cartilage explants and identified the proteins using 2-DE followed by MS/MS. Among the identified proteins were matrix proteins including Cartilage Intermediate Layer Protein (CILP), Chondroadherin (CHAD), Clusterin (CLU), Collagen Type II Alpha 1 Chain (COL2A1), Collagen VI, Collagen Type XI, Cartilage Oligomeric Matrix Protein (COMP), Secreted Protein Acidic and Rich in Cysteine (SPARC), Chitinase-3-like Protein 2 (YLK-39), Lumican (LUM) proteinases and inhibitors Matrix Metalloproteinases 1 and 2 (MMP1, MMP2), Tissue Inhibitor of Metalloproteinases 1 and 2 (TIMP1, TIMP2); regulatory molecules Connective Tissue Growth Factor (CTGF), Cytokine-Like 1 (CYTL1), Inhibin bA (INHBA). The authors demonstrated that collagen type 2 synthesis was upregulated in OA samples in comparison to the normal group. Moreover, pro-INHBA was detected in all of the samples, whereas in the normal group it was found only in half of the samples (Hermansson et al., 2004) . De Ceuninck *et al.* demonstrated similar findings however, only two osteoarthritic cartilage samples were used in their study. Among the 43 identified secreted proteins were LUM, vimentin (VIM), Thrombospondin 3 (TSP3), Cartilage Oligomeric Matrix Protein (COMP), CLU, mimecan (MIME), MMP1, MMP2, TIMP1 and YLK-39 (De Ceuninck et al., 2005).

To demonstrate the advantage of depleting protein extracts of proteoglycans and collagens to improve 2-DE Vincourt *et al.* used 2-DE separation of extracted proteins from the articular cartilage followed by Matrix-Assisted Laser Desorption/Ionization Time-of-Flight (MALDI-TOF) for protein identification. Minor protein identification could be obscured in the crude protein sample, moreover,

abundant collagen species and proteoglycans strongly reduced the isoelectric focusing during 2-DE. In this study more than 600 protein spot were observed of which 200 spots were subject to MALDI-TOF, resulting in the identification of 127 proteins. The limitation of this study was it only utilised six donors, and cartilage samples were taken from the different parts of multiple joints (hip, knee and tallus). Thus, comparative proteomics was not possible in this study (Vincourt et al., 2006) .

In another study cartilage taken from donors with no history of OA were studied. Proteoglycans, mostly aggrecan, were depleted using caesium chloride gradient ultracentrifugation. Samples were run using SDS-PAGE and bands excised followed by in-gel trypsin digestion. In total 814 proteins were identified of which 59 proteins were significantly differentially abundant in the OA group when compared to the control group. High-Temperature Requirement Protein A1 (HTRA1), TIMP2, MMP2, cystatine-C and Serpin Family A Member 5 (SERPINA5) were highly abundant in the OA group. Moreover, plasma proteins Apo A-I, II, IV, and Apo H, and fibulin protein group were upregulated compared to control samples (Wu et al., 2007).

Furthermore, 2-DE and LC-MS/MS were also used to identify differentially abundant proteins in cartilage during OA. Articular cartilage from three donors with osteoarthritis and three donors without history of OA were used for this study. After the separation of proteins using 2-DE 16 differentially abundant spots were excised and subject to protein identification using LC-MS/MS. 14 proteins were identified, six upregulated in the OA group: Alpha-Enolase (ENOA), Pyruvate Kinase Muscle (KPYM) , Alcohol Dehydrogenase (ADH), Collgen type 1 (COL1A1), Collagen type 6 (COL6A1) and Responsive Factor (RF); and eight downregulated: Annexin A1 (ANXA1), Peroxiredoxin 3 (PRDX3), Zinc Responsive Factor (Zn-RF), Folate Receptor (FR), Tubulin (TUB), Adenosine Kinase (ADK), Phosphatidylethanolamine-Binding Protein (PEBP) and Superoxide Dismutase Mitochondrial (SODM) (Guo et al., 2008).

Perez *et al.* used articular cartilage from Wistar rats with OA induced by partial menisectomy to investigate the cartilage proteome. Protein extracts were proteoglycan depleted prior to 2-DE. 147 protein spots were resolved of which 47 proteins were identified using MS/MS. These were involved in the following biological functions: cellular metabolic processes (32%), structural organisation (19%), signal transduction and molecular signalling (11%), redox homeostasis (9%), transcription and protein synthesis (6%), and transport (6%). Latexin (LXN) protein was validated using immunohistochemistry (IHC). Results revealed the presence of LXN in the middle, deep and calcified zones of articular cartilage in normal rats, and a similar abundance in the superficial and deep zones in the OA group (Pérez et al., 2010).

Many proteinases are activated in OA cartilage leading to matrix destruction. Zhen *et al.* used articular cartilage samples from two donors to identify peptides cleaved by exogenous metalloproteinases and aggrecanases. Peptides from the digested tissue samples were subjected to

LC-MS/MS. Results included cleaved peptides derived from Collagen types 1, 2 and 3, Proteoglycan 4 (PRG4), COMP, Cartilage intermediate layer proteins 1 and 2 (CILP1, CILP2), Byglican (BGN), MIME, LUM, ACAN, CLU and Decorin (DCN) (Zhen et al., 2008).

Label-free based proteomics enables differential expression of non-labelled peptides. Comparative protein quantification was performed based on the peak intensity of the peptides. Dudek *et al.* used mouse hip articular cartilage to identify proteins changing with the circadian rhythm. Samples were collected at different time points over 48h. Proteins were extracted using guanidine hydrochloride (GuHCL) and identified using LC-MS/MS. In total 1777 proteins were identified of which 14 were found as rhythmic proteins (p <0.05). During the active phase HSP90AA1, HSP90AB1, Matrilin 1, Serpine 1 and Procollagen-Lysine, 2-Oxoglutarate 5 (PLOD2) proteins demonstrated a high abundance. In the early resting period Proteasome Subunit Beta 7 (PSMB7), Proteasome 26S Subunit non-ATPase 2 (PSMD2), Proteasome 26S Subunit (PSMD) proteins were abundant, while in the mid-resting period ribosomal proteins Ribosomal Protein L5 (RPL5), Ribosomal Protein L23a (RPL23a) and Ribosomal Protein S3a1 (RPS3a1) peaked. Proteins responsible for mRNA processing and ribosomal proteins had increased abundance in the afternoon (late rest phase). Proteins related to ATP synthesis peaked in the evening (early active phase) and glucose metabolism proteins were overexpressed late at night (late active phase). Proteins associated with the cytoskeleton peaked in the morning (early resting phase) (Dudek et al., 2021) .

Peffers *et al.* studied the spatial proteome of articular cartilage using OA, aged and young horses. Proteins from the cartilage samples were identified and spatially resolved using MALDI-MSI method. Authors identified Aggrecan (ACAN), BGN, CILP2, COMP, CHAD, COL2A1, Chloride Channel Accessory 1 (CL-43), Fibromodulin (FMOD), Fibronectin 1 (FN1), Hemoglobin Subunit Alpha (HBBA), Matrilin 3 (MATN3) and Melanoma Inhibitory Activity 3 (MIA3) proteins. COMP and FMOD were more abundant in the old group in comparison to the young and OA groups. Furthermore BGN had the lowest abundance in the OA group in comparison to the young and old groups, and FN1 was more abundant in OA (Peffers et al., 2014) . In a similar study Cillero-Pastor *et al.* studied the proteome of the human articular cartilage from the knee joint using MALDI-MSI; 10 control samples without a history of OA (control group) and 10 age matched OA cartilage samples. Among the identified proteins were ACAN, BGN, DCN, Proline/arginine-rich end leucine-rich repeat protein (PRELP), CILP1, COMP, Collagen type 2, FMOD. COMP and FN1 were highly abundant in OA group in comparison to control (Cillero-Pastor et al., 2013).

Hao *et al.* used a papain induced OA rat model to assess the proteome of articular cartilage.. Label-free LC-MS/MS analysis showed that 62 proteins were significantly abundant in the OA group and 208 proteins were more abundant in the control group. MAPK signalling pathway regulation

proteins and nuclear-transcribed mRNA catabolic process proteins were downregulated in OA group (Hao et al., 2021).

Label-based and targeted proteomics have also been used to examine the OA cartilage proteome. SILAC technology was used to label newly synthesised proteins that were secreted into media by articular cartilage. Cartilage samples from three donors with OA were used in this study. Among the labelled proteins identified were Serpin Family A Member 1 (SERPINA1), Apolipoprotein D (APOD), Chitinase 3-Like 1 (CH3L1), CLUS, Collagen type 3, FN1, TIMP1, Pentraxin 3 (PTX3), PRG4, Secreted Protein Acidic And Cysteine Rich (SPARC) and MMP3. Notably, Annexin A1, A2 and A5 (ANXA1, ANXA2, ANXA5), SPARC-Related Modular Calcium Binding Protein 2 (SMOC2), LUM, MIME, CHAD, COMP, CILP1, CILP2 and Apolipoprotein L Domain Containing 6 (APSC) were identified as unlabelled by 13C6, meaning they were not newly synthesised (Polacek et al., 2010).

Önnerfjord *et al*. investigated cartilage samples from multiple sites including femoral head, humerus head, tibial knee, meniscus, vertebral disk, rib and trachea. Proteins were extracted from the tissue using GuHCl and samples were labelled by isobaric tags for relative and absolute quantitation (iTRAQ) for relative quantification of proteins using LC-MS/MS. The proteins identified varied on the tissue source and ranged between 120-190 proteins. Aggrecan was found highly abundant in the femoral head, and other tissues showed similar levels except meniscus, which had less aggrecan expression. Meanwhile, PRG4 was highly abundant in the vertebral disk compared to other tissue samples and Asporin (ASPN) was abundant in the meniscus and MATN1 in the rib and trachea. In pairwise comparisons of femoral head and tibial knee cartilage it was found that LP, CHAD and SMOC2 were more abundant in the femoral head and tibial knee had increased abundance of Collagen type 6 (aI, aII, aIII), SERPINA1, Superoxide Dismutase 3 (SOD3), MIME, LUM, ASPN and Collagen type 2 in comparison to femoral head samples (Önnerfjord et al., 2012).

A number of studies have investigated the proteome of the different zones within articular cartilage. Müller *et al*. used lateral tibial plateau and medial tibial plateau articular cartilage in a targeted proteomics study. One cartilage sample taken from lateral tibial plateau was used to identify proteins in the ECM of the articular cartilage in different zones. The sample was iTRAQ labelled for LC-MS/MS proteomics, finding 277 proteins. From these identified proteins there were 70 proteins selected for targeted Multiple reaction monitoring (MRM) approach, where four medial tibial plateu cartilage samples at different depth were used. Donors for targeted proteomics study had no history of joint disease and were aged in range of 36-65 years old. Cartilage sections were cryosectioned from the surface to the calcified zone, ten sections at 10um thickness were pooled together until the calcified zone was reached. Most of the proteins showed similar patterns of distribution across the zones in four medial tibial plateu samples, except COMP, BGN, FN1 and Versican (VCAN). In the

superficial zone of the cartilage the following proteins were found to be abundant ASPN, Tenascin C (TNC), Collagen type 6, Dermatopontin (DPT), Thrombospondin 4 (THBS4) and Perlican (PERL). MIME and Thrombospondin 1 (THBS1) were the only proteins found abundant in the middle zone. In the deep zone of articular cartilage ACAN, Osteomodulin (OMD), CHAD, Matrix Gla protein (MGP), MATN3, SPARC and HTRA1 proteins were more abundant. Among the proteins that showed even distribution across the zones were PRELP, FMOD, DCN and LUM (Müller et al., 2014).

In another study investigating the cartilage layers Hsueh *et al.* used targeted MRM proteomics to differentiate the proteome of hip and knee articular cartilage in the different zones in healthy and OA donors. Moreover, samples were collected from territorial and interterritorial regions of the cartilage using laser microdissection. Cartilage tissue samples were decellularized prior LMD in order to study ECM proteins only. Tissue samples were taken from four donors: 56-year-old female with knee OA, 64-year-old female with hip end-stage OA, 48-year-old female with acute knee trauma surgery, 35-year-old male with hip trauma surgery. Authors identified 30 proteins of which 12 showed a difference based on joint type including CHAD, CILP1, CILP2, COBA2, COMP, HPLN1, HTRA1, MATN3, MGP, ACAN, THBS1, THBS4, Collagen type 3-neo. A subsequent comparison by the disease state revealed a difference in abundance of CHAD, COMP, MGP, Collagen type 3-neo proteins. Whereas, zonal comparison demonstrated changes in abundance of CILP1, COMP, DPT, FN1, HTRA1, ACAN. Furthermore, MIME demonstrated higher abundance in the superficial zone in comparison to other zones and was more abundant in the knee joint in comparison to hip, though not after adjustment for multiple comparisons (M.-F. Hsueh et al., 2017).

Hosseininia *et al* used targeted proteomics to identify differences in proteome between OA and fractured hip articular cartilage, samples were full thickness and macroscopically intact. There were five donors in the OA group (50-80 years old) and seven in the control group (53-94 years old); all of the donors were women. Authors used 74 optimized single reaction monitoring (SRM) assays that represented 35 proteins. Seven out of 35 proteins were highly abundant in OA group in comparison to non-OA group, including ASPN, MIME, MATN3, CILP2, collagens VI, III, II (Hosseininia et al., 2019).

Qiu *et al.* used nucleus pulposus to identify age-related protein changes using Tandem Mas Tag (TMT) and Parallel reaction monitoring (PRM). In total 3259 proteins were identified of which 2691 were quantified. 11 proteins were selected for PRM validation Inteleukin-11 (IL11), CLU, Tumor necrosis factor alpha-induced protein 6 (TNFAIP6), Matrix-remodeling associated protein 5 (MXRA5), Extracellular Matrix Protein 1 (ECM1), Serpin Family E Member 1 (SERPINE1), Platelet-Derived Growth Factor C (PDGFC) were upregulated in the geriatric group, whereas Heat Shock Protein Family A Member 8 (HSPA8), MATN3 and Suppression of Tumorigenicity 13 (ST13) were downregulated (Qiu et al., 2020).

Li *et al.* used TMT label-based proteomics to study the proteome of post-traumatic OA articular cartilage in a mini-pig model. 2950 proteins were identified and 491 were differentially abundant. Proteins found to be differentially abundant in the OA cartilage group included those belonging to the cytochrome complexes, intermediate filaments, endosomal sorting complexes required for transport-III complexes, intermediate filament cytoskeleton, anchoring junctions, RAS signalling pathway and oxidative phosphorylation (Pengcui Li et al., 2020).

In another TMT label-based proteomics approach the difference between OA and Kashin-Beck disease (KBD) cartilage was studied. Despite some similarities in the ECM degradation, disruption of proteoglycans and collagens between these diseases, each had unique protein patterns. There were identified 375 proteins differentially abundant between OA and KBD. These proteins were involved in ECM - receptor interaction, focal adhesion, phosphatidylinositol 3-kinase (PI3K)-Protein kinase B (Akt), RAS signalling pathways and integrins, laminins, NF-κB (Lei et al., 2020).

Mild and moderate cartilage degeneration proteomic differences were identified in adjacent intact cartilage areas in bovine articular. Authors employed iTRAQ label-based proteomics identifying 196 proteins. Between the adjacent intact control samples significant difference were found in Collagen type 9, Osteoglycin (OGN) and C-type lectin domain family 3-member B (CLEC3B). Cartilage areas with mild degeneration showed a higher abundance of Transforming growth factor beta 1 (TGFB1), THBS1, Gelsolin (GSN), Collagen type 6(a1, a2, a3), FMOD, TNC, ANXA2 in comparison to the adjacent intact areas. ACAN, COMP, CILP, WAP Four-Disulfide Core Domain 18 (WFDC18), Lysozyme 1 (LYZ1) and Complement C4A (C4A) showed altered abundance in the intact area in comparison to the mild degeneration area. Areas with moderate degeneration had a higher abundance of MB and TGFB1 proteins and lower abundance of ACAN, C4A, LYZ1 proteins in comparison to the intact areas. Validation was undertaken using MRM targeted proteomics and also identified differences in ACAN, LYZ1 and C4A. Moreover, VIM and GSTP1 was highly abundant in the intact area in comparison to the moderate degenerated cartilage (Jacob et al., 2021).

All of the above studies used Data-dependent acquisition (DDA) in which mass spectrometer selects the most intense peptide ions, which are fragmented and analysed. Data independent acquisition (DIA) selects precursor ions in an isolation window that is set and fragments all the ions. This enables increased precision and reproducibility in comparison to DDA (Collins, et al., 2013). In a recent study Folkesson *et al.* used femoral condyle cartilage and meniscus from three donors without a history of joint disease to differentiate the proteome between the tissue types using DDA and DIA mass spectrometry methods. DDA analysis identified 673 proteins, of which 358 proteins had at least two unique peptides. Meniscus and articular cartilage showed substantial overlap in identified proteins, with only 11 (COL11a1 and a2, MATN3, HTRA3) proteins unique for articular cartilage and 40 proteins (COL4a1 and a2, HMGB1, NID2) only found in meniscus. DDA analysis revealed

four differentially abundant proteins, while DIA method found 19 proteins differentially abundant. The top 10 proteins with the highest intensity in the DDA analysis in the articular cartilage were ACAN, COMP, DCN, ALB, PRELP, FN1, FMOD, BGN, CILP1 and MIME (Elin Folkesson et al., 2018).

In a different study Folkesson *et al.* also employed DIA method to compare the proteomes of medial and lateral menisci of OA donors (n=10) to control group (n=10). 835 proteins were identified; HBA and some other plasma proteins were found to be abundant in the OA medial and lateral menisci samples. Following pathway analysis, activation of LXR/RXR pathway was increased in the medial OA group. MMP3 and TIMP1 were found to be upregulated in the OA menisci in comparison to the control group (E Folkesson et al., 2020).

All of the above studies demonstrated the results of cartilage proteome to provide greater understanding of the tissue and changes during the disease. Cartilage proteomics could also aid in the early detection of cartilage-related diseases such as OA and to help identify novel biomarkers. New diagnostic and prognostic tools can be developed with the help of the identification of proteins or peptides that are differentially expressed in diseased versus healthy cartilage.

Understanding the molecular mechanisms of cartilage formation and disease progression can be aided by proteomics research. This knowledge can be used to create more effective treatments and preventative measures for conditions affecting cartilage. Proteomics techniques are high-throughput because they permit the analysis of hundreds or thousands of proteins at once in a single experiment. When compared to conventional biochemical techniques, this high-throughput method can be more efficient and cost-effective. Understanding the development of diseases affecting cartilage and locating therapeutic targets can benefit from this data.

In this study we hypothesised that there would be protein differences identified in ageing and OA between the three layers of human cartilage using mass spectrometry proteomics.

2.2 MATERIALS AND METHODS

2.2.1 Human articular cartilage specimens

Osteoarthritic articular cartilage specimens were collected from patients undergoing total knee replacement. Samples were provided on the same day of surgery by Liverpool Musculoskeletal Biobank under Health Research Authority approval (Sponsor Ref:UoL001398) and Clatterbridge Hospital, Wirral following ethical approval (IRAS ID 242434). Normal articular cartilage from knee joints of donors with no history of OA were purchased from Proteogenex Inc. Donors of cartilage samples for LC-MS/MS proteomics were all males. Mean age of young group was 32 years old (26-35), old group 71.6 years old (67-75) and OA group 76.4 years old (69-85), each group had n=5 of donors. OA cartilage samples were placed into saline following surgery, and kept at 4°C. All the reagents used in the experimental work from Sigma-Aldrich (Dorset, UK) unless stated otherwise. A section of full thickness cartilage was cut from the femoral condyles and immersed into isopentane and snap frozen in the liquid nitrogen. Normal articular cartilage samples were obtained from cadavers and were immediately flash frozen in the liquid nitrogen. All of the samples were kept at 80°C and handled on dry-ice.

2.2.2 Equine cartilage collection

Articular cartilage was taken from the metacarpophalangeal joints of horses. Firstly, the area of the joint was de-skinned and cleaned afterwards with 70% ethanol. The joint was opened using a scalpel while the third metacarpal bone was clamped. Using a sterile scalpel full thickness articular cartilage samples were taken from the margins of the third metacarpal part of the joint (Fig. 2.1). Samples were transferred on dry ice and kept at -80°C afterwards.

Figure 2.1: Metacarpophalangeal joint of a horse. Dashed rectangles indicate the areas where cartilage samples were taken from.

2.2.3 Cryosectioning of articular cartilage

Frozen cartilage samples were processed using a cryostat CM1900 (Leica Biosystems, Milton Keynes, UK). Cartilage specimens were placed onto optimal cutting temperature (OCT) compound (ThermoFisher Scientific, Paisley, UK) in the cryostat, chamber and temperature was set to -21°C and the specimen holder at -24°C. Full thickness cartilage was cut in coronal plane at 20μm thickness. Cryosections used for laser microdissection (LMD) were collected onto polyethylene terephthalate (PET) membrane (1.4μm) slides (Leica Microsystems, Wetzlar, Germany). Cryosections were collected the day before laser microdissection and stored in 50ml falcons at -80°C. Cryosections for haematoxylin and eosin staining (H&E) were collected onto Superfrost Plus™ glass slides (ThermoFisher Scientific, Paisley, UK) and stained immediately.

2.2.4 Haematoxylin and eosin staining

Cartilage cryosections were stained with H&E manually. Firstly, cryosections were submerged into 70% ethanol (Fisher Scientific, Loughborough, UK) for 30sec, followed by brief immersion into tap water. Afterwards sections were stained with Harris haemotoxylin for 30sec and briefly washed with tap water. Then sections were placed into 1% acid alcohol (Leica Biosystems, Milton Keynes, UK) for 5sec and immediately counter stained with alcoholic eosin (Leica Biosystems, Milton Keynes, UK) for 10sec. Sections were then dehydrated with 90% ethanol for 30sec and two steps of 100% ethanol 30sec, followed by two steps of xylene (Fisher Scientific, Loughborough, UK) for 2min

each. Sections were covered with mounting media (Fisher Scientific, Loughborough, UK) and coverslips. Slides were air-dried in the fume hood overnight prior imaging.

2.2.5 Laser microdissection of cartilage zones

Different zones of the cartilage were microdissected using a LMD7000 (Leica Microsystems, Wetzlar, Germany) laser microdissection microscope. Slides with cryosections were kept on dry-ice and before loading to the specimen holder tray sections were dehydrated with 50%, 70% and 100% ethanol for 30 seconds each. Slides were air-dried and loaded onto the microscope stage. 0.5ml flat head tubes were placed into the collection tray and 40μl of freshly prepared 25mM ammonium bicarbonate (AmBic) (Sigma-Aldrich, Dorset, UK) was pipetted into the tube's cap. A collection tray was located under the specimen holding tray where the membrane slides were placed. During LMD the microdissected tissue specimen fell by gravity into the solution. LMD was carried out using the following laser parameters: Power – 50, Aperture – 29, Speed – 8, Specimen balance – 17, Head current – 100, Pulse – 228. The objective was set to 10x magnification and the same area was collected for each zone. For the superficial zone 5μm^2 total area was collected and for the middle and deep zones it was 25μm^2. After collecting all three zones tubes with samples were placed bottom-up on dry ice. Samples were stored at -80C until the sample preparation step for mass spectrometry.

2.2.6 Sample preparation for mass spectrometry proteomics

Samples were removed from the -80°C freezer and 50μl 0.1%(w/v) Rapigest SF Surfactant (Waters, Herts, UK) (freshly prepared in 25mM ammonium bicarbonate (ambic)) was added to the bottom of the upright tubes and the tubes were inverted to cover the tissue on the lid of the tube. Samples were supported cap-side down for 30min at RT then transferred to an oven set at 60°C for 60min. Samples were centrifuged at 17,000 x g for 10min which brought the liquid to the bottom of the tube (and the cap lining). 30μl of 25mM ambic added and an in-solution trypsin digestion in a final volume of 100μl undertaken. The samples were heated at 80°C for 10min followed by reduction with dithiothreitol (DTT), 5μl of a 9.2mg/mL solution in 25mM ambic at 60°C for 10min. Alkylation was carried out for 30min at RT in the dark, 33mg/mL iodoacetamide (IAA) in 25mM ambic.

5μl (33ng) of a 1:30 dilution of 0.2mg/mL stock solution of trypsin from porcine pancreas was added (1:50 Enzyme:Protein) and the digests were incubated at 37°C for 2.5h, a 5μl (33ng) trypsin'top-up' was then added and the digests were incubated overnight in a rotating incubator at 37°C .

On the following day samples were centrifuged for 10min at 17,200 x g and supernatants transferred to a protein low-bind tube. The laser capture tubes were centrifuged for 5min and residual digest recovered. Digests were acidified by the addition of 1μl trifluoroacetic acid (TFA) (Sigma-

Aldrich, Dorset, UK) and pH of each sample was checked using a pH paper. Afterwards samples were incubated at 37°C for 45min followed by centrifugation for 30min at 17,200 x g. C18 zip-tips were prepared with three membrane discs. 40µl wetting step with methanol followed by 70%(v/v) acetonitrile (ACN), following equilibration with 0.1% (v/v) TFA 20µl each sample was added and peptides washed with 40µl 0.1%(v/v) TFA. Peptides were eluted with 50% (v/v) ACN/0.1% (v/v) TFA into protein low-bind tubes and the volume reduced to approximately 3µl by vacuum centrifugation. 12µl 3% (v/v) ACN/0.1% (v/v) TFA was added to each sample. Samples were centrifuged and transferred to total recovery vials for high-resolution LC-MS analysis.

2.2.7 Liquid Chromatography and Mass spectrometry (LC-MS/MS)

Data-dependent LC-MS/MS analyses were conducted on a QExactive quadrupole-Orbitrap mass spectrometer coupled to a Dionex Ultimate 3000 RSLC nano-liquid chromatograph (Thermo Fisher, UK). Sample digest was loaded onto a trapping column (Acclaim PepMap 100 C18, 75 µm x 2 cm, 3 µm packing material, 100 Å) using a loading buffer of 0.1% (v/v) TFA, 2 % (v/v) ACN in water for 7 min at a flow rate of 9 µL min^{-1}. The trapping column was then set in-line with an analytical column (EASY-Spray PepMap RSLC C18, 75 µm x 50 cm, 2 µm packing material, 100 Å) and the peptides eluted using a linear gradient of 96.2 % A (0.1 % [v/v] formic acid):3.8 % B (0.1 % [v/v[formic acid in water:ACN [80:20] [v/v]) to 50 % A:50 % B over 30 min at a flow rate of 300nL min^{-1}, followed by washing at 1% A:99 % B for 5 min and re-equilibration of the column to starting conditions. The column was maintained at 40°C, and the digest introduced directly into the integrated nano-electrospray ionisation source operating in positive ion mode, 45 min gradient was used. The mass spectrometer was operated in DDA mode with survey scans between m/z 300-2000 acquired at a mass resolution of 70,000 (FWHM) at m/z 200. The maximum injection time was 250 ms, and the automatic gain control was set to 1e^6. The 10 most intense precursor ions with charges states of between 2+ and 5+ were selected for MS/MS at a resolution of 35,000. The maximum injection time was 100 ms, and the automatic gain control was set to 1e^5 with an isolation window of 2 m/z units. Fragmentation of the peptides was by higher-energy collisional dissociation using a normalised collision energy of 30%. Dynamic exclusion of m/z values to prevent repeated fragmentation of the same peptide was used with an exclusion time of 20sec.

2.2.8 Protein identification and quantification

For label-free quantification, the raw files of the acquired spectra were analysed using Progenesis QI software (Waters, Manchester, UK) which alignedf the files and then peak picked for quantification by peptide abundance. Spectra for each feature were exported from Progenesis QI and

utilised for peptide identification with a local Mascot server (Version 2.6.2), searching against the Unihuman Reviewed data-base with carbamidomethyl cysteine as a fixed modification and methionine oxidation as a variable modification, peptide mass tolerance of 10 ppm and fragment tolerance of 0.01 Da.

2.2.9 Data visualisation and statistical analysis

Normalised spectra values from Progenesis QI were used for data visualisation and statistical analysis. Proteins were filtered based on having at least two unique proteins used for identification. Moreover, proteins KRT85, MYOC and B2M were removed from the list of proteins as they were not present in more than three samples. All of the analysis were performed in R (version 4.1.0) using Rstudio. PCA, biplot and heatmap were generated using mixOmics package. To identify differentially abundant proteins lme4 package was used. Normalised spectra were transformed in log10 scale and spectra for proteins with missing values were imputed using local least squares (lls) of pcaMethods package, the number of similar genes used for regression (k) was set to 10. Comparison results with statistics including p values were extracted using emmeans package, family wise error rate was adjusted using Tukey HSD method (p value). Further, p values for multiple testing of each protein were adjusted using Bonferroni and Hochberg method (p.adjusted value).

2.2.10 Pathway analysis

Gene ontology (GO) analysis of molecular function (MF), cellular component (CC), biological process (BP) and biological pathways from Reactome database of identified proteins were run using online tool g:Profiler. Query was run with default settings and organism was selected Homo sapiens. Protein-protein interaction network of differentially abundant proteins were build using online tool String (version 1.10). Network type was selected as full String network, required score was set to medium confidence (0.400) and FDR stringency was set to medium (5 percent). Pathway analysis of differentially abundant proteins at significance level of p value 0.05 were carried out using Cytoscape (version 3.8.2).

2.3 RESULTS

The effect of method of collection was interrogated in equine superficial cartilage

2.3.1 LMD of equine articular cartilage

Superficial zone of cartilage samples were collected using LMD (Fig. 2.2). Different amounts of samples were collected for each sample due to the variance in the size of cartilage samples. Amount of trypsin was adjusted on the amount of tissue collected.
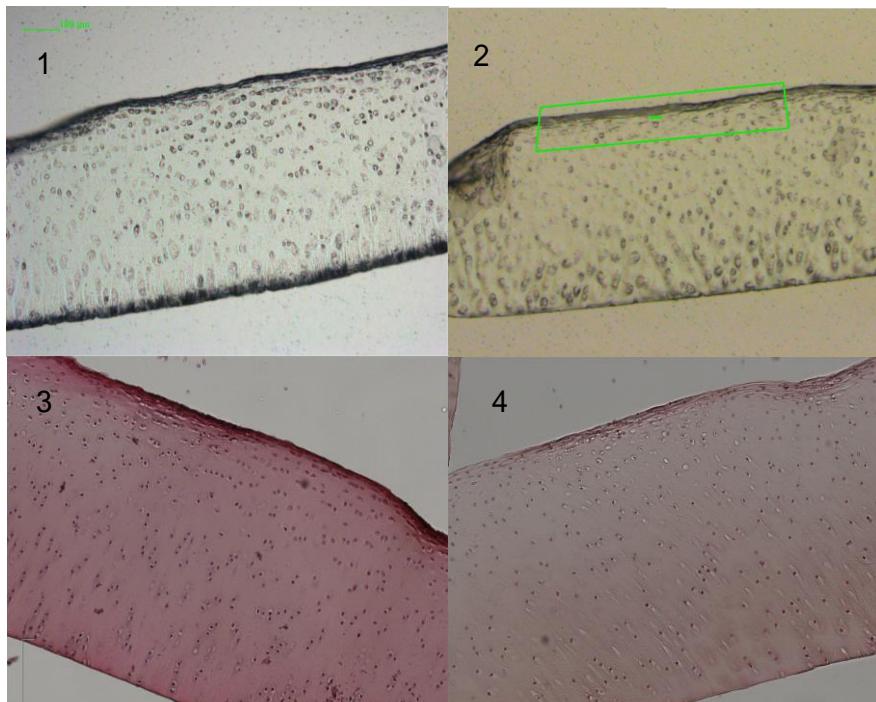
Figure 2.2: Equine articular cartilage sections under LMD microscope and upright microscope in the bright field. 1-2 unstained cartilage sections frozen in isopentane and flash frozen respectively, imaged under LMD microscope. Green rectangle represents the area collected for the analysis, green scale bar 100um. 3-4 H&E stained cartilage samples frozen in isopentane and flash frozen respectively.

2.3.2 MS spectra of the equine cartilage peptides

Base peak intensity of samples run on 45 minutes gradient demonstrated similar chromatogram (Fig. 2.3). FF2 sample demonstrated a different peak at the beginning of the run, however, there was little difference in the chromatographic profile based on the collection method.
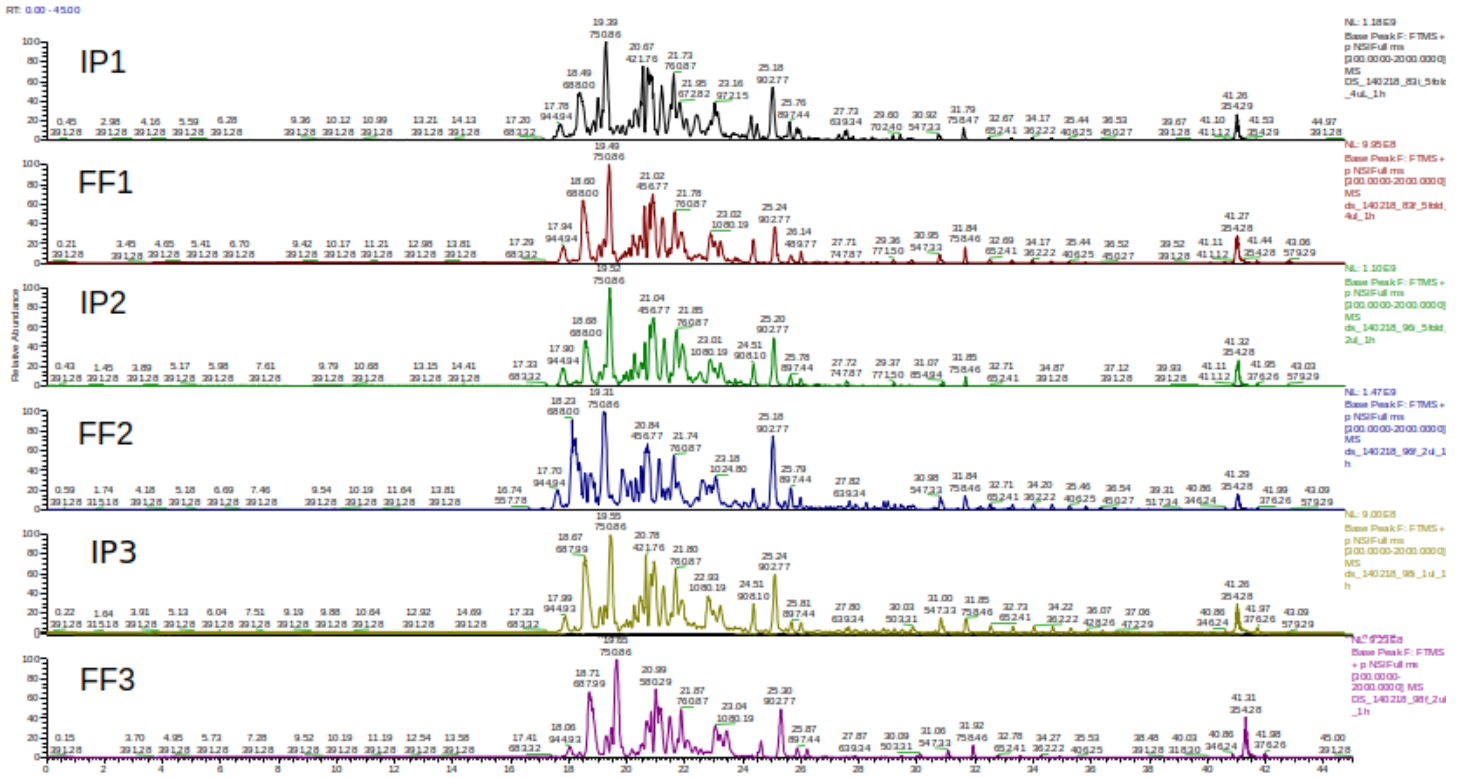
Figure 2.3: Base peak intensity chromatogram of equine cartilage samples collected in isopentane and fresh frozen on 45 minutes gradient. Normalisation level (NL) of the base peak intensity was in the range of 9.00+e8 to 1.49+e9. IP – isopentane, FF – fresh frozen.
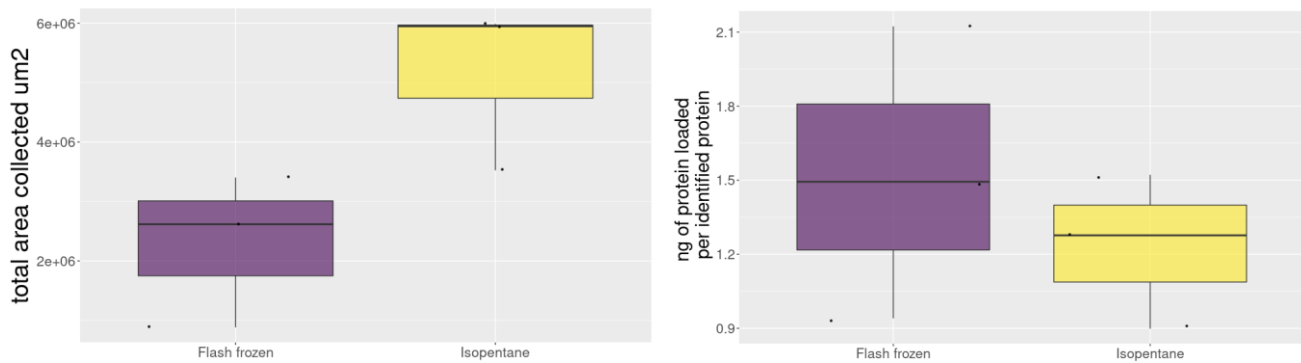
Figure 2.4: Sample area collected of equine cartilage using LMD. Total area (um2) collected from each sample for mass spectrometry sample preparation. Amount of proteins loaded (ng) per identified protein.

Due to the difference in the area collected the amount of total protein loaded varied between the samples from 79 to 233 ng, which resulted in a variation in the number of proteins identified (Fig. 2.4).

Human cartilage zonal proteomics in young, old and OA cartilage

2.3.3 Protein identification in human cartilage samples

There were in total 511 proteins identified using the label-free quantification software Progenesis and Mascot on the 45 samples from three cartilage zones in 15 donors. Progenesis software quantifies and then identifies. This enables previously low scoring proteins to be identified due to a single protein identification file being produced and searched in MASCOT. This identification file is then matched to the previously quantified protein changes in Progenesis. After removing proteins identified with only one unique peptide 236 proteins remained. Furthermore, proteins Beta-2-microglobulin (B2M), Keratin 85 (KRT85) and Myocilin (MYOC) were removed from subsequent analysis due to missing values in most samples. We took this total identification files and undertook bioinformatics on it to determine the classes of proteins identified in the samples as a whole. Gene ontology (GO) analysis on the selected proteins was performed using g:Profiler for molecular functions (MF), cellular component (CC) and biological process (BP), further biological pathways using the Reactome database (REAC) was selected (Fig. 2.5).

Molecular activities of the identified proteins subjected to GO analysis showed the following functions demonstrated significant overlap in MF: ECM structural constituent (p_{adj} 1.47x10^{-72}), structural molecule activity (p_{adj} 1.72x10^{-48}), ECM structural constituent conferring tensile strength

(p_{adj} 1.35x10^{-29}), glycosaminoglycan binding (p_{adj} 5.48x10^{-28}), heparin binding (p_{adj} 1.44x10^{-21}) and collagen binding (p_{adj} 5.44x10^{-14}). It was found that among top processes managed by multiple molecular activities termed as BP included ECM organisation (p_{adj} 5.81x10^{-49}), ECM structure organisation (p_{adj} 6.83x10^{-49}), external encapsulating structure organisation (p_{adj} 9.42x10^{-49}), platelet degranulation (p_{adj} 3.86x10^{-27}), skeletal system development (p_{adj} 4.86x10^{-18}). The locations relative to cellular structures of identified proteins demonstrated a significant overlap in CC including collagen-containing ECM (p_{adj} 3.9x10^{-126}), ECM (p_{adj} 6.86x10^{-117}), external encapsulating structure (p_{adj} 8.61x10^{-117}), extracellular region (p_{adj} 4.39x10^{-114}) and extracellular space (p_{adj} 1.33x10^{-102}). GO analysis of REAC pathways showed ECM organisation (p_{adj} 2.23x10^{-44}), collagen biosynthesis and modifying enzymes (p_{adj} 2.01x10^{-26}), ECM proteoglycans (p_{adj} 2.72x10^{-31}), integrin cell surface interactions (p_{adj} 6.02x10^{-28}), degradation of the ECM (p_{adj} 5.71x10^{-26}) were among the overlapped pathways at the significant level.
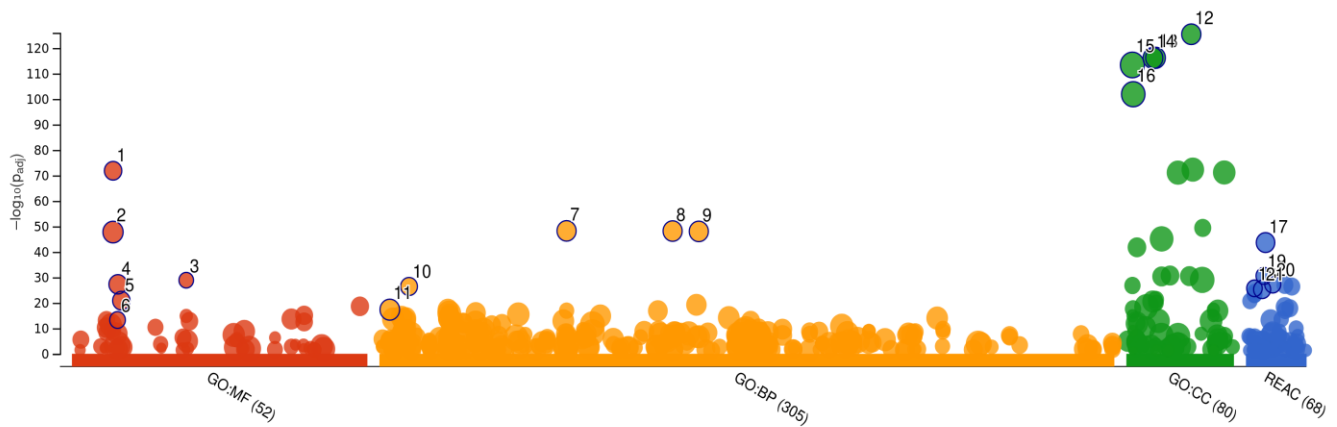
ID	Source	Term ID	Term Name	p_{adj} (query_1)
1	GO:MF	GO:0005201	extracellular matrix structural constituent	1.477×10^{-72}
2	GO:MF	GO:0005198	structural molecule activity	1.719×10^{-48}
3	GO:MF	GO:0030020	extracellular matrix structural constituent conferring tensile strength	1.348×10^{-29}
4	GO:MF	GO:0005539	glycosaminoglycan binding	5.477×10^{-28}
5	GO:MF	GO:0008201	heparin binding	1.443×10^{-21}
6	GO:MF	GO:0005518	collagen binding	5.443×10^{-14}
7	GO:BP	GO:0030198	extracellular matrix organization	5.808×10^{-49}
8	GO:BP	GO:0043062	extracellular structure organization	6.827×10^{-49}
9	GO:BP	GO:0045229	external encapsulating structure organization	9.420×10^{-49}
10	GO:BP	GO:0002576	platelet degranulation	3.859×10^{-27}
11	GO:BP	GO:0001501	skeletal system development	4.887×10^{-18}
12	GO:CC	GO:0062023	collagen-containing extracellular matrix	3.902×10^{-126}
13	GO:CC	GO:0031012	extracellular matrix	6.860×10^{-117}
14	GO:CC	GO:0030312	external encapsulating structure	8.609×10^{-117}
15	GO:CC	GO:0005576	extracellular region	4.388×10^{-114}
16	GO:CC	GO:0005615	extracellular space	1.332×10^{-102}
17	REAC	REAC:R-HSA-1474244	Extracellular matrix organization	2.227×10^{-44}
18	REAC	REAC:R-HSA-1650814	Collagen biosynthesis and modifying enzymes	2.009×10^{-26}
19	REAC	REAC:R-HSA-3000178	ECM proteoglycans	2.724×10^{-31}
20	REAC	REAC:R-HSA-216083	Integrin cell surface interactions	6.020×10^{-28}
21	REAC	REAC:R-HSA-1474228	Degradation of the extracellular matrix	5.714×10^{-26}

Figure 2.5: GO analysis of proteins in the all human cartilage zonal samples from young, old and OA donors (file made in Progenesis and searched with MASCOT with at least 2 unique)

peptides (236 proteins) using g:Profiler tool. GO – gene ontology, MF – molecular function, BP – biological process, CC – cellular component, REAC – Reactome database biological pathways.

2.3.4 Differentially abundant proteins

a. Between donor type (young, old, OA) results

Contrasts were made for each zone. We compared the young and old groups to identify the difference in the proteome during ageing, and old and OA group zones were compared to differentiate the zone-specific proteome in OA. In the superficial zone during ageing (old vs. young) 18 proteins were found to be differentially abundant at a statistically significant level ($p < 0.05$) (Tabel 1). Of these 11 proteins were more abundant in the old group and 7 proteins in the young group. After p value adjustment for multiple comparison the number of proteins was reduced to five proteins: Phospholipase A2 group IIA (PLA2G2A), and SERPINE2 were upregulated in the old group and Elastin microfibril interfacer 3 (EMILIN3), CILP2, ABI family member 3 binding protein (ABI3BP) were downregulated in the old group . The middle zone comparison of old and young groups revealed 29 proteins were differentially abundant, after p value adjustment only CILP2 was upregulated in the old group (Table 2). In the deep zone there were 34 proteins differentially abundant when old and young groups compared, nine proteins were differentially abundant at $p_{adj} < 0.05$. Of these nine proteins: SEMA3D, PCOLCE, TIMP3, KNG1, SERPINE2, HSPG2 were upregulated in the old group and CILP2, SMOC2, FBN1 were downregulated in the old group (Table 3).

Identification of OA related protein changes in the different zones was performed by comparing old and OA groups. Consequently, in the superficial zone during OA (OA vs. old) there were 72 proteins with $p < 0.05$, after p adjustment 38 proteins were identified (Table 4). OA and old groups comparison in the middle zone showed 36 proteins differentially abundant and with 2 proteins following adjustment for multiple comparison. In the deep zone proteome 29 proteins were differentially abundant and after p adjustment, 10 proteins differed.

The list of all comparisons with proteins and fold changes between the relative groups provided below.

Table 1. Superficial zone proteins (at a significant levele $p < 0.05$) during ageing (old superficial zone vs. young superficial zone)

Protein	p value	p.adj value	logFC
EMILIN3	0.002	0.029	-1.908
PLA2G2A	0.003	0.036	1.477
CILP2	0.003	0.036	-1.916
SERPINE2	0.005	0.044	2.404

ABI3BP	0.006	0.049	-1.998
HTRA1	0.012	0.077	1.971
CDH1	0.014	0.084	1.426
TGFBI	0.017	0.103	-1.824
CRP	0.019	0.112	2.124
SOD1	0.025	0.141	-1.526
APCS	0.035	0.173	2.556
HHIPL2	0.037	0.180	4.543
HP	0.039	0.187	2.036
COL4A5	0.042	0.194	0.978
IGHG4	0.044	0.199	1.612
SOD3	0.044	0.199	-0.930
ITIH6	0.045	0.199	1.581
TNXB	0.049	0.214	-2.169

Table 2. Middle zone proteins (at significant level $p < 0.05$) during ageing (old middle zone vs. young middle zone)

Protein	p value	p.adj value	log2FC
CILP2	0.000	0.025	-2.585
PPIB	0.001	0.109	1.583
HTRA1	0.003	0.164	2.058
MIA	0.004	0.185	1.689
P4HB	0.007	0.198	-0.760
COL4A5	0.007	0.198	0.491
APOD	0.008	0.198	1.363
PCOLCE	0.008	0.198	1.390
OGN	0.008	0.198	-1.207
LAG3	0.009	0.198	1.417
ITIH6	0.010	0.200	1.769
COL6A1	0.010	0.200	-1.249
TIMP3	0.010	0.201	2.384
C3	0.011	0.201	0.765
EDIL3	0.011	0.201	1.599
SMOC2	0.014	0.230	-1.413
SRPX2	0.015	0.232	-0.767
GDF10	0.017	0.240	2.046

ABI3BP	0.018	0.240	-2.205
CXCL12	0.023	0.251	2.416
C4A	0.028	0.275	1.183
TNXB	0.029	0.277	-1.550
IGHG2	0.032	0.299	2.215
COL6A3	0.040	0.339	-1.023
RAB1B	0.040	0.339	1.475
HSPG2	0.041	0.345	-0.890
COL6A2	0.043	0.350	-1.117
HP	0.047	0.362	0.871
FBN1	0.047	0.362	-0.630

Table 3. Deep zone proteins (at significant level $p < 0.05$) during ageing (old deep zone vs. young deep zone)

Protein	p value	p.adj value	logFC
SEMA3D	0.00001	0.002	2.206
CILP2	0.0001	0.011	-2.262
SMOC2	0.0002	0.016	-1.690
FBN1	0.0002	0.017	-1.249
PCOLCE	0.001	0.036	1.803
TIMP3	0.001	0.036	2.799
KNG1	0.001	0.038	2.901
SERPINE2	0.001	0.039	3.358
HSPG2	0.001	0.043	-1.290
SLC1A4	0.004	0.085	-1.669
MIA	0.004	0.085	1.881
APOD	0.004	0.091	1.184
CDH1	0.005	0.106	2.133
QSOX1	0.006	0.109	2.571
HS3ST3B1	0.008	0.133	2.888
ANXA2	0.009	0.139	-0.775
COL6A2	0.010	0.142	-0.803
HP	0.011	0.145	0.508
COL4A5	0.013	0.162	1.065
KRT83	0.017	0.184	1.833
HTRA1	0.019	0.196	2.009
COL9A1	0.022	0.211	-0.972

C3	0.024	0.218	1.304
CXCL12	0.030	0.251	1.898
APOE	0.030	0.251	1.166
APCS	0.031	0.251	-0.628
SERPINA5	0.031	0.251	2.008
TNFRSF11B	0.031	0.253	2.568
PPIB	0.034	0.256	1.723
FMOD	0.035	0.261	-0.751
COL6A3	0.037	0.264	-0.695
SRPX2	0.037	0.267	-0.799
MAMDC2	0.044	0.309	1.209
ENO1	0.049	0.325	-0.818

Table 4. Supperficial zone proteins (at significant level p < 0.05) during OA (OA superficial zone vs old superficial zone)

Protein	P value	p.adj value	logFC
HPX	0.0000001	2E-05	-3.971
GC	0.000001	2E-04	-4.550
A1BG	0.00001	1E-03	-3.274
SERPINA3	0.00001	0.001	-4.121
SERPINA1	0.00001	0.001	-3.737
ALB	0.00002	0.001	-3.773
IGHG2	0.00003	0.002	-4.176
IGKC	0.00004	0.002	-3.732
TF	0.0001	0.004	-2.429
ORM1	0.0002	0.006	-3.269
CP	0.0002	0.007	-4.270
PARK7	0.0002	0.007	-2.178
TPI1	0.0003	0.008	-1.555
IGHA1	0.0003	0.008	-4.597
A2M	0.0003	0.008	-2.855
IGHG1	0.0004	0.008	-3.316
HP	0.0004	0.008	-4.004
ASS1	0.0004	0.008	-2.641
IGHG3	0.0005	0.009	-3.120
CRP	0.0005	0.009	-3.503
PRDX6	0.0007	0.013	-1.984

CFH	0.0008	0.014	-1.034
F13A1	0.0010	0.015	-2.560
HIST1H2AG	0.0010	0.015	-0.698
RAB1B	0.001	0.017	-1.331
IGHV3-66	0.001	0.017	-4.332
GSTP1	0.002	0.026	-1.644
LBP	0.003	0.032	-2.641
HBA1	0.003	0.033	-4.398
GDI2	0.004	0.038	-1.975
PGAM1	0.004	0.043	-1.672
IGHM	0.005	0.043	-3.024
GAPDH	0.005	0.043	-0.970
IDH1	0.005	0.044	-2.505
PRDX1	0.005	0.044	-1.120
GSN	0.005	0.044	-1.484
RPS27A	0.005	0.044	-1.278
ORM2	0.006	0.049	-1.421
APOH	0.006	0.051	-1.660
APOA4	0.006	0.051	3.672
ANG	0.007	0.054	-1.309
ITIH6	0.007	0.054	-2.169
PPIB	0.008	0.057	1.069
ACAN	0.008	0.059	-1.919
RHOC	0.008	0.061	-1.797
HBB	0.009	0.061	-4.153
LAG3	0.011	0.072	2.080
TGFBI	0.012	0.080	1.924
CA1	0.013	0.083	-3.387
LDHA	0.014	0.084	-1.375
TNC	0.017	0.103	3.360
HIST1H1E	0.018	0.111	-1.872
POSTN	0.019	0.112	2.641
IGHG4	0.020	0.112	-1.875
FMOD	0.020	0.112	-1.134
TRPV4	0.020	0.112	-1.493
PGK1	0.020	0.112	-1.104
PRDX2	0.020	0.112	-3.152

C9	0.026	0.145	1.612
SCIN	0.028	0.149	-3.868
ALDOA	0.028	0.149	-1.310
COL1A1	0.030	0.156	1.492
VTN	0.031	0.162	1.348
OGN	0.033	0.165	0.909
KNG1	0.034	0.170	-2.514
CFD	0.034	0.170	-1.536
MSN	0.037	0.180	-0.939
ANXA6	0.037	0.180	-1.123
CFHR5	0.040	0.191	1.676
SOD2	0.041	0.191	-2.772
PFN1	0.041	0.192	-1.758
SOD1	0.045	0.202	1.363

Table 5. Middle zone proteins during OA (OA middle zone vs. old middle zone)

Protein	adj.p.value	BH	log2FC
APOD	0.0001	0.025	-2.410
PRG4	0.0002	0.035	-1.640
CP	0.0006	0.053	-4.053
PFN1	0.002	0.144	-1.694
HHIPL2	0.003	0.164	-3.728
SERPINC1	0.003	0.164	-2.488
CXCL12	0.004	0.175	-3.197
F13A1	0.005	0.185	-3.268
GSTP1	0.006	0.198	-1.583
THBS1	0.006	0.198	-1.626
THBS4	0.007	0.198	1.714
SMOC2	0.009	0.198	1.510
KNG1	0.010	0.200	-3.509
MATN3	0.011	0.204	2.767
SERPINA1	0.014	0.230	-2.102
CLU	0.014	0.230	-2.036
ORM1	0.015	0.233	-2.451
SERPINA3	0.015	0.233	-2.030
MATN4	0.017	0.240	2.636
ARPC4	0.017	0.240	1.057

CFD	0.018	0.240	-1.606
FBN1	0.020	0.251	0.745
HPX	0.021	0.251	-2.133
MIA	0.021	0.251	-1.317
IGHG2	0.022	0.251	-2.381
MATN2	0.022	0.251	-1.381
ASPN	0.022	0.251	1.123
P4HB	0.022	0.251	0.625
COL11A1	0.023	0.253	0.614
AHSG	0.024	0.261	-3.090
OGN	0.027	0.275	0.990
HBB	0.028	0.277	-1.619
C9	0.037	0.327	-1.062
HBA1	0.046	0.362	-1.262
ALB	0.048	0.362	-2.297
LBP	0.049	0.363	-1.087

Table 6. Deep zone proteins (p <0.05) during OA (OA deep zone vs old deep zone)

Protein	adj.p.value	BH	log2FC
SMOC2	5E-06	0.00	2.47
APOD	2E-05	0.00	-2.15
HSPG2	1E-04	0.01	1.74
FBN1	0.0002	0.015	1.304
PKM	0.001	0.036	1.129
SLC1A4	0.001	0.042	1.934
HAPLN1	0.001	0.043	1.319
PRDX1	0.002	0.064	1.106
MATN4	0.003	0.072	2.795
CLEC3A	0.003	0.072	2.443
SCIN	0.004	0.085	2.203
PGM1	0.006	0.109	1.532
ANXA2	0.006	0.109	0.832
THBS4	0.006	0.113	1.333
ANXA5	0.008	0.133	0.882
CLEC11A	0.009	0.139	3.089
IGHV3-66	0.010	0.140	-1.851
TRPV4	0.011	0.145	1.776

IGHG1	0.011	0.145	-1.169
GAPDH	0.013	0.162	0.828
MSN	0.013	0.162	0.985
IDH1	0.015	0.179	1.292
PRG4	0.019	0.196	-0.990
F13A1	0.019	0.196	-1.503
KNG1	0.019	0.196	-1.866
ACTB	0.020	0.196	1.059
APCS	0.022	0.211	0.666
ANXA6	0.023	0.216	0.953
LDHA	0.025	0.226	1.053
ARPC4	0.026	0.232	1.387
CHRDL2	0.026	0.232	2.077
CXCL12	0.027	0.232	-1.938
BGN	0.032	0.253	0.763
GDF10	0.034	0.256	1.958
EEF1A1P5	0.042	0.300	1.170
HP	0.046	0.314	-0.392

b. Between zone results; superficial, middle, deep

Within group comparisons between different zones was also conducted, thus each group had three comparisons superficial – middle, middle – deep and superficial – deep zones.

In the young group comparison between superficial and middle zones found 115 proteins with $p < 0.05$ and after p value adjustment 109 proteins were still differentially abundant at a statistically significant level. Middle and deep zones comparison in the young group revealed 53 proteins were differentially abundant, after correction for multiple comparison 19 proteins were at $p_{adj} < 0.05$. Finally, comparison between the superficial and deep zones demonstrated difference in 149 proteins' abundance at $p < 0.05$, after correction for multiple comparison 139 proteins were left.

In the old group comparisons between superficial and middle, middle and deep, superficial and deep zones found 122 proteins (108 proteins $p_{adj} < 0.05$), 80 proteins (60 proteins $p_{adj} < 0.05$), 171 proteins (168 proteins $p_{adj} < 0.05$) differentially abundant respectively.

Similarly in the OA group superficial and middle, middle and deep, superficial and deep zone comparisons had 128 proteins (112 proteins $p_{adj} < 0.05$), 84 proteins (68 proteins $p_{adj} < 0.05$), 167 proteins (163 proteins $p_{adj} < 0.05$).

2.3.5 Zonal specific protein identification in human articular cartilage

Proteins that had a statistically higher abundance in either of three zones between young, old and OA groups were merged together based on the similar proteins. Thus, proteins that were highly abundant in the superficial zone in comparison to the middle and deep zones were selected, the same analysis was undertaken for the middle and deep zones. By merging proteins with the higher abundance in the specific zone in all three groups this returned zone specific proteins despite age and disease state. 22 proteins were found to be highly abundant in the superficial zone in all three groups (Table 7). Those proteins included a1 and a2 helixes of collagen I and all three helixes of collagen VI. There were no proteins found to be specific for the middle zone that were common in all three groups. In the deep zone there were six highly abundant proteins (ANG, C2orf40, CHAD, CNMD, LYZ, PLA2G2A) shared by young, old and OA groups (Table 8). The middle zone serves as the transition zone, hence there could be an overlap in the proteome of this zone when compared to the superficial and deep zones. To get the higher contrast between the cartilage proteome in the superficial and deep zone only comparisons between these two zones was performed in all 3 groups , thus middle zone was omitted. In the superficial zone 54 proteins demonstrated higher abundance and 40 proteins in the deep zone common in all three groups.

Table 7. Proteins highly abundant in the superficial zone in comparison to the middle and deep zones at a statistically significant level ($p_{adj} < 0.05$)

	log2FC superficial-deep			log2FC superficial-middle		
Protein	Young	Old	OA	Young	Old	OA
AEBP1	2.258	2.475	3.421	3.024	1.517	3.134
APCS	1.605	4.789	5.223	1.553	3.193	4.294
APOA1	2.588	2.842	2.928	2.882	1.992	1.404
APOH	3.163	3.614	1.857	2.448	1.752	0.092
ASPN	2.818	2.372	3.185	1.842	2.200	2.960
C4A	2.230	3.298	2.167	2.903	2.899	2.201
C9	1.658	1.868	4.218	1.335	1.278	2.890
COL1A1	3.373	2.606	4.009	2.992	1.948	3.439
COL1A2	5.387	4.366	5.486	4.643	3.514	4.861
COL6A1	2.044	1.576	2.466	1.450	1.613	2.255
COL6A2	1.888	1.670	2.331	1.320	1.415	2.067
COL6A3	1.983	1.696	2.198	1.388	1.430	1.921
HSPA5	1.339	2.586	2.381	1.152	1.601	1.362
IGHG4	1.179	2.675	1.241	1.746	2.534	0.659
ITIH4	3.191	4.763	3.353	3.054	6.014	4.237
KNG1	6.167	2.744	2.095	4.901	2.976	0.462
LMNA	2.820	2.897	2.621	1.761	1.447	1.462
ORM2	3.685	3.262	2.062	2.696	1.845	0.424
SOD1	3.380	1.799	3.744	3.232	2.067	3.429
TNC	2.528	2.532	6.221	2.486	2.018	5.377

Protein						
TNXB	4.441	2.563	3.186	2.914	2.294	3.190
VTN	4.184	4.512	6.098	2.839	3.163	4.511

Table 8. Proteins highly abundant in the deep zone in comparison to the superficial and middle zones at a statistically significant level ($p_{adj} < 0.05$)

	log2FC deep-superficial			log2FC deep-middle		
Protein	Young	Old	OA	Young	Old	OA
ANG	3.883	3.361	4.970	1.763	1.814	2.114
C2orf40	5.265	3.783	2.725	2.028	1.848	1.236
CHAD	3.795	3.774	3.649	0.947	0.950	0.840
CNMD	4.184	4.464	4.152	1.648	1.985	2.438
LYZ	5.444	5.517	5.288	2.085	1.862	1.414
PLA2G2A	5.281	5.472	6.066	2.294	2.756	3.521

2.3.6 Zonal proteins pathway analysis

Inputting differentially abundant proteins from each zone separately formed a network of protein-protein interactions using StringDB that showed two distinct clusters in proteins significantly abundant in the superficial zone when compared to both middle and deep zones in all three groups (Fig. 2.6). One of the clusters consisted of collagen I and VI helices along ASPN, TNXB, AEBP1 and LMNA proteins. The second cluster contained mostly serum-related proteins. Enrichment analysis showed significant overlap with GO terms including extracellular matrix organisation (FDR 3.64×10^{-7}), secretory granule (FDR 0.0002), collagen-containing extracellular matrix (FDR 0.0002).

Figure 2.6: Protein-protein interactions with GO enrichment analysis of proteins significantly abundant in the superficial zone in comparison to both middle and deep zones in all groups.
GO terms: extracellular matrix organisation (blue); secretory granule (yellow); collagen-containing extracellular matrix (purple).

An extended list of proteins significantly abundant in the superficial zone in comparison to the deep zone had a significant overlap with GO term nucleosome (FDR 0.0009) and superoxide dismutase activity (FDR 2.41×10^{-5}) (Fig. 2.7). Moreover, GO terms extracellular matrix organisation (FDR 4.61×10^{-13}), collagen-containing extracellular matrix (FDR 9.59×10^{-14}) and secretory granule (FDR 0.0009).

Figure 2.7: Protein-protein interactions with GO enrichment analysis of proteins significantly abundant in the superficial zone in comparison to the deep zone in all groups. GO terms: nucleosome (red); superoxide dismutase activity (green); collagen-containing extracellular matrix (purple); extracellular matrix organisation (blue); secretory granule (yellow).

There were only six proteins significantly differentially abundant in the deep zone in comparison to both middle and superficial zones. This was inadequate to build an interaction network.

Protein-protein interactions were analysed of the proteins differentially abundant in the deep zone in comparison to the superficial zone (Fig. 2.8). A cluster with a substantial number of proteins with branched interactions within the cluster included GO terms: extracellular matrix organisation (FDR 8.41×10^{-9}), skeletal system development (FDR 4.98×10^{-7}), glycosaminoglycan binding (FDR 4.03×10^{-8}), collagen-containing extracellular matrix (FDR 0.0002). Functional enrichment in the network revealed a smaller cluster with GO term secretion (FDR 0.01).

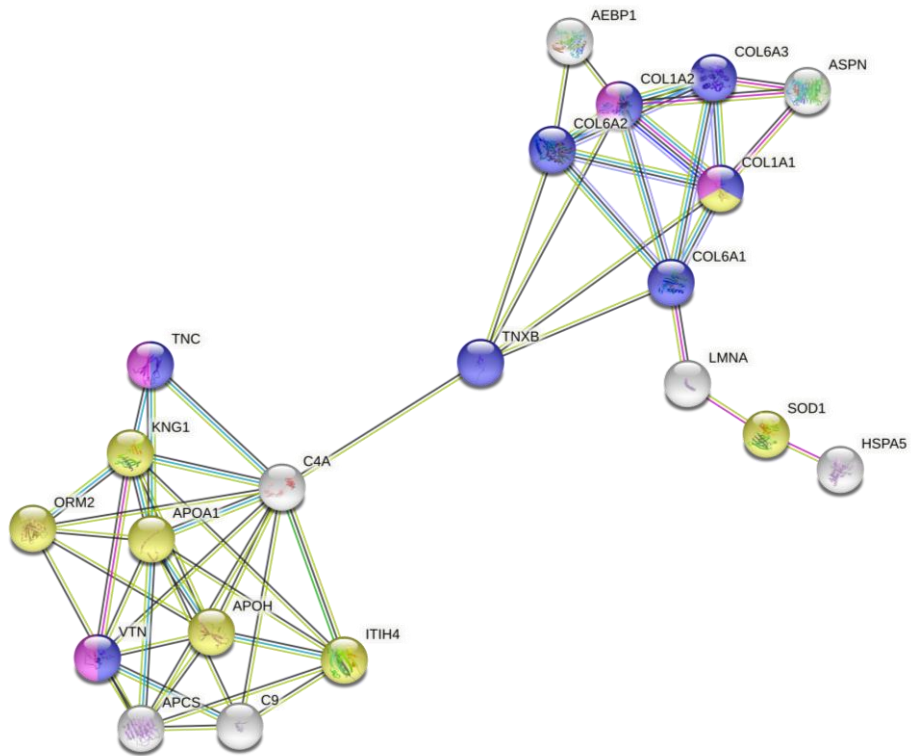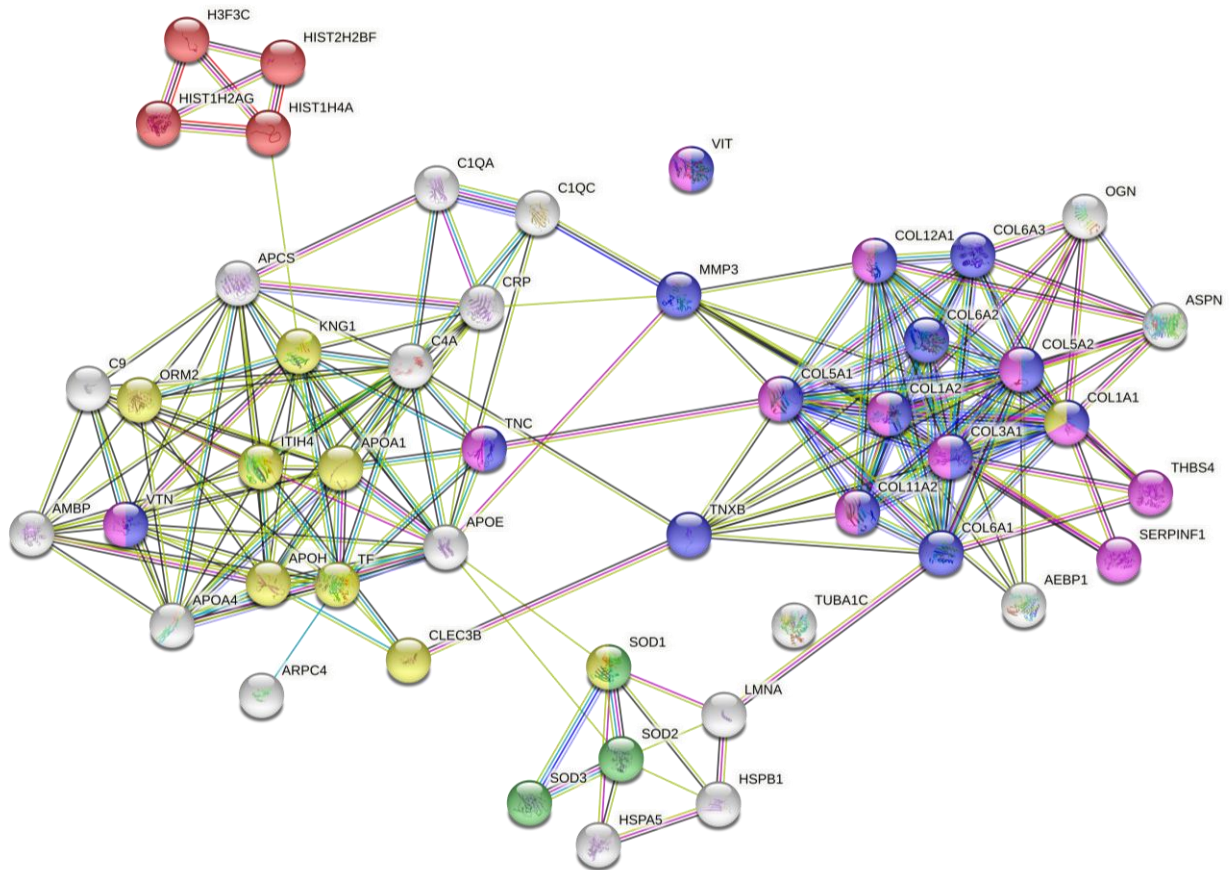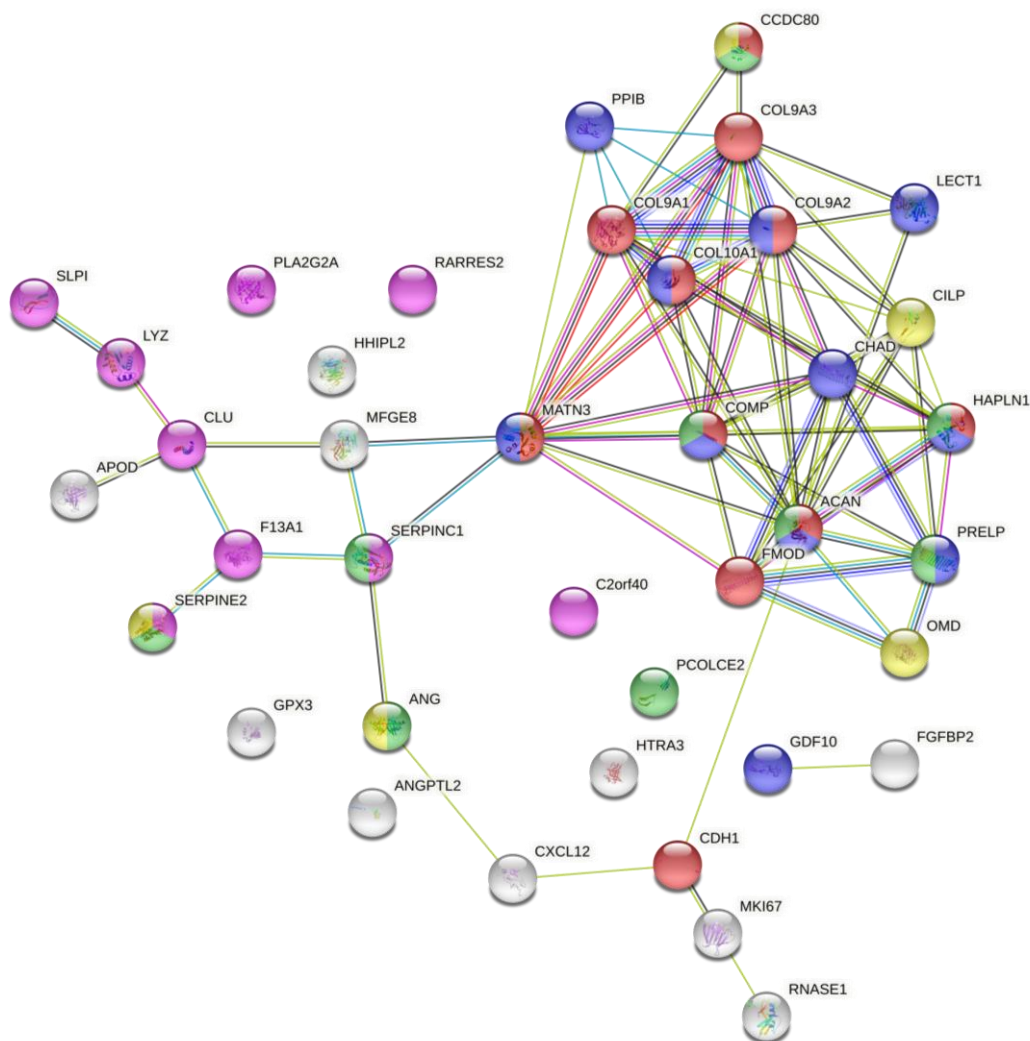**Figure 2.8: Protein-protein interaction network with GO enrichment analysis of proteins abundant in the deep zone in comparison to the superficial zone.** GO terms: extracellular matrix organisation (red), skeletal system development (blue), collagen-containing extracellular matrix (yellow), glycosaminoglycan binding (green), secretion (purple).

2.3.7 Superficial zone during OA

A protein-protein interaction network was generated using the String app in Cytoscape software. Differentially abundant proteins in the superficial zone of OA and old group comparison had an extensive network. Proteins of interest were manually selected from the network (Fig. 2.9). SERPINA3, SERPINA1, ACAN, THBS1, A2M, and GSN as these were found less abundant in the OA group in comparison to the old group. Whereas FGA, TGFBI, PCOLCE, POSTN, COL1A1 and AEBP1 were all significantly abundant during OA.

Figure 2.9: Selected protein-protein interaction network of differentially abundant proteins in the superficial zone during OA. Positive logFC (upregulation) and negative logFC

(downregulation) of protein in the superficial OA group in comparison to the superficial old group

2.3.8 Middle zone during OA

Differentially abundant proteins in the middle zone during OA formed a cluster with upregulated collagens I, XI, XII and FBN1, along with downregulated ORM2, GSTP1, CLU and THBS1 in the centre of the network (Fig. 2.10). Serine protease inhibitors (SERPINC1, SERPINA1) and metalloproteinase inhibitor TIMP3 were less abundant in the OA group in comparison to old group. ECM proteins MATN4, MATN3, SMOC2, OGN and ASPN were found more abundant in the OA group.

Figure 2.10: Cluster of protein-protein interaction network of differentially abundant proteins in the middle zone during OA. Positive logFC (upregulation) and negative logFC (downregulation) of protein in the middle OA group in comparison to the middle old group

2.3.9 Deep zone during OA

A protein-protein interaction network of differentially abundant proteins in the deep zone during OA generated two clusters (Fig. 2.11). Similarly, to the middle zone COL11A1, MATN4 and FBN1 were more abundant in the OA group. Additionally, HAPLN1 and HSPG2 proteins were also more abundant, and these five proteins formed one cluster. The second cluster had the majority of proteins (ANXA2/5/6, GAPDH, ACTB, LDHA, PRDX1, PKM, PGM1, PRDX1, MSN, SCIN, ARPC4) were abundant in the OA group, except CXCL12 and TNFRSF11B proteins.

Figure 2.11: Clusters of protein-protein interaction network of differentially abundant proteins in the deep zone during OA. Positive logFC (upregulation) and negative logFC (downregulation) of protein in the deep OA group in comparison to the deep old group

Differentially abundant proteins during ageing

2.3.10 Superficial zone during ageing

Superficial zone proteins during ageing formed a protein-protein network cluster with downregulated collagens I and VI, and upregulated COL4A5 in the middle of the network. Moreover, downregulated proteins FBN1, TNXB, TGFBI and upregulated SERPINE2 were connected with collagens. Downregulated SOD1 and SOD3 formed connections with upregulated APOE and HTRA1 (Fig. 2.12).

Figure 2.12: Cluster of protein-protein interaction network of differentially abundant proteins in the superficial zone during ageing. Positive logFC (upregulation) and negative logFC (downregulation) of protein in the superficial old group in comparison to the superficial young group

2.3.11 Middle zone during ageing

Similar to the superficial zone collagen VI, TNXB and FBN1 were downregulated in the old middle group in comparison to the young group. In close proximity to them were downregulated HSPG2 and upregulated PCOLCE which formed the core of the network (Fig. 2.13). Protease inhibitors SERPINE2 and TIMP3 were more abundant during ageing in the middle zone. Furthermore, proteins HTRA1, CDH1, CXCL12, GDF10, QSOX1, APOA1, APOD and HS3ST3B1 were more abundant in the old middle group and were connected to this network.
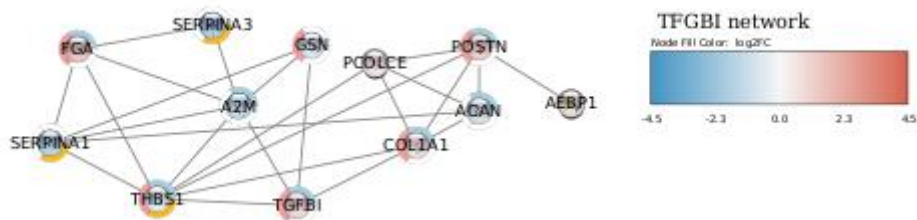
Figure 2.13: Cluster of protein-protein interaction network of differentially abundant proteins in the middle zone during ageing. Positive logFC (upregulation) and negative logFC (downregulation) of protein in the middle old group in comparison to the middle young group

2.3.12 Deep zone during ageing

Deep zone proteins formed an extensive network with 26 proteins (Fig. 2.14). COL10A1, COL11A1, FBN1 and CILP2 were less abundant in the old group in comparison to the young group. Furthermore, PDIA3, ENO1, ANXA2, HSPG2, OGN, FMOD, SMOC2 and SRPX2 were downregulated during ageing. Similar to the superficial and middle zones in ageing TIMP3, CXCL12, QSOX1, HTRA1, PCOLCE, CDH1, HS3ST3B1 were identified as more abundant in the old group. In addition, SERPINA5, C3, KNG1, PPIB, TNFRSF11B were more abundant during ageing in the deep zone.
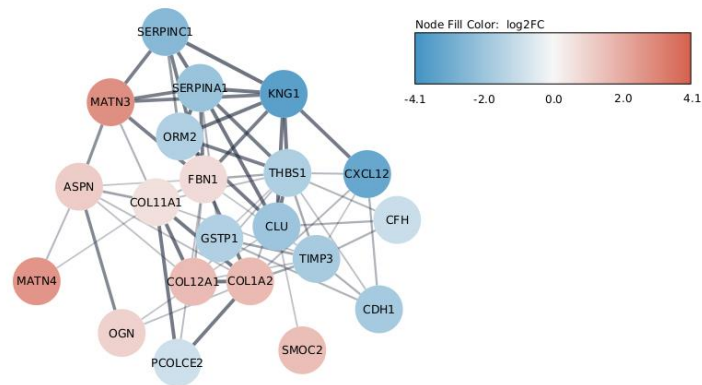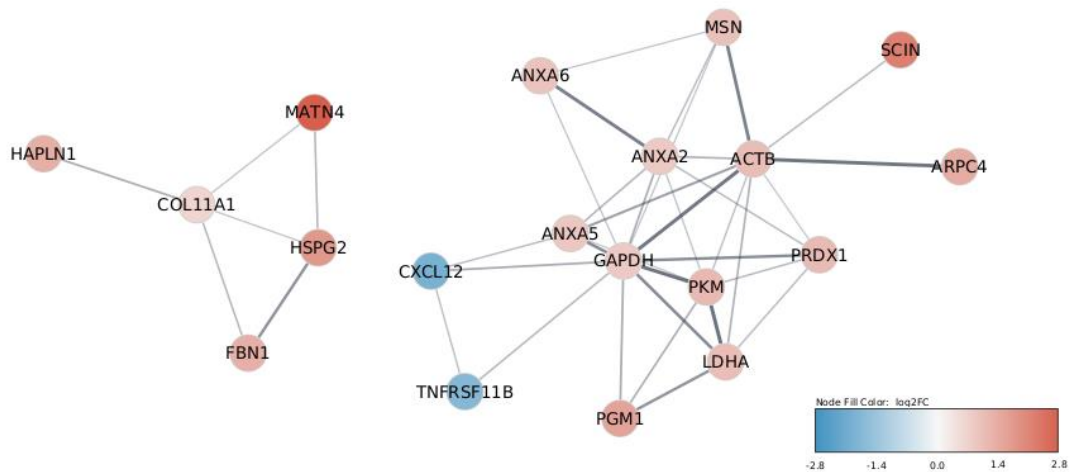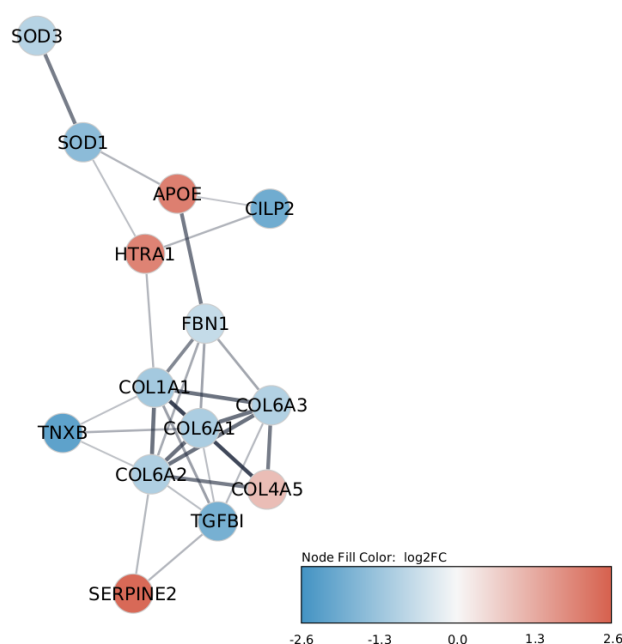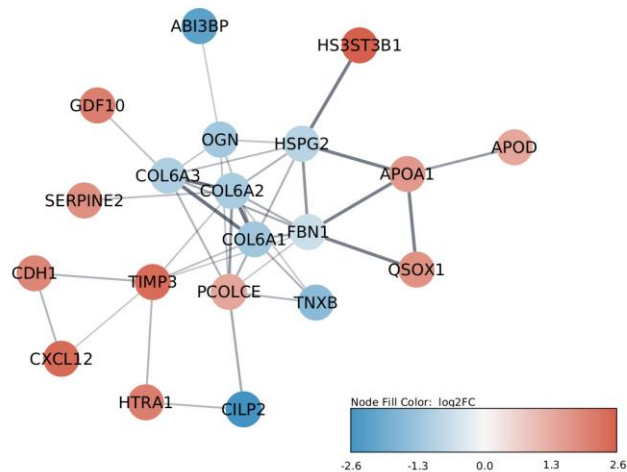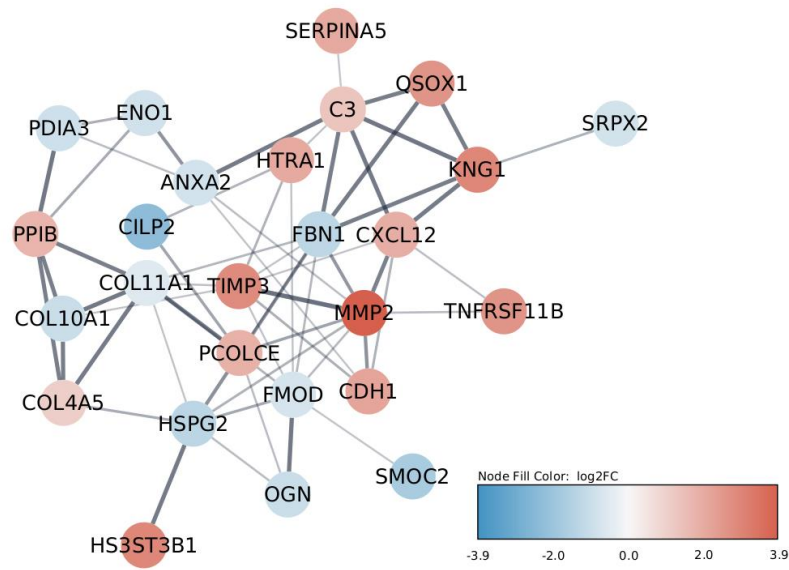
Figure 2.14: Cluster of protein-protein interaction network of differentially abundant proteins in the deep zone during ageing. Positive logFC (upregulation) and negative logFC (downregulation) of proteins in the deep old group in comparison to the deep young group

2.4 DISCUSSION

2.4.1 Optimisation of the method of collection of articular cartilage

There was no significant difference in the proteome of equine articular cartilage of the superficial zone following microdissection and stored either in isopentane or fresh frozen in liquid nitrogen. There was difference in the number of identified proteins in each sample, however, as it was shown in chromatogram the loading of samples was different. This was mainly due to the difference in the amount of tissue collected between samples. In conclusion, the comparison of isopentane and fresh frozen had no significant effect on protein abundance.

OA driven differences in the articular cartilage of different zones

2.4.2. Proteome changes in the superficial zone during OA

Transforming growth factor beta-induced protein (TGFBI) was in higher abundance in OA compared to old normal cartilage within the superficial zone. TGFBI plays an important role in cartilage homeostasis; its deficiency led to cartilage matrix degradation in a mouse OA model (Lee et al., 2015). TGFBI was more highly expression at the mRNA and protein level in the OA cartilage in comparison to healthy cartilage. TGFBI knockdown in OA chondrocytes demonstrated a significant increase in type X collagen. Furthermore, TGFBI expression was found at higher levels during chondrogenesis of MSCs. However, its addition to chondrocytes increased the expression of hypertrophic and mineralisation markers (Ruiz et al., 2019). COL1A1 was more abundant as well in the superficial OA group. It has previously been shown that TGFB1 can induce the expression of TGFBI and COL1a1 in renal carcinoma cells (Boguslawska et al., 2016). TFGBI was found to be co-expressed with THBS1 in cancer (Ahmed et al., 2007). Although Thrombospondin 1 (THBS1) was downregulated in our study; it was less abundant in the OA group. However, it may play a role in chondrogenesis, as its addition to MSCs undergoing chondrogenesis elevated chondrogenic markers. The addition of recombinant THBS1 did not reverse the osteoarthritic phenotype in chondrocytes (Maumus et al., 2017). THBS1 was more abundant during cartilage development in a mouse model, whereas TGFBI was significantly decreased (Wilson et al., 2012). A lack of THBS1 in mice lead to a persistence of inflammation in the wound healing process (Agah et al., 2002), and in comparison to other thrombospondin types THBS1 knockout mice showed the least chondrocyte growth plate disorganisation (Posey et al., 2008).

The upregulation of TGFBI in the OA cartilage could indicate the activation of the chondrogenesis process, however, THBS1 downregulation in the OA group might indicate a dysregulated process of new cartilage formation during the OA.

FGA was more abundant in the superficial OA group in our study. Peptides from FGA and COL1a1 were found to be upregulated in synovial fluid during inflammatory arthritis using label-free proteomics (Mahendran et al., 2019). FGA protein was identified as a rhythmic protein with peak abundance during the late rest period in mice femoral head cartilage (Dudek et al., 2021). Furthermore, FGA protein was found to be abundant in degraded OA cartilage in comparison to the intact cartilage (Steinberg et al., 2017), and in a separate proteomics study it was also more abundant in the OA cartilage (Wu et al., 2007). Thus the higher abundance of FGA in the OA cartilage in our study is similar to previous published work.

Serine protease inhibitors (SERPINA1, SERPINA3) were downregulated in the superficial zone of OA group. SERPINA1 and SERPINA3 were upregulated during chondrogenesis (Boeuf et al., 2008) and SERPINA1 and SERPINA3 can be inactivated by MMP3 (Mast et al., 1991). Although, MMP3 was not more abundant in the OA group of superficial zone, lower levels of SERPINA1 and A3 could be indicators of ongoing metalloproteinase activity and cartilage breakdown. and may indicate the lower ability of chondrogenesis in the superficial zone during OA.

COL1A1, the major cartilage ECM protein, was found to be more abundant in the superficial zone in the OA group in comparison to the old group. It was previously shown that COL1A1 was increased during OA progression in full thickness cartilage (Miosge et al., 2004; Zhong et al., 2016). POSTN was upregulated in the OA cartilage in the superficial zone in comparison to the old group in our study, it was also previously identified as a significantly upregulated gene in the superficial zone of articular cartilage (Fukui et al., 2008). POSTN expression was found to be upregulated in OA cartilage (Chijimatsu et al., 2015) and its deficiency protected cartilage from post-traumatic and age-related OA in mice (Attur et al., 2021). The protective effect of POSTN downregulation could be due to a possible link with IL1β, ADAMTS-4/5 and MMP13 (Attur et al., 2015; Chinzei et al., 2018). It demonstrates that in our study POSTN is specifically abundant in the superficial zone of OA and could be one of the factors leading to OA progression.

AEBP1 is an ECM protein that links with collagens and is involved in wound healing and fibroproliferative pathways (Blackburn et al., 2018). In our study AEBP1 was upregulated in OA and had a protein-protein interaction with POSTN. AEBP1 expression was identified to be upregulated during the initial steps of chondrogenesis in MSCs and decreased in the late stages when COL2A1 expression was highest (Hering, T M. et al., 2000). Thus, increased abundance of AEBP1 could be an indicator of ongoing fibrosis in the superficial zone of cartilage tissue.

Procollagen C-endopeptidase enhancer (PCOLCE) was significantly increased in the OA group when compared to the old group in the superficial zone. PCOLCE function is to cleave procollogen upon secretion from the cell. PCOLCE associates with collagens I-III, and in our study COL1A1 was also significantly more abundant in the OA group. During MSCs chondrogenesis PCOLCE

expression was found to be upregulated (Rocha et al., 2014) and also in the OA cartilage, however, there was no significant difference in abundance when compared between the zones in another study (M. F. Hsueh et al., 2016). The upregulation of PCOLCE in our study could be an indicator of the chondrogenesis process in the superficial zone during OA.

A2M protein was downregulated in the OA group when compared to the old group in the superficial zone. A2M acts as an inhibitor of ADAMTS-4/5/7/12 (Luan et al., 2008; Tortorella et al., 2004) and MMP13 (Demirag et al., 2005). Expression of A2M was found in serum, synovial fluid and cartilage, moreover, it reduced MMP13 level in chondrocytes when treated with IL-1 (S. Wang et al., 2014). All of the above may indicate the ongoing activation of chondrocytes, hence, the upregulation of proteins involved in chondrogenesis (TGFBI, AEBP1, PCOLCE). However, these proteins are found in the early stages of chondrogenesis and in later stages could stimulate hypertrophic cartilage features. Furthermore, protective capabilities of cartilage from proteases were downregulated due to low abundance of proteins with protease inhibitory activity (SERPINA1/3, A2M) and upregulation of proteins that induce the proteases (POSTN). The activation of chondrocytes suggests that restoration of cartilage tissue inclined more towards a fibrocartilage state. This was also evidenced by a higher abundance of proteins involved in fibrosis (COL1A1, FGA) and decline in cartilage core protein ACAN.

The proteins discussed above demonstrate the changes during OA the abundance of the proteins identified in our study corresponds to the studies that investigated osteoarthritic cartilage. Our study also shows that some of these proteins interact which could demonstrate that proteins involved in the OA development work together in an attempt to restore the cartilage by increasing chondrogenesis, however, it could also lead for mineralisation processes. This could be be an indicator that newly formed cartilage upon degradation does not have the features as normal healthy cartilage, and could lead to cartilage mineralisation. .

2.4.3 Proteome changes in the middle zone during OA

The middle zone demonstrated a number of proteins changed in OA. The protein-protein interactions demonstrated a cluster of closely interconnected proteins. Collagen type XI and XII were both upregulated in the middle zone of OA samples in comparison to the old group. Collagen type XI forms thin fibrils and is found in pericellular matrix, where it can form heteropolymer with collagens II and IX (Eyre, 2001; Hagg et al., 1998). Collagen XI also promotes chondrogenesis in MSCs and inhibit cartilage ECM degradation in human chondrocyte pellet (A. Li et al., 2018). Collagen XII links with collagen I in bone where it is highly expressed, moreover COL12A1 demonstrated an increased expression during mechanical strain in mouse osteoblast cells (Arai et al., 2008). The upregulation of collagen XI could indicate the proliferation of chondrocyte in the middle zone during

OA, however, the upregulation of collagen XII suggests a drive towards cartilage mineralisation. Moreover, FBN1 was also upregulated in the OA group when compared to the old group in our study. It was found that FBN1 abundance in the articular cartilage, is higher in close proximity to the subchondral bone, and it was also involved in ossification (Keene et al., 1997). Furthermore, COL1A2 was more highly abundant in the middle zone of OA group in comparison the old group which could also be a sign of abnormal cartilage ossification during OA within the middle zone.

Asporin (ASPN) was upregulated in the middle zone of OA group in comparison to the old group. ASPN can be upregulated by TGFb, but not IL-1b and TNFa, furthermore, chondrocyte dedifferentiation resulted in a decrease in ASPN (Duval et al., 2011). ASPN was shown to inhibit chondrogenesis and was highly expressed in OA cartilage (Kizawa et al., 2005; Lorenzo et al., 2001). ASPN inhibits chondrogenesis by binding to TGFb, which is important in chondrocyte proliferation and differentiation (Nakajima et al., 2007). ASPN also can induce collagen biomineralisation, which was shown in osteoblasts (Kalamajski et al., 2009). Thus, higher abundance of ASPN in the middle zone during OA could indicate of the inhibition of chondrogenesis and ossification of the cartilage tissue.

Matrilin 3 (MATN3) was upregulated in the middle zone during OA. It was shown MATN3 could be involved in OA progression, as mutations in MATN3 gene were linked to hand OA (Stefánsson et al., 2003). However, mice lacking MATN3 showed no skeletal abnormalities (Ko et al., 2004). Gene expression and protein levels of MATN3 were correlated with OA severity. The highest expression was found in severe OA cartilage tissue, moreover, protein abundance was limited to the middle and deep zones of articular cartilage (Pullig et al., 2002). MATN3 could play both catabolic and anabolic roles in articular cartilage, thus high concentrations of MATN3 may lead to upregulation of inflammatory cytokines and MMPs, whereas low concentrations of MATN3 inhibits IL-1β and promote synthesis of collagen II and ACAN (Muttigi et al., 2016). Furthermore, MATN3 interacts with TGFβ during chondrogenesis, and mutant forms of MATN3 dysregulates TGFβ induced chondrogenesis in chondroprogenitor cells (Jayasuriya et al., 2014). Another member of the matrilin family, MATN4 was upregulated in the middle zone during OA. A loss of MATN4 in mice lead to age-related spontaneous OA in comparison to normal control mice. MATN4 along with other matrilins were highly abundant in human OA cartilage in comparison to normal control (Ping Li et al., 2020). However, at the gene expression level MATN4 downregulation was associated with OA progression (Chou et al., 2015). MATN4 has broader expression patterns in different tissue types, whereas MATN3 expression is more specific to cartilage tissue (Klatt et al., 2002). The presence of MATN3 and MATN4 at higher levels during OA in the middle zone of articular cartilage in our study are in concordance with the mentioned studies. Both of matrilins have protein-protein interactions with POSTN, which could be one of the OA progression mechanisms in the middle cartilage zone.

OGN, also known as Mimecan, was upregulated in the middle zone during OA and it had protein-protein interactions with ASPN and collagens type XII and II. OGN was found to be upregulated at the mRNA level in the superficial zone in comparison to middle and deep zones of cartilage (Grogan et al., 2013). Moreover, it was upregulated in cartilage during necrosis of the femoral head (Liu et al., 2016). OGN peptides were generated following treatment of cartilage tissue with MMPs and ADAMTS-4/5 (Zhen et al., 2008). Crosstalk between OGN and ASPN could be one of the factors drivning changes in the middle zone during OA progression.

Clusterin (CLU) was downregulated in the middle zone during OA. This glycoprotein was in the middle of the protein-protein interaction network. CLU expression was previously found to be upregulated in early-stage OA cartilage, specifically in the middle zone (Connor et al., 2001) and with the disease progression CLU expression decreased. Furthermore, CLU may inhibit inflammation activated by TNFα, and silencing CLU in chondrocytes lead to accumulation of ROS and increase in MMP13 and COL10A1 (Tarquini et al., 2020). TIMP3 is one of the four members of tissue inhibitors of metalloproteinases and was less abundant in the middle zone of OA cartilage. At the gene expression level TIMP3 was upregulated in the OA cartilage, in contrast to other members of TIMPs (Kevorkian et al., 2004). The amount of TIMP3 protein extracted from normal cartilage was higher than in OA cartilage. Additionally, IL-1β and OP-1 treated chondrocytes demonstrated decrease of TIMP3 protein abundance, whereas TNFα and TGFβ treated cells lead to increase of TIMP3 (Morris et al., 2010). The downregulation of CLU in our study could be evidence of the disease progression at the later stages of OA. Furthermore, the high connectivity in the protein-protein network could mean that it plays a major role of OA progression cartilage.

Procollagen C-endopeptidase enhancer 2 (PCOLCE2) was downregulated in the middle zone of OA cartilage in comparison to the old group. PCOLCE2 similarly to PCOLCE links with collagens I-III. PCOLCE2 was highly expressed in non-ossified cartilage in developing tissues (Steiglitz et al., 2002), and PCOLCE2 was responsible for a glycosaminoglycan metabolic disorder subtype of OA (Yuan et al., 2020). The downregulation of PCOLCE2 during OA could be a result of a decrease in cartilage remodelling in the OA cartilage.

Cadherin 1 (CDH1) was downregulated in the middle zone of articular cartilage during OA. It was shown that CDH1 mediated calcium-dependant cell-cell adhesion and its downregulation at the gene and protein level were found in cancer, and promoted invasiveness (Starska et al., 2013). It can inhibit growth via suppressing β-catenin (Gottardi et al., 2001) and over-expression of CDH1 inhibited Wnt/β-catenin pathway in chondrocytes (Xu et al., 2016). Moreover, chondrocytes transfected with CDH1 demonstrated elevated expression of collagen II, SOX9 and ACAN. In our study CDH1 was downregulated along with THBS1, and this could be an evidence of a decrease in the production of essential ECM proteins in the articular cartilage.

Another protein that had connections with CDH1 in the protein-protein network was C-X-C motif chemokine ligand 12 (CXCL12), which was also downregulated in the middle zone during OA. CXCL12 binds to its receptors CXCR4 and CXCR7, which are located on chondrocytes. CXCL12 at high concentrations can induce cell death in chondrocytes (Wei et al., 2006). Furthermore, CXCL12/CXCR4 linkage can negatively regulate chondrogenesis by reducing SOX9 expression (Hu et al., 2017). The downregulation of CXCL12 in our study is contrary to cartilage destruction during the disease. However, the lower protein levels of this protein alone would not be enough to produce healthy articular cartilage in OA.

Finally, Serpins A1 and C1 along with THBS1 were downregulated in the middle zone of OA group, similar to the superficial zone. This could indicate the increase in the activity of MMPs in the middle zone during OA.

Overall, the changes in the protein abundance in the middle zone during OA demonstrate the higher activity of chondrocytes in the articular cartilage during disease within this layer. However, the activity of cartilage restoration could be hindered by the production of mineralised cartilage. This would lead to ossification and a decrease in the biomechanical properties of the tissue to withstand the loading. Moreover, the decrease in the abundance of Serpins could indicate in the activation of catabolic activity in the tissue driven by MMPs. The similarity of some of the protein patterns in the middle zone to the superficial zone could be explained by the close proximity, and the overlap during the collection of the zones during microdissection.

2.4.4 Proteome changes in the deep zone during OA

The protein-protein interaction network in the deep zone in OA revealed two distinct clusters. One of the clusters demonstrated overall upregulation in the deep zone during OA, and included Hyaluronan and Proteoglycan Link Protein 1 (HAPLN1). HAPLN1 links hyaluronic acid to ACAN, and thus plays a crucial role in cartilage homeostasis (Neame & Barry, 1993). Others found HAPLN1 gene expression was downregulated in damaged OA cartilage in comparison to the intact cartilage. At the protein level it was decreased in OA in comparison to normal cartilage (Dunn et al., 2016; Zheng et al., 2013). The contradiction of protein levels in our study in comparison to the results of other studies could demonstrate the specific changes in the deep zone, not in the whole cartilage tissue.

Other proteins in that cluster included Heparan Sulphate Proteoglycan 2 (HSPG2), Collagen type XI (COL11A1), FBN1 and MATN4, all of which were upregulated in the deep zone during OA. |A loss of HSPG2, also known as perlecan, in mice protected cartilage from post-traumatic OA (Shu et al., 2016). However, synovial mesenchymal cells extracted from HSPG2 knockout mice demonstrated a decrease in chondrogenesis and it could be regulated by affecting SOX9 (Sadatsuki

et al., 2017). These proteins demonstrate essential roles in the homeostasis of the articular cartilage. Sections of cartilage collected from the OA tissue were macroscopically intact, which could explain the activity of these proteins in the deep zone. Furthermore, the deep zones of the OA cartilage that do not have destruction of articular cartilage could be more protected from the catabolic activity in evident in the superficial and middle zones. FBN1 and collage type XI were shown to be involved in the cartilage ossification and this could be beneficial in the deep zone of articular cartilage in comparison to the superior zones.

A second cluster in the protein network of deep zone had similarly to the middle zone. CXCL12 was downregulated in the deep zone during OA. Another protein downregulated in the OA group in comparison to the old group was TNFRSF11B (Osteoprotegerin). There was a loss of this gene in mice which demonstrated an age-related cartilage loss and the appearance of bony tissue (Liang et al., 2011). Addition of TNFRSF11B to chondrocytes downregulated ADAMTS-5 and induced expression of TIMP-4 (Feng et al., 2013). This could indicate the overlap with the middle zone and similar processes ongoing during disease in the deep zone.

Members of annexin family, specifically ANXA2/5/6, were upregulated in the OA group in the deep zone in comparison to the old group in our study. ANXA2 and ANXA5 were upregulated in the upper zone of degrading OA cartilage, which in turn may have led to mineralisation of the tissue (Kirsch et al., 2000). ANXA6 can regulate Wnt/β-catenin and NF-kB pathways and overexpression of ANXA6 can increase catabolic markers in an OA model (Campbell et al., 2013; Minashima & Kirsch, 2018). In contrast to the first cluster this cluster of proteins included ANXA proteins demonstrating the possibility of catabolic activity even in the deep zone of intact cartilage during OA. This could suggest an initiation of cartilage destructive processes in the deep levels of the cartilage.

Peroxiredoxin (PRDX1) was upregulated in the deep zone of articular cartilage during OA. PRDX1 plays an important role in protecting cells from oxidative stress, moreover, it regulates osteogenesis in BMP signalling-dependent manner in pre-hypertrophic chondrocytes (Kumar et al., 2018). GAPDH, PKM, PGM1 and LDHA proteins are part of the glycolysis and glycogenesis pathways. Upregulation of these proteins may suggest increased metabolic activity during OA in the deep zone.

Overall, changes at proteome level in the deep zone during OA demonstrated the possible chondrocyte activity and ECM production. However, the ossification process was activated in the deep zone as in the superficial and middle zones. Normally, the close proximity of deep zone to the underlying subchondral bone could indicate the activity of proteins involved in ossification and hypertrophy of the articular cartilage in that zone. As the upregulation of the protein cluster including HAPLN1 might indicate restoration and homeostasis of cartilage with ANXA proteins demonstrating possible catabolic activity in the deep zone.

2.4.5 Superficial zone ageing

Oxidative stress is one of the key factors leading to cartilage degeneration during OA. Superoxide dismutase (SOD) was downregulated in the superficial zone in the old group in comparison to young group. SOD activity decreases in OA cartilage, moreover, there was a negative trend of SOD activity in cartilage during ageing (Koike et al., 2018). Here SOD3 and SOD1 abundance was lower in the superficial zone during ageing, which may indicate a decrease in antioxidant protection with ageing.

High-temperature requirement A serine peptidase 1 (HTRA1) was upregulated in the superficial zone during ageing. HTRA1 is a serine protease found to be upregulated in OA cartilage; however, HTRA1 demonstrated higher presence in the deep zone of cartilage (Tocharus et al., 2004; Wu et al., 2007). Furthermore, HTRA1 can inhibit TGFβ signalling pathway via its protease activity. This could demonstrate the possible decrease in the production of ECM in the superficial zone, as TGFβ signalling pathway is involved in the homeostasis of articular cartilage.

Collagen VI helices were downregulated in the superficial zone during ageing. It is mainly found in the pericellular matrix. It was found that Collagen VI was not present in chondrocytes expressing HTRA1, and this could indicate the involvement of HTRA1 in pericellular matrix degeneration (Polur et al., 2010).

In the superficial zone of the old group TGFBI had the lowest level of expression in comparison to both young and OA groups. TGFBI is present in the early stages of chondrogenesis, thus suggesting the presence of active chondrocytes in the young and OA cartilage in comparison to the old cartilage.

Tenascin-XB (TNXB) was downregulated in the superficial zone during ageing. TNXB is a glycoprotein involved in maintaining collagen matrix structure. TNXB deficiency has been associated with the connective tissue disorder Ehlers-Danlos syndrome (Kaufman & Butler, 2016). Moreover, in a proteomics study it was significantly more abundant in the superficial layer of the cartilage (M. F. Hsueh et al., 2016). This points to an age-related dysregulation of the collagen matrix structure.

Overall, it was evident that in the superficial zone in old cartilage versus young cartilage there was a reduction in proteins involved in chondrogenesis. Ans SOD family protein abundance also decreased this indicates a reduced ability for the superficial layer to withstand oxidative stress in ageing. However, it also appears from our proteomics results that ossification of cartilage could be decreased in ageing in the superficial zone. Furthermore, the pericellular matrix that surrounds chondrocytes is also dysregulated in the superficial zone of ageing cartilage.

2.4.6 Middle zone ageing

In the middle zone similarly to the superficial zone collagen VI, FBN1, TNXB were downregulated, whereas HTRA1 and SERPINE2 were more abundant during ageing. TIMP3, CDH1 and CXCL12 were significantlyhigher in the old group when compared to both young and OA groups. This indicates similarities shared by young and OA cartilage which could point to the higher activity of chondrocytes in young and OA cartilage in comparison to the old cartilage.

Growth differentiation factor 10 (GDF10) was upregulated in the middle zone of old group in comparison to the young group. GDF10 was downregulated in OA articular cartilage and was associated with disease severity (Chou et al., 2013). GDF10 may play an important role in cartilage homeostasis and is regulated by SOX9 (Lafont et al., 2008). Significantly, high abundance of protease inhibitors (SERPINE2, TIMP3) demonstrated protection of the matrix from enzymatic degradation during ageing. However, as it was noted previously that CDH1 could inhibit growth and CXCL12 could negatively regulate chondrogenesis. Processes during ageing in articular cartilage suggest the inhibition of enzymatic digestion of matrix, although the chondrocyte might be in an inactive state. Thus, cartilage matrix may not be being restored by synthesising new proteins. Together this could indicate a decrease in catabolic activity during ageing in the middle zone. However, similar to the superficial zone it seems that the pericellular zone is also compromised during ageing in the middle zone.

2.4.7 Deep zone ageing

Collagen XI and X were downregulated in the deep zone during ageing in our study. Collagen XI maintains the architecture of collagen fibrils and plays an essential role in endochondral ossification (Hafez et al., 2015). Collagen X is a known chondrocyte hypertrophy marker and it can be regulated by the transcription factor RUNX2 and also by COX-2 (Gu et al., 2014). ANXA2 upregulation can also lead to mineralisation. Together these findings suggest a decrease of mineralisation during ageing in the deep zone. Similar to the superficial and middle zones FBN1 was in reduced abundance in the old group in comparison to the young group. TNFRSF11B was upregulated during OA in the deep zone, however, this protein had the highest abundance in the old group. TNFRSF11B may induce TIMP4 expression, thus protecting the cartilage from degradation (Feng et al., 2013).

CXCL12 and CDH1 were abundant in the deep zone in the old group, similarly to the middle zone. Protein Disulfide Isomerase Family A Member 3 (PDIA3) was downregulated in the deep zone of the old group in comparison to the young group. PDIA3 was shown to be involved in skeletal system development, and deficiency in it led to malformation of the tibia in mice (Y. Wang et al., 2014).

MMP2 is known to be upregulated in the OA cartilage (Zeng et al., 2015), however, in our study MMP2 was found to be upregulated during the ageing in the deep zone. Nonetheless, TIMP3 was upregulated in the deep zone during ageing and this could be an indication of an ongoing attempt at inhibition of cartilage destruction in the deep zone during ageing Our findings suggest that the deep zone has the highest catabolic activity within articular cartilage during ageing.

Overall, our proteomics results suggest that the deep zone of articular cartilage during ageing displays a dysregulation in maintaining the features of deep zone articular cartilage as Collagens X and XI were downregulated. Also, the high abundance catabolic marker MMP2 could indicate the destruction of cartilage tissue in this zone. However, the upregulation of TIMP3 could counteract to MMPs activity and upregulation of TNFRSF11B could indicate the activation of TIMP4. Nevertheless, the activation of both catabolic enzymes and their inhibitors might point to the a destructive processes in the deep layers of cartilage tissue. The increase of CDH1 in the deep zone could result in an inhibition of Wnt/β-catenin signaling pathway. In articular cartilage, activation of the Wnt/β-catenin pathway promotes the differentiation of chondroprogenitor cells into mature chondrocytes, which are the cells that produce and maintain the ECM of cartilage. Additionally, Wnt/β-catenin signaling has been shown to regulate the expression of key cartilage matrix genes such as Aggrecan and Collagen II, and to promote the survival of chondrocytes under conditions of mechanical loading or injury (Wang et al., 2014).

There are a number of limitations in this study. The superficial, middle and deep zone were collected using LMD, which means the zones were selected visually on the appearance mainly of the chondrocytes. Cartilage sections were not stained as it made more difficult for sections to adhere to the membrane of the slide. The thickness of articular cartilage differed between the donors, thus some of the donors could have deeper layers present in the sample. However, deep zone was always distinguished by the columnar appearance of chondrocytes in tissue. The close proximity of the zones there means there could be some overlap between adjacent zones. In general, separating the zones and analysing proteome between the zones could enabled us to explore zone specific differences during ageing and disease. Another of the limitation of this study was the cartilage tissue itself, as it contained high amounts of ECM proteins which could mask less abundant cellular proteins that are in the tissue. This was addressed to some extent in Chapter 4 in which we undertook proteomic on cells derived from different cartilage zones.

2.5 CONCLUSION

In conclusion, proteomic analysis enabled us to look into changes at protein level that are occurring during OA and ageing. The separation of superficial, middle and deep zone showed some

similarities and differences between different zones upon disease and ageing. From our data it is evident that during OA chondrocytes are more active in comparison to the old group. This suggests that cartilage tissue is being restored upon destructive changes of the disease. However, there is a high proportion of proteins involved in mineralisation of the cartilage tissue in the superficial and middle zones during OA, which could mean the new cartilage synthesised in the tissue does not have proper biomechanical features. Overall, this would suggest the new cartilage tissue could not maintain the homoestasis and upon loading will lead to further destruction.

In contrast, during ageing protein interactions network point to the decrease in chondrocyte activity for cartilage matrix turnover. Also, pericellular matrix surrounding the chondrocytes during ageing is dysregulated, suggesting the chondrocytes surrounding environment is compromised. Furthermore, the decrease in the ability to tackle oxidative stress via SOD family members could point to the stressful environment in the superficial zone in old articular cartilage. Although, there was not any indication of catabolic activity in the superficial and middle zones of articular cartilage during ageing, it was found that both TIMP and MMP protein members were upregulated. This could point to the destructive processes of catabolic activity start from the deep zone in normal articular cartilage during ageing.

Considering all of the above it seems during OA chondrocytes are activated to produce more ECM, however, the matrix does not possess the optimal features of healthy cartilage. Whereas, during ageing chondrocytes are inactive, meaning the protein turnover is inhibited and matrix cannot be restored upon continuous loading during movement. The destructive catabolic activity is high in the deep zone during ageing, while during OA the catabolic activity is higher in the superficial zone.

However, overall our study provides novel knowledge for future investigation of individual proteins in the respective zones. The information could also be used to assess the artificial cartilage tissue made in the laboratory and for future transplantation.

CHAPTER 3

Transcriptome changes within the zones of articular cartilage during OA and ageing

3.1 Introduction

RNA sequencing (RNAseq) is a high-throughput technology that allows for the quantitative analysis of the complete transcriptome of a tissue or cell type, providing insight into the gene expression profile of that sample. It has been widely used to investigate the molecular mechanisms underlying various diseases and physiological processes in different tissues, including articular cartilage.

RNAseq was utilized by Kalamegam et al. (2019) to discover differentially expressed genes (DEGs) in OA cartilage relative to healthy cartilage. The study revealed 1,018 upregulated and 524 downregulated genes. Matrix metalloproteinase 13 (MMP13), interleukin-1 beta (IL1B), and chemokine (C-C motif) ligand 5 were among the most highly elevated genes (CCL5). Among the genes most significantly downregulated were collagen type II alpha 1 chain (COL2A1), aggrecan (ACAN), and SOX9. In another study Liao et al. (2020) examined the molecular pathways causing cartilage degradation in OA. Their research uncovered 4,287 DEGs between OA and healthy cartilage. MMP13, IL1B, and prostaglandin-endoperoxide synthase 2 (PTGS2) were amongst the genes with increased expression. Among the genes that were downregulated were COL2A1, ACAN, and SOX9.

Gene expression profiling of human chondrocytes subjected to cyclic tensile stress was assessed using RNAseq. In response to cyclic tension, the study found 2,876 DEGs. Transforming growth factor beta 1 (TGFB1), vascular endothelial growth factor A (VEGFA), and IL1B were among the genes that were elevated. Among the genes that were downregulated were COL2A1, ACAN, and fibromodulin (FMOD) (Zhang et al. (2020)). Ruan et al. (2021) investigated the gene expression profile of human articular cartilage in response to interleukin-17A using RNAseq (IL-17A). The study revealed 333 upregulated and 92 downregulated genes. Among the most significantly elevated genes were chemokine (C-X-C motif) ligand 1 (CXCL1), CXCL2, and CXCL3. Among the most significantly downregulated genes were COL2A1, ACAN, and SOX9.

In a synovium study Leong et al. (2017) found 1,665 DEGs between samples from people with normal joints and those with OA. MMP13, IL6, and IL8 were among the top genes that were upregulated, while COL1A1 and TIMP3 were among the top genes that were downregulated. In another study Ren et al. (2019) found 3,561 DEGs between samples of human articular cartilage that were normal and samples that had OA. MMP13, ADAMTS5, and IL1B were among the genes that changed the most and COL2A1 and ACAN were among the genes that changed the least.
Similar results were obtained by Liu et al. (2021), where they found 470 DEGs between samples of human articular cartilage that were normal or had OA. MMP13, TNFAIP6, and SIRT1 were among

74

the genes that changed the most and similar to the Liu et al study COL2A1 and ACAN were among the genes that changed the least.

RNA sequencing (RNAseq) is a potent technique that offers numerous advantages over conventional methods of gene expression research. RNAseq can identify novel transcripts that are absent from existing gene databases which allows for the identification of new pathways and targets that could be utilized in the creation of novel therapies. Furthermore, the great sensitivity of RNAseq enables the discovery of low-abundance transcripts that may be missed by microarray-based gene expression analyses. Its sensitivity enables the discovery of genes that play a crucial role in the aetiology of OA but may be missed by conventional approaches.

Articular cartilage consists of several zones, each with a unique makeup of cells and extracellular matrix. These zones are the superficial, middle, and deep layers. To comprehend the molecular mechanisms of cartilage growth and degeneration, it is vital to examine the gene expression patterns of these zones. RNAseq has been utilized in a number of studies to explore the gene expression patterns of distinct articular cartilage zones. RNAseq was undertaken on articular cartilage samples from patients with OA and healthy controls, revealing significant changes in gene expression patterns between the cartilage's superficial and deep zones. In addition, they found a number of DEGs that were enriched for pathways linked to extracellular matrix organization and cell adhesion, indicating a crucial role for these processes in the aetiology of OA (de Andrés MC et al., 2015). The study identified 1,254 DEGs in OA compared to healthy controls, with 805 upregulated and 449 downregulated genes. Among these DEGs, 234 genes were differentially expressed in the superficial zone, 184 genes in the middle zone, and 1,049 genes in the deep zone. The study also found significant differences in gene expression patterns between the different zones of the articular cartilage.

RNAseq was employed in another study to explore the gene expression patterns of distinct articular cartilage zones during development. They discovered significant changes in gene expression patterns between the superficial and deep zones of the cartilage, with the superficial zone displaying higher expression of genes involved in extracellular matrix assembly and cell adhesion. This study also found a number of DEGs involved in chondrocyte differentiation and maturation, indicating that these processes play a crucial role in cartilage development (Bonnin et al., 2019). A third study investigated the gene expression patterns of distinct articular cartilage zones in response to mechanical loading using RNAseq. There were significant changes in gene expression patterns between the superficial and deep zones of cartilage. In addition, a number of DEGs implicated in mechanotransduction and extracellular matrix remodelling were identified, indicating a crucial role for these processes in the response of articular cartilage to mechanical loading (Li et al., 2019).

There are several alignment tools to analyse RNAseq data. In our study we have used STAR, Tophat2, HiSat2 and Salmon tools to align RNAseq to the human genome. There some differences in the algorithms used for the analysis, thus depending on the dataset some of the tools could be more preferential.

STAR

In 2013, STAR, a prominent RNA-seq alignment tool, was initially introduced. STAR's capacity   y to align spliced reads, which are formed when introns are deleted from RNA transcripts during post-transcriptional processing, is one of its key strengths. STAR can also detect novel splice junctions, making it a helpful annotation tool for transcriptomes. Moreover, STAR has a high rate of accuracy and can process both short and lengthy reads. However, STAR demands a large amount of computational resources, and its accuracy might be impacted by the reference genome's quality.

Tophat2

Tophat2, which was first introduced in 2012, is another prominent RNA-seq alignment tool. Tophat2 is designed to handle spliced reads and uses a two-step alignment approach to do this. First, the reads are aligned with the reference genome to ascertain their approximate locations. The algorithm then identifies probable splice junctions and aligns the readings across these junctions. Tophat2 can also discover novel splice junctions and is typically faster than STAR. It has been demonstrated that Tophat2 is less accurate than STAR and produces more false positives.

HISAT2 (Hierarchical Indexing for Spliced Alignment of Transcripts)

HISAT2 is a fairly new tool for aligning RNA-Seq data. It was first used in 2015. HISAT2, like STAR and Tophat2, can process spliced readings, but its alignment technique is based on hierarchical indexing. This strategy enables HISAT2 to align reads more rapidly than previous alignment tools while retaining a high level of precision. HISAT2 is able to detect novel splice junctions and can process both short and long reads. HISAT2 requires a substantial amount of RAM, which may limit its applicability in certain computational environments.

Salmon

Salmon is an alignment tool for RNA-seq that was originally introduced in 2017. Salmon aligns reads to a reference transcriptome as opposed to a reference genome, unlike the other alignment methods. Salmon is able to reliably assess gene expression levels even in the absence of a reference genome thanks to this technique, which makes it substantially faster than other alignment tools and

enables it to operate in the lack of a reference genome. Salmon is unable of recognizing novel splice junctions and may yield less accurate results when matching reads to an inadequate or erroneous reference transcriptome.

In this chapter we determined the trancriptome of articular cartilage in the superficial, middle and deep zones during OA and ageing. We employed LMD technique to obtain three different from each cartilage sections. The aim of this work is to investigate the zonal differences during OA and ageing at the gene expression level.

3.2 MATERIALS AND METHODS

3.2.1 Human articular cartilage samples

Human articular cartilage was used with Liverpool Musculoskeletal Biobank under Health Research Authority approval (Sponsor Ref:UoL001398) and Clatterbridge Hospital, Wirral following ethical approval (IRAS ID 242434). The same cartilage samples used in the proteomics study from non-OA donors were used for RNA-seq experiments described in this chapter. However, two samples from the OA group used in the proteomics study were replaced, due to low RNA integrity number (RIN). In total three groups were analysed, each group had samples from five donors. Young group had mean age of 32±3.7 (mean±SD), old group 71.6±3.4, and OA group 77.2±7.8 years old. Mean body mass index (BMI) of the young group was 27.1±3.0, old group 25.0±0.9, and OA group 26.4±3.5.

3.2.2 Cartilage sample collection

Cartilage samples were handled in the same way as per the proteomics study. Cartilage samples were stored at -80°C and were kept frozen at all times during handling prior to LMD.

3.2.3 RNA extraction from the cartilage sections

To minimise RNA degradation and improve the amount of total extractable RNA cartilage samples were cryosectioned before proceeding with RNA extraction. Cryostat chamber temperature was set at -20°C and specimen holder temperature at -21°C, thus cartilage tissue was kept frozen at all times. Cartilage samples were placed into the cryostat and 20 sections at 10μm thickness were cut in the coronal plane. Sections were collected into 1.5ml Eppendorf tubes and were stored at -80°C until RNA extraction. To identify the most optimal RNA extraction method from cartilage two methods were used: RNeasy micro kit (Qiagen) and RNAqueous micro total RNA isolation kit (Invitrogen) and RIN was assessed. For both methods the manufacturer's instructions were followed.

3.2.4 RNA integrity assessment of cartilage samples

High RNA quality is essential for RNAseq experiments as degraded RNA could fail the library preparation and subsequent sequencing results. RIN is a standardised number from one to ten, one being the poorest and ten the highest RNA integrity. RIN is calculated based on 28s and 18s rRNA ratio, they have approximately 5kb and 2kb length respectively. rRNA makes up the majority of total RNA in cells (80%), thus a good indicator of RNA quality. Extracted RNA quality was assessed using Tapestation 2200 (Agilent Technologies) instrument and High Sensitivity RNA ScreenTape kit (Agilent Technologies). The ScreenTape had quantitative range of 500-10,000pg/μl and RIN functional range of 1,000-25,000pg/μl. The manufacturer's instructions for High Sensitivity RNA ScreenTape kit were followed.

3.2.5 Cryosection for LMD

Cryosection was carried out under the same conditions described in LMD proteomics study. However, cartilage sections were collected on RNase-free steel frame slides with PET membrane (1.4 μm) (Leica Microsystems). Tissue on slides were collected on the day before LMD, slides were stored at -80°C.

3.2.6 LMD of different cartilage zones

LMD parameters of the cartilage sections were the same as described in LMD proteomics study. The difference was in the buffer used for collection of microdissected specimen from the cartilage sections, which were collected into 60μl of lysis buffer RLT from RNeasy micro kit. Further, for collection of three zones 30 minutes time-frame was set per slide to reduce RNA degradation, as LMD was performed at room temperature. Tubes with microdissected samples were placed onto dry ice straight away and stored at -80°C until RNA extraction.

3.2.7 RNA extraction for RNA-seq

The solution with microdissected samples was brought to the bottom of the tube by brief centrifugation the tubes. Volume of the solution was brought up to 350μl with RLT buffer and the protocol described in the section 4.3.4 for RNeasy micro kit was followed. Afterwards RNA integrity was assessed as described in the section 4.3.5 using Tapestation 2200 instrument.

3.2.8 Library preparation and RNAseq

Extracted RNA was transferred to the Centre for Genomic Research (CGR) at the University of Liverpool where library preparation and RNAseq was performed by a CGR employee. The

following procedure was carried out for library preparation and sequencing. 45 samples were submitted for sequencing using NEBNext® Single Cell/Low Input RNA Library Prep Kit for Illumina®. The NEBNext® Single Cell/Low Input RNA Library Prep Kit for Illumina® uses a template switching method to generate full length cDNAs directly from single cells or 2 pg – 200 ng RNA, followed by conversion to sequence-ready libraries using the Ultra™ II FS workflow. Essentially 200pg of total RNA estimated by Bioanalyser was used per sample in the template switching reaction and the cDNA generated was amplified by 14 cycles of PCR. After accessing the quality of this on the Agilent Bioanalyser. This cDNA was fragmented, adapter ligated and barcodes added by a further 14 cycles of amplification. Libraries were accessed by Qubit assay and Bioanalyser and normalised in a pool of all the samples equally represented.

The final pool was assessed by qPCR using the Illumina Library Quantification Kit from Kapa on a Roche Light Cycler LC480II according to manufacturer's instructions. The template DNA was denatured according to the protocol described in the Illumina cBot User guide and loaded at 300 pM concentration. To improve sequencing quality control 1% PhiX was spiked-in. The sequencing was carried out on five lanes of an Illumina HiSeq 4000 with version 1 chemistry generating 2×150 bp paired end reads.

Initial processing and quality assessment of the sequence data was performed using an in-house pipeline (developed by Dr Richard Gregory). Briefly, basecalling and de-multiplexing of indexed reads was performed by CASAVA version 1.8.2 (Illumina) to produce 45 samples in FASTQ format. Flexbar v3.3.0 was used to remove the adapter sequences, the reads were further trimmed to remove low quality bases using Sickle version 1.200 with a minimum window quality score of 20. Remaining reads shorter than 20 bp were discarded of (Dodt et al., 2012).

3.2.9 Quality control (QC) of the reads

MultiQC v1.7 (Ewels et al., 2016) was used to assess the reads and select samples for the differential gene expression analysis. Reads were aligned to the Human genome gencode version 31 using STAR version 2.7.2b (Dobin et al., 2013). Genome indexes for STAR were generated using gencode version 31, --sjdbOverhang was set to 149. Reads were counted using featureCounts from Subread package version 1.6.5 (Liao et al., 2014) and differential gene expression analysis was carried out using DESeq2 package version 1.6.2 (Love et al., 2014) in R version 4.0.0. Differentially expressed (DE) genes were selected with p adjusted values of less than 0.05.

3.2.10 Data visualisation

Multilevel PCA and biplots were generated using mixOmics package version 6.16.1 in R version 4.0.3. The top 500 genes by variance were used to generate plots.

3.2.11 Pathway analysis of DE genes

Pathway analysis was performed in Ingenuity Pathway Analysis (IPA) (Qiagen). GO analysis was performed using gProfiler with the same parameters as in the proteomics part. For validation of RNA-seq results the upstream regulators picked up by IPA specific for the superficial and deep zone in the OA group were studied. Genes for the OA deep zone were selected from the upstream regulators in IPA based on the prediction significance and novelty in the OA field. Genes for the superficial zone were selected using Significance Analysis of Microarrays (samr) for differential expression analysis package v3.0 in R. Genes from samr output for validation were selected on the basis of the high expression in the superficial OA group and novelty in the involvement with OA.

3.2.12 Chondrocyte extraction

Chondrocyte cell extraction was carried out using the following protocol provided by collaborator Professor Brian Johnstone. In a clean cell-culture hood, femoral condyles were placed into Petri dishes filled with phosphate-buffered saline (PBS). Using 8mm Biopsy punches (Medisave) areas with macroscopically intact cartilage surface were cut all the way down to the subchondral bone. Using surgical clippers ostechondral plugs were cut and placed into separate Petri dish filled with PBS. Articular cartilage was divided into thirds (Superficial 1/3, middle 1/3, and deep 1/3). Superficial and deep zone thirds were placed into their respective PBS filled Petri dishes. Cartilage tissue from the respective zones was cut into small pieces using sterile scalpel. Pronase (Roche) at the concentration 10mg/ml was dissolved in 3-4ml of low-glucose Dulbecco's modified Eagle medium (DMEM)(ThermoFisher) were added to 15ml Falcon tube and samples were transferred into the solution. Tubes were placed on a rotator and incubated at 37°C for 1 hour with moderate rotation speed. Pronase solution was removed from the tube and cartilage samples were rinsed with 2ml of PBS. 3-4 ml of the 1300 U/ml collagenase type 2 dissolved in DMEM was added to each tube and incubated with rotation at 37°C for 3 hours. The pieces of tissue at this point were diminished in size, and the chondrocytes dissociated from the cartilage matrix were in the collagenase-DMEM solution. Carefully using a P1000 pipette the solution containing the cells was passed through a cell strainer (40µm) fitted onto a clean 50ml conical tube. Strained cells were centrifuged at 500 x g for 5 min. Cells for tissue culture were resuspended in DMEM supplemented with 10% fetal bovine serum (FBS)(ThermoFisher), 1% Penicillin-Streptomycin (Pen-strep), and 0.2% Amphotericin. Cells were plated in T75 flask. Cells for freezing were resuspended in 1ml of DMEM/FBS/DMSO solution at proportion 4/5/1 and transferred into 1.5ml cryovials. Cells were frozen at -80°C overnight in a freezing container providing 1°C/min cooling rate of samples.

3.2.13 Tissue culture and collection of cells

Chondrocytes extracted from the superficial and deep zones that were frozen straight away or used for RNA extraction were labelled as 'native' chondrocytes. Chondrocytes were labelled 'unattached' when on the day after plating the cells media was replaced, and unattached cells were pelleted by centrifugation at 500 x g for 5min. Upon reaching confluence chondrocyte samples were labelled P0 and further passaging was labelled P1, P2, etc.

DMEM low glucose was used for cell culturing supplemented with 10% FBS, 1% Penicllin/streptomycin, and 0.2% fungizone, and media was changed three times a week. Upon reaching confluence chondrocytes were detached from the plastic using 5ml of trypsin for 5min at 37°C.

Chondrocytes extracted from the superficial and deep zones were either cultured until reaching confluence in the flask or RNA was extracted. These cells were treated as native chondrocytes. After plating the extracted cells on the next day media was changed and unattached cells were collected and labelled P0.

3.2.14 RNA extraction from cells

RNA from cells were extracted using TRIzol method (Invitrogen) using protocol provided by manufacturer with minor modifications. The RNA pellet was dissolved in 20μL RNase-free water.

The extracted RNA concentration and purity was measured using Nanodrop 2000 spectrophotometer.

3.2.15 cDNA synthesis

Total RNA was reverse transcribed into cDNA for mRNA quantification using the M-MLV reverse transcriptase (Promega, Southampton, UK). 500ng of total RNA was converted into cDNA. This was mixed with 0.5μL of random primers (Promega, Southampton, UK) and with nuclease-free water up to final volume of 18.3μL. This was incubated at 70°C for 5min to dissociate secondary RNA structures. Then, the mixture was mixed with 5μL of M-MLV 5X Reaction Buffer (Promega, Southampton, UK), 0.6μL of 25mM PCR Nucleotide Mix (Promega, Southampton, UK), 0.6μL of RNasin(R) Plus RNase Inhibitor (Promega, Southampton, UK) and 0.5μL M-MLV Reverse Transcriptase, up to final volume of 25μL. The final mixture was mixed well and incubated at 37°C for 60min for reverse transcription. Reverse transcriptase was inactivated at 93°C for 5min and cDNA stored at -20°C.

3.2.16 qPCR for gene expression analysis

mRNA amplification by qPCR was carried out using the QuantiTect SYBR Green PCR Master Mix (Qiagen, Manchester, UK). Primers were either designed by the author or OriGene (OriGene, Herford, Germany) and synthesised by Eurogentec (Seraing, Belgium), or designed and synthesised by Primerdesign (Chandler's Ford, UK). cDNA was diluted with nuclease-free water at a working concentration of 2.5ng/μL. Eurogentec forward and reverse primers were mixed and diluted at a working concentration of 20μM per primer. Primerdesign primers were resuspended as a primer mix at a working concentration of 6μM. In a 96-well Semi-Skirted PCR Plate, the following were added per well: 4μL of diluted cDNA (10ng per reaction), 5μL of QuantiTect SYBR Green PCR Master Mix, 0.2μL of Eurogentec primer mix (final concentration in reaction: 400nM) or 0.67μL of Primerdesign primer mix (final concentration in reaction: 400nM). Nuclease-free water was added up to 10μL final volume per reaction. Each reaction was set up in duplicate or triplicate. MRNA amplification was carried out by a LightCycler® 96 Instrument under the following cycling conditions:1 cycle of: 95°C for 15min, for HotStarTaq DNA Polymerase activation; 45 cycles of: 94°C for 15sec, for double strand dissociation; 55°C for 30sec, for primer annealing 70°C for 30sec, for strand elongation; Melting curve: 95°C for 10sec, 65°C for 60sec, 97°C for 1sec (acquisition mode: continuous). mRNA expression was calculated using the 2 -ΔCT method (Livak & Schmittgen, 2001), relative to the appropriate reference genes.

3.2.17 Reference gene selection for qPCR gene expression normalisation

Candidates for reference genes were selected from RNAseq results after DE analysis in Deseq2. Coefficient matrix from Deseq2 was extracted for each group and on the log scale standard deviation (stdev) was calculated. Genes with stdev less than 0.4 were used for reference gene selection. Moreover, candidate genes were selected on the basis of high expression in the samples which had high numbers of counts.

RefFinder (Xie, Xiao, Chen, Xu, & Zhang, 2012) is a free online tool used to select the best reference genes for qPCR gene expression normalisation between different sample groups. It integrates four different tools: geNorm (Vandesompele et al., 2002), Normfinder (Andersen, Jensen, & Ørntoft, 2004), BestKeeper (Pfaffl, Tichopad, Prgomet, & Neuvians, 2004), and the comparative Delta-C_T method (Silver, Best, Jiang, & Thein, 2006), to rank the best reference genes for the samples of interest. C_T values of the candidate genes were obtained after qPCR analysis in the sample groups of interest. These C_T values were input in the field provided on the online tool and analysed. RefFinder suggested the best reference gene based on each of the four programmes used, but also a comprehensive ranking that considers all four programmes together.

3.2.18 In situ hybridisation RNAscope

RNAscope employs novel *in situ hybridisation* method for detecting RNA in the intact cells within the tissue or cell pellet. In order to generate a signal from the RNA molecule adjacent two probes for the target gene need to hybridise to the RNA. Probes form a Z shape which has around 18-25 nucleotide at the base that hybridise to the target gene, and 14 base sequence at the top. The top part of the Z probe used as binding site for the pre-amplifier. Signal from RNA can be detected only when to adjacent Z probes hybridise to the target molecule. Afterwards amplifiers can bind to the pre-amplifier's binding site. In the final steps either fluorescent molecule or chromogenic enzyme would bind to the multiple sites of amplifiers and generates a signal in the form of dot within the cell. To validate the spatial distribution of gene expression in the articular cartilage AMTN, SEMA3A and FGFBP2 genes were selected. RNAscope® 2.5 HD RED detection kit and protocol provided by the manufacturer for fresh frozen tissue were used with minor modifications.

Cartilage samples were cryosectioned at the same conditions as described in Chapter 2. Tissue sections were collected onto Superfrost plus slides (Thermofisher), sections were dried at -20C for 1 hour, and stored at -80C prior to RNAscope sample preparation. After slides were taken from the freezer sections were immediately fixed using 4% paraformaldehyde (PFA) for 20 minutes at 4C. Followed by subsequent steps of dehydration in 50%, 70% and 100% ethanol, each step was performed at RT for 5 min. Slides were then dried for 5 min at RT and area around the tissue was outlined by Immedge™ hydrophobic barrier pen. To improve the adherence of sections to the glass slides they were incubated for 30 min at 37°C. Afterwards two drops of RNAscope® Hydrogen Peroxide was added per section and incubated at RT for 10 min. Followed by rinse in PBS and addition of 2 drops of RNAscope Protease IV per section, and incubated for 30 minutes at RT. At the end of incubation slides were briefly washed twice in PBS. Probes were pre-warmed at 40C for 10 min prior to adding them to the sections. Probes were hybridised for 2 hours at 40C in the HybEZ oven. Afterwards sections were taken from the oven and washed twice at RT for 2 min using RNAscope 1X Wash buffer. AMP1 was then added to sections and incubated at 40C for 30 min in the oven. After the incubation sections were washed with 1X Wash buffer as above. AMP2 was then hybridised for 15 min at 40C and washed as in the previous steps. Afterwards AMP3 was added to the sections and incubated for 30 min at 40C, followed by a wash step. AMP4 was added afterwards and hybridised for 15 min at 40C. At the end of incubation sections were washed as in the previous steps. All of the following steps were performed at RT. Two drops of AMP5 was added to each section and incubated for 30 min followed by a wash step. The final amplifier AMP6 was added to each section and hybridised for 15 min, the amplifier was washed off afterwards. To detect the signal Red Working Solution was prepared by using 1:60 ratio of Red-B and Red-A reagents. 40μL of Red Working Solution was added to each section and incubated for 10 min at RT. Immediately at the end of incubation period solution was discarded by tipping the slide to a waste container and slide was

immersed into tap water. Slides were then placed into a fresh tap water to wash the sections. Cell nuclei were stained with Gill's Hematoxylin I Solution (Sigma-Aldrich) for 2 min at RT. Afterwards slides were washed with tap water until slides are clear and sections remain purple. Slides were dried at 60C for 15 min, then the slides were briefly immersed into pure xylene and 1-2 drops of Ecomount were added to each section before xylene dried. Slides were left to dry in the fume hood overnight.

3.3 RESULTS

3.3.1 RNA extraction method optimisation and RNA integrity

RNA from the cartilage samples were extracted using RNeasy micro kit (Qiagen) and RNAqueous micro total RNA isolation kit (Invitrogen). RNA integrity was compared between the two methods using a Tapestation 2200 (Agilent).
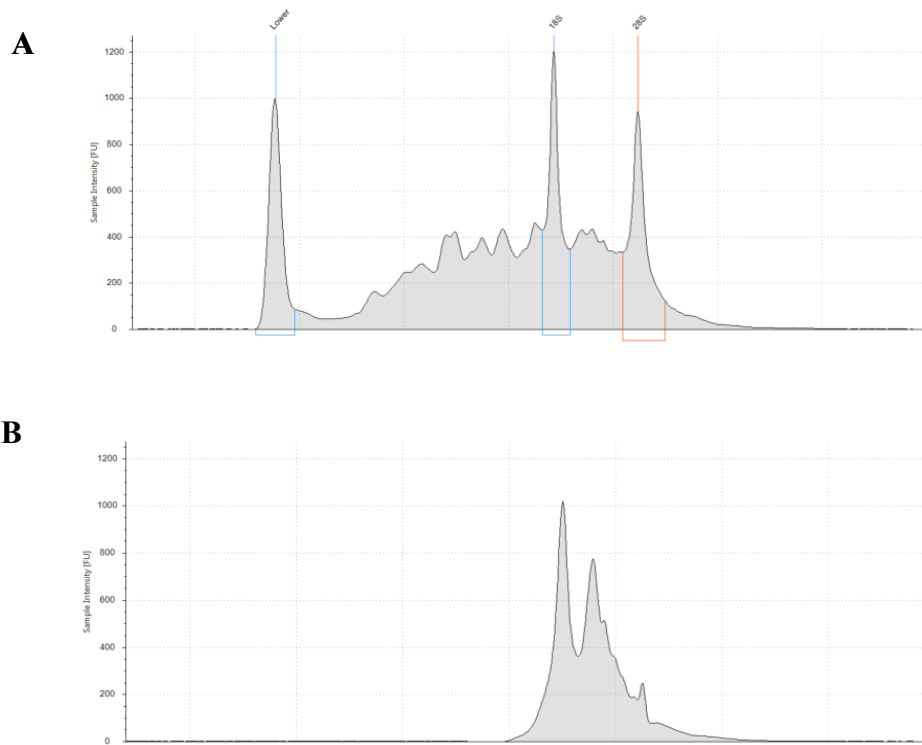
Figure 3.1: RNA integrity of the cartilage samples, two RNA extraction methods compared.
(A) RNeasy micro kit, RIN 5.9. (B) RNAqueous micro total RNA isolation kit, RIN measurement failed.

The RNeasy method demonstrated fair RIN of 5.9 in the cartilage sample. Two distinct peaks representing 18s and 28s rRNAs were seen on the electropherogram (Fig. 3.1A). Whereas RNAaqueous method failed to measure RIN due to poor resolution of the sample (Fig. 3.2B). This could be an effect of interfering particles in the sample with Tapestation reagents. Thus RNeasy micro kit was chosen as RNA extraction method for RNAseq.

Prior to LMD RNA integrity was checked in all samples by extracting RNA from full thickness cartilage. All of the samples had RIN > 6.5, except one sample with RIN 5.7 (Fig. 3.2A). Two samples from the OA group had low RIN < 3 (Fig. 3.2B), which points to the RNA degradation in the tissue. These samples were replaced with cartilage samples form OA patients undergoing TKA surgery, samples had a RIN > 7 (Fig. 3.2C).
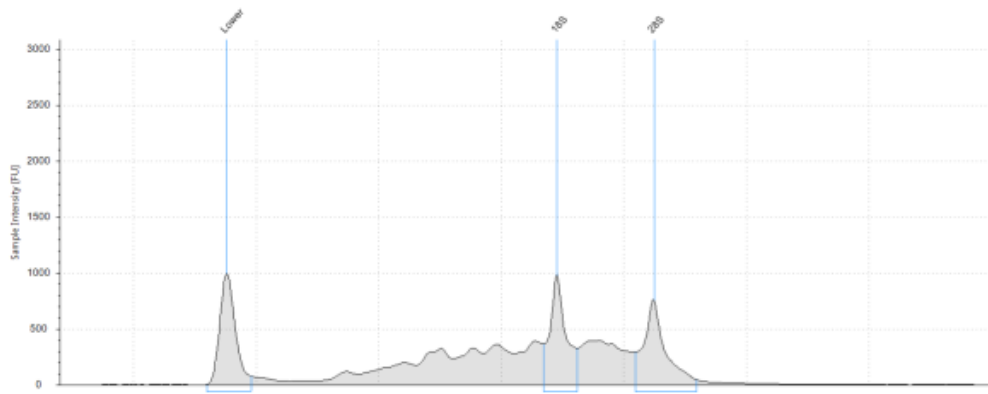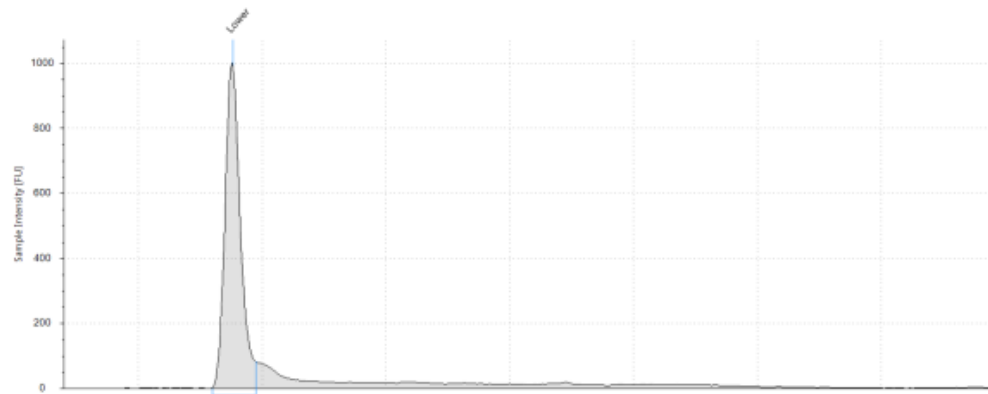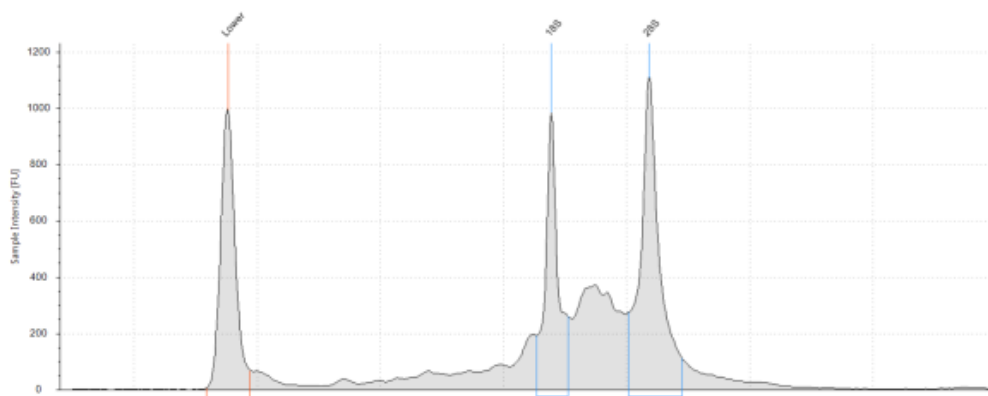
Figure 3.2: RNA integrity of cartilage samples. (A) Sample with the lowest RIN 5.7 included for RNAseq. (B) Sample from the OA group with RIN 2.9 which was replaced. (C) Sample with the highest RIN 8.5

3.3.2 LMD of the cartilage samples
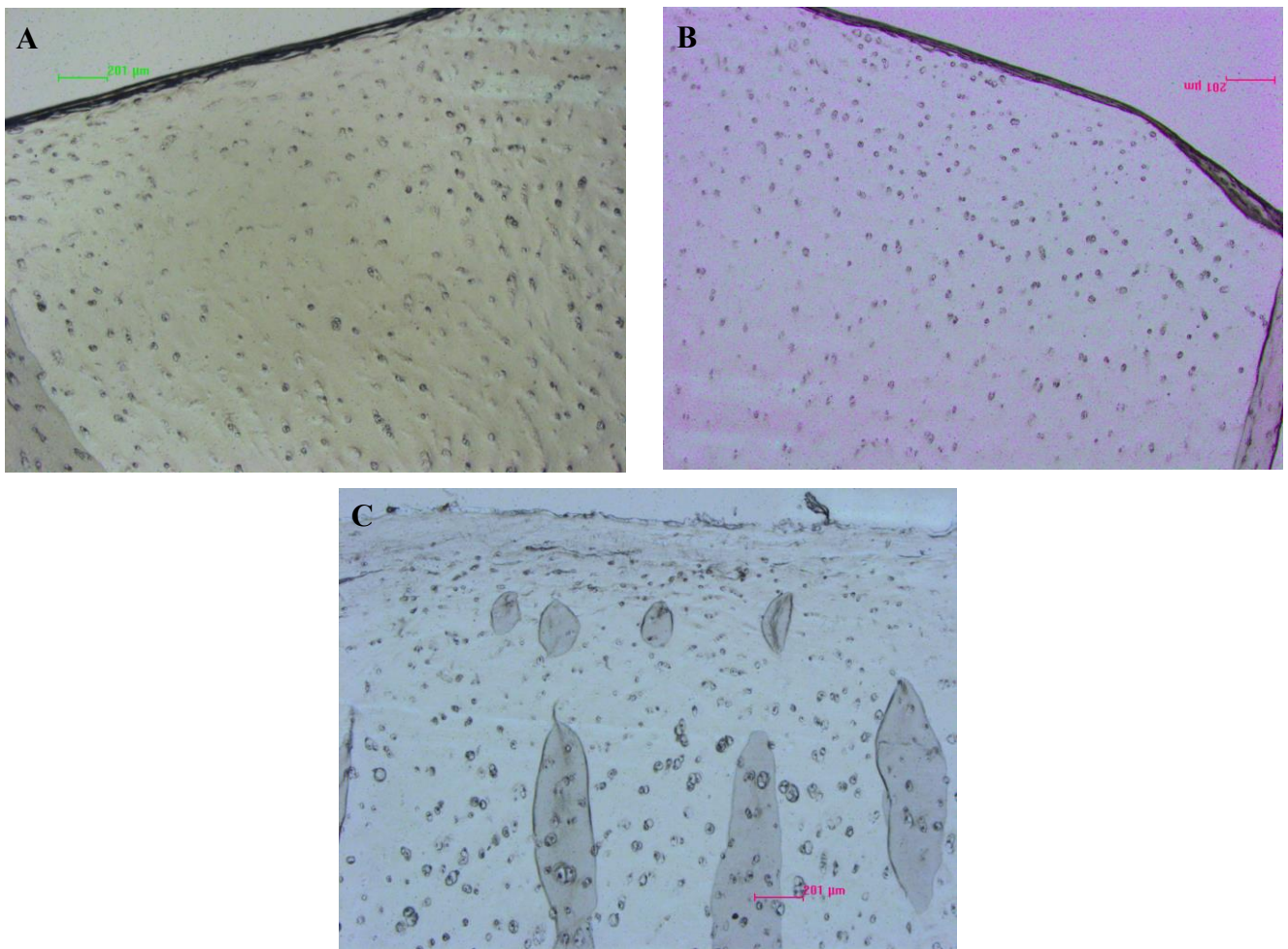
Figure 3.3: Cartilage sections under LMD microscope LMD7000 (Leica Microsystems).
Cartilage sections from the young(A), old (B) and OA (C) groups. Scale bar 201µm

LMD for RNAseq the time spent on acquiring each section was the foremost important factor to prevent RNA degradation. Thus, area collected for each sample varied, for the superficial zone area > 3×10^6 um^2 was collected. For the middle and deep zone area collected was around $8.5\text{-}21 \times 10^6$ um^2.

3.3.3 RNA extraction from LMD tissue

RNA from the LMD samples was extracted using RNeasy micro kit. RNA concentration and integrity were measured on Tapestation 2200. Quantitative range of High sensitivity RNA ScreenTape was 500-10000 pg/ul and RIN functional range was 1000-25000 pg/ul. In only a couple of samples' RNA concentration fell into that range and RIN was measured. All of these samples were derived from the superficial zone. Sample from the young group that had RIN 8 when full thickness cartilage was extracted from the tissue demonstrated RIN 7.8 in the superficial zone after LMD.

The superficial zone showed highest RNA concentrations in comparison to the middle and deep zones. While the area collected from the superficial zone was significantly less in comparison to other zones.

Table 3.1 Area of tissue microdissected from each cartilage zone and extracted RNA concentration

Zone	Area collected, mean (µm2)	RNA concentration, mean (pg/µl)
Superficial	5,159,097	162.9
Middle	20,850,145	115.9
Deep	21,465,281	109.9

3.3.4 QC of the reads

Quality control of the sequence reads was assessed using MultiQC tool. Quality of the reads can be assessed based on the sequence counts, quality scores, GC content and overrepresented sequences. Reads from the five samples were discarded due to high GC content per sequence and high percentage of overrepresented sequences (Fig. 3.5). Of these five samples two were superficial OA and three from superficial, middle and deep zones of the same donor from the young group. Because of the pair-end sequencing each sample had two reads (R1 and R2), and the pair of reads were assessed independently. Overrepresented sequences in these samples were in the range of 18% and 37.5% of total reads. Whereas GC content per sequence peaked at 50% GC in these five samples. Deviation of values in these two parameters could be an indicator of overamplification of the same reads in the library.

A

FastQC: Overrepresented sequences

● Top over-represented sequence   ● Sum of remaining over-represented sequences

Created with MultiQC

B

FastQC: Per Sequence GC Content

Created with MultiQC
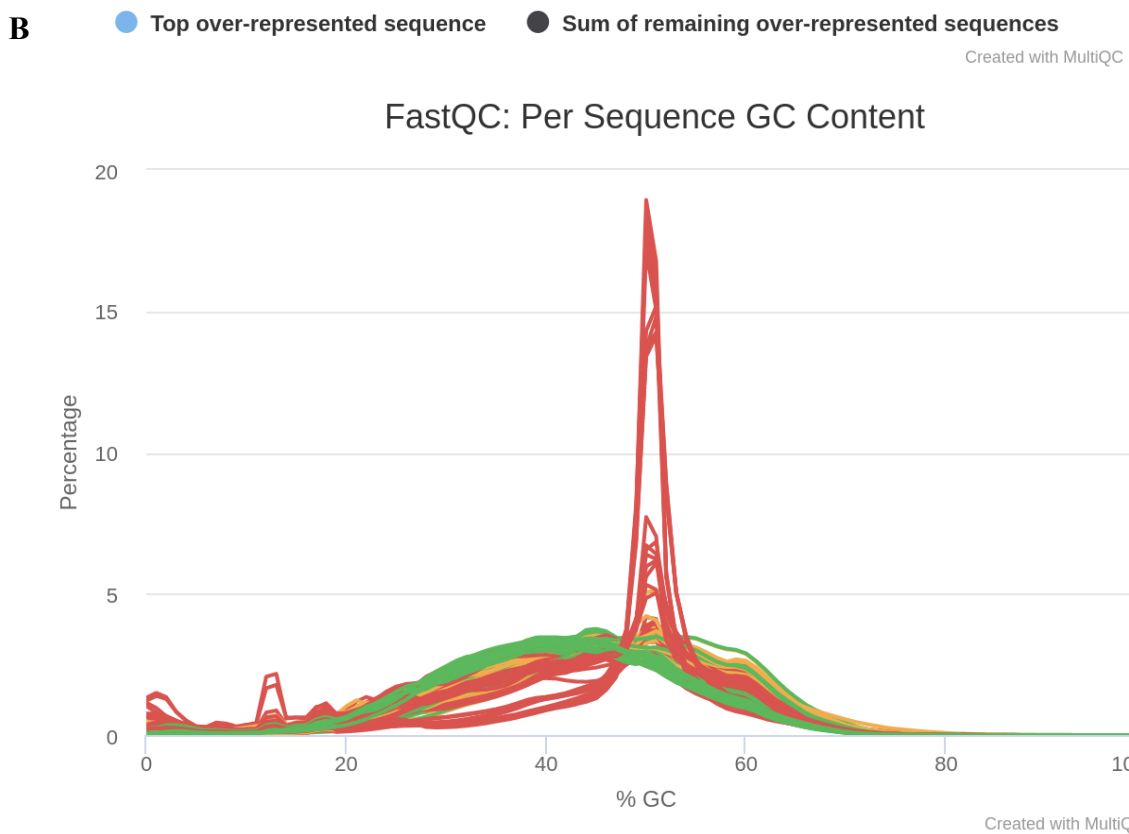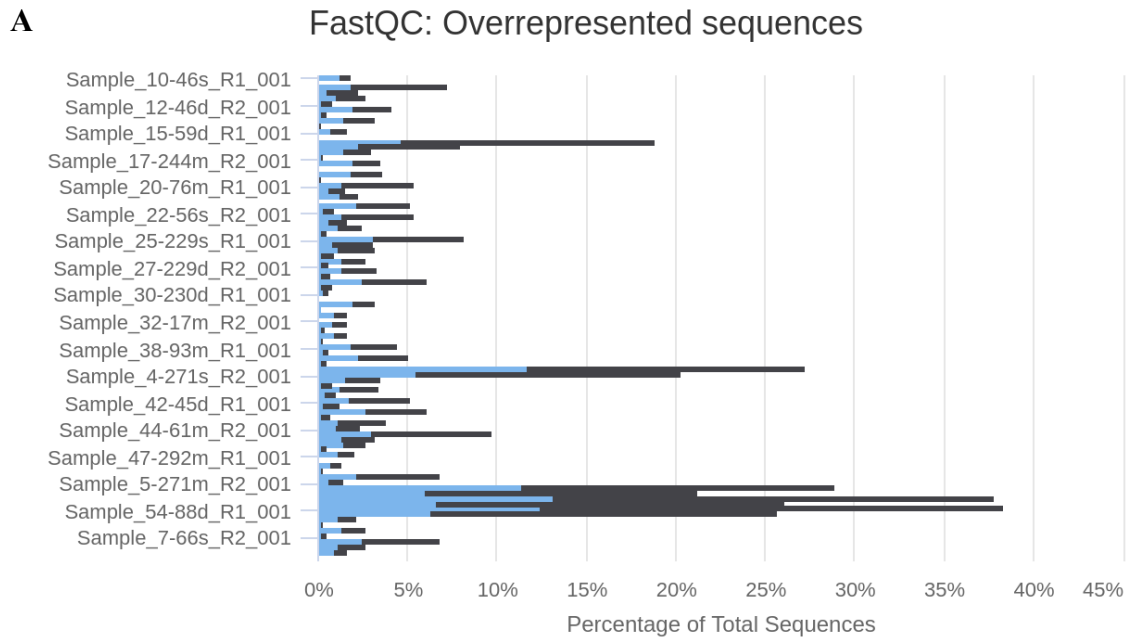
Figure 3.5 Quality control of the sequence reads. Each sample had a pair of reads (R1 and R2) due to the pair-end sequence method (A) Highest overrepresented sequences were identified in five samples (>10%): two superficial samples from the OA group and three sample zones from one young donor. (B) The same five samples had high percentage of per sequence GC content peaking at 50% GC.

3.3.5 Alignment of the reads to the genome

Prior to differential expression analysis reads had to be aligned to the human genome. Four different alignment methods were used: TopHat2 v1.2.0, HiSat2 v2.1.0, STAR v2.7.19 and mapping-based mode Salmon v1.3.0. STAR outperformed other alignment methods in terms of rate of successfully mapped reads to the genome (Fig. 3.6). However, TopHat2 was run using an older version of human genome Ensembl 84 which was released in March 2016, whereas the other three tools used gencode v31 human genome that was released in June 2019.
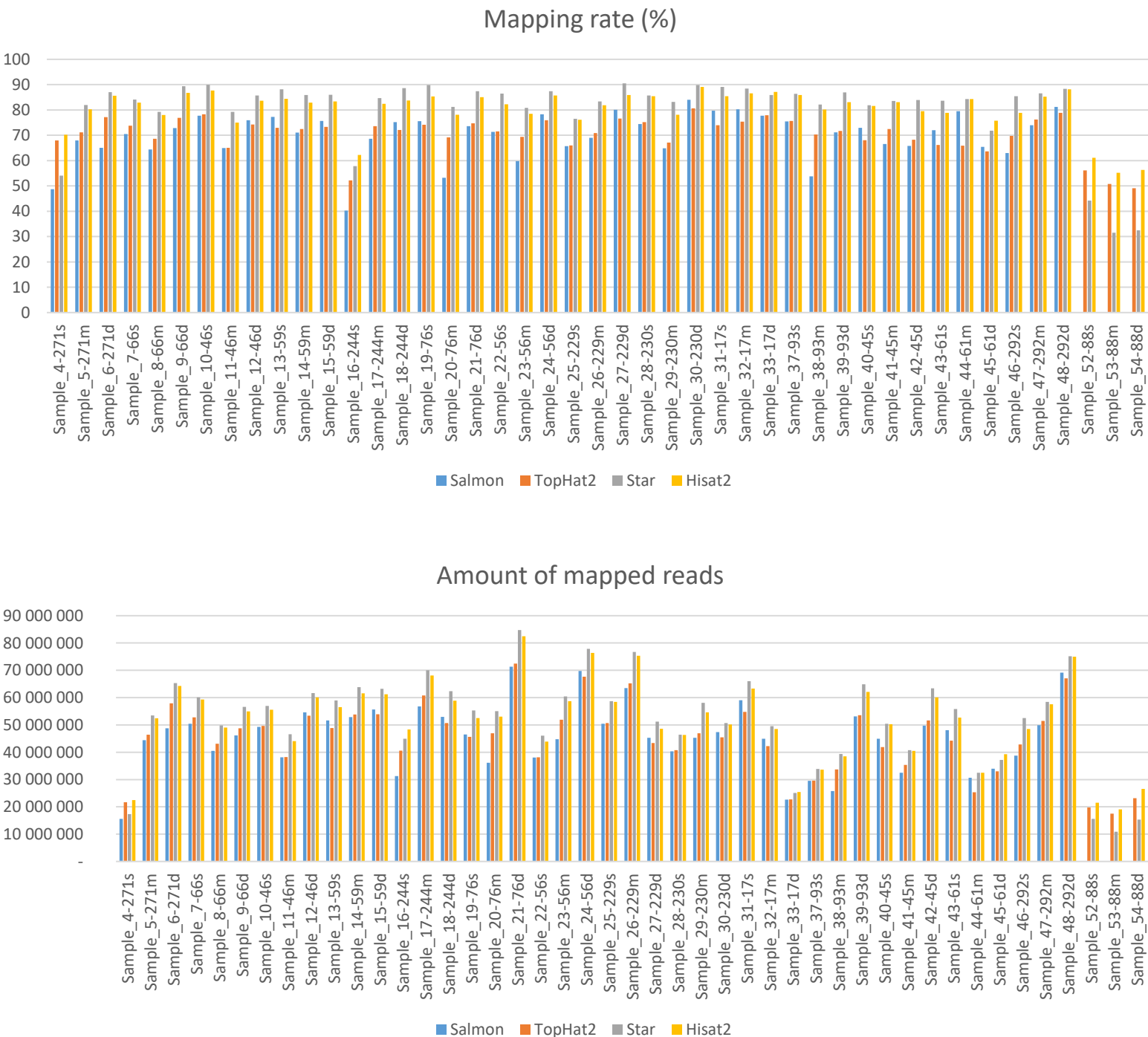
Figure 3.6: Comparison of Salmon, TopHat2, STAR and HiSat2 alignment tools.

STAR alignment tool demonstrated the highest mapping rate, however Hisat2 had second best mapping rate equalling to STAR in some samples. Salmon and TopHat2 showed similar mapping rates although there was between sample variability when either Salmon or TopHat2 had higher mapping rate. STAR was outperformed in samples with poor read quality. The amount of mapped reads on average was around 40M reads. The same five samples with poor quality of reads showed mapping rate of 50% with the STAR alignment tool.

3.3.6 Differential expression analysis

Mapped reads from STAR alignment tool were counted using featureCounts and differential expression (DE) analysis was performed using DEseq2 v1.30.0 package in R. Five samples with poor quality of reads and low mapping rate were excluded from the DE analysis. Zones were used as "condition" and Age was used as groups. Each donor was given the same identification for a different zone. A nested sample approach was used to acknowledge the dependable samples in donors when different zones were compared within the same group. Comparisons between the same zones of different groups were extracted using contrasts.

Table 3.2 DE genes (p_{adj}<0.05) during ageing and OA in the different zones

Comparisons	DE genes, p.adj <0.05
Superficial OA vs. Old	1583
Middle OA vs. Old	2195
Deep OA vs. Old	1985
Superficial Old vs. Young	978
Middle Old vs. Young	2014
Deep Old vs. Young	1440

Table 3.3 DE genes between superficial and deep zones

Group	DE genes, p.adj <0.05
Young	1848
Old	2189
OA	1713

3.3.7 Data visualisation

To reduce the dimensionality and maximise the variance PCA was performed. Moreover, zones from the same group were dependant since they were extracted from the same donor. To meet the requirement of independent variables in the dataset multilevel PCA from Mixomics package was used. The use of all gene counts for PCA demonstrated higher variance within the groups Principal component 1 (PC1) was 8% and some variance between the zones was explained by PC2 6% (Fig 3.7A). Genes were sorted based on the variance and top 500 of the most variable genes were selected

to generate a multilevel PCA (Fig 3.7B). Top 500 genes showed greater variance between the groups. Highest variance was found between the superficial and deep zones explained by PC1 (22%), whereas middle zone samples were between them. PC2 explained 10% of variance where in superficial zone samples were separated by the groups. Superficial OA and old groups were separated by PC2, young superficial group was situated between them. Middle zone samples were found to be sparse, where some were closer to the superficial and others to the deep zone samples. Deep zone samples were less clustered in comparison to the superficial zone, however, it seemed that old and young groups clustered together and OA group separately.
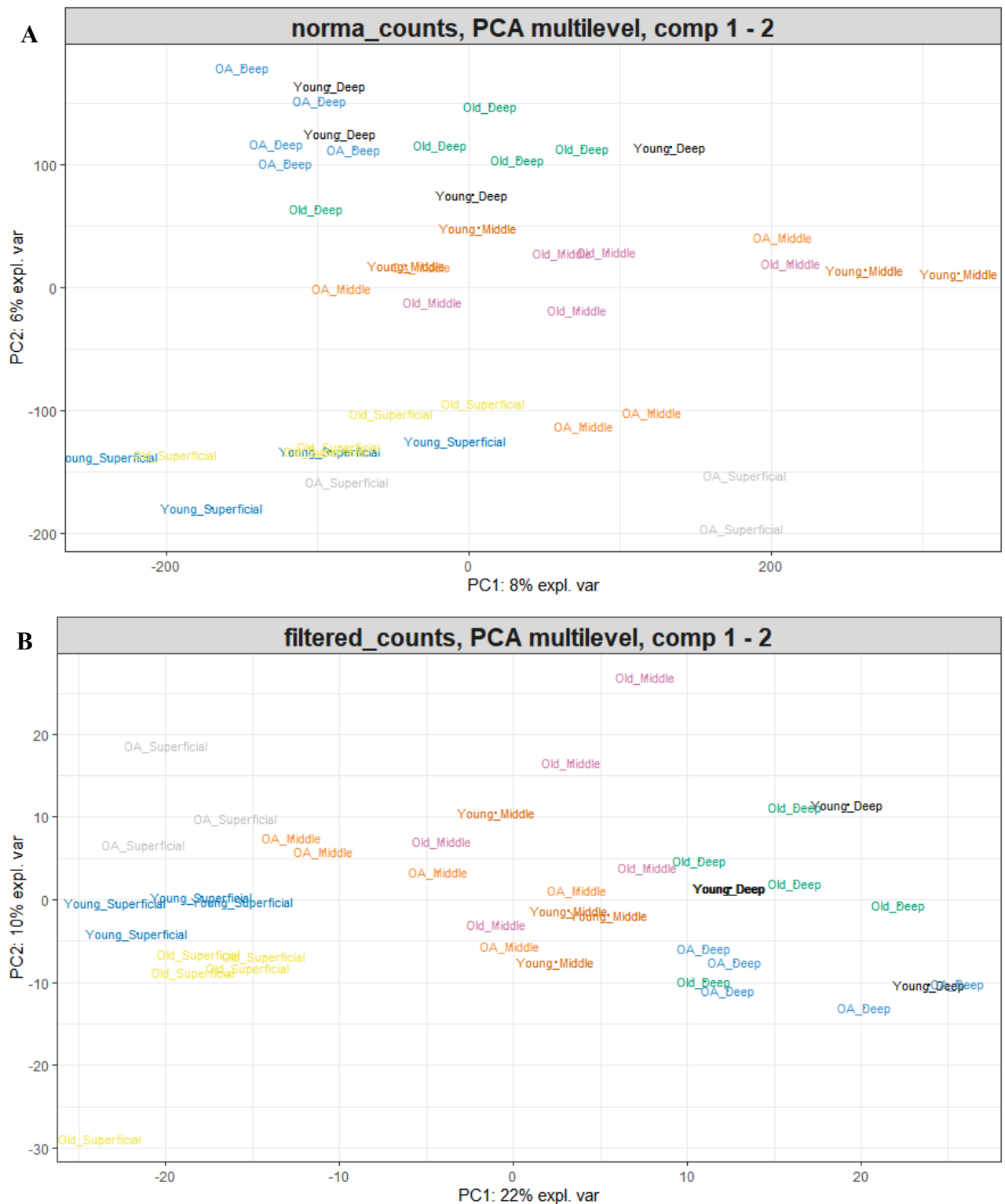
Figure 3.7 Multilevel PCA generated using all gene counts (A) and top 500 sorted by variance (B). Multilevel PCA generated using all gene counts had the highest variance within the groups (PC1 8%). However, variance of PC2 (6%) was able to separate the zones. Multilevel PCA performed better with selected top 500 genes with the highest variance. The highest variance was demonstrated between the zones (PC1 22%), and some of the variance between the groups in the superficial zone was found (PC2 10%). MixOmics package was used, counts were log transformed, scale and centre were set to false.

To visualise the genes accountable for driving the separation of samples a biplot was generated, where variables were overlaid with the samples (Fig 3.8).
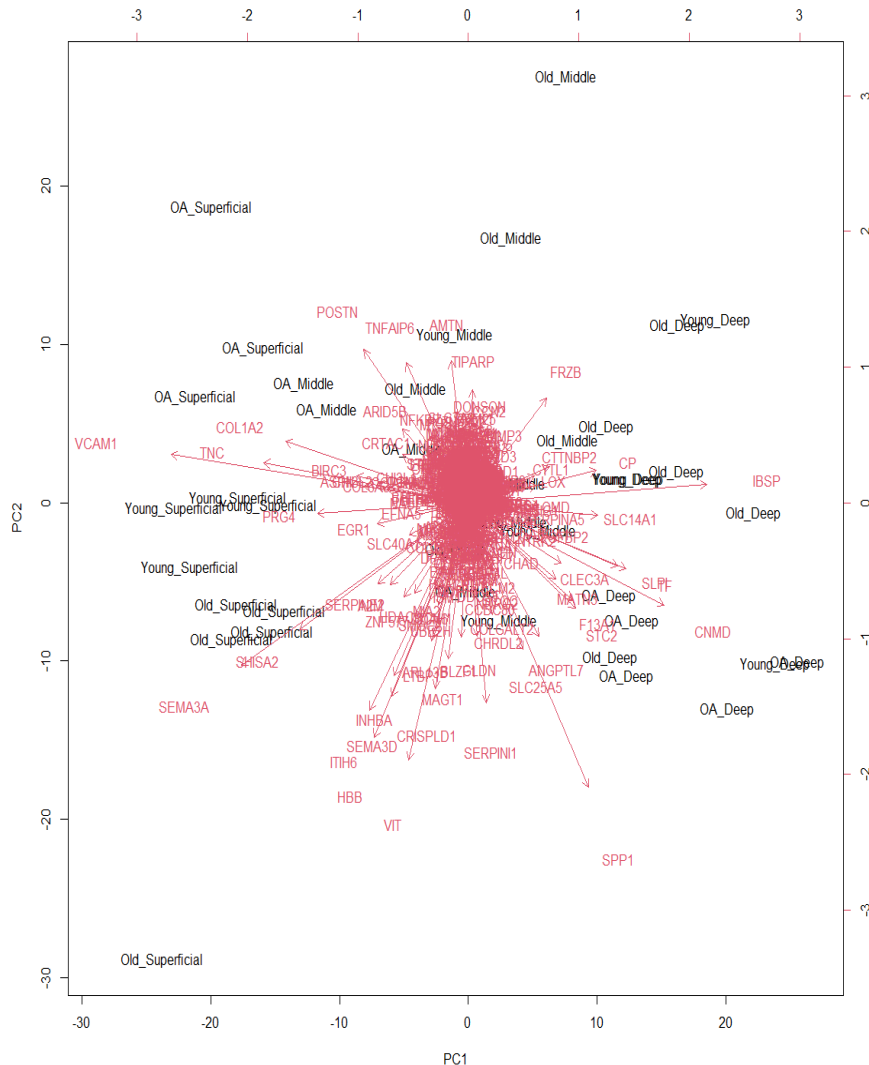
Figure 3.8: Biplot of 500 top genes generated using multilevel parameters. Biplot represents the genes that demonstrate the highest variance between the samples thus samples separate into clusters. The genes that are located closer to the cluster represent the genes that had shown similar expression level in that cluster in comparison to others. For instance, POSTN, COL1A2 and VCAM1 gene expression levels were the main factors for clustering OA superficial group.

POSTN, COL1A2, TNC and VCAM were found to be the variables separating OA superficial zone (Fig 3.8). PRG4 and ERG1 were responsible for separation of the young superficial group. SEMA3A, SHISA2 and SERPINE2 had the most weight for separating the old superficial group. AMTN, TNFAIP6 and TIPARP was separating the groups by PC2 component. Whereas, SERPINI1, VIT and CRISPLD1 guide the separation opposite way on PC2 plane. Gene responsible for the deep zone clustering included FRZB, CP, IBSP, SLPI, CNMD, STC2 and SPP1.

sPCA (Shen and Huang, 2008) was used to de-composite singular values, especially to deal with large data sets. In mixOmics, 'sparsity' was achieved via LASSO penalizations. sPCA can remove some of the non-informative variables in PCA and generate 'tighter' sample clusters. sPCA was generated using three principal components, with the parameter to keep 50 variables for PC1 and PC2, and 30 variables for PC3. PC3 revealed poor separation accounting for 6% of variation and groups of samples were mixed.
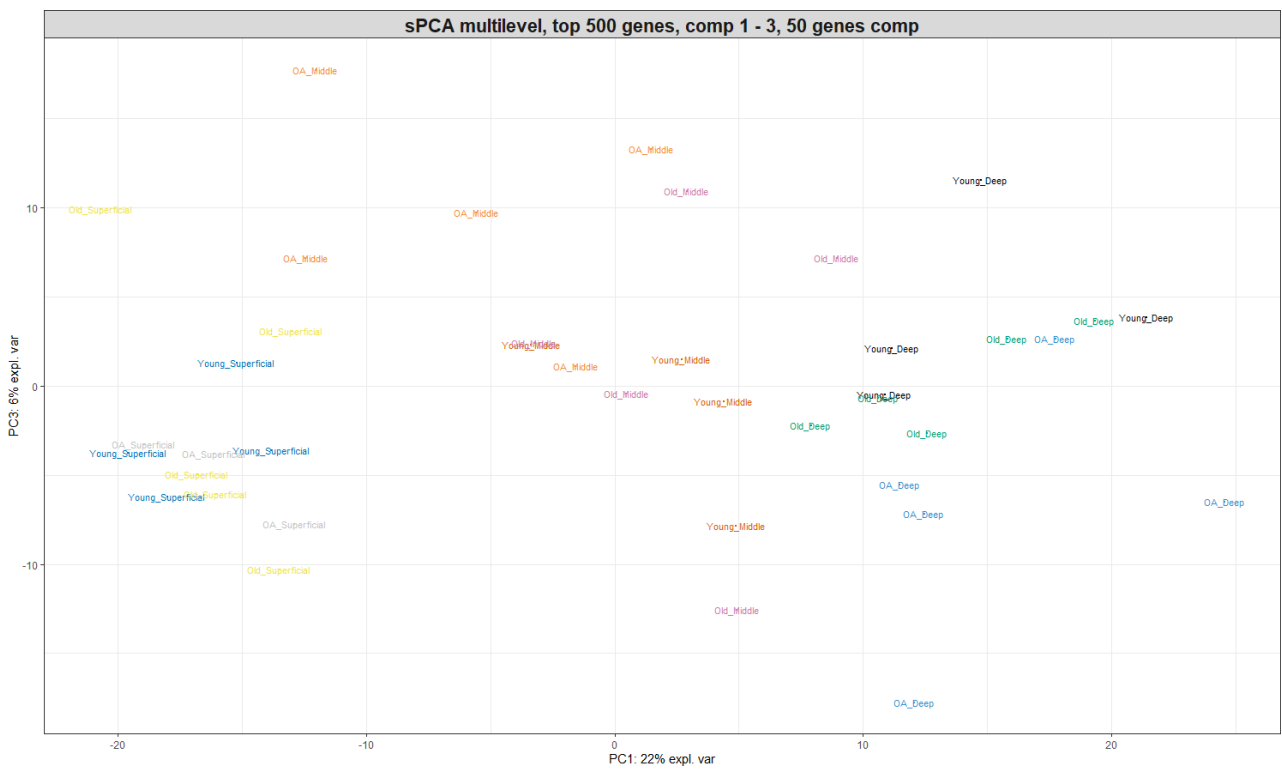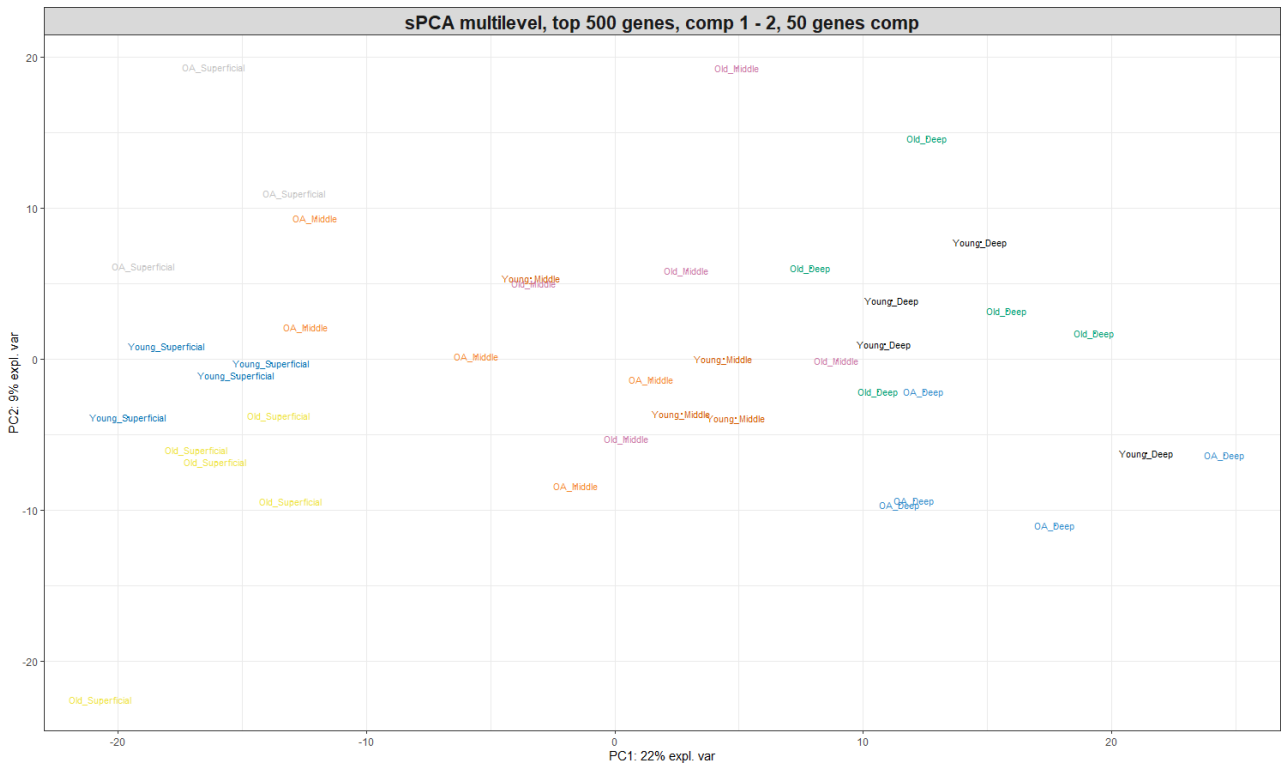
Figure 3.9: sPCA plot displayed with PC1 (22%) and PC2 (9%) (A), and with PC1 and PC3 (6%) (B).
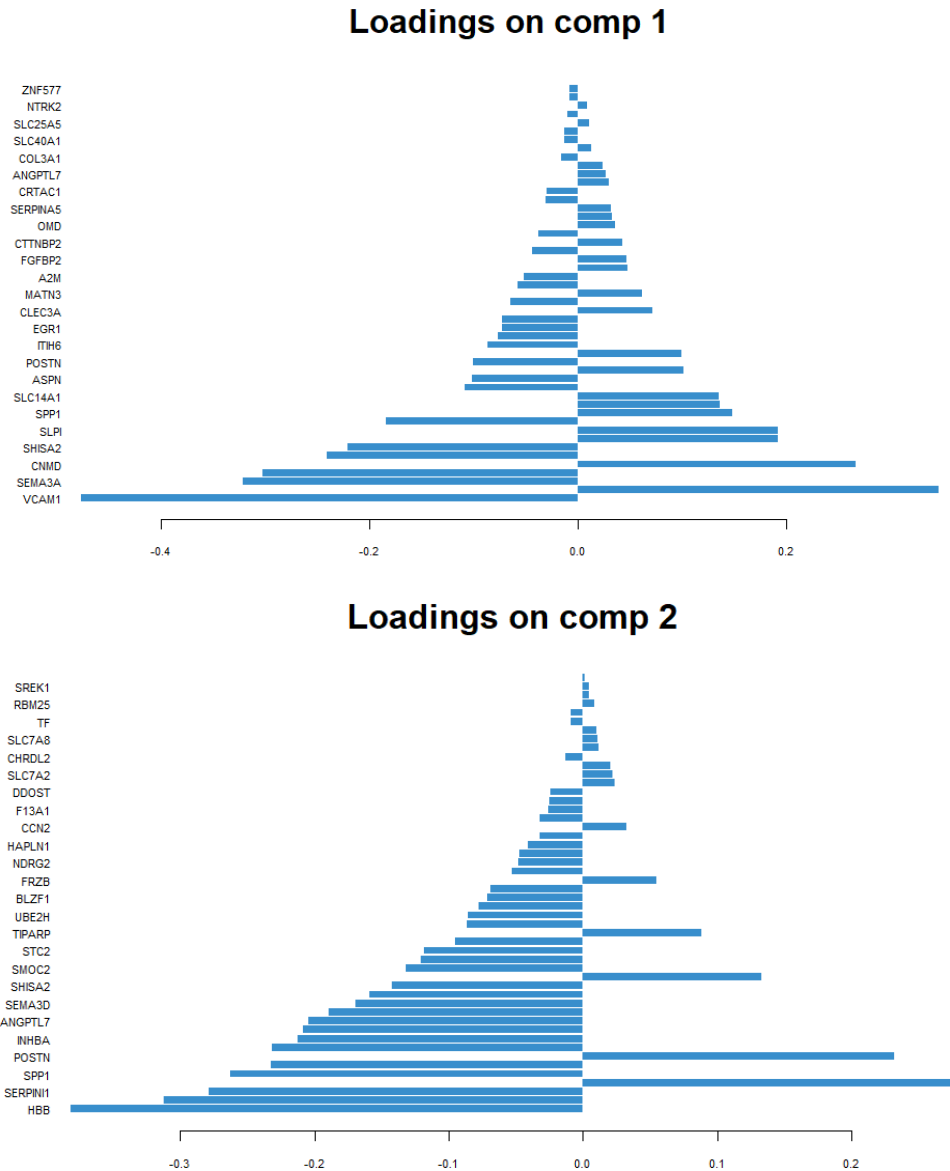
Figure 3.10: Loadings of components 1 and 2 sorted selected by sPCA analysis to identify the genes with the greatest variance in the dataset that explains the separation of clusters on the plot

3.3.8 Reference genes selection for qPCR data normalisation

180 genes were found to have stdev < 0.4, these genes were checked as to whether they had been previously used as a reference gene in qPCR experiments. Among those genes C1orf43, GPI and CHMP2A had been used as reference genes (Eisenberg & Levanon, 2013). Furthermore, ATP5F1 and PGK1 were revealed as the most stable genes in iPS cells (Panina et al., 2018). Whereas in the articular cartilage SDHA, YWHAZ and RPL4 were shown to be most stable genes during mechanical

loading (Al-Sabah et al., 2016). Although YWHAZ was not found in the list of candidate genes of RNAseq data, a different member of 14-3-3 family YWHAE was found. Finally, the genes selected with the least variability in the RNAseq data were METAP2 and RPL3. Based on the level of gene expression, genes with the highest counts were selected for experimental analysis. ATP5F1, YWHAE, RPL4 and RPL3 were selected. Moreover, GAPDH was also selected for identification of the most stable gene, it was used previously in our group as a reference gene in qPCR.

Ranking Order (Better--Good--Average)					
Method	1	2	3	4	5
Delta CT	GAPDH	YWHAE	RPL3	RPL4	ATP5F1
BestKeeper	ATP5F1	YWHAE	GAPDH	RPL3	RPL4
Normfinder	GAPDH	YWHAE	RPL3	RPL4	ATP5F1
Genorm	GAPDH	RPL3	YWHAE	RPL4	ATP5F1
Recommended comprehensive ranking	GAPDH	YWHAE	RPL3	ATP5F1	RPL4

Comprehensive Ranking | Delta CT | BestKeeper | Normfinder | Genorm

Genes Geomean of ranking values
GAPDH 1.32
YWHAE 2.21
RPL3 2.45
ATP5F1 3.34
RPL4 4.23

Comprehensive gene stability

<== Most stable genes   Least stable genes ==>

Figure 3.11: Gene expression of the reference genes in the articular cartilage from the different zones compared using refFinder. GAPDH and YWHAE were the most stable genes, whereas RPL4 was found to be the most variable between the samples.

RNA was extracted from the superficial, middle and deep zones of articular cartilage. Three donor samples were used, each sample was run in duplicate. The mean C_T values of each sample were uploaded to refFinder and compared using DeltaCT, BestKeeper, Normfinder and Genorm. The comprehensive ranking identified GAPDH and YWHAE as the most stable genes across the five tested genes. GAPDH ranked the most stable gene in all of the methods except BestKeeper, which revealed ATP5F1 as the gene with least variance across the samples. Apart from BestKeeper ATP5F1

99

was the least stable genes in the rest of the methods used. On the other hand, YWHAE was the second stable gene in all of the methods (Fig. 4.11). Based on these results GAPDH and YWHAE were selected as the reference genes for qPCR data normalisation.

3.3.9 Validation of OA specific genes in chondrocytes from the superficial and deep zones

An upstream regulator is defined by IPA broadly as "any molecule that can affect the expression of other molecules" ("Upstream Regulator Analysis", Qiagen). IPA analyses the quantity of targets for transcription regulators in the RNAseq dataset and denotes the direction of change (upregulated/downregulated). The significance of the upstream regulator is denoted by the overlap p-value and activation z-score. The overlap p-value is the degree of overlap between the dataset genes and regulated targets. The activation Z-score is the measure of how accurate the up/down-regulation indicator is. Upstream regulators identified by IPA in superficial and deep zones in the OA group were studied. Any upstream regulator also found in old or young groups were removed. From RNASeq results three genes were upregulated in the deep zone over the superficial zone (Lymphotoxin beta receptor (LTBR), TGF-beta activated kinase 1 (TAB1), Teratocarcinoma-derived growth factor 1 (TDGF1) and one upregulated in the superficial zone over the deep zone HIC ZBTB Transcriptional repressor 1 (HIC1) in the OA group. Moreover, samr package was used to identify the upregulated gene specific for the superficial OA group. The top 20 upregulated genes were used to select genes for the validation (Table 4.2). Baculoviral IAP Repeat Containing 7 (BIRC7) was selected from the list for validation based on the high fold change and it was not reported previously in connection to OA.

Table 3.4 Top 20 upregulated genes in the superficial OA group identified using samr package

Gene	logFC
CX3CL1	6.18
NRGN	5.517
BIRC7	3.871
AQP1	3.858
DLX3	3.69
PDE1A	3.429
AC092535.1	3.409
U82695.1	3.404

PCOLCE	3.287
TNC	3.243
MXRA5	3.167
GALNT16	3.148
KCNN4	3.146
F5	3.112
AC021205.1	3.066
PODXL	2.988
LRP5	2.879
ITGA9	2.839
TDGF1	2.839
AL356489.2	2.819

Positive LFC means the expression was higher in the superficial OA

Superficial and deep chondrocytes extracted from the OA cartilage were used for the validation. Chondrocytes extracted from the tissue and not cultured were designated as native chondrocytes, and chondrocytes that were plated into the flask but failed to attach to the plastic were designated as P0. In total samples from six donors were used, three for each set of samples. Gene expression level of BIRC7 was low in the samples and were excluded from the analysis.

In P0 cells LTBR and TAB1 were significantly ($p<0.05$) upregulated in the deep zone chondrocytes. Difference in HIC1 and TDGFB1 gene expression were not statistically significant (Fig 3.12A). However, in the native cells only LTBR was differentially expressed at the significant level ($p<0.05$). On the contrary to P0 cells LTBR was highly expressed in the superficial zone (Fig 3.12B).
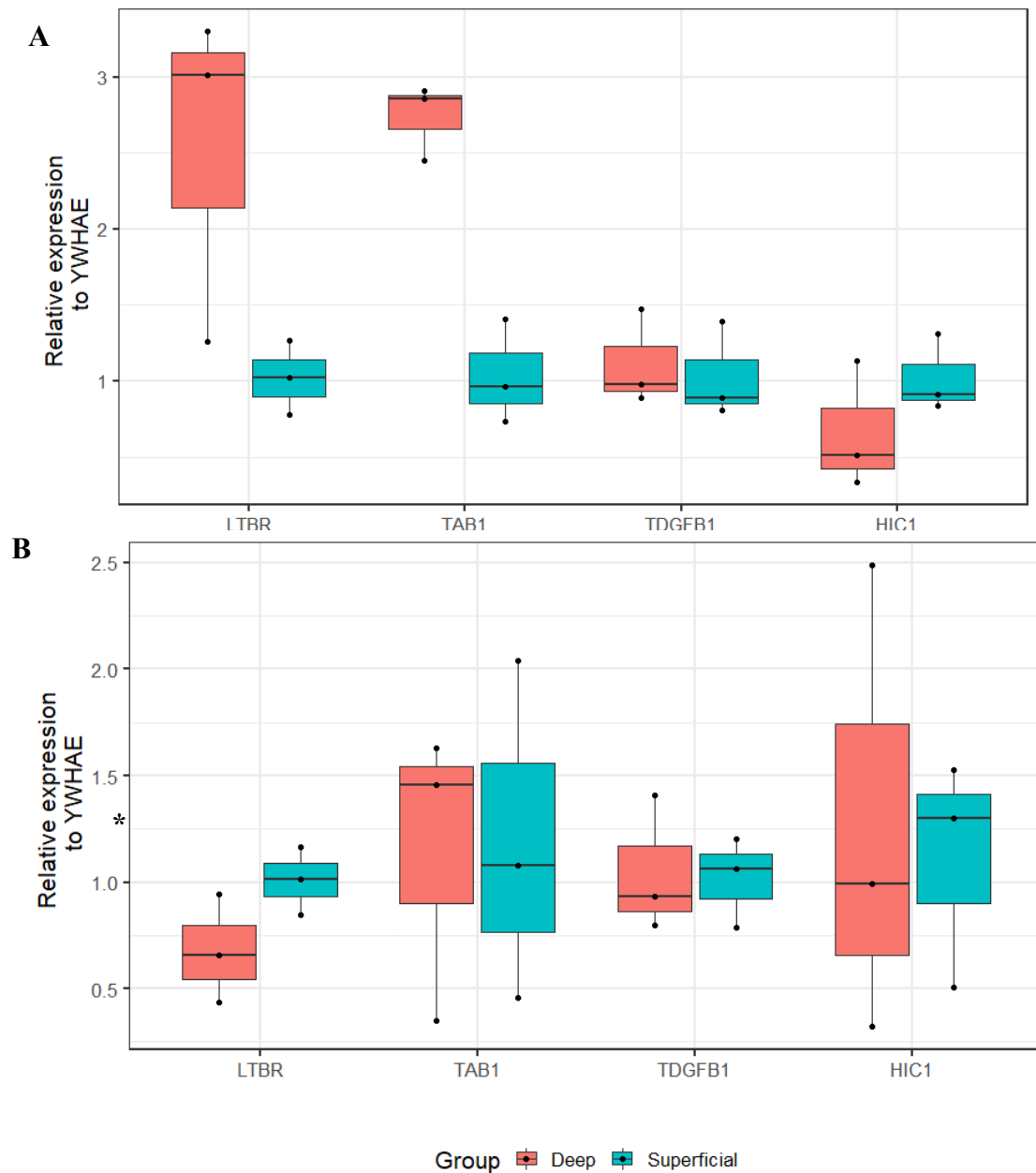
Figure 3.12: Gene expression level of LTBR, TAB1, TDGF1 and HIC1 in the superficial and deep chondrocytes extracted from the OA tissue. (A) LTBR and TAB1 significantly (p<0.05) upregulated in the deep zone of unattached chondrocytes. (B) LTBR significantly (p<0.05) upregulated in the superficial zone of native chondrocytes* P<0.05 statistics undertaken in R version 4.0.3.

3.3.10 In situ hybridisation RNAscope of the articular cartilage

Human control slides of formalin fixed paraffin embeded (FFPE) cultured cell pellets of human HeLa cells were used to test the RNAscope method. Probes against ubiquitously expressed PPIB were used as positive controls and bacterial gene dapB was used as a negative control (Fig 3.13).
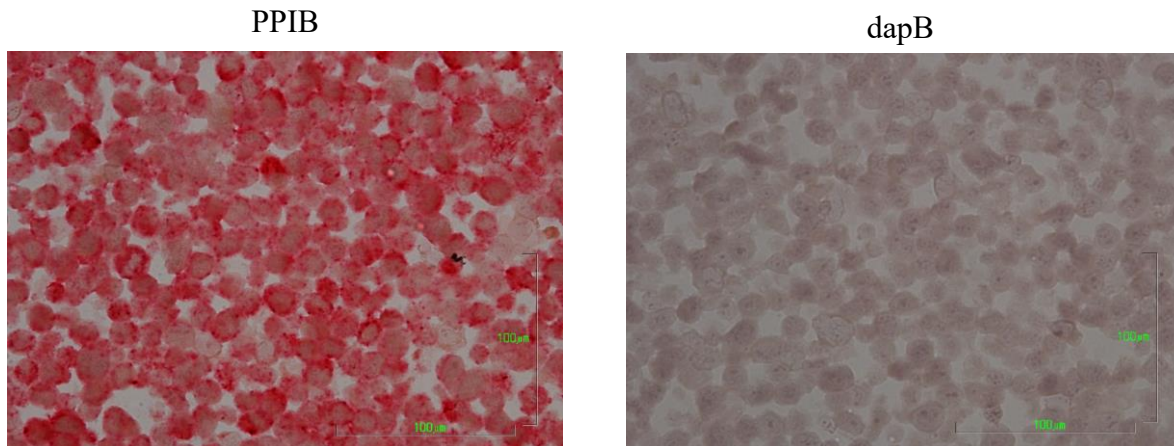
Figure 3.13: Gene expression of PPIB (positive control) and dapB (negative control) in HeLA cell pellet. Each red dot represents gene expression signal, meaning probe was bound to the RNA molecule, in the case when complementary probes are not available no hybridisation would occur. PPIB is abundantly expressed gene in the human cells, and dapB is a bacterial gene. a Scale bars are 100um

Cell pellet samples probed for PPIB gene demonstrated a strong signal, multiple red dots denoting RNA molecules hybridised with the probe were present in cells. There was no signal detected in the samples used for bacterial dapB gene negative control. To identify the most suitable probes for the articular cartilage tissue PPIB, UBC and COL2A1 were tested (Fig 3.14). UBC and COL2A1 probes demonstrated positive signal in more cells in comparison to PPIB. It was in concordance with RNAseq results, where UBC and COL2A1 gene counts were higher in comparison to PPIB gene.

Target probes for SEMA3A, FGFBP2 and AMTN genes were investigated in the articular cartilage (Fig 3.15). Only a few dots were found in the tissue of which SEMA3A gene demonstrated expression in the superficial zone. Gene expression of FGFBP2 was found in the middle zone of cartilage tissue.
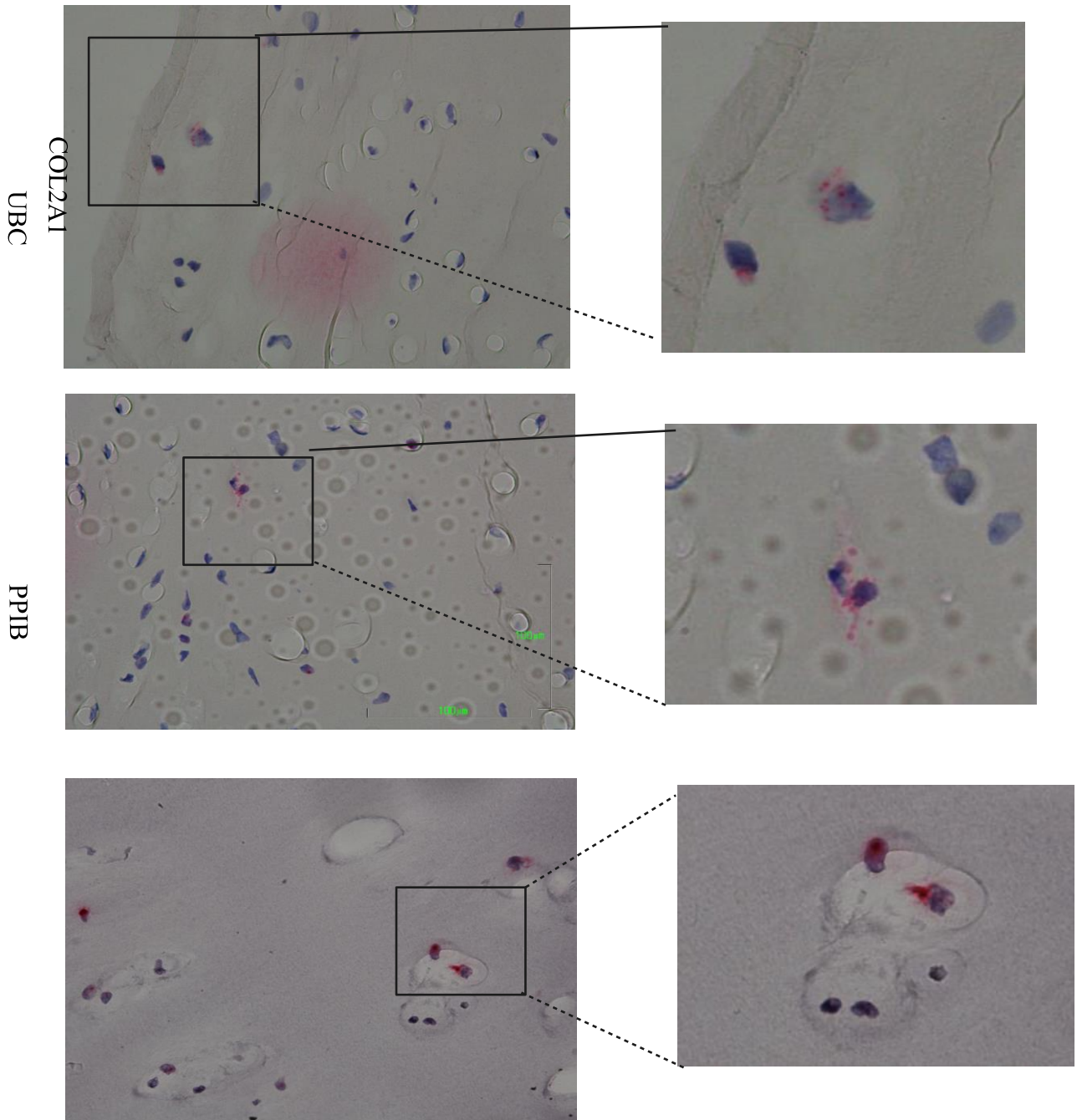
Figure 3.14: RNAScope of articular cartilage sections. UBC, PPIB and COL2A1 probes were tested on cryosectioned articular cartilage from an OA donor.
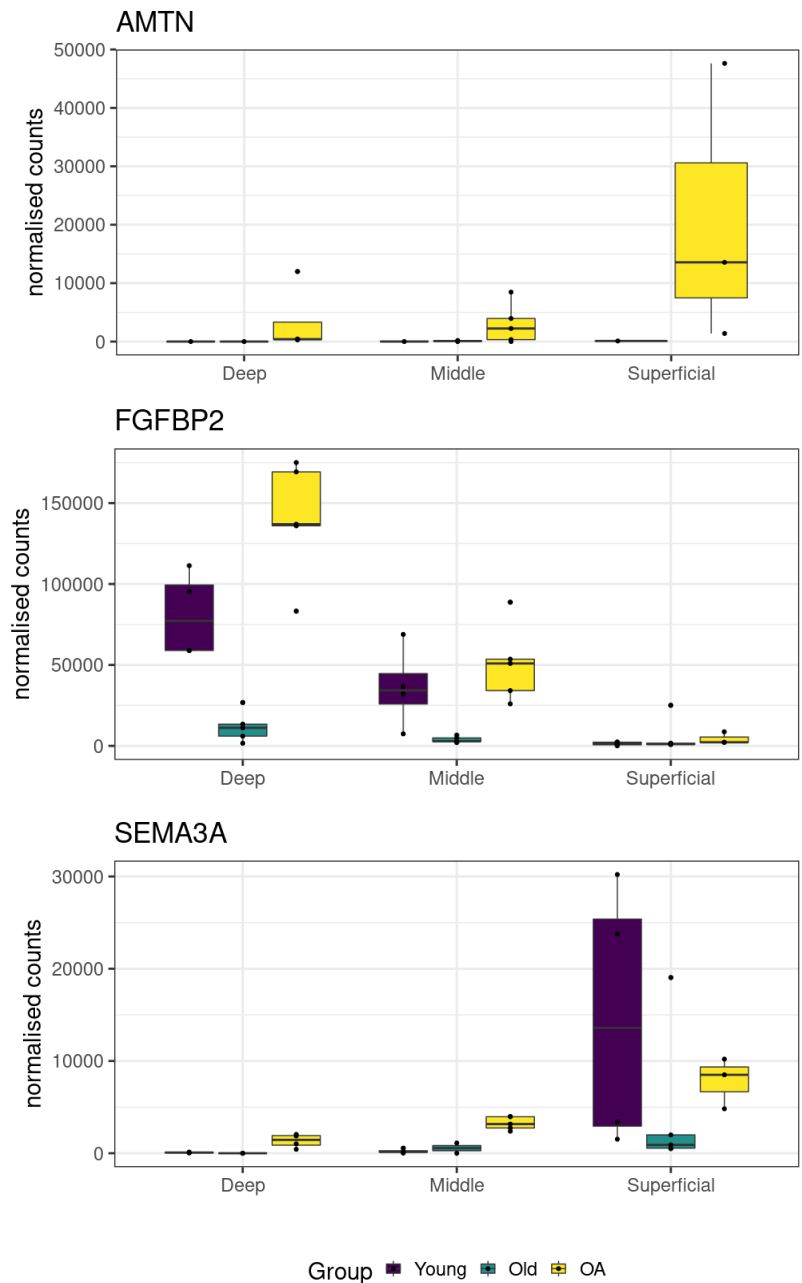
Figure 3.15: Normalised counts from RNAseq dataset of AMTN, FGFBP2 and SEMA3 genes in the different zones of young, old and OA groups. AMTN gene expression in the OA group was higher in all zones when compared to the respective zones of young and old groups. FGFBP2 was upregulated in the middle and deep zones of young and OA groups in comparison to the old group, with the highest upregulation in the OA deep zone. SEMA3A had shown gradual increase in the OA group, with the highest expression level in the young and OA superficial zone group.
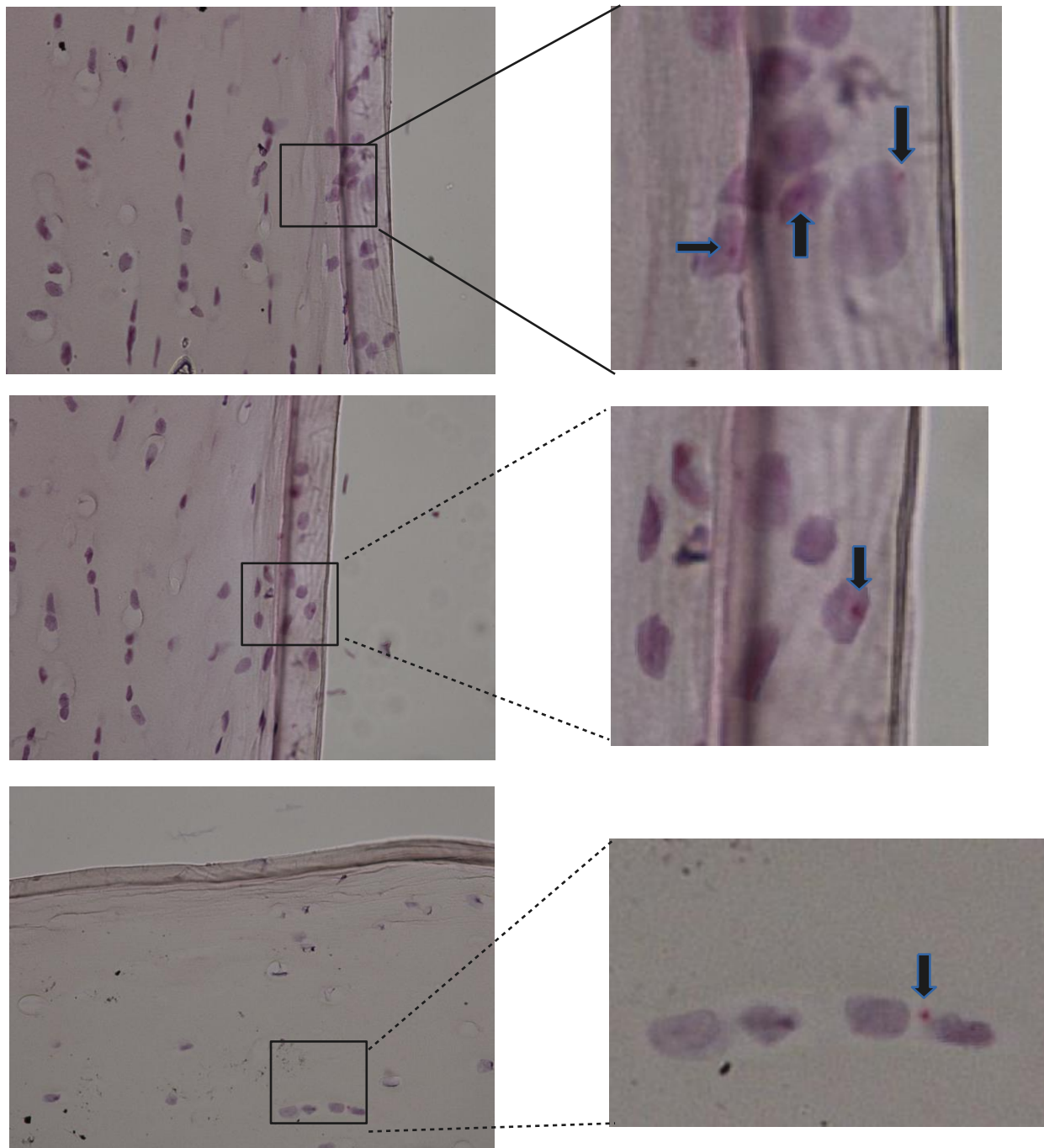
Figure 3.16: In situ hybridisation of human cartilage samples. The presence of gene expression of SEMA3A in the superficial zone of the cartilage from the young group (A) and FGFBP2 gene expression was detected in the middle zone of OA cartilage (B). The gene expression could not be obtained in the majority of chondrocytes, thus comparative gene expression between different groups was not possible.

3.4 DISCUSSION

In this study we identified age and OA related change in gene expression in the three layers of articular cartilage.

Quality control of the RNASeq data revealed that some samples had GC content in the sequences and overrepresented sequences. The presence of biases during PCR amplification or library preparation can result in a high GC content. GC-rich areas may be preferentially amplified during PCR amplification, resulting to an overrepresentation of these regions in the final library. Similarly, certain library preparation procedures, such as those employing random hexamers for reverse transcription, may favor GC-rich sequences. On the other hand, overrepresented sequences can be the result of contamination that was introduced during the sample preparation or sequencing process. For instance, adapter sequences, PCR primers, or other sequencing artifacts may be overrepresented in the final library, which might result in an increase in their representation in the sequencing data. This can also happen with other sequencing artifacts. Similarly, contamination from other sources, such as bacteria or fungi, can also contribute to the existence of overrepresented sequences in the sequencing data. This can occur for a variety of reasons. For these reasons one of the donor sample was excluded from the RNAseq analysis, and two samples from the OA superficial group were removed as well for that reason.

Alignment is a crucial stage in the study of RNA-seq data, in which the reads generated by the sequencing instrument are mapped to a reference genome. STAR, Tophat2, HISAT2, and Salmon are some of the software tools available for RNA-seq alignment. While all of these tools have been developed to perform the same function, there are significant distinctions between them and must be considered when choosing an alignment tool for their investigations. In our study of all the compared genome alignment tools STAR demonstrated higher genome coverage when our RNAseq data was aligned to the human genome. STAR can outperform other genome alignment tools during RNA-seq analysis due in large part to its ability to align spliced reads accurately and efficiently. In transcriptomics, where RNA transcripts undergo post-transcriptional processing resulting in the elimination of introns and splicing of exons into a mature mRNA transcript, this is of particular importance. Many studies comparing STAR's performance to those of other RNA-seq alignment algorithms have confirmed its superiority. For instance, Engstrom et al. (2013) examined STAR, TopHat2, and GSNAP for the alignment of Illumina RNA-seq data and found that STAR provided the most accurate alignment, especially for spliced reads. Dobin et al. (2013) examined the alignment performance of STAR, TopHat2, and HISAT for RNA-seq data and found that STAR had the highest alignment accuracy and the lowest false positive rate. The higher genome coverage of STAR was the reason we have used mapped reads from it for the subsequent analysis of the RNAseq dataset.

PCA is a method of dimensionality reduction that can identify patterns and trends in large datasets. This is accomplished by reducing the number of variables to a smaller set of orthogonal variables, which are referred to as principal components. Plots of principal components can be used to help identify outlier samples, which are samples that are significantly different from the other samples in a dataset. Also the proximity of two samples in a PCA plot can be used to identify clusters of samples that have similar patterns of gene expression. This is done by comparing the two samples to one another. In our study it was found that the highest variance was between the different zones rather than the disease state or age. As the superficial zone and deep zones have distinctive functions in the overall architecture of the cartilage they also sustain different loading and shearing forces during the movement of the limbs. We have used top 500 genes with the most variance in our dataset to produce the PCAs. PC1, which explained the difference between the zones had the highest variance of 22%, while PC2 showed some variance between the disease state and ageing and accounted for 11% of variance in our dataset. The superficial zone samples of each group clustered closer and the highest variance was found between OA and healthy old superficial zone samples.

Plots of principal components using PCA can be also used to determine which principal components capture the most variation in the data. Based on that we performed biplot to overlay loadings of each gene to explain the variance of clusters. POSTN was significantly upregulated in the superficial zone of OA group in comparison to the young and old groups. It was one of the main factors driving the separation of clusters in PCA. It was previously discovered that POSTN expression was elevated in OA cartilage relative to healthy cartilage, and that this elevation was proportional to the severity of OA. The involvement of POSTN in the development of OA in a rat model was also examined. POSTN expression was elevated in OA cartilage and that inhibiting POSTN expression with RNA interference decreased cartilage deterioration and enhanced joint function in rats. Also, the function of POSTN in regulating chondrocyte metabolism and its possible significance in OA were studied. POSTN expression was elevated in OA cartilage and that it increased chondrocyte catabolism and inflammation via Wnt/-catenin signaling pathway. From the results of our study the role of POSTN could specific to the superficial zone of articular cartilage during OA. Moreover, Vascular cell adhesion molecule-1 (VCAM1), a cell surface protein that is involved in the adhesion and migration of leukocytes during inflammatory responses was also upregulated in the superficial zone of OA group. It was previously found that VCAM1 expression was increased in OA cartilage compared to healthy cartilage, and that this increase was correlated with the severity of OA. It was also shown that VCAM1 expression was increased in OA cartilage and that it promoted chondrocyte apoptosis and cartilage degeneration through the JNK signaling pathway (Liao et al., 2021).

SEMA3A was upregulated in the superficial zone of old and OA samples in comparison to the young group. It was shown previously that the expression of SEMA3A was found to be lower in

OA cartilage than in healthy cartilage, and this decrease was correlated with the severity of OA. Matrix metalloproteinases (MMPs) and aggrecanases may also be inhibited by treatment with recombinant SEMA3A. Activation of the ERK1/2 signaling pathway was identified as the mechanism by which SEMA3A stimulated chondrocyte proliferation and differentiation (Liu et al. 2017). SEMA3A has been identified as a potential therapeutic target for the treatment of OA. SEMA3A treatment could decrease the expression of interleukin-1β (IL-1β) and tumor necrosis factor-α (TNF-α), which are key pro-inflammatory cytokines in OA .

SHISA2 (also known as CKLFSF2 or CKLF-like MARVEL transmembrane domain-containing protein 2) is a gene that encodes a transmembrane protein involved in cellular adhesion and signaling pathways. In our study it was downregulated in the superficial zone of OA group in comparison to the old group. It was earlier found that SHISA2 expression was significantly decreased in OA cartilage compared to healthy cartilage, and that this decrease was correlated with the severity of OA. Moreover, SHISA2 knockdown in chondrocytes resulted in decreased cell proliferation, migration, and adhesion, and increased expression of MMPs (Wang et al 2019). Moreover, SHISA2 overexpression could decrease the expression of interleukin-1β (IL-1β) and tumor necrosis factor-α (TNF-α), which are key pro-inflammatory cytokines in OA . All of the above suggests the PCA analysis can be used for identifying the most differentially expressed genes in the dataset and could used for further analysis of the findings. As the results from our study correlates to the earlier published research findings. However, using our dataset we could identify the anatomical regions within the cartilage tissue where gene expression patterns change.

We have also used Sparse Principal Component Analysis (sPCA) in our study, it is a variant of Principal Component Analysis (PCA) that is used in the analysis of high-dimensional and sparse datasets, such as RNA-seq data. Unlike traditional PCA, sPCA can handle missing values in the data, which is a common issue in RNA-seq datasets due to dropout events. This means that sPCA can extract useful information from incomplete datasets, leading to better dimensionality reduction and clustering results (Hoffman et al., 2013). In RNA-seq datasets, there are often many genes that are not informative or are only weakly associated with the biological signal of interest. sPCA can identify the genes that are most informative for explaining the variation in the data, and focus on those genes for downstream analysis. We have looked into the loadings from sPCA analysis to identify the genes that have higher variance leading to the separation of clusters on the plot. Thus, the genes from the PC1 of sPCA could indicate genes that change the gene expression levels depending on the zone, while PC2 could explain to a lesser amount the difference between the OA, old and young groups.

To identify the zone-specific upstream regulators in the OA cartilage we used IPA analysis with dataset on the superficial and deep zone DEGs. LTBR (Lymphotoxin Beta Receptor) was predicted to be upregulated in the deep zone of donor chondrocytes in both unattached and native

cells. It is a gene that encodes a tumour necrosis factor receptor. Its protein is involved in signalling during the development of lymphoid organs, apoptosis, lipid metabolism and immune responses. LTBR acts as an upstream regulator of VCAM1 and DSG2. VCAM 1 transcription is predicted to increase with LTBR engagement. VCAM1 gene encodes a cell surface sialoglycoprotein present on cytokine-activated endothelium. VCAM-1 is involved in leucocyte-endothelial adhesion and signal transduction. It is hypothesized to contribute to rheumatoid arthritis pathogenesis. DSG2 is a gene that encodes a desmoglein group protein. Desmoglein proteins are Calcium-binding glycoprotein components of desmosomes and form cell to cell junctions.

TAB1 was also predicted to be decreased in the superficial zone of OA in comparison to the deep zone. TAB1 is a regulator of the MAP kinase kinase kinase pathway (MAP3K7/TAK1). TAB1 influences the intracellular signalling pathways of TGF-beta, Interleukin 1 and WNT-1. TAB1 has been identified as an upstream regulator of MMP13 and XAF1. MMP13 is a matrix metalloproteinase involved in the breakdown of extracellular matrix in normal physiology; it has also been identified as having a role in metastasis and arthritis. TAB1 is predicted to upregulate and increase the transcription of MMP13. TAB1 is also predicted to upregulate and increase the transcription of XAF1. XAF1 gene encodes a protein that opposes the inhibitory action of the IAP. Our validation results with chondrocytes extracted from the superficial and deep zones demonstrated the similar pattern of gene expression with TAB1 and LTBR genes. Whereas, TDGFB1 and HIC1 gene expression was not different when superficial and deep zones of OA chondrocytes were compared. This result suggest zone specific changes in the articular cartilage during OA, and while inflammatory processes activated in the whole cartilage tissue, different zones demonstrate unique genes in driving those processes.

Results of the RNAseq were also used to predict the most stable genes in all groups, including OA, old and young cartilage samples. This would mean the gene expression does not change between those groups and the least variance. These genes were selected to use as reference gene for qPCR normalisation. Selected genes included GAPDH, YWHAE, RPL3, ATP5F1 and RPL4. It was shown by qPCR analysis that GAPDH and YWHAE genes have the similar expression levels in the superficial and deep zones. Furthermore, AMTN, FGFBP2 and SEMA3A were selected for validation study using *in situ* hybridisation method. The genes were selected based on the number of reads in the RNAseq data, as high number of reads would suggest high expression levels in chondrocytes. By using PPIB positive control on the cartilage tissue it was decided to use the genes with higher expression levels, as the genes with lower numbers of reads could be difficult to detect in the tissue using in situ hybridisation.

The AMTN (Amelotin) gene encodes a protein that belongs to the secretory calcium-binding phosphoprotein (SCPP) family. It is expressed in various tissues, including dental enamel, oral

epithelium, and bone. The precise function of AMTN is not fully understood, but it has been suggested to play a role in enamel formation, tooth eruption, and biomineralization of bone (Yoshida et al., 2009). This gene was a subject of interest as there was no available information of its involvement in the articular cartilage and osteoarthritis. In our dataset it was shown to be upregulated in the superficial zone of OA group, and there was negligible level of gene expression in other zones of all groups. We validated our RNASeq finding using this *in situ* hybridisation.

FGFBP2 (Fibroblast Growth Factor Binding Protein 2) is a gene that encodes a protein that binds to fibroblast growth factors (FGFs), which are involved in a variety of biological processes, including development, wound healing, and tissue repair. FGFBP2 may play a role in the regulation of chondrocyte metabolism, ECM remodeling, and inflammation in the joint. In our validation study there was a weak signal in the middle zone in one of the samples.

SEMA3A (semaphorin 3A) is a gene that encodes a semaphorin protein that regulates cell migration, proliferation, and differentiation throughout development and tissue repair. The protein SEMA3A is essential for axon guidance and brain development. SEMA3A has been linked in the pathophysiology of OA, in addition to its role in the neurological system. SEMA3A signal was detected in the superficial zone of articular cartilage in one of the samples.

Unfortunately, *in situ* hybridisation did not provide results for most of cartilage samples. As the method has many steps of washing most of the cartilage sections were washed off the slides. We tried many optimisation methods, including the increase of time for drying slides, different thickness of sections and timing for probe incubation we could not get the results from almost all of the samples.

Overall, the usage of RNAseq on articular cartilage, specifically from the superficial, middle and deep zones of the tissue demonstrated the ability to distinguish the different patterns of gene expression during disease and ageing. There is still needed further analysis of these datasets, especially in the aspect of ageing. The sparse availability of normal cartilage from young and old donors is one of the main obstacles in studying the age specific changes. Our results have confirmed the results of some of the previously published work in the field. Furthermore, it could point to the zone specific changes in the articular cartilage.

3.5 CONCLUSSION

In this study we have identified differentially expressed genes within the zones of articular cartilage and the zone specific changes in cartilage during OA and ageing. It was shown that the use of the most suitable bioinformatic tool for the dataset can aid the data analysis. Furthermore, we have validated LTBR and TAB1 genes with the superficial and deep zones of chondrocytes extracted from

the cartilage. Initially these gene were predicted by the pathway analysis tool (IPA) as the upstream regulators of the genes in our dataset and the gene expression levels of LTBR and TAB1 were upregulated in the deep zone chondrocytes extracted from the OA cartilage in comparison to the superficial zone upon validation.

CHAPTER 4

Zonal differences in proteome of chondrocytes during age-related OA

4.1 INTRODUCTION

Proteomics of chondrocytes extracted from the articular cartilage can give insightful information on cellular changes. Moreover, cultured chondrocytes can be used for *in vitro* secretome experiments, in which proteins secreted from the cells can be studied to understand the changes upon external stimuli.

Earlier published works have demonstrated that proteomics of chondrocytes can provide potential biomarkers and signalling pathways involved in the osteoarthritis (OA) progression. In one study the proteome of human normal chondrocytes was investigated, and 93 proteins were identified as involved in cell organization, energy, protein fate, metabolism, and cell stress. The proteome of chondrocytes was enriched in proteins related with actin remodelling, such as vimentin (VIM), transgelin (TAGL), cofilins (CFLs), and destrin (DSTN). This work demonstrated that actin-cytoskeleton architecture is a key regulator of chondrocyte phenotype (Ruiz-Romero et al.,).

In a further proteomic analysis of OA chondrocytes compared to normal chondrocytes, OA chondrocytes express 19 proteins at higher levels and 9 proteins at lower levels. The bulk of the proteins were involved in metabolic pathways, although other cellular activities such as protein synthesis, cell stress and defence, signalling, and transport were also represented.

In a cartilage proteomic analysis the differential expression of 17 proteins between OA and normal chondrocytes was found. The majority were engaged in metabolic pathways and oxidative stress defence. The role of vimentin (VIM) and other cytoskeleton proteins in the development of osteoarthritis was also demonstrated. A separate study found that the expression pattern of 76 proteins differed between OA and normal chondrocytes. The authors identified 48 proteins that were upregulated in OA compared to normal chondrocytes and 28 proteins that were downregulated. In particular, the inflammatory proteins interleukin 1 (IL-1), IL-6, and C-C motif chemokine receptor 3 (CCR3) were found to be elevated in OA chondrocytes.

Furthermore a proteomics analysis of chondrocytes isolated from healthy and arthritic cartilage revealed the presence of 73 proteins with altered levels of expression in OA cells and mitochondrial superoxide dismutase 2 (SOD2) was shown to be significantly downregulated in OA chondrocytes.. Proteomic analysis of chondrons was performed to detect alterations in the proteome of chondrocytes and the pericellular matrix. The majority of pericellular matrix abundant proteins were discovered, including different types Collagen type VI. Morevoer, TGF induced protein-2 (LTBP-2), TPIS, HLPN1, neurexin- 2- (NRXN2) and PRDX4.

Label-free proteomics was used for the proteome analysis of normal and OA chondrocytes from the knee articular cartilage, which resulted in the discovery approximately 2400 proteins. The two groups had significantly different levels of synthesis in 269 of proteins. Proteins involved in

pathways related to actin cytoskeleton regulation, epidermal growth factor receptor signaling, transforming growth factor beta signaling, mitogen-activated protein kinase signaling, integrin-mediated cell adhesion, and lipid metabolism were significantly enriched in the OA samples, as determined by functional annotation.

All of these studies used a label-free proteomics approach to identify differentially abundant proteins in chondrocytes. Label-free proteomics is a method that allows for the quantification and identification of proteins without the need for chemical labels. One of the main limitations is the complexity of the data generated by mass spectrometry, which can be difficult to interpret and require sophisticated computational methods for analysis. Furthermore, the analysis of the label-free proteomics needs a normalisation across the samples in order to perform relative changes in the abundance of proteins between the groups. The normalisation of samples can be performed by using total ion counts or based on the specific protein that is stable across the samples. Although, label-free proteomics are more robust in terms of sample preparation and available tools for data analysis it is less accurate in performing relative and absolute quantification of proteins for group comparison. Label-based proteomics can be used for quantitative analysis of proteins in the different groups of samples.

One method of label-based proteomics is SILAC (Stable Isotope Labelling by Amino acids in Cell culture). It is a widely used technique that enables quantitative analysis of protein expression levels and post-translational modifications. The SILAC method involves labelling proteins with stable isotopes of amino acids *in vitro,* which enables precise and accurate quantification of changes in protein expression levels between different samples. SILAC requires the use of two cell populations that are grown in culture, each with a different isotopically labelled amino acid. For example, one population may be grown in culture medium containing light isotopes of essential amino acids (such as 12C and 14N), while the other population is grown in medium containing isotopically heavy amino acids (such as 13C and 15N). After labelling the cells with heavy and light amino acids, the cells from the different populations are mixed in equal ratios, and the proteins are extracted and processed for mass spectrometry analysis. By using mass-spectrometry analysis peptides the proteins can be identified and measured. The ratio of heavy to light peptides is used to calculate the relative expression levels of the proteins in the two cell populations. SILAC is a highly accurate method for quantifying protein expression levels because the cells are labelled with stable isotopes, which eliminates experimental variability. The relative abundance of proteins can be determined with high accuracy and precision, which allows for comparative analyses of protein expression levels in different samples.

Another method of label-based proteomics is iTRAQ (Isobaric Tags for Relative and Absolute Quantitation). It is a mass spectrometry-based proteomics method that permits the simultaneous quantitative analysis of up to ten samples. It involves labelling peptides with isobaric tags, which are molecules with the same mass but differing chemical characteristics, enabling their differentiation during mass spectrometry. Extracted proteins from the sample are digested into peptides by protease enzymes. The peptides are labelled with isobaric tags via a chemical reaction that selectively attaches the tags to the peptides' N-terminus and lysine residues. Each iTRAQ reagent contains a different mass tag, allowing for the simultaneous analysis of up to ten samples. Following labelling, the peptides are fractionated using techniques such as high-performance liquid chromatography (HPLC) or strong cation exchange (SCX) chromatography, which separate the peptides based on their net charge. A mass spectrometer is then used to ionize and separate the fractionated peptides based on their mass-to-charge ratio (m/z). The iTRAQ tags on the peptides generate reporter ions, which are then quantified. The resulting mass spectrometry data is analysed using software tools that identify and quantify the labelled peptides and proteins, and compare the relative abundances of the peptides across the different samples.

In our study we have decided to used iTRAQ labelling mass spectrometry. The aim of study was firstly to identify the proteins that are differentially abundant between the superficial and deep zone chondrocytes derived from normal and OA cartilage human cartilage. It has been shown that chondrocytes undergo certain changes upon culture. Chondrocytes change in phenotype when removed from their extracellular matrix and cultured in the media, in particular cells expand and acquire elongated form. Whilst chondrocytes residing in the cartilage tissue appear round and sparsely situated in the tissue. Moreover, gene expression changes in chondrocytes that are cultured with the upregulation of collagen type I and a reduction in type II. Furthermore, the response of cultured chondrocytes to the mechanical loading showed significant changes in the genes expressed. It was found that cartilage ECM proteins downregulate after mechanical stimuli and inflammatory genes upregulate. For this reason, we also assessed the gene expression levels of chondrogenic, hypertrophic and zone specific genes in cultured and native chondrocytes extracted from the superficial and deep zones.

4.2 MATERIALS AND METHODS

4.2.1 Extraction of chondrocytes from human articular cartilage

Human OA cartilage was collected by the Liverpool Musculoskeletal Biobank following Sponsorship Approval (Sponsor Ref: UoL001398) and Clatterbridge Hospital, Wirral following ethical approval for the isolation of human primary OA chondrocytes (IRAS ID 242434; Main Investigator: Dr Simon Tew, Senior Lecturer, University of Liverpool). Chondrocytes extracted from the articular cartilage of young group was kindly provided by Professor Brian Johnstone. Chondrocytes were extracted from the femoral condyles. The mean age of the donors from young group was 21 years old, the mean age of the donors from OA group was 65 years old with n=5 of donors in each group. All of the donors in OA group were from total knee arthroplasty of males, in the young group there were four males and one female.

Human primary chondrocytes were isolated from cartilage tissue under sterile conditions in a class II laminar flow hood, and all items were sprayed with 70% ethanol prior to use to maintain sterility.

Once in the laboratory, the tissue was placed in a sterile hood. A sterile 5mm punch biopsy tool was used to biopsy the articular cartilage until reaching the underlying subchondral bone. Surgical clippers were used to cut through the articular cartilage and subchondral bone to obtain osteochondral plug. 4-5 subchondral plugs were collected from the macroscopically intact areas of the femoral condyles. Using scalpel upper third was cut out and designated as superficial zone, underlying second third was cut out and discarded off. The lower third was cut from the subchondral bone and noted as the deep zone. Excised cartilage tissue was washed in the sterile phosphate buffered saline (PBS) and cut into smaller pieces using scalpel. Collected cartilage tissue pieces were washed twice with sterile complete media containing Dulbecco's Modified Eagle Medium (DMEM) to remove debris and blood (ThermoFisher Scientific, Paisley, UK). Cartilage was cut into 2-3mm pieces and placed in a 15mL falcon tube with 12ml of DMEM media containing 0.08% collagenase type 2 (Worthington Biochemicals, Danehill, UK). The falcon was kept in a 37°C shaking incubator overnight to allow tissue digestion and chondrocyte extraction from the ECM. The solution was then passed through a 70m sterile cell strainer (Fisher Scientific, Loughborough, UK) the following day to remove undigested cartilage pieces. The solution was centrifuged for 4 min at 1400 rpm at room temperature. The supernatant was removed after the chondrocytes were pelleted. Chondrocytes were resuspended in 5ml complete media, washed, and spun down as before.

Chondrocyte samples selected for the subsequent proteomics analysis were frozen down in DMEM medium supplemented with 50% final concentration of 10% foetal bovine serum (FBS)

(Gibco/ThermoFisher Scientific, Paisley, UK) and 10% Dimethyl sulfoxide. Chondrocytes that were not selected for the purpose of proteomics study were cultured in the DMEM medium with low glucose (1g/L), pyruvate (110.0mg/L), 1% L-glutamine, phenol-red (15mg/L), 1% penicillin-streptomycin (P/S) (Gibco/ThermoFisher Scientific, Paisley, UK) and 0.2% amphotericin B/fungizone (F/Z) (Gibco/ThermoFisher Scientific, Paisley, UK) in T75 flask (Greiner Bio-One, Stonehouse, UK). Flasks with the cells were placed in a tissue culture incubator at 37°C, supplied with 20% O_2 and 5% CO_2 .

4.2.2 Tissue culture of the chondrocytes

Following chondrocyte isolation, human chondrocytes were placed in T75 flasks to proliferate. Complete media was changed twice a week until chondrocytes reached 90% confluence. To collect or passage chondrocytes, media was removed and cells were washed twice with 5mL 1x Dulbecco's phosphate buffered saline (DPBS) (Sigma-Aldrich, Dorset, UK). DPBS was removed and 5mL of 1x trypsin-Ethylenediaminetetraacetic acid (EDTA) (Sigma- Aldrich, Dorset, UK) was added to the cells. Cells were placed at 37°C for 3min to detach from plastic and trypsin-EDTA was deactivated by adding 5ml of complete media. Cells were collected and centrifuged at 1400rpm for 4min. Supernatant was removed and cell pellet was resuspended in 5mL of complete media. Cells were counted with a haemocytometer (Hawksley, Sussex, UK) and cell number was calculated by using the formula below:

total cell number = number of cells counted in four corner squares / 4 x 10^3 x initial volume

Cells were either collected and lysed or seeded in well plates in appropriate density according to the experimental procedure downstream.

4.2.3 Total RNA extraction from cells using TRIzol method

The guanidinium thiocyanate-phenol-chloroform method (TRIzol) (Ambion by Life Technologies, Paisley, UK) is considered as the standard method for RNA extraction. Prior to addition of TRIzol cells were first scrapped off the flask in the DPBS and then pelleted down at 1400rpm for 4min. DPBS was then removed and the following protocol was used for RNA extraction of chondrocytes. 500µL of TRIzol was added to the cell pellet and the sample was lysed by vortexing for 2min. 200µL of chloroform (or less, dependent on amount of TRIzol added, TRIZol:chloroform 5:1) was added to the lysate and shaken vigorously to mix. The sample was left at room temperature for 2-3min until the aqueous phase appeared on top. The sample was then centrifuged at 13,000rpm at 4°C for 20min for phase separation. The aqueous phase was transferred to a new 1.5mL tube. 2µL

of GlycoBlue™ Coprecipitant (Invitrogen by ThermoFisher Scientific, Paisley, UK) was added to the aqueous phase and mixed. An equal amount of isopropanol (Sigma-Aldrich, Dorset, UK) was added and the tube was inverted ten times to mix. The sample was left on ice for 30min to precipitate total RNA. The sample was centrifuged at 13,000rpm at 4°C for 20min to pellet RNA. Supernatant was discarded. The pelleted RNA was washed with 1mL of 75% ice-cold molecular biology-grade ethanol. The sample was centrifuged at 13,000rpm at 4°C for 5min. Most of the ethanol was discarded by decanting. To remove any ethanol left, the sample was pulse spun and the excess of ethanol was pipetted out of the tube. The sample was left on the bench to air dry (approximately for 10min). The RNA pellet was dissolved in 15μL of nuclease-free water. RNA concentration and purity were measured using a Nanodrop 2000 Spectrophotometer. RNA was stored at -80°C.

4.2.4 cDNA synthesis for mRNA quantification

Total RNA was reverse transcribed into cDNA for mRNA quantification using the M-MLV reverse transcriptase (Promega, Southampton, UK) (Promega, 2016). 500ng of total RNA was converted into cDNA. This was mixed with 0.5μL of random primers (Promega, Southampton, UK) and with nuclease-free water up to final volume of 18.3μL. This was incubated at 70°C for 5min to dissociate secondary RNA structures. Then, the mixture was mixed with 5μL of M- MLV 5X Reaction Buffer (Promega, Southampton, UK), 0.6μL of 25mM PCR Nucleotide Mix (Promega, Southampton, UK), 0.6μL of RNasin(R) mRNA expression was calculated using the 2 -ΔCT method (Livak & Schmittgen, 2001), relative to the appropriate reference genes. Plus RNase Inhibitor (Promega, Southampton, UK) and 0.5μL M-MLV Reverse Transcriptase, up to final volume of 25μL. The final mixture was mixed well and incubated at 37°C for 60min for reverse transcription. Reverse transcriptase was inactivated at 93°C for 5min and cDNA stored at -20°C.

4.2.5 qPCR for mRNA quantification

mRNA amplification by qPCR was carried out using the QuantiTect SYBR Green PCR Master Mix (Qiagen, Manchester, UK). Primers were either designed by the Panagiotis Balaskas (Phd student) and synthesised by Eurogentec (Seraing, Belgium), or designed and synthesised by Primerdesign (Chandler's Ford, UK). cDNA was diluted with nuclease-free water at a working concentration of 2.5ng/μL. Eurogentec forward and reverse primers were mixed and diluted at a working concentration of 20μM per primer. Primerdesign primers were resuspended as a primer mix at a working concentration of 6μM. In a 96-Well Semi-Skirted PCR Plate, the following were added per well:

4μL of diluted cDNA (10ng per reaction), 5μL of QuantiTect SYBR Green PCR Master Mix, 0.2μL

of Eurogentec primer mix (final concentration in reaction: 400nM) or 0.67μL of Primerdesign primer mix (final concentration in reaction: 400nM). Nuclease-free water was added up to 10μL final volume per reaction. Each reaction was set up in duplicate or triplicate. MRNA amplification was carried out by a LightCycler® 96 Instrument under the following cycling conditions: 1 cycle of: 95°C for 15min, 45 cycles of: 94°C for 15sec, 55°C for 30sec, 70°C for 30sec. Melting curve: 95°C for 10sec, 65°C for 60sec, 97°C for 1sec (acquisition mode: continuous). mRNA expression was calculated using the $2^{-\Delta CT}$ method (Livak & Schmittgen, 2001), relative to the appropriate reference genes.

4.2.6 Sodium dodecyl sulphate–polyacrylamide gel electrophoresis on proteins extracted from the cells

Sodium dodecyl sulphate–polyacrylamide gel electrophoresis (SDS-PAGE) was used to separate proteins extracted from the chondrocytes. Proteins were detected using silver staining or Coomassie Brilliant Blue staining. 7.5μL of 2x Novex™ Tris-Glycine SDS Sample Buffer (ThermoFisher Scientific, Paisley, UK), supplemented with 8% of 2-Mercaptoethanol (Sigma-Aldrich, Dorset, UK), was added to 7.5μL of sample (2μg of protein). Samples were mixed and heated at 100°C for 10min to denature proteins. Samples were placed immediately on ice. A NuPAGE™ 4% to 12%, Bis-Tris gel (ThermoFisher Scientific, Paisley, UK) was placed in the electrophoretic tank and the tank was filled with 1x NuPAGE® MES Running Buffer (ThermoFisher Scientific, Paisley, UK) (diluted from the 20x stock in ultrapure water). Samples were loaded onto the gel alongside 6μL of the Novex™ Sharp Pre-stained Protein Standard ladder (ThermoFisher Scientific, Paisley, UK). The gel was run at 80V for 10min and then 100V for the remaining time of electrophoresis.

4.2.7 Silver staining of polyacrylamide gels

A silver staining method was used to detect protein bands on the polyacrylamide gel. The Pierce Silver Stain Kit (ThermoFisher Scientific, Paisley, UK) was used to assess quality and molecular weight distribution of proteins run on polyacrylamide gels according to manufacturer's instructions (ThermoFisherScientific, 2016).

4.2.8 Removal of foetal bovine serum from the chondrocyte medium

As it was mentioned earlier cells for proteomics analysis were frozen in DMEM consisting of 50% foetal bovine serum (FBS) and 10% dimethyl sylfoxide. However, for the label-based proteomics using iTRAQ method samples needed to be free of FBS. To remove the FBS from the samples cells were first thawed at room temperature and then spun down at 400 x g for 4 min. Afterwards supernatant was removed and 1ml of Dulbecco's phosphate buffered saline (DPBS) was

added gently to the tube with the sample and gently mixed by slowly pipetting up and down. Then the tubes were centrifuged as before and cells were washed again with DPBS, in total wash step was completed three times. After discarding the supernatant at the finish of the final step 200μL of ammonium bicarbonate (25mM) was added to the sample.

4.2.9 Sample preparation using S-trap columns for LC-MS/MS analysis of cells

S-trap columns (Protifi, Fairport, USA) were used for sample preparation of chondrocytes for the proteomics analysis. S-trap columns enable the use of SDS in proteomics sample preparation. SDS is a nearly universal protein solvent that dissolves even poorly-soluble molecules like membrane proteins which are often discarded as pellets. The manufacturer's protocol was followed for the sample preparation, lysis buffer contained 5% SDS at the final concentration and proteins were digested using Trypsin/Lys-C Mix (Promega, Southampton, UK).

4.2.10 Sample preparation using SPEED method for LC-MS/MS analysis of cells

Sample Preparation by Easy Extraction and Digestion (SPEED) was used to prepare protein samples for further LC-MS/MS analysis. The protocol provided by the authors were followed. In brief in consisted of three steps, acidification, neutralization and digestion. Pure TFA was used to lyse the cells and extract proteins. Proteins were digested using Trypsin/Lys-C Mix.

4.2.11 Sample preparation using sonication method for LC-MS/MS analysis of cells

The standard method of protein sample preparation used in our group was performed on the cells to extract proteins from the cells and digest the proteins. This method is covered in detail in Chapter 2 methods. In brief, sonication method was used to disrupt the cells followed by the addition of Rapigest Surfactant that helps to digest the proteins during the sample preparation. Samples were then reduced and alkylated to keep at the denatured state. proteins were digested using Trypsin/Lys-C Mix.

4.2.12 Sample preparation for LC-MS/MS analysis of chondrocytes from the different zones

The sample preparation was undertaken in the Centre for Proteome Research (University of Liverpool, UK) by the qualified scientists at the facility. In brief, the protocol consisted of the following steps.

100μL of Lysis buffer was added to the sample. Lysis buffer was made of the following 100mM Triethylammonium bicarbonate (TEAB) 0.05% (W/V), RapiGest (5 vials per 10mL), 1x protease inhibitor (cOmplete Mini EDTA-free, Roche), 250 U benzonase per 10 mL of Lysis buffer.

Cells were sonicated for 1min at 30% amplitude (10s on, 10s off cycles). Samples were boiled 80°C for 10 min. Protein concentration was determined using Bradford protein assay. 12.5 µg lysate were diluted in 100 mM TEAB to give a total volume of 75 µl. Proteins were reduced with DTT: 5 µl of 11 mg/ml in 100mM TEAB (72 mM) stock (4 mM Final) at 60°C for 10 min. Samples were put in the fridge for 5 minutes. Proteins were alkylated with Iodoacetamide (IAA): 5 µl of 46.6 mg/ml in 100mM TEAB (266 mM) stock (14 mM Final) at room temperature in the dark for 30 min. IAA was quenched with Dithiothreitol (DTT) by adding 4.7 µl of 11 mg/ml in 100mM TEAB (72 mM) stock (7mM Final). Proteins were digested by the addition of 0.250ug Trypsin (1.25uL) (0.2 ug/ul stock) for 50:1 protein:trypsin ratio and incubated at 37°C on the rocker overnight. On the next day samples were dried and resuspended in 20 µl of TEAB. TMT 10plex (ThermoFisher Scientific, UK) was used label the peptides according to the manufacturer's protocol.

4.2.13 Bioinformatic analysis of LC-MS/MS experiment

Bioinformatic analysis of LC-MS/MS data was performed by appropriate personnel at CPR, as described in (Timur et al., 2020). For label-free quantification, the raw files of the acquired spectra were aligned by the Progenesis QI for proteomics software (Waters, Manchester, UK), which peak picks for quantification by peptide ion abundance. One reference sample was selected and the retention times of the other samples were aligned. The top five spectra for each feature were exported from Progenesis QI and used for peptide identification with our local Mascot server (Version 2.6.2) searching against the Unihuman Reviewed database, containing 22,640 protein sequences. Search parameters were adjusted to mass tolerance of 10ppm, fragment mass tolerance of 0.01Da, one missed cleavage allowed, with carbamidomethyl cysteine as a fixed modification and methionine, proline, lysine oxidation as variable modifications. Statistical analysis was performed using Progenesis QI in-build statistical tool that provided q-value, the expected proportion of false positives if that feature's p-value is chosen as the significance threshold. This provides greater power for finding truly significant features.

4.3 RESULTS

4.3.1 Tissue culture of human chondrocytes extracted from the articular cartilage

Chondrocytes extracted from the articular cartilage where either frozen down for the proteomics analysis or were cultured in the media and passaged. Due to the difference of cellularity in the different zones of articular cartilage there were a higher number of cells extracted from the

superficial zone in comparison to the deep zone. Furthermore, cells derived from the superficial zone of articular cartilage showed higher proliferation rates in culture. Cells showed drastic change in the phenotype upon culturing in the medium (Fig. 4.1). On the following day of plating cells in the culture medium they appeared round in shape, however, after just ten days in culture the cells resembled fibroblast like shape.
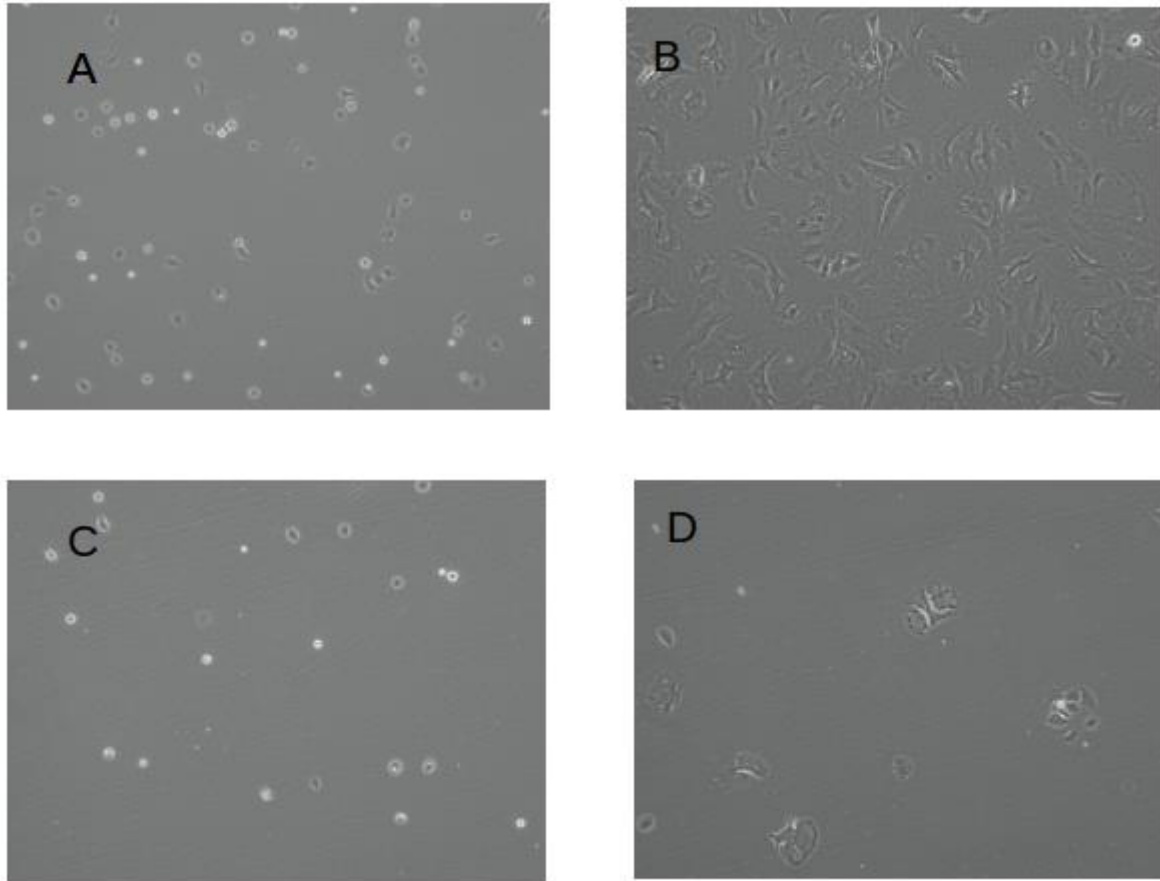
Figure 4.1: Chondrocytes extracted from the articular cartilage were cultured in the medium. (A) There were higher number of chondrocytes extracted from the superficial zone in comparison to the (B) chondrocytes extracted from the deep zone. After ten days of culturing (C, D) chondrocytes changed the phenotype and the cells from the superficial zone had higher proliferation rate.

4.3.2 Gene expression analysis of chondrocytes extracted from the superficial and deep zones of articular cartilage

To assess the gene expression profile of chondrocytes extracted from the superficial and deep zones we used qPCR analysis. In order to find the differences in the gene expression levels of chondrogenic (SOX9, ACAN, COL2A1), zone specific (COL10A1, RUNX2, PRG4) and inflammatory (MMP13) genes upon culturing we have passaged the cells until P3 (Fig 4.2). Furthermore, on the following media change after plating the chondrocytes we have changed the

medium in the flask to a fresh medium. The medium that was collected from the flask contained cells that were not attached to the plastic. These cells were also used for RNA extraction and qPCR analysis. These cells were designated as unattached (U). The gene expression level of SOX9, COL2A1 and ACAN were significantly downregulated upon culturing in the media both in the superficial and deep zone chondrocytes. The gene expression level of PRG4 decreased upon culturing in the medium when compared to the U cells. RUNX2 gene expression was not significantly different between the superficial and deep zone chondrocytes, however, there was an increase in gene expression of RUNX2 in P2 of deep zone chondrocytes. COL10A was only expressed in the unattached chondrocytes derived from the deep zone, and following passaging the gene expression levels were not observed in the deep zone chondrocytes, neither in the superficial zone chondrocytes. There was no significant change in the gene expression of MMP13 between the zones and upon culturing.
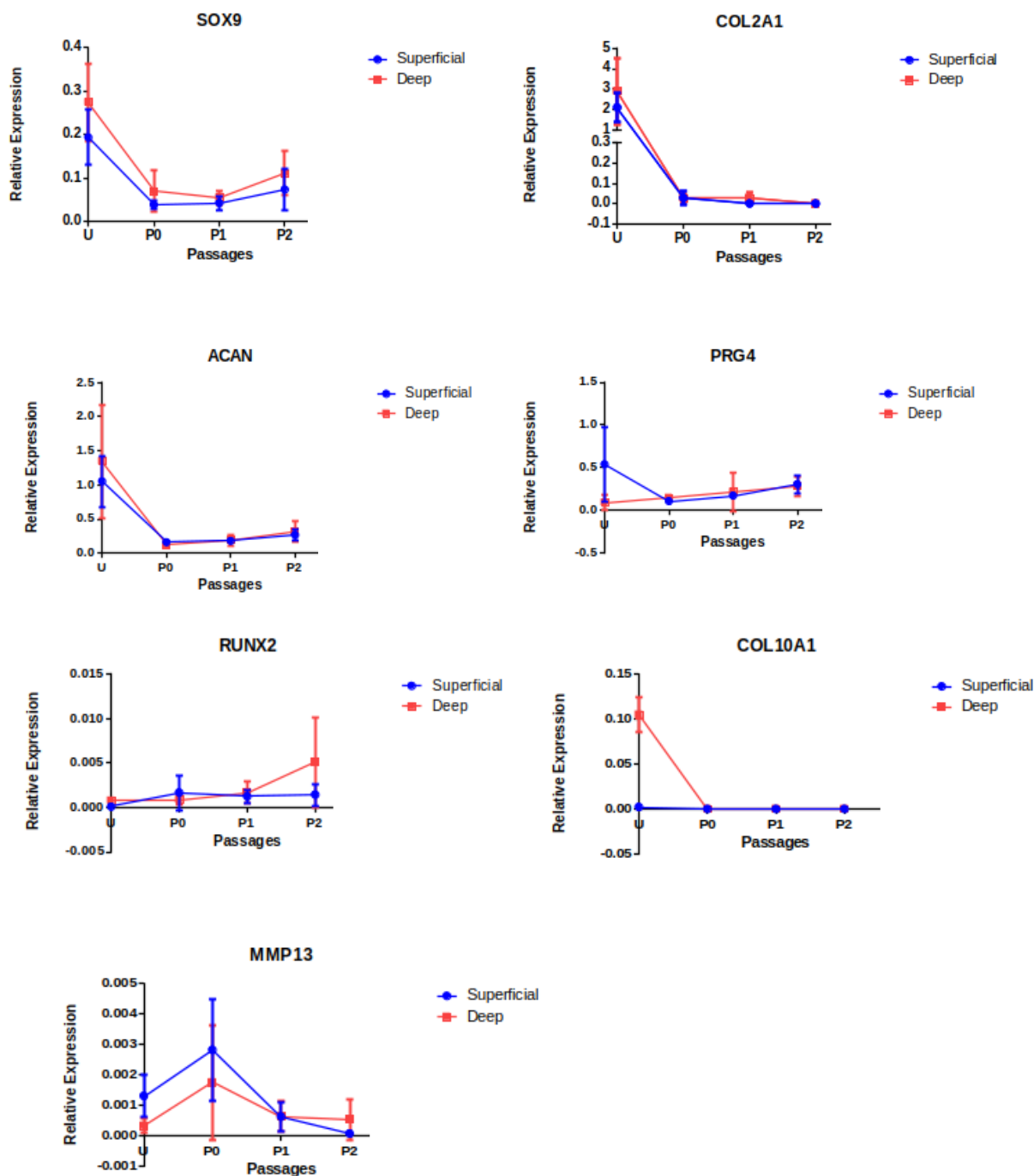
Figure 4.2: Gene expression levels of chondrogenic (SOX9, COL2A1, ACAN), zone specific (PRG4, COL10A1, RUNX2) and inflammatory (MMP13) genes. SOX9, COL2A1, ACAN genes were downregulated upon passaging. PRG4 and RUNX2 gene expression level were not changed between the zones and upon passaging. COL10A1 was only expressed in the U cells of the deep zone. MMP13 gene expression levels were not significantly changed upon between the zones, however at P2 superficial zone chondrocytes demonstrated the lowest level of MMP13 gene expression. Error bars represent standard deviation of the relative gene expression to the reference gene (GAPDH)

4.3.3 Optimisation of sample preparation of proteins for LC-MS/MS

We used three methods to prepare samples for proteomics using LC-MS/MS, namely SPEED, S-trap columns and standard method using sonication. The samples were prepared from the same donor of human chondrocytes extracted from the OA cartilage and the same number of cells. SPEED demonstrated the lowest amount of proteins identified (281 proteins) after LC-MS/MS. Standard method using sonication has produced the largest amount of proteins identified (1218 proteins) and S-trap column-based method allowed to identify 810 proteins in the sample (Fig 4.3). The chromatograms produced by LC-MS/MS of SPEED method has the lowest peaks, whilst S-trap columns had equal and sharper peaks.
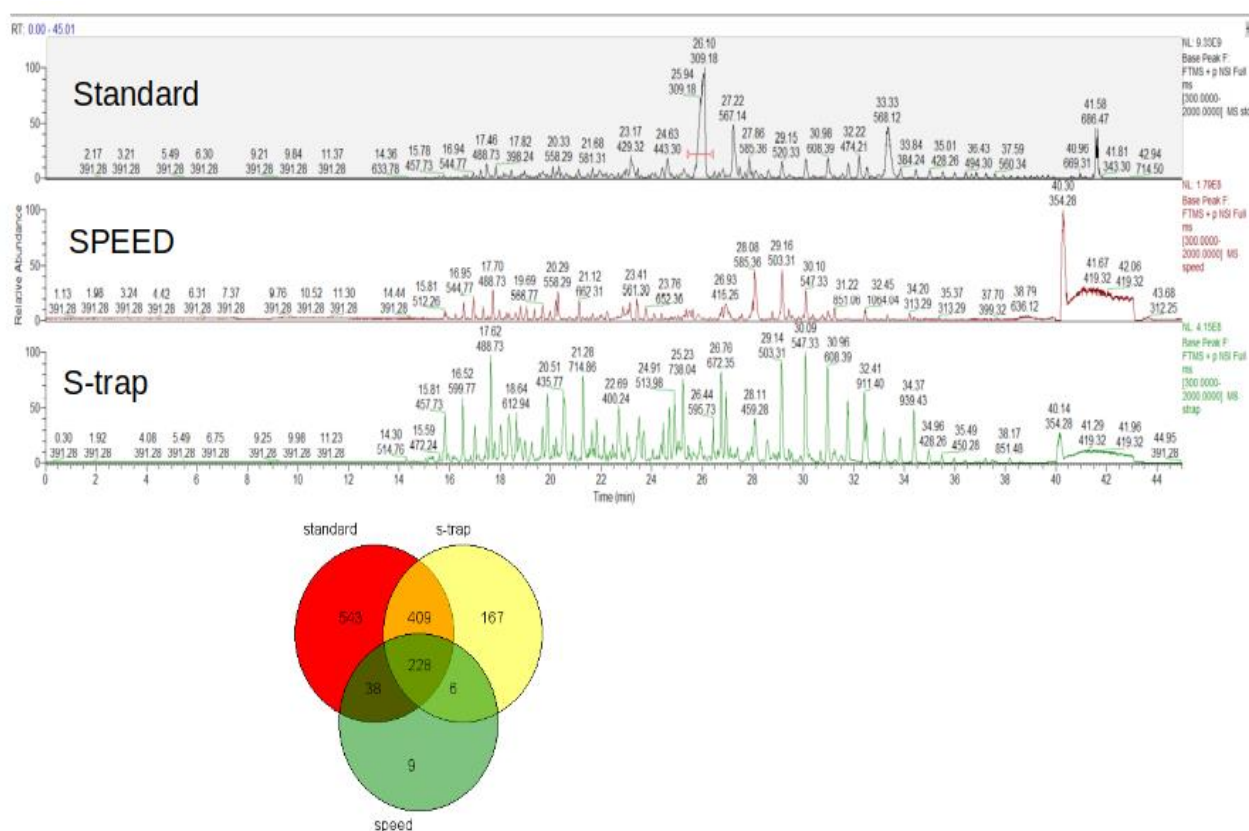
Figure 4.3. Proteins from chondrocytes were extracted and prepared for LC-MS/MS using Standard sonication, SPEED and S-trap methods. A. Chromatograms for Standard method had higher and a greater number of peaks in comparison to the SPEED method. S-trap method had sharper and higher peaks in the chromatogram. B. Venn diagram of number of proteins identified. Standard method lead to the identification of 1218 proteins in the sample, S-trap method had 810 proteins and SPEED method identified only 281 proteins in the sample. Standard and S-trap methods had identified 637 proteins that were present in both methods (Venn diagram was made in GeneVenn).

4.3.4 The depletion of FBS from the chondrocyte samples

FBS present in the sample could inhibit the TMT labelling of samples for LC-MS/MS, thus we attempted to remove it. We performed PBS washes on the chondrocyte pellet after thawing them and then protein extracted from the cells were assessed using Silver stain method. SDS-PAGE was run on the same sample of chondrocytes that had different amount of cells and the different number of wash steps (Fig. 4.4). FBS produced distinct protein band at 260kDa, 160kDa and 60kDa. After just one

PBS wash the aforementioned bands were significantly reduced on the gel. Three steps of PBS wash demonstrated the similar results of one wash step with PBS.

Lane	Amount of cells	PBS washes	Protein conc. (ug/ml)	Total protein (ug)
1*	50,000	1	32.9	6.6
2*	50,000	3	30.5	6.1
3	150,000	No	576.4	115.3
4	150,000	1	214.0	42.8
5	150,000	3	57.4	11.5
6	500,000	1	1137.1	227.4
7	500,000	3	1266.8	253.4
8	Media (50% FBS, 10% DMSO)			

4-12% Bis-Tris gel
600ng loaded per lane
*300ng loaded
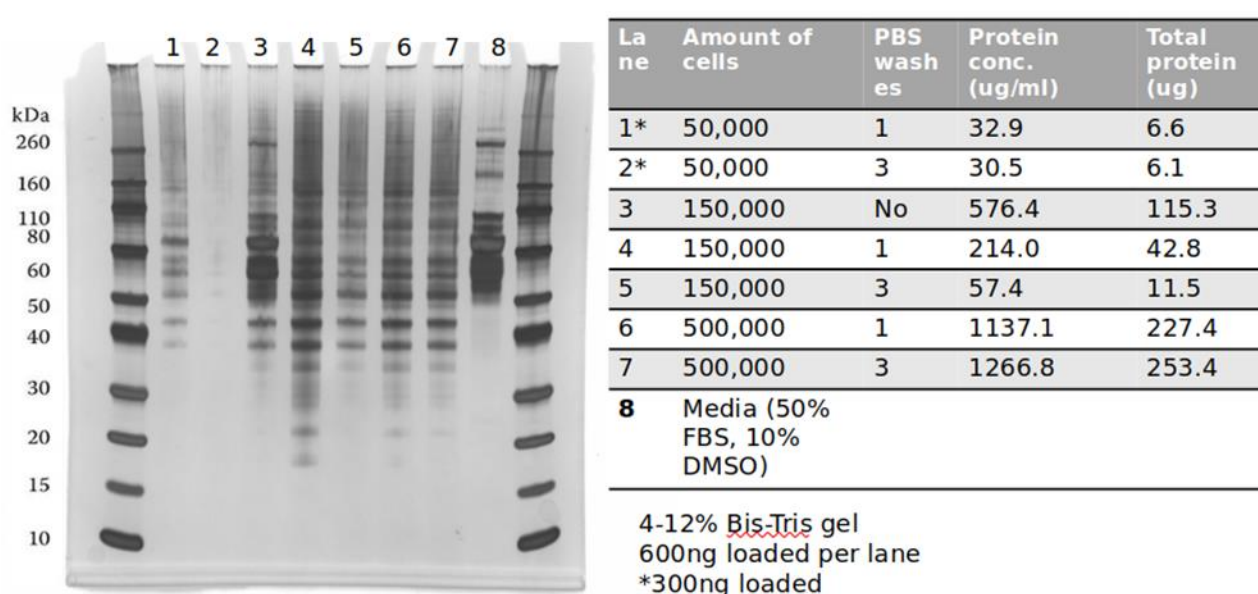
Figure 4.4. Proteins extracted from the chondrocytes following PBS washing.   Washes were undertaken either once (lanes 1, 4, 6), three times (lanes 2, 5 and 7) or no wash (lane 3). Also media with FBS and DMSO was run on the SDS-PAGE (lane 8). Media with FBS demonstrated distinct bands at 260kDa, 160kDa and 60kDa. The sample that was not washed with PBS had these bands in the gel (lane 3).

4.3.5 Label-based proteomics of chondrocytes extracted from the superficial and deep zone of cartilage in young and OA groups

The standard method of sample preparation was selected for LC-MS/MS analysis. The proteins were then labelled with 10plex TMT tags, each tag had a unique reporter ion to distinguish the samples during the data analysis. However, during the experiment it was found that the maximum label efficiency of 40%, thus experiment was stopped and was not completed.

4.3.6 Label-free proteomics of chondrocytes extracted from the superficial and deep zones of cartilage in young and OA samples

1ug of each sample was saved before the label-based proteomics. After the failure of label-based proteomics these 1ug samples were used for label-free proteomics. Proteomics analysis showed that there were in total 1124 proteins identified in all samples. The comparison of OA superficial and OA deep zone chondrocytes showed only Prostoglandin 1 (PTGS1) upregulation at the significant level (q < 0.05) in the superficial zone. The comparison of young superficial and young deep zone chondrocytes demonstrated no change in protein abundance at FDR 0.05 significant level between the groups. Superficial zone comparison between young and OA groups revealed three proteins differentially abundant: CD44 antigen (CD44), 40s ribosomal protein (RSP14) and Tubulin beta chain (TUBB). All of the three proteins were significantly upregulated in the superficial zone of OA group in comparison to the superficial zone of young samples. The comparison of the deep zone between OA and young groups found 344 proteins deferentially abundant at FDR<0.05.

Table 4.1 OA group superficial vs. deep zone (q <0.05)

Protein	q-Value (FDR)	Fold change	Full name
PTGS1	0.03	7.566	Prostaglandin G/H synthase

Table 4.2 Superficial zone OA vs. young group (q<0.05)

Protein	q-Value (FDR)	Fold change	Full name
CD44	0.026	9.80	CD44 antigen
RPS14	0.028	2.076	40S ribosomal protein S14
TUBB	0.028	4.472	Tubulin beta chain

Table 4.3 Deep zone OA vs. young group (q<0.05)

Protein	q Value	Fold change	Full name
QSOX1	0.00398	-4.70	Sulfhydryl oxidase 1
MFGE8	0.0238	-3.20	Lactadherin
APEH	0.0294	-2.26	Acylamino-acid-releasing enzyme
CLEC3B	0.029	-3.94	Tetranectin
PPP1CC	0.029	-16.07	Serine/threonine-protein phosphatase PP1-gamma catalytic subunit
F5	0.029	-4.243	Coagulation factor V
KRT31	0.029	-3.277	Keratin, type I cuticular Ha1
RPL32	0.029	-28.25	60S ribosomal protein L32
COL1A2	0.034	-14.55	Collagen alpha-2(I) chain
C9	0.034	-2.746	Complement component C9
THBS1	0.036	-2.927	Thrombospondin-1
AGO3	0.039	-2.487	Protein argonaute-3
NIPSNAP1	0.040	-3.159	Protein NipSnap homolog 1
LRP1	0.043	-2.232	Prolow-density lipoprotein receptor-related protein 1
CD44	0.005	5.503	CD44 antigen
HNRNPA2B1	0.014	4.421	Heterogeneous nuclear ribonucleoproteins A2/B1
PUF60	0.023	3.657	Poly(U)-binding-splicing factor PUF60
SCARB2	0.028	2.019	Lysosome membrane protein 2
LMNA	0.028	2.441	Prelamin-A/C
KRT5	0.029	4.646	Keratin, type II cytoskeletal 5
LNPEP	0.0294	4.49	Leucyl-cystinyl aminopeptidase
SF3B2	0.0294	2.910	Splicing factor 3B subunit 2
CRIP2	0.0294	12.77	Cysteine-rich protein 2
H2AFY	0.0294	2.418	Core histone macro-H2A.1
NONO	0.02942	2.050	Non-POU domain-containing octamer-binding protein
CDC37	0.02942	2.635	Hsp90 co-chaperone Cdc37

AHNAK	0.02942	1.991	Neuroblast differentiation-associated protein AHNAK
TUBB4B	0.02942	2.283	Tubulin beta-4B chain
CLIC4	0.02942	3.017	Chloride intracellular channel protein 4
SEC23A	0.02942	3.638	Protein transport protein Sec23A
CTSD	0.02942	2.858	Cathepsin D
KHSRP	0.02942	2.398	Far upstream element-binding protein 2
KPNB1	0.02942	3.721	Importin subunit beta-1
SF3B3	0.02942	2.18	Splicing factor 3B subunit 3
HAPLN1	0.02942	3.64	Hyaluronan and proteoglycan link protein 1
LMNB2	0.02942	1.83	Lamin-B2
TRIM28	0.02942	3.34	Transcription intermediary factor 1-beta
PABPC1	0.02942	2.89	Polyadenylate-binding protein 1
ERH	0.02942	2.71	Enhancer of rudimentary homolog
RAC1	0.02942	2.53	Ras-related C3 botulinum toxin substrate 1
RTN4	0.02942	5.86	Reticulon-4
HNRNPA1	0.02942	3.28	Heterogeneous nuclear ribonucleoprotein A1
ARL6IP5	0.02942	2.58	PRA1 family protein 3
VIM	0.02942	2.85	Vimentin
PCBP1	0.02942	4.05	Poly(rC)-binding protein 1
NPM1	0.02942	2.49	Nucleophosmin
AHCY	0.02942	2.20	Adenosylhomocysteinase
PSPC1	0.02942	3.21	Paraspeckle component 1
S100A10	0.02942	2.55	Protein S100-A10
ANXA2	0.02942	2.06	Annexin A2
RAN	0.02942	2.11	GTP-binding nuclear protein Ran
RPL10A	0.02942	3.82	60S ribosomal protein L10a
RPL23	0.02942	4.13	60S ribosomal protein L23
HNRNPK	0.02942	2.71	Heterogeneous nuclear ribonucleoprotein K
SACM1L	0.02942	13.2	Phosphatidylinositide phosphatase SAC1
SNRPD3	0.02942	2.105	Small nuclear ribonucleoprotein Sm D3
DDX5	0.02942	2.794	Probable ATP-dependent RNA helicase DDX5
GRN	0.02942	3.175	Granulins

VAPA	0.02942	2.702	Vesicle-associated membrane protein-associated protein A
RHOA	0.02942	3.014	Transforming protein RhoA
XRCC6	0.02942	2.39	X-ray repair cross-complementing protein 6
NFIX	0.02942	3.66	Nuclear factor 1 X-type
ILF2	0.02942	3.22	Interleukin enhancer-binding factor 2
LMAN2	0.02942	1.65	Vesicular integral-membrane protein VIP36
EFTUD2	0.02942	2.63	116 kDa U5 small nuclear ribonucleoprotein component
RPS20	0.02942	2.398	40S ribosomal protein S20
PSAP	0.02942	2.32	Prosaposin
RPL13A	0.02942	2.68	60S ribosomal protein L13a
RPL12	0.02942	2.78	60S ribosomal protein L12
RPS17	0.02942	4.62	40S ribosomal protein S17
RAB7A	0.02942	1.95	Ras-related protein Rab-7a
PRPF19	0.02942	6.05	Pre-mRNA-processing factor 19
GORASP2	0.02942	5.61	Golgi reassembly-stacking protein 2
GNB1	0.03	2.58	Guanine nucleotide-binding protein G(I)/G(S)/G(T) subunit beta-1
ATL3	0.03	3.53	Atlastin-3
TKT	0.03	2.83	Transketolase
RPL24	0.03	4.39	60S ribosomal protein L24
SURF4	0.03	2.44	Surfeit locus protein 4
EEF1A1P5	0.03	3.39	Putative elongation factor 1-alpha-like 3
RAB2A	0.03	2.15	Ras-related protein Rab-2A
TUBB2B	0.03	6.53	Tubulin beta-2B chain
DDAH2	0.03	2.22	N(G),N(G)-dimethylarginine dimethylaminohydrolase 2
RPLP1	0.03	3.32	60S acidic ribosomal protein P1
TARDBP	0.03	2.54	TAR DNA-binding protein 43
RPL37A	0.03	3.55	60S ribosomal protein L37a
RTCB	0.03	1.93	tRNA-splicing ligase RtcB homolog
SH3BGRL3	0.03	4.41	SH3 domain-binding glutamic acid-rich-like protein 3

131

PRELP	0.03	4.37	Prolargin
TRPV4	0.03	4.00	Transient receptor potential cation channel subfamily V member 4
RPL10	0.03	2.98	60S ribosomal protein L10
TAF15	0.02942	5.88	TATA-binding protein-associated factor 2N
CYP20A1	0.02942	3.01	Cytochrome P450 20A1
ERO1A	0.02942	8.80	ERO1-like protein alpha
PDIA5	0.02942	2.597	Protein disulfide-isomerase A5
RPL35A	0.02942	2.27	60S ribosomal protein L35a
SEC22B	0.02942	2.24	Vesicle-trafficking protein SEC22b
TBL2	0.02942	2.25	Transducin beta-like protein 2
HNRNPC	0.02942	3.16	Heterogeneous nuclear ribonucleoproteins C1/C2
ASAH1	0.02942	2.76	Acid ceramidase
PICALM	0.02942	3.80	Phosphatidylinositol-binding clathrin assembly protein
PDLIM5	0.02968	2.82	PDZ and LIM domain protein 5
MYADM	0.02968	3.43	Myeloid-associated differentiation marker
TXNL1	0.03	3.06	Thioredoxin-like protein 1
HSPA8	0.03	2.97	Heat shock cognate 71 kDa protein
HSP90AB1	0.03	2.49	Heat shock protein HSP 90-beta
TNS3	0.03	7.09	Tensin-3
ITPR2	0.03	3.02	Inositol 1,4,5-trisphosphate receptor type 2
CALR	0.03	1.73	Calreticulin
PYGL	0.03	2.28	Glycogen phosphorylase, liver form
SF3A1	0.03	3.08	Splicing factor 3A subunit 1
TXNDC5	0.03	1.82	Thioredoxin domain-containing protein 5
NOP58	0.03	2.50	Nucleolar protein 58
SEC61B	0.03	2.48	Protein transport protein Sec61 subunit beta
SNX6	0.03	2.26	Sorting nexin-6
HNRNPR	0.03	1.60	Heterogeneous nuclear ribonucleoprotein R
SEPT2	0.03	2.44	Septin-2
AP2M1	0.03	2.03	AP-2 complex subunit mu
SRPRB	0.03	2.87	Signal recognition particle receptor subunit beta
VCP	0.03	2.54	Transitional endoplasmic reticulum ATPase

ATP2A2	0.03	2.38	Sarcoplasmic/endoplasmic reticulum calcium ATPase 2
CLTC	0.03	1.79	Clathrin heavy chain 1
RUVBL1	0.03	2.19	RuvB-like 1
HNRNPD	0.03	2.51	Heterogeneous nuclear ribonucleoprotein D0
HDLBP	0.03	2.10	Vigilin
METTL7A	0.03	2.46	Methyltransferase-like protein 7A
S100A11	0.03	3.25	Protein S100-A11
RNH1	0.03	2.93	Ribonuclease inhibitor
RPL11	0.03	2.70	60S ribosomal protein L11
RPL35	0.03	4.42	60S ribosomal protein L35
RPL9	0.03	4.30	60S ribosomal protein L9
SNRPD2	0.03	2.60	Small nuclear ribonucleoprotein Sm D2
RPS15A	0.03	3.66	40S ribosomal protein S15a
RPL30	0.03	3.26	60S ribosomal protein L30
RACK1	0.03	2.47	Receptor of activated protein C kinase 1
ACSL3	0.03	3.62	Long-chain-fatty-acid--CoA ligase 3
PAPSS2	0.03	2.88	Bifunctional 3'-phosphoadenosine 5'-phosphosulfate synthase 2
THRAP3	0.03	1.90	Thyroid hormone receptor-associated protein 3
CPPED1	0.03	2.58	Serine/threonine-protein phosphatase CPPED1
AP1G1	0.03	3.44	AP-1 complex subunit gamma-1
COMT	0.032	2.31	Catechol O-methyltransferase
RPL7A	0.032	2.16	60S ribosomal protein L7a
LIN7C	0.032	1.99	Protein lin-7 homolog C
GMPPA	0.032	5.06	Mannose-1-phosphate guanyltransferase alpha
UBE2N	0.032	3.53	Ubiquitin-conjugating enzyme E2 N
ISOC2	0.032	1.82	Isochorismatase domain-containing protein 2
KHDRBS1	0.0.33	4.34	KH domain-containing, RNA-binding, signal transduction-associated protein 1
TMPO	0.034	2.86	Lamina-associated polypeptide 2, isoforms beta/gamma
HNRNPUL2	0.034	3.27	Heterogeneous nuclear ribonucleoprotein U-like protein 2

SRRM2	0.034	17.7	Serine/arginine repetitive matrix protein 2
PLEC	0.034	1.65	Plectin
HNRNPU	0.034	2.45	Heterogeneous nuclear ribonucleoprotein U
SRSF5	0.034	1.84	Serine/arginine-rich splicing factor 5
TOLLIP	0.034	2.24	Toll-interacting protein
RALY	0.034	3.54	RNA-binding protein Raly
RAB11B	0.034	1.64	Ras-related protein Rab-11B
ELAVL1	0.034	2.34	ELAV-like protein 1
NFIC	0.034	3.90	Nuclear factor 1 C-type
PLCD1	0.034	3.51	1-phosphatidylinositol 4,5-bisphosphate phosphodiesterase delta-1
GNG12	0.034	2.37	Guanine nucleotide-binding protein G(I)/G(S)/G(O) subunit gamma-12
CAPZA1	0.034	3.60	F-actin-capping protein subunit alpha-1
PRKCSH	0.034	1.86	Glucosidase 2 subunit beta
RCN2	0.034	2.99	Reticulocalbin-2
COPB1	0.034	3.00	Coatomer subunit beta
EEF1G	0.034	2.41	Elongation factor 1-gamma
CNP	0.034	4.35	2',3'-cyclic-nucleotide 3'-phosphodiesterase
HNRNPA0	0.034	2.74	Heterogeneous nuclear ribonucleoprotein A0
EEF1B2	0.034	2.05	Elongation factor 1-beta
RPRD1B	0.034	3.16	Regulation of nuclear pre-mRNA domain-containing protein 1B
TUBB	0.034	2.47	Tubulin beta chain
RPS16	0.034	2.99	40S ribosomal protein S16
TPD52	0.034	7.29	Tumor protein D52
C1QBP	0.034	2.43	Complement component 1 Q subcomponent-binding protein, mitochondrial
NPTN	0.034	1.91	Neuroplastin
FUBP1	0.034	2.03	Far upstream element-binding protein 1
HUWE1	0.034	3.01	E3 ubiquitin-protein ligase HUWE1
ILF3	0.034	2.02	Interleukin enhancer-binding factor 3
VPS35	0.034	2.33	Vacuolar protein sorting-associated protein 35
COPB2	0.034	2.23	Coatomer subunit beta'

CILP	0.034	2.22	Cartilage intermediate layer protein 1
RRBP1	0.034	2.07	Ribosome-binding protein 1
PSMA1	0.034	2.59	Proteasome subunit alpha type-1
ACTB	0.034	2.90	Actin, cytoplasmic 1
HNRNPA3	0.034	1.74	Heterogeneous nuclear ribonucleoprotein A3
GNAI2	0.034	2.09	Guanine nucleotide-binding protein G(i) subunit alpha-2
GAPDH	0.034	3.412	Glyceraldehyde-3-phosphate dehydrogenase
RPL28	0.034	5.14	60S ribosomal protein L28
PGK1	0.034	4.18	Phosphoglycerate kinase 1
CALM1	0.034	4.30	Calmodulin-1
IDH1	0.034	2.73	Isocitrate dehydrogenase [NADP] cytoplasmic
SH3BGRL	0.034	5.40	SH3 domain-binding glutamic acid-rich-like protein
RPSA	0.034	2.46	40S ribosomal protein SA
DKC1	0.034	2.29	H/ACA ribonucleoprotein complex subunit 4
HNRNPDL	0.034	2.46	Heterogeneous nuclear ribonucleoprotein D-like
H2AFY2	0.034	1.99	Core histone macro-H2A.2
GLS	0.034	3.02	Glutaminase kidney isoform, mitochondrial
SNRPF	0.034	3.04	Small nuclear ribonucleoprotein F
PSMC4	0.034	3.36	26S proteasome regulatory subunit 6B
RCN1	0.034	2.47	Reticulocalbin-1
RPL8	0.035	3.06	60S ribosomal protein L8
SERPINH1	0.035	3.79	Serpin H1
KTN1	0.035	4.15	Kinectin
ACBD3	0.035	2.99	Golgi resident protein GCP60
PRKRA	0.035	1.89	Interferon-inducible double-stranded RNA-dependent protein kinase activator A
PPT1	0.036	2.71	Palmitoyl-protein thioesterase 1
SEC62	0.036	3.77	Translocation protein SEC62
RECQL	0.036	2.81	ATP-dependent DNA helicase Q1
PSMB4	0.036	2.23	Proteasome subunit beta type-4
RAP1B	0.036	2.07	Ras-related protein Rap-1b
PPIB	0.037	2.05	Peptidyl-prolyl cis-trans isomerase B

RAB14	0.037	1.39	Ras-related protein Rab-14
TMED2	0.037	2.61	Transmembrane emp24 domain-containing protein 2
NME2	0.037	4.22	Nucleoside diphosphate kinase B
SNRPN	0.037	2.62	Small nuclear ribonucleoprotein-associated protein N
ITGB1	0.037	1.662	Integrin beta-1
PRAF2	0.038	2.58	PRA1 family protein 2
HNRNPF	0.038	2.39	Heterogeneous nuclear ribonucleoprotein F
NSFL1C	0.038	3.15	NSFL1 cofactor p47
ADSSL1	0.038	2.60	Adenylosuccinate synthetase isozyme 1
HDGF	0.038	2.32	Hepatoma-derived growth factor
SMU1	0.038	2.01	WD40 repeat-containing protein SMU1
CCT8	0.038	1.61	T-complex protein 1 subunit theta
RPL5	0.038	2.82	60S ribosomal protein L5
DDX3X	0.038	3.76	ATP-dependent RNA helicase DDX3X
RPN2	0.038	1.68	Dolichyl-diphosphooligosaccharide--protein glycosyltransferase subunit 2
CAPG	0.038	4.78	Macrophage-capping protein
ETFB	0.038	1.48	Electron transfer flavoprotein subunit beta
UGP2	0.038	2.45	UTP--glucose-1-phosphate uridylyltransferase
DDX1	0.038	2.16	ATP-dependent RNA helicase DDX1
PARK7	0.038	2.96	Protein/nucleic acid deglycase DJ-1
FKBP2	0.038	2.58	Peptidyl-prolyl cis-trans isomerase FKBP2
RPS19	0.038	2.52	40S ribosomal protein S19
KRT18	0.038	2.08	Keratin, type I cytoskeletal 18
TPI1	0.039	3.02	Triosephosphate isomerase
CAVIN1	0.039	2.54	Caveolae-associated protein 1
AP2B1	0.039	2.23	AP-2 complex subunit beta
RAP1A	0.039	3.62	Ras-related protein Rap-1A
EIF5A	0.039	3.14	Eukaryotic translation initiation factor 5A-1
RPA1	0.039	2.35	Replication protein A 70 kDa DNA-binding subunit
CPNE3	0.039	1.72	Copine-3

PPIA	0.039	2.29	Peptidyl-prolyl cis-trans isomerase A
GANAB	0.039	1.63	Neutral alpha-glucosidase AB
SRSF7	0.039	1.85	Serine/arginine-rich splicing factor 7
SH3GLB1	0.039	3.97	Endophilin-B1
SAR1B	0.039	3.31	GTP-binding protein SAR1b
CMAS	0.039	3.15	N-acylneuraminate cytidylyltransferase
PSMD14	0.039	3.30	26S proteasome non-ATPase regulatory subunit 14
LDHA	0.039	3.13	L-lactate dehydrogenase A chain
HSPB6	0.039	12.4	Heat shock protein beta-6
TAGLN2	0.039	1.55	Transgelin-2
TOR1AIP1	0.039	2.71	Torsin-1A-interacting protein 1
PRPF8	0.04	2.09	Pre-mRNA-processing-splicing factor 8
SYNCRIP	0.04	1.75	Heterogeneous nuclear ribonucleoprotein Q
PABPN1	0.04	2.72	Polyadenylate-binding protein 2
ACAN	0.04	2.87	Aggrecan core protein
YWHAZ	0.04	2.32	14-3-3 protein zeta/delta
CYB5R3	0.04	2.09	NADH-cytochrome b5 reductase 3
CCT6A	0.04	3.05	T-complex protein 1 subunit zeta
TXNDC12	0.04	1.99	Thioredoxin domain-containing protein 12
RPL4	0.04	3.92	60S ribosomal protein L4
RPLP2	0.04	3.58	60S acidic ribosomal protein P2
RPL15	0.04	2.19	60S ribosomal protein L15
AK1	0.04	3.08	Adenylate kinase isoenzyme 1 O
GPI	0.04	3.42	Glucose-6-phosphate isomerase
RPS5	0.04	2.34	40S ribosomal protein S5
YWHAE	0.04	2.75	14-3-3 protein epsilon
PRKDC	0.041	1.59	DNA-dependent protein kinase catalytic subunit
SFPQ	0.041	1.63	Splicing factor, proline- and glutamine-rich
HSD17B12	0.042	1.99	Very-long-chain 3-oxoacyl-CoA reductase
STX7	0.042	3.30	Syntaxin-7
RPS2	0.042	2.56	40S ribosomal protein S2
SNRPE	0.042	2.30	Small nuclear ribonucleoprotein E
GOLGA3	0.042	1.95	Golgin subfamily A member 3

PHLDB1	0.042	1.72	Pleckstrin homology-like domain family B member 1
CANX	0.042	1.40	Calnexin
RPL13	0.042	3.21	60S ribosomal protein L13
RRAS	0.042	2.38	Ras-related protein R-Ras
NAP1L1	0.042	2.35	Nucleosome assembly protein 1-like 1
ERLIN2	0.042	2.48	Erlin-2
RPN1	0.042	1.45	Dolichyl-diphosphooligosaccharide--protein glycosyltransferase subunit 1
YWHAQ	0.042	1.79	14-3-3 protein theta
ARF4	0.042	3.05	ADP-ribosylation factor 4
EEF1D	0.043	1.88	Elongation factor 1-delta
CAPZA2	0.043	1.64	F-actin-capping protein subunit alpha-2
FUS	0.043	2.00	RNA-binding protein FUS
SLC35B2	0.043	1.49	Adenosine 3'-phospho 5'-phosphosulfate transporter 1
NCL	0.043	1.56	Nucleolin
RPL3	0.043	2.45	60S ribosomal protein L3
NEBL	0.043	3.17	Nebulette
CNN3	0.044	1.77	Calponin-3
RPLP0	0.044	2.30	60S acidic ribosomal protein P0
UBA1	0.044	2.60	Ubiquitin-like modifier-activating enzyme 1
MIF	0.044	4.42	Macrophage migration inhibitory factor
RPS21	0.044	1.95	40S ribosomal protein S21
AK4	0.044	1.66	Adenylate kinase 4, mitochondrial
DCN	0.044	2.58	Decorin
PRDX2	0.044	2.39	Peroxiredoxin-2
RAB6A	0.044	1.99	Ras-related protein Rab-6A
SRP14	0.044	1.77	Signal recognition particle 14 kDa protein
OCIAD1	0.044	2.19	OCIA domain-containing protein 1
CRELD2	0.044	2.49	Cysteine-rich with EGF-like domain protein 2
HK1	0.044	1.70	Hexokinase-1
PDIA3	0.044	1.51	Protein disulfide-isomerase A3
HNRNPM	0.044	1.26	Heterogeneous nuclear ribonucleoprotein M

RPS11	0.044	2.08	40S ribosomal protein S11
MAP4	0.045	2.09	Microtubule-associated protein 4
NAXE	0.045	3.42	NAD(P)H-hydrate epimerase
PYGB	0.045	2.74	Glycogen phosphorylase, brain form
ACADM	0.045	2.27	Medium-chain specific acyl-CoA dehydrogenase, mitochondrial
RPS28	0.045	2.70	40S ribosomal protein S28
DARS	0.045	2.85	Aspartate--tRNA ligase, cytoplasmic
ACIN1	0.045	2.32	Apoptotic chromatin condensation inducer in the nucleus
ANP32E	0.045	3.17	Acidic leucine-rich nuclear phosphoprotein 32 family member E
SEC61A1	0.045	1.79	Protein transport protein Sec61 subunit alpha isoform 1
PSMC6	0.045	1.96	26S proteasome regulatory subunit 10B
USP5	0.045	4.07	Ubiquitin carboxyl-terminal hydrolase 5
EEF2	0.045	2.30	Elongation factor 2
RPS3	0.045	2.02	40S ribosomal protein S3
SND1	0.045	1.77	Staphylococcal nuclease domain-containing protein 1
GOLIM4	0.045	3.04	Golgi integral membrane protein 4
MVP	0.045	1.87	Major vault protein
ARPC2	0.045	2.51	Actin-related protein 2/3 complex subunit 2
MATR3	0.046	2.37	Matrin-3
ENO1	0.046	3.40	Alpha-enolase
RPS25	0.046	4.38	40S ribosomal protein S25
ARPC1B	0.046	2.10	Actin-related protein 2/3 complex subunit 1B
RPL17	0.046	4.29	60S ribosomal protein L17
ACTR2	0.046	1.75	Actin-related protein 2
LRPAP1	0.046	1.72	Alpha-2-macroglobulin receptor-associated protein
PA2G4	0.046	2.34	Proliferation-associated protein 2G4
RPL6	0.046	2.12	60S ribosomal protein L6
CYCS	0.047	1.75	Cytochrome c

MYO1D	0.047	2.68	Unconventional myosin-Id
RPS9	0.048	2.42	40S ribosomal protein S9
PGAM1	0.048	2.60	Phosphoglycerate mutase 1
FBL	0.048	1.39	rRNA 2'-O-methyltransferase fibrillarin
ALDOA	0.048	2.71	Fructose-bisphosphate aldolase A
ATP6V1A	0.048	1.87	V-type proton ATPase catalytic subunit A
MYO1C	0.049	2.23	Unconventional myosin-Ic
EIF4A1	0.049	3.47	Eukaryotic initiation factor 4A-I
ADGRG2	0.049	3.71	Adhesion G-protein coupled receptor G2
CBR1	0.049	2.43	Carbonyl reductase [NADPH] 1
HSD17B4	0.049	1.55	Peroxisomal multifunctional enzyme type 2
TNPO1	0.0495	2.84	Transportin-1
TNS2	0.0495	2.69	Tensin-2

4.4 DISCUSSION

We have used chondrocytes extracted from the superficial and deep zones of OA and young articular cartilage to define the proteomic changes in the cells during OA and zonal distribution. In the previous chapters we have used articular cartilage tissue to study the proteome and transcriptome during the disease and ageing in the different zones. Hence, the chondrocytes in the tissue were in their native state. The aim of the chondrocyte proteomics was to study the proteome change at the cellular level, as it was reported in the Chapter 2 the majority of proteins identified from the cartilage tissue were ECM proteins. Thus, we wanted to justify the selection of native chondrocytes for the proteomics study and not the cultured chondrocytes. For that reason we have used chondrocytes that were not passaged (unattached cells) and passaged cells to assess the level of gene expression change in the chondrocytes extracted from the superficial and deep zones. We decided to exclude the middle zone chondrocytes as it was found in our study the protein and gene expression levels of some samples overlap with the adjacent regions. Moreover, the zone selection was performed macroscopically from the intact regions of the cartilage tissue, and it would greatly increase the variability between the samples of the same group. Furthermore, the iTRAQ method we used only could analyse 10 samples simultaneously. And from the results of our previous chapters n=5 of donors for each group proved to be an adequate number of samples to identify genes and proteins that were deferentially expressed within the zones and disease state.

Selection of native chondrocytes was also justified by the change in phenotype of cells upon culture. It was evident from the start of tissue culturing how drastically chondrocytes change in the monolayer culture. This would suggest the dedifferention of chondrocytes in the culture. It was shown before that during the process of dedifferentiation chondrocytes become fibroblast-like cells, characterized by an increase in the expression of type I collagen (COL-1) and a decrease of cartilage-specific markers, such as type II, XI, IX collagens (COL-2, COL-11, COL-9) and aggrecan (ACAN) (Duan et al., 2015). It was also confirmed by assessing the gene expression levels of chondrogenic and zone specific genes in the chondrocytes derived from the superficial and deep zones. We found that the gene expression levels of the main ECM proteins Collagen type 2 (COL2A1) and Aggrecan (ACAN) were significantly downregulated when unattached cells were compared to P0, P1 and P2 cells. Furthermore, chondrogenic transcription factor SOX9 was also downregulated in chondrocytes of both zones in cultured cells in comparison to the unattached cells. There was a high variability in the expression of Proteoglycan 4 (PRG4) which is a zone specific protein expressed in the superficial zone of the articular cartilage between the donors, hence the difference between the unattached cells of the superficial and deep zone was not significant. Furthermore, it the expression of PRG4 had incremental trend in both zones upon culturing in vitro. RUNX2 gene is a transcription factor

involved in chondrocyte maturation and normal endochondral bone formation, it is highly expressed in the deep zone and during OA. There was no significant change in the gene expression level RUNX2 when compared between the zones and upon in vitro culture. The cells that we used in the gene expression analysis were extracted from the OA cartilage, it could be for that reason we did not see a significant change in the expression of RUNX2 when superficial and deep zone, as it was shown to be upregulated in cartilage during OA. Another gene that is found to be highly expressed in the deep zone is Collagen type X (COL10A1), because its involved in mediating endochondral ossification. In our study the expression of COL10A1 was only observed in the unattached chondrocytes derived from the deep zone of articular cartilage. Matrix metalloproteinase-13 (MMP13) is the primary MMP involved in the cartilage degradation during OA by cleaving Collagen type 2. In our study the gene expression levels of MMP13 was not significantly expressed between the zones and during tissue culture.

As it was mentioned before in this study there was a high variability in gene expression levels of aforementioned cartilage markers. However, when each donor's cells were compared between the superficial and deep zones there was a significant difference in the genes that are zone specific in some of the donors. Overall, our justification of using native chondrocytes instead of cultured chondrocytes was confirmed by the changes that we have seen in the phenotype and gene expression levels in chondrocytes derived from the different zones upon tissue culture.

The cartilage tissue from the healthy individuals is extremely hard to obtain. And we could not find the source where could get fresh cartilage samples from the knee joints of healthy individuals of old age. Usually these samples are collected after performing surgical procedures after sustaining femoral chondyle fracture in old people, however, the most prevalent type of a fracture in older people is of femoral head. Our collaborator Professor Brian Johnstone (Oregon Health and Science University, USA) was working on chondrocytes extracted from the healthy articular cartilage collected from people of young age and he was also studying chondrocytes derived from the different zones. He kindly provided us with the cells extracted from the superficial and deep zones of articular cartilage from the femoral chondyles. Although there were two major confounding factors between the groups of young and OA, namely disease state and age, it was of great interest to study the zonal changes of chondrocytes in their native state in healthy cartilage and during the disease at proteome level. Therefore it was the main aim to study the differences of proteome between the superficial and deep zones of young individuals and separately between these zones in the OA chondrocytes. And then to compare the changes within zones between young and OA group. Another reason of studying firstly the zonal differences within the young and OA group was the technical con-founder, because the extraction of OA samples was performed by us, while the cartilage tissue of young individuals were processed at Prof. Brian Johnstone's laboratory. Hence, the difference found in the protein

abundance between respective zones of OA and young chondrocytes (for instance, Superficial OA group vs. Superficial Young) could be due to the technical variability.

PTSG1 was the only protein found to be differentially abundant when the chondrocytes of the superficial and deep zones of OA were compared, it was significantly upregulated in the superficial zone. PTGS1 gene, also known as COX-1 (cyclooxygenase-1), encodes an enzyme called prostaglandin-endoperoxide synthase 1, which plays a crucial role in the synthesis of prostaglandins. Prostaglandins are lipid signaling molecules that are involved in a wide range of physiological processes, including inflammation, pain. It was previously shown that PTGS1 was highly expressed in the OA chondrocytes in comparison to the chondrocytes of normal cartilage (Sun et al., 2015). Furthermore, the gene expression of PTGS1 was upregulated upon treatment of chondrocytes with the inflammatory cytokine interleukin-1b (IL1B) and was downregulated after the addition of cyclooxygenase-2 (COX-2) inhibitor to the chondrocytes. This would confirm the involvement of PTGS1 in the inflammation processes in chondrocytes during OA. It could also suggest the higher inflammatory activity in the superficial zone in comparison to the deep zone based on the results of our study. There was no protein found to be differentially abundant when the superficial and deep zone chondrocytes of the young group were compared.

In our study found three proteins (CD44, RPS14 and TUBB) to be upregulated in the superficial zone of OA chondrocytes in comparison to the chondrocytes of superficial young group. CD44 is a transmembrane glycoprotein that is encoded by the CD44 gene. It is a cell-surface receptor that plays a key role in cell adhesion, cell migration and signal transduction. It was previously found the high protein levels of CD44 in the articular cartilage during OA has a positive correlation with the disease severity (Zhang et al., 2013). Furthermore, the synthesis of intracellular domain of CD44 resulted in dedifferentiation of chondrocytes upon mechanical stress and during OA (Sobue et al., 2019). The inhibition of CD44 intracellular domain lead to the increase of ACAN and Collagen type 2 in chondrocyte monolayer after induction of mechanical stress.

RPS14 was also found to be upregulated in the superficial zone of OA chondrocytes when compared to the superficial zone of young chondrocytes. RPS14 protein is a component of the 40S ribosomal subunit, which is essential for the translation of messenger RNA (mRNA) into protein. Specifically, the RPS14 protein is involved in the binding of mRNA to the ribosome, as well as in the initiation of translation. It was previously found that RPS14 is upregulated during OA (Ge et al., 2021) and involved in the senescence of cartilage by binding to the CircRNA CircZSWIM6 (Gong et al., 2023). In our study OA donors were of old age in comparison to the young group, hence, both of these factors could confirm the involvement of RPS14 during OA and ageing.

The third protein that was upregulated in the superficial OA chondrocytes in comparison to the superficial young chondrocytes was Beta-tubulin protein (TUBB). TUBB protein is an essential

component of microtubules in cells. Microtubules are part of the cytoskeleton, which provides structural support for cells and plays a role in cell division, intracellular transport, and other cellular processes. TUBB gene was shown to be downregulated after the addition of IL1B to the chondrocytes (Joos et al., 2008). Furthemore, the inhibition of p38 mitogen-activated protein kinase (MAPK) increased the gene expression level of TUBB in the chondrocytes treated with IL1B, suggesting the involvement of MAPK signalling pathway in the regulation of TUBB during inflammation initiated by IL1B. However, this contradicts our findings, as this would suggest higher inflammation rates in the superficial zone of young cartilage in comparison to the superficial zone of OA cartilage.

There were 344 proteins identified to be differentially abundant in the chondrocytes extracted from the deep zone of old OA cartilage in comparison to the chondrocytes of the young cartilage of respective zone. Similar to the superficial zone comparison, here in the deep zone OA chondrocytes demonstrated a significant upregulation of TUBB and CD44 proteins in comparison to the deep zone chondrocytes in the young group. Notably, Hyaluronan and proteoglycan link protein 1 (HAPLN1) and Annexin A2 (ANXA2) proteins were upregulated in the deep zone chondrocytes of the OA group in comparison to the deep zone chondrocytes of young group. These proteins were also upregulated in the deep zone of OA cartilage in comparison to the deep zone of old cartilage in articular cartilage tissue proteomics (Chapter 2). As it was discussed in Chapter 2 the contradiction of our findings to the published studies could be due to the zonal differences in protein distribution rather than in whole cartilage tissue. In the previously published work it was found that ANXA2 was upregulated in the OA cartilage and could be involved the mineralisation of the cartilage tissue (Kirsch et al., 2000). Furthermore, 14-3-3 epsilon (YWHAE) protein was significantly increased in the deep zone of OA chondrocytes in comparison the deep zone of young chondrocytes. However, the gene expression levels of YWHAE in our RNAseq study suggested it was one of the stable genes expressed across the zones and it was validated in our qPCR analysis that YWHAE was expressed at the same level in chondrocytes extracted from the cartilage. Also we have used YWHAE as the reference gene in our qPCR analysis.

Overall, the proteomics study of chondrocytes extracted from the different zones of articular cartilage in the OA and young donors found only minor change in the proteome when the superficial and deep zones were compared. However, our proteomics study (Chapter 2) found a higher number of proteins that were differentially abundant at a significant level when the superficial and deep zones of OA cartilage was compared. Moreover, our RNAseq study (Chapter 3) also demonstrated higher variability between the zones rather than between the disease state and ageing when respective zones were compared. The limitation of the study we describe in this chapter is that we only were able to use 1ug of protein for LC-MS/MS, the majority of the samples were used for label-based proteomics that failed. Furthermore, label-based proteomics experiment failed due to the presence of free amines

from the FBS. Although our removal of FBS from the chondrocyte mixture demonstrated the actual reduction of FBS presence in the sample mixture it was not enough to obtain chondrocyte mixture free from FBS. The reason of using FBS was that our collaborators from whom we obtained the cells were freezing the cells using FBS in the medium. In order to reduce the technical variability we have extracted and stored the samples in the same way. The contamination of samples with FBS could also be a reason in the low amount of proteins identified at a significant level. Taking into account aforementioned issues with this experiment, in my personal opinion, the results of this study should be taken carefully and further mechanistic study and validation of the results needed.

4.5 CONCLUSION

The findings of this chapter found the dedifferentiation changes in the chondrocytes extracted from the different zones of articular cartilage. Chondrocyte phenotype changes drastically upon culturing both in chondrocytes from the superficial and deep zones. Furthermore, the gene levels of chondrogenic genes (COL2A1, ACAN, SOX9) significantly downregulate upon tissue culture. Also, the hypertrophic marker COL10A1 was only expressed in the unattached chondrocytes of the deep zone. Label-free proteomics identified only few proteins differentially abundant at a statistically significant level when superficial and deep zone chondrocytes were compared. Nevertheless, non-cultured chondrocytes can be used to discover cellular alterations at the proteome level in their native state.

CHAPTER 5

General discussion and future work

5.1 GENERAL DISCUSSION

The main aim of this thesis was to define the proteome and/or transcriptome changes in the anatomical regions of human articular cartilage or chondrocytes derived from these zones during OA and ageing. In order to investigate the proteome changes in the articular cartilage during OA and ageing we collected superficial, middle and deep zones of human knee cartilage tissue. Additionally, we isolated chondrocytes from the superficial and deep zone of young and OA cartilage from the femoral chondyles of the knee joint.

In our cartilage studies the three distinctive zones of cartilage were collected using LMD method. For proteomics studies the extracted proteins were analysed using LC-MS/MS. To study the transcriptome changes in the cartilage during OA and ageing in the aforementioned zones we utilised RNAseq. Furthermore, we aimed to establish the zone-specific proteome changes in the chondrocytes extracted from the OA and young cartilage. This was because mass spectrometry proteomics does not identify all proteins in a sample. In order to define a deeper cartilage proteome with increased representative cellular proteins chondrocyte isolation was necessary. This is because cartilage contains only 1% cells; the single cell type being the chondrocytes. By, in essence fractionating the cartilage by isolating the cellular component we were able to interrogate the cellular part of cartilage more extensively. Thus, the superficial and deep zones of articular cartilage collected from OA and young donors were zonally dissected and cells extracted from these zones. Extracted chondrocytes were subjected to the proteome analysis by using LC-MS/MS proteomics. Our initial aim was to use a labelled proteomics approach (TMT labelling) however interference with labelling efficiency meant we could not undertake this study. Therefore, we used a label-free approach. The results of the studies in this thesis demonstrated the zone-specific changes at protein and RNA level in the cartilage. This suggests that considering the anatomical regions of the tissue as separate specimens we were able to establish a greater understanding of how the different zones contribute to cartilage homeostasis in ageing and OA.

In Chapter 2 the proteomic approach of establishing the changes of protein abundance in the different zones of articular cartilage allowed us to identify the proteins that changed significantly between the zones. Unsurprisingly there was a greater number of differentially abundant proteins identified when the superficial zone was compared to the deep zone, whilst the comparison of the middle zone to either superficial or deep zone produced a lower number of proteins that were differentially abundant when a filter of significance of (p_{adj} <0.05) was used. This is explained by the overlap of the middle zone to the adjacent zones, as the zones of the cartilage were microdissected from unstained tissue.

We attempted to stain the tissue in order to get an optimal representation of cells. However, it complicated the collection protocol and was incompatible with the membranes on the slides required for LCM. The tissue sections tended to detach from the membrane. Furthermore, in Chapter 3 we used the same method to isolate the zones from the tissue for RNA extraction and staining of the tissue would have resulted in higher RNA degradation. This can be an issue especially with low cellularity high ECM tissues for RNASeq. Nevertheless, the cells were visible under the LMD microscope and the superficial zone was selected as the area with high amount cells on the margins of the tissue. To reduce cross over between zones we left an area that was not collected before selecting the middle zone for isolation and collection. The deep zone was selected based on the columnar structures of cells in the tissue.

We could not quantify the protein concentration in the tissue prior to LC-MS/MS because firstly, there was only small amount of the tissue collected and secondly, we were using *in situ* digestion of the proteins. Thus, we did not extract proteins from the tissue prior to sample preparation for LC-MS/MS. However, we normalised sample loading to the LC-MS/MS instrument by collecting the same area from all three zones. The superficial zone is the thinnest zone of the cartilage; therefore we collected less area of the tissue from that zone, however during the loading of the samples to the LC/MS-MS samples were normalised proportionally to the area collected.

The majority of proteins identified in our cartilage study were unsurprisingly ECM proteins. The superficial zone is highly cellular in comparison to the underlying middle and deep zones, hence there could be higher protein levels of intracellular and pericellular matrix proteins. This should be taken with the note that the difference in protein levels of those proteins when the superficial zone was compared to the middle or deep zone. We realised this may lead to discrepancies in cellular content between zones as this varies. This could have had a knock-on effect of the proteins isolated in each zone. However, given that cartilage is only 1% cells we discounted this as a potential bias. Furthermore, we believe that overall, the identification of proteins across the zones in young, old and OA explains the protein architecture of the articular cartilage. The impact of this additional knowledge could be used in the production and assessment of artificially engineered cartilage.

We have also analysed the proteome difference in each of the zone during ageing and OA. Ageing is an important factor in OA pathogenesis (Loeser, 2009). Therefore, by understanding cartilage changes in ageing we can elucidate how these changes could contribute to age-related OA. In order to define the proteins that are differentially abundant during ageing we compared old and young cartilage from the respective zones. To identify the proteins that are differentially abundant during OA we performed comparison of OA and old cartilage (thus as age-matched as possible) from the respective zones. We compared the results of this work to the previously published studies. Based on the results we obtained we suggest that cells in the superficial zone of both OA and young cartilage

are more active, as the proteins involved (discussed in Chapter 2) in proliferation were highly abundant in these groups than in the old superficial zone. Young cartilage tissue has a higher capability for ECM turnover to support the homeostasis. While in OA cartilage the higher activity of cells could be to due to the fact the cells are trying to restore the destruction of the tissue caused by the inflammatory and catabolic activity. We hypothesise that articular cartilage in the superficial zone during ageing is in passive state, and there are lower levels of protein turnover. Additional experiments are required to establish this.

There were proteome changes in the middle zone during ageing and OA. We suggest that the environment in the middle zone of cartilage during OA is similar to the superficial zone. There were conflicting findings in our study based on the published literature, as some of the chondrogenic proteins were downregulated and the others were upregulated. These proteins would need further validation in order to have a definite conclusion. However, these changes could be indicative that protein restoration in the OA cartilage does not undergo optimal restoration leading to the formation of a less functional matrix. Moreover, it was found that during OA cartilage mineralisation processes were activated, which in turn would also hinder the biomechanical properties of the tissue. From our results it could be suggested that during ageing the cartilage in the middle zone has less capabilities for growth and proliferation. Nevertheless, there were conflicting findings in regards to the activation of chondrogenesis. Moreover, there were higher level of protease inhibitor (TIMP3) in the middle zone during ageing. This could suggest that although we have not identified protease activity in that zone there could be an elevation in inflammatory activity. On the other hand, the higher levels of protease inhibitors could further halt the process of protein turnover during ageing and would lead for protein accumulation in the matrix.

The results of the differentially abundant proteins in the deep zone of cartilage during OA demonstrated further cartilage degradation that was seen in the superficial and middle zones. The proteins that were found to be involved in OA progression based on the published literature were upregulated in the OA cartilage in our study. Moreover, the metabolic activity could be upregulated in the deep zone of OA cartilage based on the protein levels involved in glycolysis and glycogenesis. From the proteomics results the deep zone of OA cartilage could also have increased mineralisation of the tissue.

Our findings on the proteome changes in the deep zone of articular cartilage during ageing support the idea that there is a higher inflammatory activity in the middle and deep zones. The reason for this is that the protease (MMP2) was upregulated in the deep zone during ageing, however, like the middle zone protease inhibitor was also upregulated in the deep zone cartilage during ageing. Moreover, based on the results it could proposed that in the deep zone there is disruption in the fibril organisation of collagens. There were inconclusive results of the mineralisation of the tissue,

however, hypertrophy markers of the articular cartilage were found to be downregulated which could indicate the possible disorganisation in the matrix or altered phenotype.

Overall, considering the findings of the work in Chapter 2 we believe that during OA there is an increase in chondrogenic, metabolic activity, and cartilage mineralisation and degradation. All of this could lead to matrix disorganisation, even in the macroscopically intact cartilage during OA, which would result in the biomechanical properties of the tissue. However, during ageing a decrease in the chondrocyte activity and protein turnover, especially in the superficial and middle zones occurs. Based on our results the destructive changes in the articular cartilage might be initiated from the deep zone.

In our transcriptome analysis (Chapter 3) of cartilage we have used RNAseq method to identify the differences in the gene expression within the zones of articular cartilage during OA and ageing. The cartilage samples of the same donors from the young and old group that were used in the Chapter 2 were also used in this study. Cartilage samples of two donors were replaced due to low RNA integrity number. It was of great interest to use the same samples in proteomics and transcriptomics studies in order to perform the omics analysis with both datasets, this would be discussed below in the future directions. RNAseq is a powerful tool that is used to define the whole transcriptome of the cells. However, it generates vast amounts of data that needs high-throughput bioinformatic analysis. For this reason, we have analysed our transcriptome dataset using different bioinformatics tools, and we found that using the STAR alignment tool we produced a greater amount of genome coverage. Using an unsupervised method for the distribution of variation the results of the RNAseq analysis demonstrated that at the gene expression level derived from the different zones account for higher variance irrespective of age or disease state. Although it is considered that the only cells residing in the articular cartilage are chondrocytes, our findings suggest that the articular cartilage chondrocytes of different zones should be considered as separate biological cells in regards to gene expression. Indeed, work using single cell sequencing has demonstrated that not all chondrocytes are the same (Li et al., 2019). This can be explained by the fact that the different zones within the articular cartilage have different biomechanical properties and protein distribution due to their different roles.

The gene expression levels during OA and ageing had a high number of genes differentially expressed at a significant level. In order to explain the high number of genes that were differentially expressed during OA and ageing we employed pathway analysis software (IPA, Qiagen) to identify the upstream regulators of these genes. We hypothesised that validation of the upstream regulator would explain the expression in a given gene interaction network. However, we did not have a source to obtain fresh articular cartilage from the young and old donors in order to perform qPCR analysis on chondrocytes extracted from the different zones. For this reason, we only selected the upstream

regulators that were predicted to be upregulated/downregulated exclusively between the superficial and deep zones of OA cartilage. In our validation study using qPCR the upstream regulators LTBR and TAB1 were confirmed to be upregulated in the deep zone of OA chondrocytes (as predicted by IPA) in unattached chondrocytes. However, only LTBR gene expression was confirmed in the native chondrocytes. We used unattached cells to assess the gene expression pattern in chondrocytes extracted from the superficial and deep zones in Chapter 4, and these cells demonstrated high expression levels of chondrogenic and hypertrophy markers. The validation of this upstream regulators allowed us to assume with higher confidence that the expression levels of genes downstream of the regulator were true. For instance, in our data set NFKB2 and VCAM1 were downregulated in the deep zone of OA cartilage in comparison to the superficial zone OA, and it was predicted by IPA this could be a result of downregulation of LTBR. By validating the gene expression of LTBR in the deep zone of OA cartilage we can assume that NFKB2 and VCAM1 gene expression levels are also validated to some extent.

As our transcriptome analysis identified number of genes that were not scrutinised excessively in the literature in regards to the OA or ageing, in the articular cartilage we have selected SEMA3A, AMTN, and TGFBP1 genes for validation using *in situ* hybridisation method. However, this method proved to be hard to use on fresh frozen articular cartilage samples. We used different optimisation methods for this technique, including different incubation times, different section thickness, different fixation timing and temperature. However, the tissue sections were either detached completely from the glass slides during the protocol or the sections that were not detached completely produced false positive signal, due to probe getting between the tissue and glass slide. Out of many sections we used only three had single signals, thus we could not use the results for quantitative or qualitative analysis. The images provided in the Chapter 3 on *in situ* hybridisation should be only considered as attempt to validate the gene expression.

The proteomics study that we conducted on the articular tissue allowed us to investigate proteome of articular cartilage in the different zones during ageing and OA. However, as cartilage matrix accounts for the majority of tissue, we identified only small proportion of cellular proteins. For that reason we decided to analyse proteome of chondrocytes extracted from the superficial and deep zones of articular cartilage. In the study we used cartilage samples derived from young and old OA donors. Firstly, we attempted determine using label-based proteomics the differences in the protein abundance of the chondrocytes. However, this experiment failed as there were issues during the sample preparation for label-based proteomics. Therefore, we performed label-free proteomics to identify and quantify proteins in the cells. Nevertheless, both sets of results were described in Chapter 4 Although, label-free proteomics of chondrocytes identified 1125 proteins in total, only few proteins were found to be differentially abundant when cells from the the superficial and deep zones were

compared in young and OA chondrocytes. As discussed in Chapter 4 our main aim was to first identify the changes in protein abundance between the superficial and deep zone of young chondrocytes, and then identify the protein changes between the in these zones in OA chondrocytes. It was for this reason that the chondrocytes from young cartilage were extracted and processed not by us and in a different laboratory. This could have produced technical variability when high-throughput proteomics or transcriptomics studies were conducted as previously described (Fei et al., 2018). Nevertheless, we have also compared the superficial zone chondrocytes of young to the superficial zone chondrocytes of OA, and the same for the deep zone. Superficial zone comparison between young and OA found CD44, RPS14 and TUBB proteins to be differentially abundant, whereas deep zone comparison found 344 proteins to be differentially abundant.

5.2 FUTURE WORK

In our work in Chapters 2 and 3 we used the cartilage from the same young and old donors. There were two samples replaced in OA group to the cartilage of other donors in Chapter 3 due to the low RNA integrity. The use of samples from the same donors could be used in integrative omics studies, to explore the changes in both RNA and protein level and for instance, to define the regulation of proteins by the transcription factors. This could be undertaken in the future using programs such as MFuzz or Joint Dimensionality Reduction (jDR) efficient approach to integrate multi-omics data using MOFA. This is a multi-omics integration method that uses factor analysis. It is similar to using PCA but for multiple omics and can be used to interpret the reduced dimensions as your "factors" (made up of genes/proteins). Factors correlated with features in the phenotype table (which for our data would include cartilage zone and age) can be used to determine if they captured relevant sources of biological variation. In our studies we have would have liked to undertake this work but due to the time constraints we could only optimise the simultaneous extraction of RNA and protein from the same sample of the different zones in articular cartilage.

Further validation of our findings could be undertaken with further gene expression work by performing qPCR and we could also validate protein abundance by performing western blot or ELISA. Ideally both of these would be undertaken on an independent cohort of samples to show that our findings are also relevant to the wider population and not just in our small sample set. Furthermore, validation in both sexes and in samples from different ethnicities would be valid.

Moreover, mechanistic studies could be performed to validate the effect of a certain gene on chondrogenic, zone specific or catabolic genes and proteins. In our work we also optimised protocols to knockdown gene in the superficial and deep zone chondrocytes, however, the work was not finished due to the time constraints.

5.3 CONCLUSION

Human articular cartilage tissue and cells were investigated in this thesis to discover disease and age-related alterations at the proteome and transcriptome levels. Furthermore, separate anatomical zones of cartilage tissue were stratified to address molecular changes during osteoarthritis and ageing, as well as to gain understanding about the tissue's molecular makeup. This thesis' analyses indicated zone-specific changes in protein abundance and gene expression during disease and ageing, laying the groundwork for future research in the field.

REFERENCES

Agah, A., Kyriakides, T. R., Lawler, J., & Bornstein, P. (2002). The lack of thrombospondin-1 (TSP1) dictates the course of wound healing in double-TSP1/TSP2-null mice. The American Journal of Pathology, 161(3), 831–839. https://doi.org/10.1016/S0002-9440(10)64243-5

Ahmed, A. A., Mills, A. D., Ibrahim, A. E. K., Temple, J., Blenkiron, C., Vias, M., Massie, C. E., Iyer, N. G., McGeoch, A., Crawford, R., Nicke, B., Downward, J., Swanton, C., Bell, S. D., Earl, H. M., Laskey, R. A., Caldas, C., & Brenton, J. D. (2007). The extracellular matrix protein TGFBI induces microtubule stabilization and sensitizes ovarian cancers to paclitaxel. Cancer Cell, 12(6), 514–527. https://doi.org/10.1016/j.ccr.2007.11.014

Alsalameh, S., Amin, R., Gemba, T., & Lotz, M. (2004). Identification of mesenchymal progenitor cells in normal and osteoarthritic human articular cartilage. Arthritis and Rheumatism, 50(5), 1522–1532. https://doi.org/10.1002/art.20269

Arai, K., Nagashima, Y., Takemoto, T., & Nishiyama, T. (2008). Mechanical strain increases expression of type XII collagen in murine osteoblastic MC3T3-E1 cells. Cell Structure and Function, 33(2), 203–210. https://doi.org/10.1247/csf.08025

Attur, M., Duan, X., Cai, L., Han, T., Zhang, W., Tycksen, E. D., Samuels, J., Brophy, R. H., Abramson, S. B., & Rai, M. F. (2021). Periostin loss-of-function protects mice from post-traumatic and age-related osteoarthritis. Arthritis Research & Therapy, 23(1), 104. https://doi.org/10.1186/s13075-021-02477-z

Attur, M., Yang, Q., Shimada, K., Tachida, Y., Nagase, H., Mignatti, P., Statman, L., Palmer, G., Kirsch, T., Beier, F., & Abramson, S. B. (2015). Elevated expression of periostin in human osteoarthritic cartilage and its potential role in matrix degradation via matrix metalloproteinase-13. FASEB Journal : Official Publication of the Federation of American Societies for Experimental Biology, 29(10), 4107–4121. https://doi.org/10.1096/fj.15-272427

Bader, D. L., Salter, D. M., & Chowdhury, T. T. (2011). Biomechanical influence of cartilage homeostasis in health and disease. Arthritis, 2011, 979032. https://doi.org/10.1155/2011/979032

Baert, I. A. C., Jonkers, I., Staes, F., Luyten, F. P., Truijen, S., & Verschueren, S. M. P. (2013). Gait characteristics and lower limb muscle strength in women with early and established knee osteoarthritis. Clinical Biomechanics (Bristol, Avon), 28(1), 40–47. https://doi.org/10.1016/j.clinbiomech.2012.10.007

Bank, R. A., Bayliss, M. T., Lafeber, F. P., Maroudas, A., & Tekoppele, J. M. (1998). Ageing and zonal variation in post-translational modification of collagen in normal human articular cartilage. The age-related increase in non-enzymatic glycation affects biomechanical properties of cartilage. The Biochemical Journal, 330 (Pt 1(Pt 1), 345–351. https://doi.org/10.1042/bj3300345

Bernardo, B. C., Belluoccio, D., Rowley, L., Little, C. B., Hansen, U., & Bateman, J. F. (2011). Cartilage intermediate layer protein 2 (CILP-2) is expressed in articular and meniscal cartilage

and down-regulated in experimental osteoarthritis. The Journal of Biological Chemistry, 286(43), 37758–37767. https://doi.org/10.1074/jbc.M111.248039

Bhosale, A. M., & Richardson, J. B. (2008). Articular cartilage: structure, injuries and review of management. British Medical Bulletin, 87(1), 77–95. https://doi.org/10.1093/bmb/ldn025

Bijlsma, J. W. J., Berenbaum, F., & Lafeber, F. P. J. G. (2011). Osteoarthritis: an update with relevance for clinical practice. Lancet (London, England), 377(9783), 2115–2126. https://doi.org/10.1016/S0140-6736(11)60243-2

Blackburn, P. R., Xu, Z., Tumelty, K. E., Zhao, R. W., Monis, W. J., Harris, K. G., Gass, J. M., Cousin, M. A., Boczek, N. J., Mitkov, M. V, Cappel, M. A., Francomano, C. A., Parisi, J. E., Klee, E. W., Faqeih, E., Alkuraya, F. S., Layne, M. D., McDonnell, N. B., & Atwal, P. S. (2018). Bi-allelic Alterations in AEBP1 Lead to Defective Collagen Assembly and Connective Tissue Structure Resulting in a Variant of Ehlers-Danlos Syndrome. American Journal of Human Genetics, 102(4), 696–705. https://doi.org/10.1016/j.ajhg.2018.02.018

Blaschke, U. K., Eikenberry, E. F., Hulmes, D. J., Galla, H. J., & Bruckner, P. (2000). Collagen XI nucleates self-assembly and limits lateral growth of cartilage fibrils. The Journal of Biological Chemistry, 275(14), 10370–10378. https://doi.org/10.1074/jbc.275.14.10370

Bliddal, H., Leeds, A. R., & Christensen, R. (2014). Osteoarthritis, obesity and weight loss: evidence, hypotheses and horizons - a scoping review. Obesity Reviews : An Official Journal of the International Association for the Study of Obesity, 15(7), 578–586. https://doi.org/10.1111/obr.12173

Boeuf, S., Steck, E., Pelttari, K., Hennig, T., Buneb, A., Benz, K., Witte, D., Sültmann, H., Poustka, A., & Richter, W. (2008). Subtractive gene expression profiling of articular cartilage and mesenchymal stem cells: serpins as cartilage-relevant differentiation markers. Osteoarthritis and Cartilage, 16(1), 48–60. https://doi.org/10.1016/j.joca.2007.05.008

Boguslawska, J., Kedzierska, H., Poplawski, P., Rybicka, B., Tanski, Z., & Piekielko-Witkowska, A. (2016). Expression of Genes Involved in Cellular Adhesion and Extracellular Matrix Remodeling Correlates with Poor Survival of Patients with Renal Cancer. The Journal of Urology, 195(6), 1892–1902. https://doi.org/https://doi.org/10.1016/j.juro.2015.11.050

Bolduc, J. A., Collins, J. A., & Loeser, R. F. (2019). Reactive oxygen species, aging and articular cartilage homeostasis. Free Radical Biology & Medicine, 132, 73–82. https://doi.org/10.1016/j.freeradbiomed.2018.08.038

Brandl, A., Hartmann, A., Bechmann, V., Graf, B., Nerlich, M., & Angele, P. (2011). Oxidative stress induces senescence in chondrocytes. Journal of Orthopaedic Research : Official Publication of the Orthopaedic Research Society, 29(7), 1114–1120. https://doi.org/10.1002/jor.21348

Brody, L. T. (2015). Knee osteoarthritis: Clinical connections to articular cartilage structure and function. Physical Therapy in Sport, 16(4), 301–316. https://doi.org/https://doi.org/10.1016/j.ptsp.2014.12.001

Buckwalter, J. A., & Mankin, H. J. (1998). Articular cartilage: tissue design and chondrocyte-matrix interactions. Instructional Course Lectures, 47, 477–486.

Campbell, K. A., Minashima, T., Zhang, Y., Hadley, S., Lee, Y. J., Giovinazzo, J., Quirno, M., & Kirsch, T. (2013). Annexin A6 interacts with p65 and stimulates NF-κB activity and catabolic events in articular chondrocytes. Arthritis and Rheumatism, 65(12), 3120–3129. https://doi.org/10.1002/art.38182

Campisi, J., & d'Adda di Fagagna, F. (2007). Cellular senescence: when bad things happen to good cells. Nature Reviews Molecular Cell Biology, 8(9), 729–740. https://doi.org/10.1038/nrm2233

Canovas, F., & Dagneaux, L. (2018). Quality of life after total knee arthroplasty. Orthopaedics & Traumatology: Surgery & Research, 104(1, Supplement), S41–S46. https://doi.org/https://doi.org/10.1016/j.otsr.2017.04.017

Chijimatsu, R., Kunugiza, Y., Taniyama, Y., Nakamura, N., Tomita, T., & Yoshikawa, H. (2015). Expression and pathological effects of periostin in human osteoarthritis cartilage. BMC Musculoskeletal Disorders, 16, 215. https://doi.org/10.1186/s12891-015-0682-3

Chinzei, N., Brophy, R. H., Duan, X., Cai, L., Nunley, R. M., Sandell, L. J., & Rai, M. F. (2018). Molecular influence of anterior cruciate ligament tear remnants on chondrocytes: a biologic connection between injury and osteoarthritis. Osteoarthritis and Cartilage, 26(4), 588–599. https://doi.org/10.1016/j.joca.2018.01.017

Chisari, E., Yaghmour, K. M., & Khan, W. S. (2020). The effects of TNF-alpha inhibition on cartilage: a systematic review of preclinical studies. Osteoarthritis and Cartilage, 28(5), 708–718. https://doi.org/https://doi.org/10.1016/j.joca.2019.09.008

Choi, M.-C., Jo, J., Park, J., Kang, H. K., & Park, Y. (2019). NF-κB Signaling Pathways in Osteoarthritic Cartilage Destruction. Cells, 8(7). https://doi.org/10.3390/cells8070734

Chou, C.-H., Lee, C.-H., Lu, L.-S., Song, I.-W., Chuang, H.-P., Kuo, S.-Y., Wu, J.-Y., Chen, Y.-T., Kraus, V. B., Wu, C.-C., & Lee, M. T. M. (2013). Direct assessment of articular cartilage and underlying subchondral bone reveals a progressive gene expression change in human osteoarthritic knees. Osteoarthritis and Cartilage, 21(3), 450–461. https://doi.org/https://doi.org/10.1016/j.joca.2012.11.016

Chou, C.-H., Lee, M. T. M., Song, I.-W., Lu, L.-S., Shen, H.-C., Lee, C.-H., Wu, J.-Y., Chen, Y.-T., Kraus, V. B., & Wu, C.-C. (2015). Insights into osteoarthritis progression revealed by analyses of both knee tibiofemoral compartments. Osteoarthritis and Cartilage, 23(4), 571–580. https://doi.org/https://doi.org/10.1016/j.joca.2014.12.020

Cillero-Pastor, B., Eijkel, G. B., Kiss, A., Blanco, F. J., & Heeren, R. M. A. (2013). Matrix-assisted laser desorption ionization–imaging mass spectrometry: A new methodology to study human osteoarthritic cartilage. Arthritis \& Rheumatism, 65(3), 710–720. https://doi.org/https://doi.org/10.1002/art.37799

Coggon, D., Reading, I., Croft, P., McLaren, M., Barrett, D., & Cooper, C. (2001). Knee osteoarthritis and obesity. International Journal of Obesity and Related Metabolic Disorders :

Journal of the International Association for the Study of Obesity, 25(5), 622–627. https://doi.org/10.1038/sj.ijo.0801585

Connor, J. R., Kumar, S., Sathe, G., Mooney, J., O'Brien, S. P., Mui, P., Murdock, P. R., Gowen, M., & Lark, M. W. (2001). Clusterin expression in adult human normal and osteoarthritic articular cartilage. Osteoarthritis and Cartilage, 9(8), 727–737. https://doi.org/10.1053/joca.2001.0475

Custers, R. J. H., Creemers, L. B., Verbout, A. J., van Rijen, M. H. P., Dhert, W. J. A., & Saris, D. B. F. (2007). Reliability, reproducibility and variability of the traditional Histologic/Histochemical Grading System vs the new OARSI Osteoarthritis Cartilage Histopathology Assessment System. Osteoarthritis and Cartilage, 15(11), 1241–1248. https://doi.org/10.1016/j.joca.2007.04.017

De Ceuninck, F., Marcheteau, E., Berger, S., Caliez, A., Dumont, V., Raes, M., Anract, P., Leclerc, G., Boutin, J. A., & Ferry, G. (2005). Assessment of some tools for the characterization of the human osteoarthritic cartilage proteome. Journal of Biomolecular Techniques : JBT, 16(3), 256–265.

Demirag, B., Sarisozen, B., Ozer, O., Kaplan, T., & Ozturk, C. (2005). Enhancement of tendon-bone healing of anterior cruciate ligament grafts by blockage of matrix metalloproteinases. The Journal of Bone and Joint Surgery. American Volume, 87(11), 2401–2410. https://doi.org/10.2106/JBJS.D.01952

Doege, K. J., Sasaki, M., Kimura, T., & Yamada, Y. (1991). Complete coding sequence and deduced primary structure of the human cartilage large aggregating proteoglycan, aggrecan. Human-specific repeats, and additional alternatively spliced forms. The Journal of Biological Chemistry, 266(2), 894–902.

Dowthwaite, G. P., Bishop, J. C., Redman, S. N., Khan, I. M., Rooney, P., Evans, D. J. R., Haughton, L., Bayram, Z., Boyer, S., Thomson, B., Wolfe, M. S., & Archer, C. W. (2004). The surface of articular cartilage contains a progenitor cell population. Journal of Cell Science, 117(Pt 6), 889–897. https://doi.org/10.1242/jcs.00912

Duan L, Ma B, Liang Y, Chen J, Zhu W, Li M, Wang D. Cytokine networking of chondrocyte dedifferentiation in vitro and its implications for cell-based cartilage therapy. Am J Transl Res. 2015 Feb 15;7(2):194-208. PMID: 25901191; PMCID: PMC4399086.

Duance, V. C. (1983). Surface of articular cartilage: immunohistological studies. Cell Biochemistry and Function, 1(3), 143–144. https://doi.org/10.1002/cbf.290010304

Dudek, M., Angelucci, C., Pathiranage, D., Wang, P., Mallikarjun, V., Lawless, C., Swift, J., Kadler, K. E., Boot-Handford, R. P., Hoyland, J. A., Lamande, S. R., Bateman, J. F., & Meng, Q.-J. (2021). Circadian time series proteomics reveals daily dynamics in cartilage physiology. Osteoarthritis and Cartilage. https://doi.org/10.1016/j.joca.2021.02.008

Dudhia, J. (2005). Aggrecan, aging and assembly in articular cartilage. Cellular and Molecular Life Sciences : CMLS, 62(19–20), 2241–2256. https://doi.org/10.1007/s00018-005-5217-x

Dunn, S. L., Soul, J., Anand, S., Schwartz, J.-M., Boot-Handford, R. P., & Hardingham, T. E. (2016). Gene expression changes in damaged osteoarthritic cartilage identify a signature of non-chondrogenic and mechanical responses. Osteoarthritis and Cartilage, 24(8), 1431–1440. https://doi.org/https://doi.org/10.1016/j.joca.2016.03.007

Duval, E., Bigot, N., Hervieu, M., Kou, I., Leclercq, S., Galéra, P., Boumediene, K., & Baugé, C. (2011). Asporin expression is highly regulated in human chondrocytes. Molecular Medicine (Cambridge, Mass.), 17(7–8), 816–823. https://doi.org/10.2119/molmed.2011.00052

Egloff, C., Hügle, T., & Valderrabano, V. (2012). Biomechanics and pathomechanisms of osteoarthritis. Swiss Medical Weekly, 142, w13583. https://doi.org/10.4414/smw.2012.13583

Eyre DR, W. J. (1987). Type XI or 1α2α3α collagen. In Structure and Function of Collagen Types. New York: Academic Press, 261–281.

Eyre, D. (2001). Articular cartilage and changes in Arthritis: Collagen of articular cartilage. Arthritis Research & Therapy, 4(1), 30. https://doi.org/10.1186/ar380

Eyre, D. (2002). Collagen of articular cartilage. Arthritis Research, 4(1), 30–35. https://doi.org/10.1186/ar380

Eyre, D. R. (1991). The collagens of articular cartilage. Seminars in Arthritis and Rheumatism, 21(3, Supplement 2), 2–11. https://doi.org/https://doi.org/10.1016/0049-0172(91)90035-X

Fan, Z., Söder, S., Oehler, S., Fundel, K., & Aigner, T. (2007). Activation of interleukin-1 signaling cascades in normal and osteoarthritic articular cartilage. The American Journal of Pathology, 171(3), 938–946. https://doi.org/10.2353/ajpath.2007.061083

Feng, Z.-Y., He, Z.-N., Zhang, B., & Chen, Z. (2013). Osteoprotegerin promotes the proliferation of chondrocytes and affects the expression of ADAMTS-5 and TIMP-4 through MEK/ERK signaling. Molecular Medicine Reports, 8(6), 1669–1679. https://doi.org/10.3892/mmr.2013.1717

Flannery, C. R., Hughes, C. E., Schumacher, B. L., Tudor, D., Aydelotte, M. B., Kuettner, K. E., & Caterson, B. (1999). Articular cartilage superficial zone protein (SZP) is homologous to megakaryocyte stimulating factor precursor and Is a multifunctional proteoglycan with potential growth-promoting, cytoprotective, and lubricating properties in cartilage metabolism. Biochemical and Biophysical Research Communications, 254(3), 535–541. https://doi.org/10.1006/bbrc.1998.0104

Folkesson, E, Turkiewicz, A., Ali, N., Rydén, M., Hughes, H. V, Tjörnstrand, J., Önnerfjord, P., & Englund, M. (2020). Proteomic comparison of osteoarthritic and reference human menisci using data-independent acquisition mass spectrometry. Osteoarthritis and Cartilage, 28(8), 1092–1101. https://doi.org/https://doi.org/10.1016/j.joca.2020.05.001

Folkesson, Elin, Turkiewicz, A., Englund, M., & Önnerfjord, P. (2018). Differential protein expression in human knee articular cartilage and medial meniscus using two different proteomic methods: a pilot analysis. BMC Musculoskeletal Disorders, 19(1), 416. https://doi.org/10.1186/s12891-018-2346-6

Forsyth, C. B., Cole, A., Murphy, G., Bienias, J. L., Im, H.-J., & Loeser, R. F. J. (2005). Increased matrix metalloproteinase-13 production with aging by human articular chondrocytes in response to catabolic stimuli. The Journals of Gerontology. Series A, Biological Sciences and Medical Sciences, 60(9), 1118–1124. https://doi.org/10.1093/gerona/60.9.1118

Franceschi, C., Bonafè, M., Valensin, S., Olivieri, F., De Luca, M., Ottaviani, E., & De Benedictis, G. (2000). Inflamm-aging. An evolutionary perspective on immunosenescence. Annals of the New York Academy of Sciences, 908, 244–254. https://doi.org/10.1111/j.1749-6632.2000.tb06651.x

Freund, A., Orjalo, A. V, Desprez, P.-Y., & Campisi, J. (2010). Inflammatory networks during cellular senescence: causes and consequences. Trends in Molecular Medicine, 16(5), 238–246. https://doi.org/10.1016/j.molmed.2010.03.003

Fukui, N., Miyamoto, Y., Nakajima, M., Ikeda, Y., Hikita, A., Furukawa, H., Mitomi, H., Tanaka, N., Katsuragawa, Y., Yamamoto, S., Sawabe, M., Juji, T., Mori, T., Suzuki, R., & Ikegawa, S. (2008). Zonal gene expression of chondrocytes in osteoarthritic cartilage. Arthritis and Rheumatism, 58(12), 3843–3853. https://doi.org/10.1002/art.24036

Garcia, B. A., Platt, M. D., Born, T. L., Shabanowitz, J., Marcus, N. A., & Hunt, D. F. (2006). Protein profile of osteoarthritic human articular cartilage using tandem mass spectrometry. Rapid Communications in Mass Spectrometry : RCM, 20(20), 2999–3006. https://doi.org/10.1002/rcm.2692

Ghouri, A., & Conaghan, P. G. (2019). Update on novel pharmacological therapies for osteoarthritis. Therapeutic Advances in Musculoskeletal Disease, 11, 1759720X19864492. https://doi.org/10.1177/1759720X19864492

Gilbert, S. J., & Blain, E. J. (2018). Chapter 4 - Cartilage mechanobiology: How chondrocytes respond to mechanical load. In S. W. Verbruggen (Ed.), Mechanobiology in Health and Disease (pp. 99–126). Academic Press. https://doi.org/https://doi.org/10.1016/B978-0-12-812952-4.00004-0

Gilmore, T. D. (2006). Introduction to NF-κB: players, pathways, perspectives. Oncogene, 25(51), 6680–6684. https://doi.org/10.1038/sj.onc.1209954

Goldring, M. B., & Marcu, K. B. (2009). Cartilage homeostasis in health and rheumatic diseases. Arthritis Research & Therapy, 11(3), 224. https://doi.org/10.1186/ar2592

Gottardi, C. J., Wong, E., & Gumbiner, B. M. (2001). E-cadherin suppresses cellular transformation by inhibiting beta-catenin signaling in an adhesion-independent manner. The Journal of Cell Biology, 153(5), 1049–1060. https://doi.org/10.1083/jcb.153.5.1049

Gregory, K. E., Keene, D. R., Tufa, S. F., Lunstrum, G. P., & Morris, N. P. (2001). Developmental distribution of collagen type XII in cartilage: association with articular cartilage and the growth plate. Journal of Bone and Mineral Research : The Official Journal of the American Society for Bone and Mineral Research, 16(11), 2005–2016. https://doi.org/10.1359/jbmr.2001.16.11.2005

Gress, K., Charipova, K., An, D., Hasoon, J., Kaye, A. D., Paladini, A., Varrassi, G., Viswanath, O., Abd-Elsayed, A., & Urits, I. (2020). Treatment recommendations for chronic knee osteoarthritis. Best Practice & Research Clinical Anaesthesiology, 34(3), 369–382. https://doi.org/https://doi.org/10.1016/j.bpa.2020.06.006

Grogan, S. P., & D'Lima, D. D. (2010). Joint aging and chondrocyte cell death. International Journal of Clinical Rheumatology, 5(2), 199–214. https://doi.org/10.2217/ijr.10.3

Grogan, S. P., Duffy, S. F., Pauli, C., Koziol, J. A., Su, A. I., D'Lima, D. D., & Lotz, M. K. (2013). Zone-specific gene expression patterns in articular cartilage. Arthritis and Rheumatism, 65(2), 418–428. https://doi.org/10.1002/art.37760

Grogan, S. P., Miyaki, S., Asahara, H., D'Lima, D. D., & Lotz, M. K. (2009). Mesenchymal progenitor cell markers in human articular cartilage: normal distribution and changes in osteoarthritis. Arthritis Research & Therapy, 11(3), R85. https://doi.org/10.1186/ar2719

Gu, J., Lu, Y., Li, F., Qiao, L., Wang, Q., Li, N., Borgia, J. A., Deng, Y., Lei, G., & Zheng, Q. (2014). Identification and characterization of the novel Col10a1 regulatory mechanism during chondrocyte hypertrophic differentiation. Cell Death & Disease, 5(10), e1469–e1469. https://doi.org/10.1038/cddis.2014.444

Guo, D., Tan, W., Wang, F., Lv, Z., Hu, J., Lv, T., Chen, Q., Gu, X., Wan, B., & Zhang, Z. (2008). Proteomic analysis of human articular cartilage: Identification of differentially expressed proteins in knee osteoarthritis. Joint Bone Spine, 75(4), 439–444. https://doi.org/https://doi.org/10.1016/j.jbspin.2007.12.003

H, K. J., & Lawrence, J. S. (1957). Radiological assessment of osteo-arthrosis. Annals of the Rheumatic Diseases, 16(4), 494–502. https://doi.org/10.1136/ard.16.4.494

Hafez, A., Squires, R., Pedracini, A., Joshi, A., Seegmiller, R. E., & Oxford, J. T. (2015). Col11a1 Regulates Bone Microarchitecture during Embryonic Development. Journal of Developmental Biology, 3(4), 158–176. https://doi.org/10.3390/jdb3040158

Hagg, R., Bruckner, P., & Hedbom, E. (1998). Cartilage fibrils of mammals are biochemically heterogeneous: differential distribution of decorin and collagen IX. The Journal of Cell Biology, 142(1), 285–294. https://doi.org/10.1083/jcb.142.1.285

Hao, Y., Wu, Y., Wang, S., Wang, C., Qu, S., Li, L., Yu, G., Liu, Z., Zhao, Z., Fan, P., Zhang, Z., & Shi, Y. (2021). Quantitative proteomics reveal the protective effects of EDS against osteoarthritis via attenuating inflammation and modulating immune response. Journal of Ethnopharmacology, 271, 113780. https://doi.org/https://doi.org/10.1016/j.jep.2021.113780

Hayden, M. S., & Ghosh, S. (2008). Shared principles in NF-kappaB signaling. Cell, 132(3), 344–362. https://doi.org/10.1016/j.cell.2008.01.020

Heinegård, D., & Saxne, T. (2011). The role of the cartilage matrix in osteoarthritis. Nature Reviews Rheumatology, 7(1), 50–56. https://doi.org/10.1038/nrrheum.2010.198

Hering, T M.; Kollar, J; Flory, D; Johnstone, B. (2000). Characterization of cartilage-derived AEBP1/ACLP and analysis of its expression during chondrogenic differentiation in-vitro.. 46th Annual Meeting, Orthopaedic Research Society, 0909.

Hermansson, M., Sawaji, Y., Bolton, M., Alexander, S., Wallace, A., Begum, S., Wait, R., & Saklatvala, J. (2004). Proteomic analysis of articular cartilage shows increased type II collagen synthesis in osteoarthritis and expression of inhibin betaA (activin A), a regulatory molecule for chondrocytes. The Journal of Biological Chemistry, 279(42), 43514–43521. https://doi.org/10.1074/jbc.M407041200

Hidaka, C., Cheng, C., Alexandre, D., Bhargava, M., & Torzilli, P. A. (2006). Maturational differences in superficial and deep zone articular chondrocytes. Cell and Tissue Research, 323(1), 127–135. https://doi.org/10.1007/s00441-005-0050-y

Hosseininia, S., Önnerfjord, P., & Dahlberg, L. E. (2019). Targeted proteomics of hip articular cartilage in OA and fracture patients. Journal of Orthopaedic Research : Official Publication of the Orthopaedic Research Society, 37(1), 131–135. https://doi.org/10.1002/jor.24158

Hsueh, M. F., Khabut, A., Kjellström, S., Önnerfjord, P., & Kraus, V. B. (2016). Elucidating the Molecular Composition of Cartilage by Proteomics. Journal of Proteome Research, 15(2), 374–388. https://doi.org/10.1021/acs.jproteome.5b00946

Hsueh, M.-F., Kraus, V. B., & Önnerfjord, P. (2017). Cartilage matrix remodelling differs by disease state and joint type. European Cells & Materials, 34, 70–82. https://doi.org/10.22203/eCM.v034a05

Hu, Q.-X., Li, X.-D., Xie, P., Wu, C.-C., Zheng, G.-Z., Lin, F.-X., Xie, D., Zhang, Q.-H., Liu, D.-Z., Wang, Y.-G., Chang, B., & Du, S.-X. (2017). All-trans-retinoic acid activates SDF-1/CXCR4/ROCK2 signaling pathway to inhibit chondrogenesis. American Journal of Translational Research, 9(5), 2296–2305.

Hui, W., Young, D. A., Rowan, A. D., Xu, X., Cawston, T. E., & Proctor, C. J. (2016). Oxidative changes and signalling pathways are pivotal in initiating age-related changes in articular cartilage. Annals of the Rheumatic Diseases, 75(2), 449–458. https://doi.org/10.1136/annrheumdis-2014-206295

Ikegawa, S., Sano, M., Koshizuka, Y., & Nakamura, Y. (2000). Isolation, characterization and mapping of the mouse and human PRG4 (proteoglycan 4) genes. Cytogenetics and Cell Genetics, 90(3–4), 291–297. https://doi.org/10.1159/000056791

Jacob, B., Jüllig, M., Middleditch, M., Payne, L., Broom, N., Sarojini, V., & Thambyah, A. (2021). Protein Levels and Microstructural Changes in Localized Regions of Early Cartilage Degeneration Compared with Adjacent Intact Cartilage. Cartilage, 12(2), 192–210. https://doi.org/10.1177/1947603518809401

Jayasuriya, C. T., Zhou, F. H., Pei, M., Wang, Z., Lemme, N. J., Haines, P., & Chen, Q. (2014). Matrilin-3 chondrodysplasia mutations cause attenuated chondrogenesis, premature hypertrophy and aberrant response to TGF-β in chondroprogenitor cells. International Journal of Molecular Sciences, 15(8), 14555–14573. https://doi.org/10.3390/ijms150814555

Jin, X., Wang, B. H., Wang, X., Antony, B., Zhu, Z., Han, W., Cicuttini, F., Wluka, A. E., Winzenberg, T., Blizzard, L., Jones, G., & Ding, C. (2017). Associations between endogenous

sex hormones and MRI structural changes in patients with symptomatic knee osteoarthritis. Osteoarthritis and Cartilage, 25(7), 1100–1106. https://doi.org/10.1016/j.joca.2017.01.015

Kalamajski, S., Aspberg, A., Lindblom, K., Heinegård, D., & Oldberg, A. (2009). Asporin competes with decorin for collagen binding, binds calcium and promotes osteoblast collagen mineralization. The Biochemical Journal, 423(1), 53–59. https://doi.org/10.1042/BJ20090542

Kapoor, M., Mahomed, N. N., & Medicine, P. (2015). Osteoarthritis. https://doi.org/10.1007/978-3-319-19560-5

Kassner, A., Hansen, U., Miosge, N., Reinhardt, D. P., Aigner, T., Bruckner-Tuderman, L., Bruckner, P., & Grässel, S. (2003). Discrete integration of collagen XVI into tissue-specific collagen fibrils or beaded microfibrils. Matrix Biology : Journal of the International Society for Matrix Biology, 22(2), 131–143. https://doi.org/10.1016/s0945-053x(03)00008-8

Kaufman, C. S., & Butler, M. G. (2016). Mutation in TNXB gene causes moderate to severe Ehlers-Danlos syndrome. World Journal of Medical Genetics, 6(2), 17–21. https://doi.org/10.5496/wjmg.v6.i2.17

Keene, D. R., Jordan, C. D., Reinhardt, D. P., Ridgway, C. C., Ono, R. N., Corson, G. M., Fairhurst, M., Sussman, M. D., Memoli, V. A., & Sakai, L. Y. (1997). Fibrillin-1 in human cartilage: developmental expression and formation of special banded fibers. The Journal of Histochemistry and Cytochemistry : Official Journal of the Histochemistry Society, 45(8), 1069–1082. https://doi.org/10.1177/002215549704500805

Kerr, J. F., Wyllie, A. H., & Currie, A. R. (1972). Apoptosis: a basic biological phenomenon with wide-ranging implications in tissue kinetics. British Journal of Cancer, 26(4), 239–257. https://doi.org/10.1038/bjc.1972.33

Kevorkian, L., Young, D. A., Darrah, C., Donell, S. T., Shepstone, L., Porter, S., Brockbank, S. M. V, Edwards, D. R., Parker, A. E., & Clark, I. M. (2004). Expression profiling of metalloproteinases and their inhibitors in cartilage. Arthritis and Rheumatism, 50(1), 131–141. https://doi.org/10.1002/art.11433

Khan, I. M., Salter, D. M., Bayliss, M. T., Thomson, B. M., & Archer, C. W. (2001). Expression of clusterin in the superficial zone of bovine articular cartilage. Arthritis and Rheumatism, 44(8), 1795–1799. https://doi.org/10.1002/1529-0131(200108)44:8<1795::AID-ART316>3.0.CO;2-K

Kiani, C., Lee, V., Cao, L., Chen, L., Wu, Y., Zhang, Y., Adams, M. E., & Yang, B. B. (2001). Roles of aggrecan domains in biosynthesis, modification by glycosaminoglycans and product secretion. The Biochemical Journal, 354(Pt 1), 199–207. https://doi.org/10.1042/0264-6021:3540199

Killen, M.-C., & Charalambous, C. P. (2020). Chapter 6 - Advances in cartilage restoration techniques. In W. Ahmed, D. A. Phoenix, M. J. Jackson, & C. P. Charalambous (Eds.), Advances in Medical and Surgical Engineering (pp. 71–83). Academic Press. https://doi.org/https://doi.org/10.1016/B978-0-12-819712-7.00006-1

King, L. K., March, L., & Anandacoomarasamy, A. (2013). Obesity & osteoarthritis. The Indian Journal of Medical Research, 138(2), 185–193.

Kirsch, T., Swoboda, B., & Nah, H. (2000). Activation of annexin II and V expression, terminal differentiation, mineralization and apoptosis in human osteoarthritic cartilage. Osteoarthritis and Cartilage, 8(4), 294–302. https://doi.org/10.1053/joca.1999.0304

Kizawa, H., Kou, I., Iida, A., Sudo, A., Miyamoto, Y., Fukuda, A., Mabuchi, A., Kotani, A., Kawakami, A., Yamamoto, S., Uchida, A., Nakamura, K., Notoya, K., Nakamura, Y., & Ikegawa, S. (2005). An aspartic acid repeat polymorphism in asporin inhibits chondrogenesis and increases susceptibility to osteoarthritis. Nature Genetics, 37(2), 138–144. https://doi.org/10.1038/ng1496

Klatt, A. R., Paulsson, M., & Wagener, R. (2002). Expression of matrilins during maturation of mouse skeletal tissues. Matrix Biology : Journal of the International Society for Matrix Biology, 21(3), 289–296. https://doi.org/10.1016/s0945-053x(02)00006-9

Knudson, C. B., & Knudson, W. (2001). Cartilage proteoglycans. Seminars in Cell and Developmental Biology, 12(2), 69–78. https://doi.org/10.1006/scdb.2000.0243

Ko, Y., Kobbe, B., Nicolae, C., Miosge, N., Paulsson, M., Wagener, R., & Aszódi, A. (2004). Matrilin-3 is dispensable for mouse skeletal growth and development. Molecular and Cellular Biology, 24(4), 1691–1699. https://doi.org/10.1128/MCB.24.4.1691-1699.2004

Koch, M., Schulze, J., Hansen, U., Ashwodt, T., Keene, D. R., Brunken, W. J., Burgeson, R. E., Bruckner, P., & Bruckner-Tuderman, L. (2004). A novel marker of tissue junctions, collagen XXII. The Journal of Biological Chemistry, 279(21), 22514–22521. https://doi.org/10.1074/jbc.M400536200

Koike, M., Nojiri, H., Kanazawa, H., Yamaguchi, H., Miyagawa, K., Nagura, N., Banno, S., Iwase, Y., Kurosawa, H., & Kaneko, K. (2018). Superoxide dismutase activity is significantly lower in end-stage osteoarthritic cartilage than non-osteoarthritic cartilage. PloS One, 13(9), e0203944. https://doi.org/10.1371/journal.pone.0203944

Koike, M., Nojiri, H., Ozawa, Y., Watanabe, K., Muramatsu, Y., Kaneko, H., Morikawa, D., Kobayashi, K., Saita, Y., Sasho, T., Shirasawa, T., Yokote, K., Kaneko, K., & Shimizu, T. (2015). Mechanical overloading causes mitochondrial superoxide and SOD2 imbalance in chondrocytes resulting in cartilage degeneration. Scientific Reports, 5(1), 11722. https://doi.org/10.1038/srep11722

Komiya, Y., & Habas, R. (2008). Wnt signal transduction pathways. Organogenesis, 4(2), 68–75. https://doi.org/10.4161/org.4.2.5851

Komori, T. (2017). Roles of Runx2 in Skeletal Development. Advances in Experimental Medicine and Biology, 962, 83–93. https://doi.org/10.1007/978-981-10-3233-2_6

Krishnan, Y., & Grodzinsky, A. J. (2018). Cartilage diseases. Matrix Biology : Journal of the International Society for Matrix Biology, 71–72, 51–69. https://doi.org/10.1016/j.matbio.2018.05.005

Kumar, Y., Biswas, T., Thacker, G., Kanaujiya, J. K., Kumar, S., Shukla, A., Khan, K., Sanyal, S., Chattopadhyay, N., Bandyopadhyay, A., & Trivedi, A. K. (2018). BMP signaling-driven osteogenesis is critically dependent on Prdx-1 expression-mediated maintenance of chondrocyte prehypetrophy. Free Radical Biology & Medicine, 118, 1–12. https://doi.org/10.1016/j.freeradbiomed.2018.02.016

Lafont, J. E., Talma, S., Hopfgarten, C., & Murphy, C. L. (2008). Hypoxia promotes the differentiated human articular chondrocyte phenotype through SOX9-dependent and -independent pathways. The Journal of Biological Chemistry, 283(8), 4778–4786. https://doi.org/10.1074/jbc.M707729200

Lee, J.-M., Lee, E.-H., Kim, I.-S., & Kim, J.-E. (2015). Tgfbi deficiency leads to a reduction in skeletal size and degradation of the bone matrix. Calcified Tissue International, 96(1), 56–64. https://doi.org/10.1007/s00223-014-9938-4

Lei, J., Amhare, A. F., Wang, L., Lv, Y., Deng, H., Gao, H., Guo, X., Han, J., & Lammi, M. J. (2020). Proteomic analysis of knee cartilage reveals potential signaling pathways in pathological mechanism of Kashin-Beck disease compared with osteoarthritis. Scientific Reports, 10(1), 6824. https://doi.org/10.1038/s41598-020-63932-6

Li, A., Wei, Y., Hung, C., & Vunjak-Novakovic, G. (2018). Chondrogenic properties of collagen type XI, a component of cartilage extracellular matrix. Biomaterials, 173, 47–57. https://doi.org/10.1016/j.biomaterials.2018.05.004

Li, Pengcui, Che, X., Gao, Y., & Zhang, R. (2020). Proteomics and Bioinformatics Analysis of Cartilage in Post-Traumatic Osteoarthritis in a Mini-Pig Model of Anterior Cruciate Ligament Repair. Medical Science Monitor : International Medical Journal of Experimental and Clinical Research, 26, e920104. https://doi.org/10.12659/MSM.920104

Li, Ping, Fleischhauer, L., Nicolae, C., Prein, C., Farkas, Z., Saller, M. M., Prall, W. C., Wagener, R., Heilig, J., Niehoff, A., Clausen-Schaumann, H., Alberton, P., & Aszodi, A. (2020). Mice Lacking the Matrilin Family of Extracellular Matrix Proteins Develop Mild Skeletal Abnormalities and Are Susceptible to Age-Associated Osteoarthritis. International Journal of Molecular Sciences, 21(2). https://doi.org/10.3390/ijms21020666

Liang, Q.-Q., Li, X.-F., Zhou, Q., Xing, L., Cheng, S.-D., Ding, D.-F., Xu, L.-Q., Tang, D.-Z., Bian, Q., Xi, Z.-J., Zhou, C., Shi, Q., & Wang, Y.-J. (2011). The expression of osteoprotegerin is required for maintaining the intervertebral disc endplate of aged mice. Bone, 48(6), 1362–1369. https://doi.org/10.1016/j.bone.2011.03.773

Lin, Z., Willers, C., Xu, J., & Zheng, M.-H. (2006). The chondrocyte: biology and clinical application. Tissue Engineering, 12(7), 1971–1984. https://doi.org/10.1089/ten.2006.12.1971

Liu, B., Balkwill, A., Banks, E., Cooper, C., Green, J., & Beral, V. (2007). Relationship of height, weight and body mass index to the risk of hip and knee replacements in middle-aged women. Rheumatology (Oxford, England), 46(5), 861–867. https://doi.org/10.1093/rheumatology/kel434

Liu, R., Liu, Q., Wang, K., Dang, X., & Zhang, F. (2016). Comparative analysis of gene expression profiles in normal hip human cartilage and cartilage from patients with necrosis of the femoral head. Arthritis Research & Therapy, 18(1), 98. https://doi.org/10.1186/s13075-016-0991-4

Loeser, R. F., Collins, J. A., & Diekman, B. O. (2016). Ageing and the pathogenesis of osteoarthritis. Nature Reviews. Rheumatology, 12(7), 412–420. https://doi.org/10.1038/nrrheum.2016.65

Lorenz, H., & Richter, W. (2006). Osteoarthritis: Cellular and molecular changes in degenerating cartilage. Progress in Histochemistry and Cytochemistry, 40(3), 135–163. https://doi.org/https://doi.org/10.1016/j.proghi.2006.02.003

Lorenzo, P., Aspberg, A., Onnerfjord, P., Bayliss, M. T., Neame, P. J., & Heinegard, D. (2001). Identification and characterization of asporin. a novel member of the leucine-rich repeat protein family closely related to decorin and biglycan. The Journal of Biological Chemistry, 276(15), 12201–12211. https://doi.org/10.1074/jbc.M010932200

Lorenzo, P., Bayliss, M. T., & Heinegård, D. (1998). A novel cartilage protein (CILP) present in the mid-zone of human articular cartilage increases with age. The Journal of Biological Chemistry, 273(36), 23463–23468. https://doi.org/10.1074/jbc.273.36.23463

Lotz, M, Hashimoto, S., & Kühn, K. (1999). Mechanisms of chondrocyte apoptosis. Osteoarthritis and Cartilage, 7(4), 389–391. https://doi.org/10.1053/joca.1998.0220

Lotz, Martin, & Loeser, R. F. (2012). Effects of aging on articular cartilage homeostasis. Bone, 51(2), 241–248. https://doi.org/10.1016/j.bone.2012.03.023

Luan, Y., Kong, L., Howell, D. R., Ilalov, K., Fajardo, M., Bai, X.-H., Di Cesare, P. E., Goldring, M. B., Abramson, S. B., & Liu, C.-J. (2008). Inhibition of ADAMTS-7 and ADAMTS-12 degradation of cartilage oligomeric matrix protein by alpha-2-macroglobulin. Osteoarthritis and Cartilage, 16(11), 1413–1420. https://doi.org/10.1016/j.joca.2008.03.017

Lum, Z. C., Shieh, A. K., & Dorr, L. D. (2018). Why total knees fail-A modern perspective review. World Journal of Orthopedics, 9(4), 60–64. https://doi.org/10.5312/wjo.v9.i4.60

Luo, W., Kuwada, T. S., Chandrasekaran, L., Zheng, J., & Tanzer, M. L. (1996). Divergent secretory behavior of the opposite ends of aggrecan. The Journal of Biological Chemistry, 271(28), 16447–16450. https://doi.org/10.1074/jbc.271.28.16447

Luo, Y., Sinkeviciute, D., He, Y., Karsdal, M., Henrotin, Y., Mobasheri, A., Önnerfjord, P., & Bay-Jensen, A. (2017). The minor collagens in articular cartilage. Protein & Cell, 8(8), 560–572. https://doi.org/10.1007/s13238-017-0377-7

Madry, H., Kon, E., Condello, V., Peretti, G. M., Steinwachs, M., Seil, R., Berruto, M., Engebretsen, L., Filardo, G., & Angele, P. (2016). Early osteoarthritis of the knee. Knee Surgery, Sports Traumatology, Arthroscopy, 24(6), 1753–1762. https://doi.org/10.1007/s00167-016-4068-3

Mahendran, S. M., Keystone, E. C., Krawetz, R. J., Liang, K., Diamandis, E. P., & Chandran, V. (2019). Elucidating the endogenous synovial fluid proteome and peptidome of inflammatory

arthritis using label-free mass spectrometry. Clinical Proteomics, 16, 23.
https://doi.org/10.1186/s12014-019-9243-3

Mankin, H. J., Dorfman, H., Lippiello, L., & Zarins, A. (1971). Biochemical and metabolic
abnormalities in articular cartilage from osteo-arthritic human hips. II. Correlation of
morphology with biochemical and metabolic data. The Journal of Bone and Joint Surgery.
American Volume, 53(3), 523–537.

Marcelino, J., & McDevitt, C. A. (1995). Attachment of articular cartilage chondrocytes to the
tissue form of type VI collagen. Biochimica et Biophysica Acta, 1249(2), 180–188.
https://doi.org/10.1016/0167-4838(95)00026-q

Martel-Pelletier, J., Barr, A. J., Cicuttini, F. M., Conaghan, P. G., Cooper, C., Goldring, M. B.,
Goldring, S. R., Jones, G., Teichtahl, A. J., & Pelletier, J.-P. (2016a). Osteoarthritis. Nature
Reviews Disease Primers, 2(1), 16072. https://doi.org/10.1038/nrdp.2016.72

Martel-Pelletier, J., Barr, A. J., Cicuttini, F. M., Conaghan, P. G., Cooper, C., Goldring, M. B.,
Goldring, S. R., Jones, G., Teichtahl, A. J., & Pelletier, J.-P. (2016b). Osteoarthritis. Nature
Reviews. Disease Primers, 2, 16072. https://doi.org/10.1038/nrdp.2016.72

Martin, J. A., & Buckwalter, J. A. (2002). Aging, articular cartilage chondrocyte senescence and
osteoarthritis. Biogerontology, 3(5), 257–264. https://doi.org/10.1023/A:1020185404126

Mast, A. E., Enghild, J. J., Nagase, H., Suzuki, K., Pizzo, S. V, & Salvesen, G. (1991). Kinetics
and physiologic relevance of the inactivation of alpha 1-proteinase inhibitor, alpha 1-
antichymotrypsin, and antithrombin III by matrix metalloproteinases-1 (tissue collagenase), -2
(72-kDa gelatinase/type IV collagenase), and -3 (stromelysin). The Journal of Biological
Chemistry, 266(24), 15810–15816.

Maumus, M., Manferdini, C., Toupet, K., Chuchana, P., Casteilla, L., Gachet, M., Jorgensen, C.,
Lisignoli, G., & Noël, D. (2017). Thrombospondin-1 Partly Mediates the Cartilage Protective
Effect of Adipose-Derived Mesenchymal Stem Cells in Osteoarthritis. Frontiers in
Immunology, 8, 1638. https://doi.org/10.3389/fimmu.2017.01638

Meng, W., Adams, M. J., Palmer, C. N. A., Shi, J., Auton, A., Ryan, K. A., Jordan, J. M.,
Mitchell, B. D., Jackson, R. D., Yau, M. S., McIntosh, A. M., & Smith, B. H. (2019). Genome-
wide association study of knee pain identifies associations with GDF5 and COL27A1 in UK
Biobank. Communications Biology, 2, 321. https://doi.org/10.1038/s42003-019-0568-2

Mengshol, J. A., Vincenti, M. P., & Brinckerhoff, C. E. (2001). IL-1 induces collagenase-3
(MMP-13) promoter activity in stably transfected chondrocytic cells: requirement for Runx-2
and activation by p38 MAPK and JNK pathways. Nucleic Acids Research, 29(21), 4361–4372.
https://doi.org/10.1093/nar/29.21.4361

Minashima, T., & Kirsch, T. (2018). Annexin A6 regulates catabolic events in articular
chondrocytes via the modulation of NF-κB and Wnt/ß-catenin signaling. PloS One, 13(5),
e0197690. https://doi.org/10.1371/journal.pone.0197690

Miosge, N., Hartmann, M., Maelicke, C., & Herken, R. (2004). Expression of collagen type I and type II in consecutive stages of human osteoarthritis. Histochemistry and Cell Biology, 122(3), 229–236. https://doi.org/10.1007/s00418-004-0697-6

Mitsuyama, H., Healey, R. M., Terkeltaub, R. A., Coutts, R. D., & Amiel, D. (2007). Calcification of human articular knee cartilage is primarily an effect of aging rather than osteoarthritis. Osteoarthritis and Cartilage, 15(5), 559–565. https://doi.org/10.1016/j.joca.2006.10.017

Morris, K. J., Cs-Szabo, G., & Cole, A. A. (2010). Characterization of TIMP-3 in human articular talar cartilage. Connective Tissue Research, 51(6), 478–490. https://doi.org/10.3109/03008201003686958

Müller, C., Khabut, A., Dudhia, J., Reinholt, F. P., Aspberg, A., Heinegård, D., & Önnerfjord, P. (2014). Quantitative proteomics at different depths in human articular cartilage reveals unique patterns of protein distribution. Matrix Biology : Journal of the International Society for Matrix Biology, 40, 34–45. https://doi.org/10.1016/j.matbio.2014.08.013

Muttigi, M. S., Han, I., Park, H.-K., Park, H., & Lee, S.-H. (2016). Matrilin-3 Role in Cartilage Development and Osteoarthritis. International Journal of Molecular Sciences, 17(4). https://doi.org/10.3390/ijms17040590

Nakajima, M., Kizawa, H., Saitoh, M., Kou, I., Miyazono, K., & Ikegawa, S. (2007). Mechanisms for asporin function and regulation in articular cartilage. The Journal of Biological Chemistry, 282(44), 32185–32192. https://doi.org/10.1074/jbc.M700522200

Neame, P. J., & Barry, F. P. (1993). The link proteins. Experientia, 49(5), 393–402. https://doi.org/10.1007/BF01923584

Neogi, T. (2013). The epidemiology and impact of pain in osteoarthritis. Osteoarthritis and Cartilage, 21(9), 1145–1153. https://doi.org/10.1016/j.joca.2013.03.018

Neogi, Tuhina, & Zhang, Y. (2013). Epidemiology of osteoarthritis. Rheumatic Diseases Clinics of North America, 39(1), 1–19. https://doi.org/10.1016/j.rdc.2012.10.004

Nogaeva, M. G. (2015). [Osteoarthritis in the adult population of the Republic of Kazakhstan]. Terapevticheskii arkhiv, 87(5), 65–68. https://doi.org/10.17116/terarkh201587565-68

Önnerfjord, P., Khabut, A., Reinholt, F. P., Svensson, O., & Heinegård, D. (2012). Quantitative proteomic analysis of eight cartilaginous tissues reveals characteristic differences as well as similarities between subgroups. The Journal of Biological Chemistry, 287(23), 18913–18924. https://doi.org/10.1074/jbc.M111.298968

Oo, W. M., Little, C., Duong, V., & Hunter, D. J. (2021). The Development of Disease-Modifying Therapies for Osteoarthritis (DMOADs): The Evidence to Date. Drug Design, Development and Therapy, 15, 2921–2945. https://doi.org/10.2147/DDDT.S295224

Otsuki, S., Brinson, D. C., Creighton, L., Kinoshita, M., Sah, R. L., D'Lima, D., & Lotz, M. (2008). The effect of glycosaminoglycan loss on chondrocyte viability: a study on porcine cartilage explants. Arthritis and Rheumatism, 58(4), 1076–1085. https://doi.org/10.1002/art.23381

Outerbridge, R. E. (1961). The etiology of chondromalacia patellae. The Journal of Bone and Joint Surgery. British Volume, 43-B, 752–757. https://doi.org/10.1302/0301-620X.43B4.752

Papas, P. V., Congiusta, D., & Cushner, F. D. (2019). Cementless versus Cemented Fixation in Total Knee Arthroplasty. The Journal of Knee Surgery, 32(7), 596–599. https://doi.org/10.1055/s-0039-1678687

Peffers, M. J., Cillero-Pastor, B., Eijkel, G. B., Clegg, P. D., & Heeren, R. M. A. (2014). Matrix assisted laser desorption ionization mass spectrometry imaging identifies markers of ageing and osteoarthritic cartilage. Arthritis Research & Therapy, 16(3), R110. https://doi.org/10.1186/ar4560

Pérez, E., Gallegos, J. L., Cortés, L., Calderón, K. G., Luna, J. C., Cázares, F. E., Velasquillo, M. C., Kouri, J. B., & Hernández, F. C. (2010). Identification of latexin by a proteomic analysis in rat normal articular cartilage. Proteome Science, 8, 27. https://doi.org/10.1186/1477-5956-8-27

Phinyomark, A., Osis, S. T., Hettinga, B. A., Kobsar, D., & Ferber, R. (2016). Gender differences in gait kinematics for patients with knee osteoarthritis. BMC Musculoskeletal Disorders, 17, 157. https://doi.org/10.1186/s12891-016-1013-z

Polacek, M., Bruun, J.-A., Johansen, O., & Martinez, I. (2010). Differences in the secretome of cartilage explants and cultured chondrocytes unveiled by SILAC technology. Journal of Orthopaedic Research : Official Publication of the Orthopaedic Research Society, 28(8), 1040–1049. https://doi.org/10.1002/jor.21067

Polur, I., Lee, P. L., Servais, J. M., Xu, L., & Li, Y. (2010). Role of HTRA1, a serine protease, in the progression of articular cartilage degeneration. Histology and Histopathology, 25(5), 599–608. https://doi.org/10.14670/HH-25.599

Poole, C A, Flint, M. H., & Beaumont, B. W. (1987). Chondrons in cartilage: ultrastructural analysis of the pericellular microenvironment in adult human articular cartilages. Journal of Orthopaedic Research : Official Publication of the Orthopaedic Research Society, 5(4), 509–522. https://doi.org/10.1002/jor.1100050406

Poole, C Anthony. (1997). Review. Articular cartilage chondrons: form, function and failure. Journal of Anatomy, 191(1), 1–13. https://doi.org/10.1046/j.1469-7580.1997.19110001.x

Porée, B., Kypriotou, M., Chadjichristos, C., Beauchef, G., Renard, E., Legendre, F., Melin, M., Gueret, S., Hartmann, D.-J., Malléin-Gerin, F., Pujol, J.-P., Boumediene, K., & Galéra, P. (2008). Interleukin-6 (IL-6) and/or Soluble IL-6 Receptor Down-regulation of Human Type II Collagen Gene Expression in Articular Chondrocytes Requires a Decrease of Sp1·Sp3 Ratio and of the Binding Activity of Both Factors to the COL2A1 Promoter*. Journal of Biological Chemistry, 283(8), 4850–4865. https://doi.org/https://doi.org/10.1074/jbc.M706387200

Posey, K. L., Hankenson, K., Veerisetty, A. C., Bornstein, P., Lawler, J., & Hecht, J. T. (2008). Skeletal abnormalities in mice lacking extracellular matrix proteins, thrombospondin-1, thrombospondin-3, thrombospondin-5, and type IX collagen. The American Journal of Pathology, 172(6), 1664–1674. https://doi.org/10.2353/ajpath.2008.071094

Pritzker, K. P. H., Gay, S., Jimenez, S. A., Ostergaard, K., Pelletier, J.-P., Revell, P. A., Salter, D., & van den Berg, W. B. (2006). Osteoarthritis cartilage histopathology: grading and staging. Osteoarthritis and Cartilage, 14(1), 13–29. https://doi.org/10.1016/j.joca.2005.07.014

Pullig, O., Weseloh, G., Klatt, A. R., Wagener, R., & Swoboda, B. (2002). Matrilin-3 in human articular cartilage: increased expression in osteoarthritis. Osteoarthritis and Cartilage, 10(4), 253–263. https://doi.org/10.1053/joca.2001.0508

Qiu, C., Wu, X., Bian, J., Ma, X., Zhang, G., Guo, Z., Wang, Y., Ci, Y., Wang, Q., Xiang, H., & Chen, B. (2020). Differential proteomic analysis of fetal and geriatric lumbar nucleus pulposus: immunoinflammation and age-related intervertebral disc degeneration. BMC Musculoskeletal Disorders, 21(1), 339. https://doi.org/10.1186/s12891-020-03329-8

Rocha, B., Calamia, V., Casas, V., Carrascal, M., Blanco, F. J., & Ruiz-Romero, C. (2014). Secretome analysis of human mesenchymal stem cells undergoing chondrogenic differentiation. Journal of Proteome Research, 13(2), 1045–1054. https://doi.org/10.1021/pr401030n

Roos, E. M., & Arden, N. K. (2016). Strategies for the prevention of knee osteoarthritis. Nature Reviews Rheumatology, 12(2), 92–101. https://doi.org/10.1038/nrrheum.2015.135

Ruiz, M., Maumus, M., Fonteneau, G., Pers, Y.-M., Ferreira, R., Dagneaux, L., Delfour, C., Houard, X., Berenbaum, F., Rannou, F., Jorgensen, C., & Noël, D. (2019). TGFβi is involved in the chondrogenic differentiation of mesenchymal stem cells and is dysregulated in osteoarthritis. Osteoarthritis and Cartilage, 27(3), 493–503. https://doi.org/10.1016/j.joca.2018.11.005

Rutgers, M., van Pelt, M. J. P., Dhert, W. J. A., Creemers, L. B., & Saris, D. B. F. (2010). Evaluation of histological scoring systems for tissue-engineered, repaired and osteoarthritic cartilage. Osteoarthritis and Cartilage, 18(1), 12–23. https://doi.org/10.1016/j.joca.2009.08.009

Sadatsuki, R., Kaneko, H., Kinoshita, M., Futami, I., Nonaka, R., Culley, K. L., Otero, M., Hada, S., Goldring, M. B., Yamada, Y., Kaneko, K., Arikawa-Hirasawa, E., & Ishijima, M. (2017). Perlecan is required for the chondrogenic differentiation of synovial mesenchymal cells through regulation of Sox9 gene expression. Journal of Orthopaedic Research : Official Publication of the Orthopaedic Research Society, 35(4), 837–846. https://doi.org/10.1002/jor.23318

Scheller, J., Chalaris, A., Schmidt-Arras, D., & Rose-John, S. (2011). The pro- and anti-inflammatory properties of the cytokine interleukin-6. Biochimica et Biophysica Acta (BBA) - Molecular Cell Research, 1813(5), 878–888. https://doi.org/https://doi.org/10.1016/j.bbamcr.2011.01.034

Shen, G. (2005). The role of type X collagen in facilitating and regulating endochondral ossification of articular cartilage. Orthodontics & Craniofacial Research, 8(1), 11–17. https://doi.org/10.1111/j.1601-6343.2004.00308.x

Shu, C. C., Jackson, M. T., Smith, M. M., Smith, S. M., Penm, S., Lord, M. S., Whitelock, J. M., Little, C. B., & Melrose, J. (2016). Ablation of Perlecan Domain 1 Heparan Sulfate Reduces Progressive Cartilage Degradation, Synovitis, and Osteophyte Size in a Preclinical Model of

Posttraumatic Osteoarthritis. Arthritis & Rheumatology (Hoboken, N.J.), 68(4), 868–879. https://doi.org/10.1002/art.39529

Skou, S. T., & Roos, E. M. (2019). Physical therapy for patients with knee and hip osteoarthritis: supervised, active treatment is current best practice. Clinical and Experimental Rheumatology, 37 Suppl 1(5), 112–117.

Slattery, C., & Kweon, C. Y. (2018). Classifications in Brief: Outerbridge Classification of Chondral Lesions. Clinical Orthopaedics and Related Research, 476(10), 2101–2104. https://doi.org/10.1007/s11999.0000000000000255

Sophia Fox, A. J., Bedi, A., & Rodeo, S. A. (2009). The basic science of articular cartilage: structure, composition, and function. Sports Health, 1(6), 461–468. https://doi.org/10.1177/1941738109350438

Srikanth, V. K., Fryer, J. L., Zhai, G., Winzenberg, T. M., Hosmer, D., & Jones, G. (2005). A meta-analysis of sex differences prevalence, incidence and severity of osteoarthritis. Osteoarthritis and Cartilage, 13(9), 769–781. https://doi.org/10.1016/j.joca.2005.04.014

Starska, K., Forma, E., Lewy-Trenda, I., Papież, P., Woś, J., & Bryś, M. (2013). Diagnostic impact of promoter methylation and E-cadherin gene and protein expression levels in laryngeal carcinoma. Contemporary Oncology (Poznan, Poland), 17(3), 263–271. https://doi.org/10.5114/wo.2013.35284

Stefánsson, S. E., Jónsson, H., Ingvarsson, T., Manolescu, I., Jónsson, H. H., Olafsdóttir, G., Pálsdóttir, E., Stefánsdóttir, G., Sveinbjörnsdóttir, G., Frigge, M. L., Kong, A., Gulcher, J. R., & Stefánsson, K. (2003). Genomewide scan for hand osteoarthritis: a novel mutation in matrilin-3. American Journal of Human Genetics, 72(6), 1448–1459. https://doi.org/10.1086/375556

Steiglitz, B. M., Keene, D. R., & Greenspan, D. S. (2002). PCOLCE2 encodes a functional procollagen C-proteinase enhancer (PCPE2) that is a collagen-binding protein differing in distribution of expression and post-translational modification from the previously described PCPE1. The Journal of Biological Chemistry, 277(51), 49820–49830. https://doi.org/10.1074/jbc.M209891200

Steinberg, J., Ritchie, G. R. S., Roumeliotis, T. I., Jayasuriya, R. L., Clark, M. J., Brooks, R. A., Binch, A. L. A., Shah, K. M., Coyle, R., Pardo, M., Le Maitre, C. L., Ramos, Y. F. M., Nelissen, R. G. H. H., Meulenbelt, I., McCaskie, A. W., Choudhary, J. S., Wilkinson, J. M., & Zeggini, E. (2017). Integrative epigenomics, transcriptomics and proteomics of patient chondrocytes reveal genes and pathways involved in osteoarthritis. Scientific Reports, 7(1), 8935. https://doi.org/10.1038/s41598-017-09335-6

Sun, S.-C. (2011). Non-canonical NF-κB signaling pathway. Cell Research, 21(1), 71–85. https://doi.org/10.1038/cr.2010.177

Suter, L. G., Smith, S. R., Katz, J. N., Englund, M., Hunter, D. J., Frobell, R., & Losina, E. (2017). Projecting Lifetime Risk of Symptomatic Knee Osteoarthritis and Total Knee Replacement in Individuals Sustaining a Complete Anterior Cruciate Ligament Tear in Early Adulthood. Arthritis Care & Research, 69(2), 201–208. https://doi.org/10.1002/acr.22940

Swain, S., Sarmanova, A., Mallen, C., Kuo, C. F., Coupland, C., Doherty, M., & Zhang, W. (2020). Trends in incidence and prevalence of osteoarthritis in the United Kingdom: findings from the Clinical Practice Research Datalink (CPRD). Osteoarthritis and Cartilage, 28(6), 792–801. https://doi.org/https://doi.org/10.1016/j.joca.2020.03.004

Tarquini, C., Pucci, S., Scioli, M. G., Doldo, E., Agostinelli, S., D'Amico, F., Bielli, A., Ferlosio, A., Caredda, E., Tarantino, U., & Orlandi, A. (2020). Clusterin exerts a cytoprotective and antioxidant effect in human osteoarthritic cartilage. Aging, 12(11), 10129–10146. https://doi.org/10.18632/aging.103310

Taylor, D. W., Ahmed, N., Parreno, J., Lunstrum, G. P., Gross, A. E., Diamandis, E. P., & Kandel, R. A. (2015). Collagen type XII and versican are present in the early stages of cartilage tissue formation by both redifferentating passaged and primary chondrocytes. Tissue Engineering. Part A, 21(3–4), 683–693. https://doi.org/10.1089/ten.TEA.2014.0103

Temple, M. M., Bae, W. C., Chen, M. Q., Lotz, M., Amiel, D., Coutts, R. D., & Sah, R. L. (2007). Age- and site-associated biomechanical weakening of human articular cartilage of the femoral condyle. Osteoarthritis and Cartilage, 15(9), 1042–1052. https://doi.org/10.1016/j.joca.2007.03.005

Tocharus, J., Tsuchiya, A., Kajikawa, M., Ueta, Y., Oka, C., & Kawaichi, M. (2004). Developmentally regulated expression of mouse HtrA3 and its role as an inhibitor of TGF-beta signaling. Development, Growth & Differentiation, 46(3), 257–274. https://doi.org/10.1111/j.1440-169X.2004.00743.x

Tortorella, M. D., Arner, E. C., Hills, R., Easton, A., Korte-Sarfaty, J., Fok, K., Wittwer, A. J., Liu, R.-Q., & Malfait, A.-M. (2004). Alpha2-macroglobulin is a novel substrate for ADAMTS-4 and ADAMTS-5 and represents an endogenous inhibitor of these enzymes. The Journal of Biological Chemistry, 279(17), 17554–17561. https://doi.org/10.1074/jbc.M313041200

Urban, J. P. G. (1994). THE CHONDROCYTE: A CELL UNDER PRESSURE. Rheumatology, 33(10), 901–908. https://doi.org/10.1093/rheumatology/33.10.901

Valko, M., Leibfritz, D., Moncol, J., Cronin, M. T. D., Mazur, M., & Telser, J. (2007). Free radicals and antioxidants in normal physiological functions and human disease. The International Journal of Biochemistry & Cell Biology, 39(1), 44–84. https://doi.org/https://doi.org/10.1016/j.biocel.2006.07.001

Vaughan-Thomas, A., Dudhia, J., Bayliss, M. T., Kadler, K. E., & Duance, V. C. (2008). Modification of the composition of articular cartilage collagen fibrils with increasing age. Connective Tissue Research, 49(5), 374–382. https://doi.org/10.1080/03008200802325417

Verzijl, N., Bank, R. A., TeKoppele, J. M., & DeGroot, J. (2003). AGEing and osteoarthritis: a different perspective. Current Opinion in Rheumatology, 15(5), 616–622. https://doi.org/10.1097/00002281-200309000-00016

Vincent, T. (2000). The effect of age on proteoglycan aggregation in human cartilage. Arthritis Research & Therapy, 3(1), 66797. https://doi.org/10.1186/ar-2000-66797

Vincourt, J.-B., Lionneton, F., Kratassiouk, G., Guillemin, F., Netter, P., Mainard, D., & Magdalou, J. (2006). Establishment of a reliable method for direct proteome characterization of human articular cartilage. Molecular & Cellular Proteomics : MCP, 5(10), 1984–1995. https://doi.org/10.1074/mcp.T600007-MCP200

Wachsmuth, L., Söder, S., Fan, Z., Finger, F., & Aigner, T. (2006). Immunolocalization of matrix proteins in different human cartilage subtypes. Histology and Histopathology, 21(5), 477–485. https://doi.org/10.14670/HH-21.477

Wang L, Shang X, Feng Y, et al. Wnt/β-catenin signaling regulates the proliferation and differentiation of mesenchymal progenitor cells through the p53 pathway. PLoS One. 2014;9(6):e97283. doi:10.1371/journal.pone.0097283

Wang, S., Wei, X., Zhou, J., Zhang, J., Li, K., Chen, Q., Terek, R., Fleming, B. C., Goldring, M. B., Ehrlich, M. G., Zhang, G., & Wei, L. (2014). Identification of α2-macroglobulin as a master inhibitor of cartilage-degrading factors that attenuates the progression of posttraumatic osteoarthritis. Arthritis & Rheumatology (Hoboken, N.J.), 66(7), 1843–1853. https://doi.org/10.1002/art.38576

Wang, Y., Nizkorodov, A., Riemenschneider, K., Lee, C. S. D., Olivares-Navarrete, R., Schwartz, Z., & Boyan, B. D. (2014). Impaired bone formation in Pdia3 deficient mice. PloS One, 9(11), e112708. https://doi.org/10.1371/journal.pone.0112708

Wang, Y., Zhao, X., Lotz, M., Terkeltaub, R., & Liu-Bryan, R. (2015). Mitochondrial biogenesis is impaired in osteoarthritis chondrocytes but reversible via peroxisome proliferator-activated receptor γ coactivator 1α. Arthritis & Rheumatology (Hoboken, N.J.), 67(8), 2141–2153. https://doi.org/10.1002/art.39182

Warner, S. C., & Valdes, A. M. (2017). Genetic association studies in osteoarthritis: is it fairytale? Current Opinion in Rheumatology, 29(1), 103–109. https://doi.org/10.1097/BOR.0000000000000352

Wei, L., Sun, X., Kanbe, K., Wang, Z., Sun, C., Terek, R., & Chen, Q. (2006). Chondrocyte death induced by pathological concentration of chemokine stromal cell-derived factor-1. The Journal of Rheumatology, 33(9), 1818–1826.

Wieland, H. A., Michaelis, M., Kirschbaum, B. J., & Rudolphi, K. A. (2005). Osteoarthritis - an untreatable disease? Nature Reviews. Drug Discovery, 4(4), 331–344. https://doi.org/10.1038/NRD1693

Wilson, R., Norris, E. L., Brachvogel, B., Angelucci, C., Zivkovic, S., Gordon, L., Bernardo, B. C., Stermann, J., Sekiguchi, K., Gorman, J. J., & Bateman, J. F. (2012). Changes in the chondrocyte and extracellular matrix proteome during post-natal mouse cartilage development. Molecular & Cellular Proteomics : MCP, 11(1), M111.014159. https://doi.org/10.1074/mcp.M111.014159

Wilusz, R. E., Sanchez-Adams, J., & Guilak, F. (2014). The structure and function of the pericellular matrix of articular cartilage. Matrix Biology : Journal of the International Society for Matrix Biology, 39, 25–32. https://doi.org/10.1016/j.matbio.2014.08.009

Wu, J. J., & Eyre, D. R. (1995). Structural analysis of cross-linking domains in cartilage type XI collagen. Insights on polymeric assembly. The Journal of Biological Chemistry, 270(32), 18865–18870. https://doi.org/10.1074/jbc.270.32.18865

Wu, J., Liu, W., Bemis, A., Wang, E., Qiu, Y., Morris, E. A., Flannery, C. R., & Yang, Z. (2007). Comparative proteomic characterization of articular cartilage tissue from normal donors and patients with osteoarthritis. Arthritis and Rheumatism, 56(11), 3675–3684. https://doi.org/10.1002/art.22876

Wu, J.-J., Weis, M. A., Kim, L. S., & Eyre, D. R. (2010). Type III collagen, a fibril network modifier in articular cartilage. The Journal of Biological Chemistry, 285(24), 18537–18544. https://doi.org/10.1074/jbc.M110.112904

Xi, H., Li, C., Ren, F., Zhang, H., & Zhang, L. (2013). Telomere, aging and age-related diseases. Aging Clinical and Experimental Research, 25(2), 139–146. https://doi.org/10.1007/s40520-013-0021-1

Xia, Y., Darling, E. M., & Herzog, W. (2018). Functional properties of chondrocytes and articular cartilage using optical imaging to scanning probe microscopy. Journal of Orthopaedic Research : Official Publication of the Orthopaedic Research Society, 36(2), 620–631. https://doi.org/10.1002/jor.23757

Xu, H., Zheng, Q., Song, J., Li, J., Wang, H., Liu, P., Wang, J., Wang, C., & Zhang, X. (2016). Intermittent cyclic mechanical tension promotes endplate cartilage degeneration via canonical Wnt signaling pathway and E-cadherin/β-catenin complex cross-talk. Osteoarthritis and Cartilage, 24(1), 158–168. https://doi.org/10.1016/j.joca.2015.07.019

Youn, I., Choi, J. B., Cao, L., Setton, L. A., & Guilak, F. (2006). Zonal variations in the three-dimensional morphology of the chondron measured in situ using confocal microscopy. Osteoarthritis and Cartilage, 14(9), 889–897. https://doi.org/10.1016/j.joca.2006.02.017

Yuan, C., Pan, Z., Zhao, K., Li, J., Sheng, Z., Yao, X., Liu, H., Zhang, X., Yang, Y., Yu, D., Zhang, Y., Xu, Y., Zhang, Z.-Y., Huang, T., Liu, W., & Ouyang, H. (2020). Classification of four distinct osteoarthritis subtypes with a knee joint tissue transcriptome atlas. Bone Research, 8(1), 38. https://doi.org/10.1038/s41413-020-00109-x

Zelenski, N. A., Leddy, H. A., Sanchez-Adams, J., Zhang, J., Bonaldo, P., Liedtke, W., & Guilak, F. (2015). Type VI Collagen Regulates Pericellular Matrix Properties, Chondrocyte Swelling, and Mechanotransduction in Mouse Articular Cartilage. Arthritis & Rheumatology (Hoboken, N.J.), 67(5), 1286–1294. https://doi.org/10.1002/art.39034

Zeng, G. Q., Chen, A. B., Li, W., Song, J. H., & Gao, C. Y. (2015). High MMP-1, MMP-2, and MMP-9 protein levels in osteoarthritis. Genetics and Molecular Research : GMR, 14(4), 14811–14822. https://doi.org/10.4238/2015.November.18.46

Zhen, E. Y., Brittain, I. J., Laska, D. A., Mitchell, P. G., Sumer, E. U., Karsdal, M. A., & Duffin, K. L. (2008). Characterization of metalloprotease cleavage products of human articular cartilage. Arthritis and Rheumatism, 58(8), 2420–2431. https://doi.org/10.1002/art.23654

Zheng, J., Wu, C., Ma, W., Zhang, Y., Hou, T., Xu, H., Wu, S., Yao, X., & Guo, X. (2013). Abnormal expression of chondroitin sulphate N-acetylgalactosaminyltransferase 1 and Hapln-1 in cartilage with Kashin-Beck disease and primary osteoarthritis. International Orthopaedics, 37(10), 2051–2059. https://doi.org/10.1007/s00264-013-1937-y

Zhong, L., Huang, X., Karperien, M., & Post, J. N. (2016). Correlation between Gene Expression and Osteoarthritis Progression in Human. International Journal of Molecular Sciences, 17(7). https://doi.org/10.3390/ijms17071126